frontiers | Research Topics

Case reports in cardiovascular genetics and systems medicine 2022

Edited by
Neil Morgan

Published in
Frontiers in Cardiovascular Medicine

ISSN 1664-8714
ISBN 978-2-8325-3559-2
DOI 10.3389/978-2-8325-3559-2

About Frontiers

Frontiers is more than just an open access publisher of scholarly articles: it is a pioneering approach to the world of academia, radically improving the way scholarly research is managed. The grand vision of Frontiers is a world where all people have an equal opportunity to seek, share and generate knowledge. Frontiers provides immediate and permanent online open access to all its publications, but this alone is not enough to realize our grand goals.

Frontiers journal series

The Frontiers journal series is a multi-tier and interdisciplinary set of open-access, online journals, promising a paradigm shift from the current review, selection and dissemination processes in academic publishing. All Frontiers journals are driven by researchers for researchers; therefore, they constitute a service to the scholarly community. At the same time, the *Frontiers journal series* operates on a revolutionary invention, the tiered publishing system, initially addressing specific communities of scholars, and gradually climbing up to broader public understanding, thus serving the interests of the lay society, too.

Dedication to quality

Each Frontiers article is a landmark of the highest quality, thanks to genuinely collaborative interactions between authors and review editors, who include some of the world's best academicians. Research must be certified by peers before entering a stream of knowledge that may eventually reach the public - and shape society; therefore, Frontiers only applies the most rigorous and unbiased reviews. Frontiers revolutionizes research publishing by freely delivering the most outstanding research, evaluated with no bias from both the academic and social point of view. By applying the most advanced information technologies, Frontiers is catapulting scholarly publishing into a new generation.

What are Frontiers Research Topics?

Frontiers Research Topics are very popular trademarks of the *Frontiers journals series*: they are collections of at least ten articles, all centered on a particular subject. With their unique mix of varied contributions from Original Research to Review Articles, Frontiers Research Topics unify the most influential researchers, the latest key findings and historical advances in a hot research area.

Find out more on how to host your own Frontiers Research Topic or contribute to one as an author by contacting the Frontiers editorial office: frontiersin.org/about/contact

Case reports in cardiovascular genetics and systems medicine: 2022

Topic editor
Neil Morgan — University of Birmingham, United Kingdom

Citation
Morgan, N., ed. (2023). *Case reports in cardiovascular genetics and systems medicine: 2022*. Lausanne: Frontiers Media SA. doi: 10.3389/978-2-8325-3559-2

Table of contents

frontiers | Frontiers in Cardiovascular Medicine

TYPE Editorial
PUBLISHED 11 September 2023
DOI 10.3389/fcvm.2023.1282147

OPEN ACCESS

EDITED AND REVIEWED BY
Masanori Aikawa,
Brigham and Women's Hospital and Harvard Medical School, United States

*CORRESPONDENCE
Neil V. Morgan
n.v.morgan@bham.ac.uk

RECEIVED 23 August 2023
ACCEPTED 04 September 2023
PUBLISHED 11 September 2023

CITATION
Morgan NV (2023) Editorial: Case reports in cardiovascular genetics and systems medicine: 2022.
Front. Cardiovasc. Med. 10:1282147.
doi: 10.3389/fcvm.2023.1282147

Editorial: Case reports in cardiovascular genetics and systems medicine: 2022

Neil V. Morgan*

Institute of Cardiovascular Sciences, College of Medical and Dental Sciences, University of Birmingham, Birmingham, United Kingdom

KEYWORDS

case-report, clinical cases, genetics, cardiovascular disease, rare variants, genotype-phenotype

Editorial on the Research Topic
Case reports in cardiovascular genetics and systems medicine: 2022

Case reports remain a very useful resource especially for rare genetic conditions where only a handful of reported mutations maybe reported. Indeed, it has previously been reported that case-reports, are a compendium of useful ideas for our daily activity in the context of clinical management of patients (1).

But more specifically for rarer genetic diseases, there may be situations where an additional family with a distinct mutation is needed to prove the disease gene(s) is linked to the phenotype of the specific genetic disorder. Further, the clinical work up of rare cases will allow for genotype-phenotype correlations. In situations where rare genetic variants are classed as Variants of Uncertain Significance (VUS) characterising variants for clinical action is extremely important. Internationally there are many efforts ongoing to address this such as the ClinGen Gene Curation Working Group (2). This grouping has developed a method to qualitatively define the "clinical validity" of a gene-disease relationship using a semiquantitative method to assess the clinical validity of gene-disease relationships. More recently this has been applied to a well-known cardiovascular disease, Dilated Cardiomyopathy (DCM) (3). More specifically in this study they have investigated evidence-based assessment of genes in DCM where the authors carried out a large-scale analysis of 51 genes previously associated with DCM, providing strong evidence for DCM associated genes that can be used to define and improve clinical practice and management of patients. Overall case reports may also highlight new clinical findings for a particular disease/syndrome, that have not been previously documented thus can extend the phenotypic spectrum. This can be true even for genetic diseases with mutations in the same gene, known as allelic heterogeneity.

In this latest exciting series of case reports, we illustrate the value of publishing such case reports in a range of cardiovascular genetic diseases including cardiomyopathies, tetralogy of fallot (TOF), and other rare syndromes including Ehlers Danlos syndrome. The series includes 2 case reports highlighting where specific mutations in a Cardiomyopathy can be linked to sudden cardiac death, a situation where defining the genetics can not only give a reason for this devasting outcome, but also inform genetics for future cases within the same family and allowing for accurate genetic counselling. One of these cases published by Jin et al. report a variant in the Myosin Binding Protein C3 encoding *MYBPC3*, which

is an apparent "silent" variant which although doesn't change the amino acid, results in altered splicing of the transcript leading to reduced expression of the gene.

An interesting case published by Wang et al. report a family with TOF, which is the most common cyanotic congenital heart disease (CHD), but only a small number of familial TOF cases have been reported to date. Using whole exome sequencing (WES) the authors report a novel heterozygous missense variant in the *MYOM2* gene, thus expanding the spectrum of the gene variants that lead to TOF.

Two other case reports are focused on Ehlers Danlos syndrome, a rare connective tissue disorder characterised by spontaneous arterial, bowel or organ rupture. In one case Manhas et al. functionally characterise a missense variant in *COL3A1*, classifying it as pathogenic. A further case of Ehlers-Danlos syndrome was reported by Taurino et al. with complex arterial findings and death at young age identified a novel *COL3A1* variant which concludes early diagnosis could lead to treatment choices, improved management, and ultimately, better outcomes.

In summary, this series of case reports include rare genetic diseases that are important to publish and extend the phenotype-genotype correlations of this collection of rare cardiovascular diseases. They highlight the challenges and value in assigning pathogenicity of the specific genetic variant where functional characterisation is often required, in order to ultimately improve patient management and introduce personalised treatments where possible.

Author contributions

NM: Conceptualization, Data curation, Writing – original draft, Writing – review and editing.

Funding

The author declare that no financial support was received for the research, authorship, and/or publication of this article.

Acknowledgments

The author would like to thank Samantha Montague for proofreading this manuscript.

Conflict of interest

The author declares that the research was conducted in the absence of any commercial or financial relationships that could be construed as a potential conflict of interest.

The author declared that they were an editorial board member of Frontiers, at the time of submission. This had no impact on the peer review process and the final decision.

Publisher's note

References

1. Novoa NM. Editorial: case-reports, a compendium of useful ideas for our daily activity. *Front Surg*. (2022) 9:1026401. doi: 10.3389/fsurg.2022.1026401

2. Ramos EM, Din-Lovinescu C, Berg JS, Brooks LD, Duncanson A, Dunn M, et al. Characterizing genetic variants for clinical action. *Am J Med Genet C Semin Med Genet*. (2014) 166C(1):93–104. doi: 10.1002/ajmg.c.31386

3. Jordan E, Peterson L, Ai T, Asatryan B, Bronicki L, Brown E, et al. Evidence-based assessment of genes in dilated cardiomyopathy. *Circulation*. (2021) 144(1):7–19. doi: 10.1161/CIRCULATIONAHA.120.053033

frontiers in Cardiovascular Medicine

CASE REPORT
published: 02 March 2022
doi: 10.3389/fcvm.2022.806977

Case Report: Identification of the First Synonymous Variant of Myosin Binding Protein C3 (c.24A>C, p.P8P) Altering RNA Splicing in a Cardiomyopathy and Sudden Cardiac Death Case

Jie-Yuan Jin[1†], *Jiao Xiao*[2†], *Yi Dong*[1], *Yue Sheng*[1], *Ya-Dong Guo*[2,3,4*] and *Rong Xiang*[1,3,4*]

[1] School of Life Sciences, Central South University, Changsha, China, [2] Department of Forensic Science, School of Basic Medical Sciences, Central South University, Changsha, China, [3] Hunan Key Laboratory of Animal Models for Human Diseases, School of Life Sciences, Central South University, Changsha, China, [4] Hunan Key Laboratory of Medical Genetics, School of Life Sciences, Central South University, Changsha, China

OPEN ACCESS

Edited by:
Emma Louise Robinson,
University of Colorado, United States

Reviewed by:
Sakthivel Sadayappan,
University of Cincinnati, United States
Richard Gilbert,
Warren Alpert Medical School of Brown University, United States

***Correspondence:**
Rong Xiang
shirlesmile@csu.edu.cn
Ya-Dong Guo
gyd82@126.com

[†]These authors have contributed equally to this work

Specialty section:
This article was submitted to Cardiovascular Genetics and Systems Medicine, a section of the journal Frontiers in Cardiovascular Medicine

Received: 01 November 2021
Accepted: 17 January 2022
Published: 02 March 2022

Citation:
Jin J-Y, Xiao J, Dong Y, Sheng Y, Guo Y-D and Xiang R (2022) Case Report: Identification of the First Synonymous Variant of Myosin Binding Protein C3 (c.24A>C, p.P8P) Altering RNA Splicing in a Cardiomyopathy and Sudden Cardiac Death Case. Front. Cardiovasc. Med. 9:806977. doi: 10.3389/fcvm.2022.806977

Background: Sudden cardiac death (SCD), based on sudden cardiac ejection cessation, is an unexpected death. Primary cardiomyopathies, including dilated cardiomyopathy (DCM), are one of main causes of SCD. The DCM is characterized by a cardiac dilatation and a reduced systolic function with a prevalence of 1/250 in adults. The DCM has been reported with more than 60 disease-causing genes, and *MYBPC3* variants are one of the most common and well-known causes of DCM.

Methods: We identified a 29-year-old female who died of SCD. We performed a whole-exome sequencing (WES) to detect her genetic etiology and used minigene modeling and immunohistochemistry staining to verify the pathogenicity.

Results: We determined that the woman died of SCD caused by DCM due to an identified novel synonymous variant of *MYBPC3* (NM_000256.3: c.24A>C, p.P8P) in the deceased. The variant can result in abnormal splicing, which was confirmed by minigene models and immunohistochemistry staining.

Conclusion: We may have identified the first deleterious synonymous variant of *MYBPC3* in an SCD case and verified its significant impact on RNA splicing. Our description enriched the spectrum of *MYBPC3* variants and emphasized the significance of synonymous variants that are always disregarded in genetic screening.

Keywords: *MYBPC3*, sudden cardiac death, dilated cardiomyopathy, synonymous variant, splicing

INTRODUCTION

Sudden cardiac death (SCD) is an unexpected death based on sudden cardiac ejection cessation. It accounts for 15–20% of unnatural death in developed countries (1, 2). The prominent symptoms of SCD include chest pain, dyspnea, palpitations, presyncope, and syncope. Primary electrical disorders, atherosclerosis, congenital cardiovascular diseases, and cardiomyopathies are the four main causes of SCD (3).

Cardiomyopathies can be divided into dilated cardiomyopathy (DCM), hypertrophic cardiomyopathy (HCM), restrictive cardiomyopathy (RCM), arrhythmogenic right ventricular cardiomyopathy (ARVC), and myocarditis (4). Among these cardiomyopathies, DCM is the most frequent, with a prevalence in adults of at least 1/250 (5). The DCM is characterized by cardiac dilatation and reduced systolic function. A heritable pattern is present in 20–35% of cases (6). Most of inherited DCMs show an autosomal dominant pattern and are usually present in the second or third decade of life (5).

Dilated cardiomyopathy (DCM) has been reported with more than 60 disease-causing genes, involving the sarcomere, Z disc, sarcoglycans, cytoskeletal complex, nuclear envelope, potassium and sodium channels, heat shock proteins, transcription factors, and mitochondria proteins (5).

The *MYBPC3* variants are one of the most common and well-known causes of DCM. The *MYBPC3* encodes the cardiac isoform of myosin-binding protein C and is located in the cross-bridge-bearing zone of A bands in striated muscle (7). An *MYBPC3* defect would result in a striking pattern of sarcomere disorganization and dysgenesis, triggering cardiomyopathy (8).

In the study, we identified a 29-year-old female who died of SCD caused by DCM. We detected a synonymous variant of *MYBPC3* (NM_000256.3: c.24A>C, p.P8P) in the deceased. The variant occurred in the penultimate base of exon 1 and resulted in abnormal splicing. Minigene and immunohistochemistry verified its pathogenicity. To the best of our knowledge, the variant may be the first reported deleterious synonymous variant of *MYBPC3*. Our identification enriched the spectrum of *MYBPC3* variants and emphasized the significance of synonymous variants which are always disregarded in genetic screening.

MATERIALS AND METHODS

Subjects

The study was approved by the Institutional Review Board of Changsha Forensic Appraisal Center. Written informed consent was obtained from the legal guardian and/or next of kin of the deceased for the publication of any potentially identifiable images or data included in this article. The sample was evaluated according to postmortem measures of the International Society and Federation of Cardiology. The anatomical assessment was performed by an expert forensic pathologist and confirmed by a second independent pathologist.

DNA/RNA Extraction and Reverse Transcription

Genomic DNA was extracted by the DNeasy Blood and Tissue Kit (Qiagen, Valencia, USA), and RNA was extracted by the RNeasy Mini Kit (Qiagen, Valencia, USA). Reverse transcription was performed using the RevertAid First Strand cDNA Synthesis Kit (Thermo, Vilnius, Lithuania).

Whole-Exome Sequencing

Berry Genomics Company Limited (Chengdu, China) performed an exome capture, a high-throughput sequencing, and a common filtering, as described in a previous article (9). In this study, we retained all synonymous variants. After common filtering, we predicted the influence of these variants on splicing using NetGene2-2.42 (https://services.healthtech.dtu.dk/service.php?NetGene2-2.42). Causative variants were screened by the list of cardiopathy-related genes (**Supplementary Table S1**) and were classified based on the American College of Medical Genetics and Genomics (ACMG) Standards and Guidelines (10).

Sanger Sequencing and Agarose gel Electrophoresis

The *MYBPC3* reference sequence and coding region (NM_000256.3) were obtained from NCBI (https://www.ncbi.nlm.nih.gov/gene/4607). Primer pairs (*MYBPC3* f: 5′-CCTCAGCTCTCTGGAATTCATC-3′, r: 5′-GGGTTTACCTTCACCTCTCATC-3′; minigene validated f: 5′-GGACTACAAGGATGACGATGAC-3′, r: 5′-CCAGCAATGACTGCGTAAGA-3′) were designed. Target fragments were amplified by polymerase chain reaction (PCR) and were analyzed using the ABI 3100 Genetic Analyzer (ABI, Foster City, USA). The PCR products were electrophoresed on 1% agarose gels.

MYBPC3 Minigene Model

The pcDNA3.1-MYBPC3-minigene plasmids (including exon 1, intron 1, and exon 2) were obtained from WZ Biosciences Inc. (Jinan, China). The mutagenesis of c.10G>A (pcDNA3.1-MYBPC3-10G>A) and c.24A>C (pcDNA3.1-MYBPC3-24A>C) was operated by Fast Mutagenesis Kit V2 (Vazyme, Nanjing, China).

Hematoxylin-Eosin Staining and Immunohistochemistry Staining

Paraformaldehyde-fixed left ventricle tissue was embedded in paraffin and sliced into sections. The sections were stained with hematoxylin-eosin (HE) or immunohistochemistry of *MYBPC3* (Proteintech, 19977-1-AP, 1:200), following the protocol in our previous paper (11).

RESULTS

Postmortem

We recruited a family with history of SCD from Central-South China (**Figure 1A**). The deceased (II:1) was a 29-year-old woman. At 12:00 on February 22, 2017, she expired when she sat on the sofa for a rest at home. She was diagnosed with DCM 8 years ago without other comorbidities. Pathological and toxicological tests (involving ethanol, benzodiazepines, barbitone, benzedrine, methamphetamine, ketamine, morphine, dimethylenedioxyamphetamine, and tetrahydrocannabinol acid) showed no abnormalities. Her serum IgE level was normal (27 IU/ml; reference range: 0–358 IU/ml). There was no increase of eosinophilic granulocyte (4.7%; reference range: 0.5–5%). Postmortem revealed that her heart was enlarged with valve incrassation and myocardial fibrosis, and a congestion in multiple organs with no obvious degranulation of mast cells (heart weight was 363 g; normal level: 240–260 g). The HE staining showed that cardiac muscle cells did not present the hypertrophies or other anomalies (**Figure 1B**). No other fatal

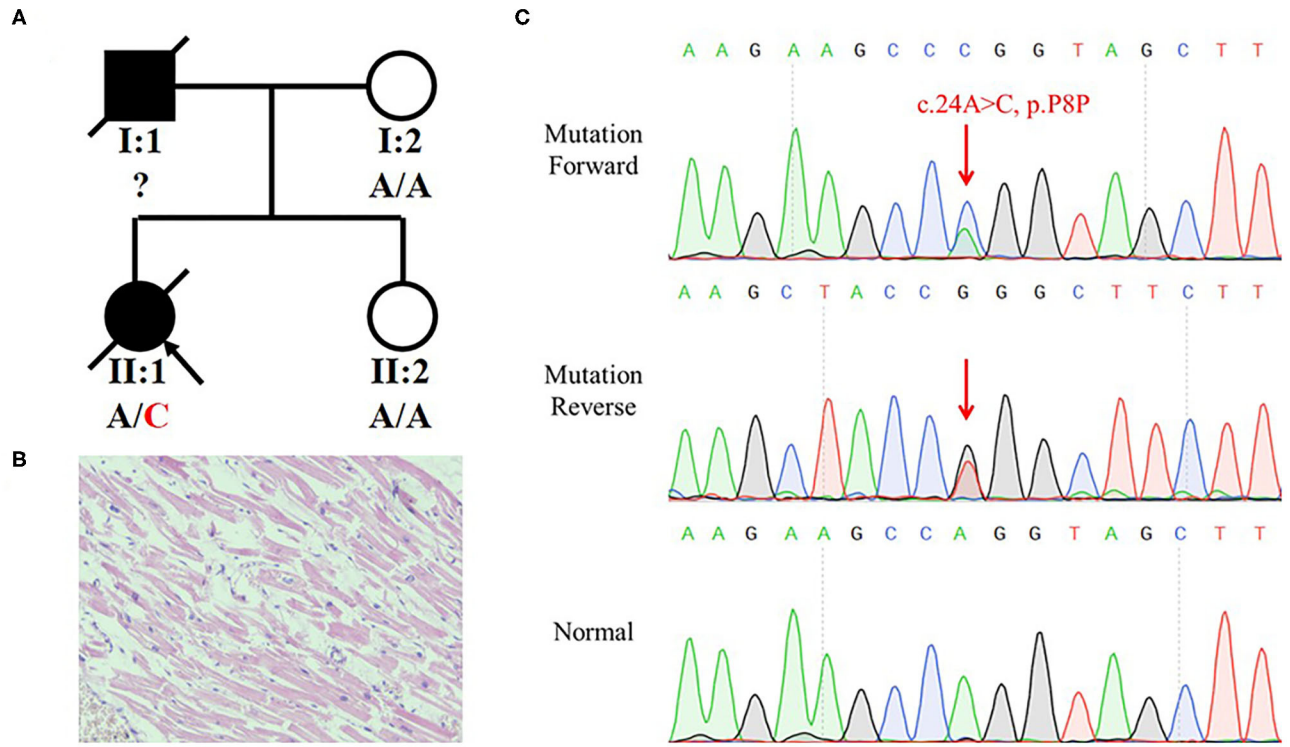

FIGURE 1 | Identification of a synonymous variant of *MYBPC3* in a family with history of Sudden Cardiac Death (SCD). **(A)** Pedigree of the family with SCD. The black symbols represent the affected members and arrows indicate probands. Genotypes are identified by letters and a slash, with red representing variants. **(B)** H and E staining of left ventricle tissue of II:1 did not present hypertrophies and other anomalies. **(C)** Sequencing result of the *MYBPC3* variant (c.24A>C, p.P8P) using Sanger sequencing. Red arrow indicates the variant site.

injury or disease was observed. We concluded that she died of SCD that might have been triggered by DCM. According to a description from her mother (I:2), we speculated that her father (I:1) might have died of a heart attack at 37. The mother and sister (II:2) were unaffected.

Genetic Analysis

The mother hoped to know whether her other daughter had a risk of SCD and turned to us for help. Blood from the heart of the deceased was collected and stored in a refrigerator at −80°C. We extracted a DNA from the blood and preformed a whole-exome sequencing (WES). We eliminated common variants using Genome Aggregation Database (GnomAD; http://gnomad.broadinstitute.org) and Chinese Millionome Database (CMDB; http://cmdb.bgi.com/cmdb/) and predicted the pathogenicity of variants using MutationTaster (http://www.mutationtaster.org/), Polyphen-2 (http://genetics.bwh.harvard.edu/pph2/), and SIFT (http://provean.jcvi.org/index.php). Five variants in cardiopathy-related genes were identified in the deceased (**Table 1**). Based on the ACMG classification of these variants, we highly suspected that *MYBPC3* variant (NM_000256.3: c.24A>C, p.P8P) was the genetic etiology of the deceased. The variant was classified as "Likely pathogenic" following the ACMG evidence PS3, PM2, PP1, and PP3. Although the variant was synonymous, it occurred in the penultimate base of exon 1, which may affect the RNA splicing. Sanger sequencing verified the *MYBPC3* variant in the deceased (**Figure 1C**). Her mother and sister did not harbor this variant.

Minigene Modeling and Immunohistochemistry Staining

To investigate whether the synonymous variant altered the RNA splicing, we constructed minigene models (**Figure 2A**). Sanger sequencing validated the mutagenesis of c.10G>A and c.24A>C in the minigene (**Figure 2B**). The pcDNA3.1-MYBPC3-c.10G>A plasmid was used to exclude the possibility that the mutagenesis, itself, broke the splicing site. The HEK293 cells were used in transfection. Agarose gel electrophoresis indicated that pcDNA3.1-MYBPC3-minigene model and pcDNA3.1-MYBPC3-c.10G>A model had a minigene full-length band (approximately 1,500 bp) and a spliceosome band (approximately 300 bp), while the pcDNA3.1-MYBPC3-c.24A>C model did not produce the spliceosome band, suggesting that c.24A>C caused abnormal splicing (**Figure 2C**). The abnormal splicing may lead to intron 1 retention and frame shift. Immunohistochemistry staining showed that compared with the deceased without SCD, the *MYBPC3* expression was decreased in the left ventricle tissue of II:1 (**Figure 2D**). Therefore, we inferred that the synonymous variant damaged the

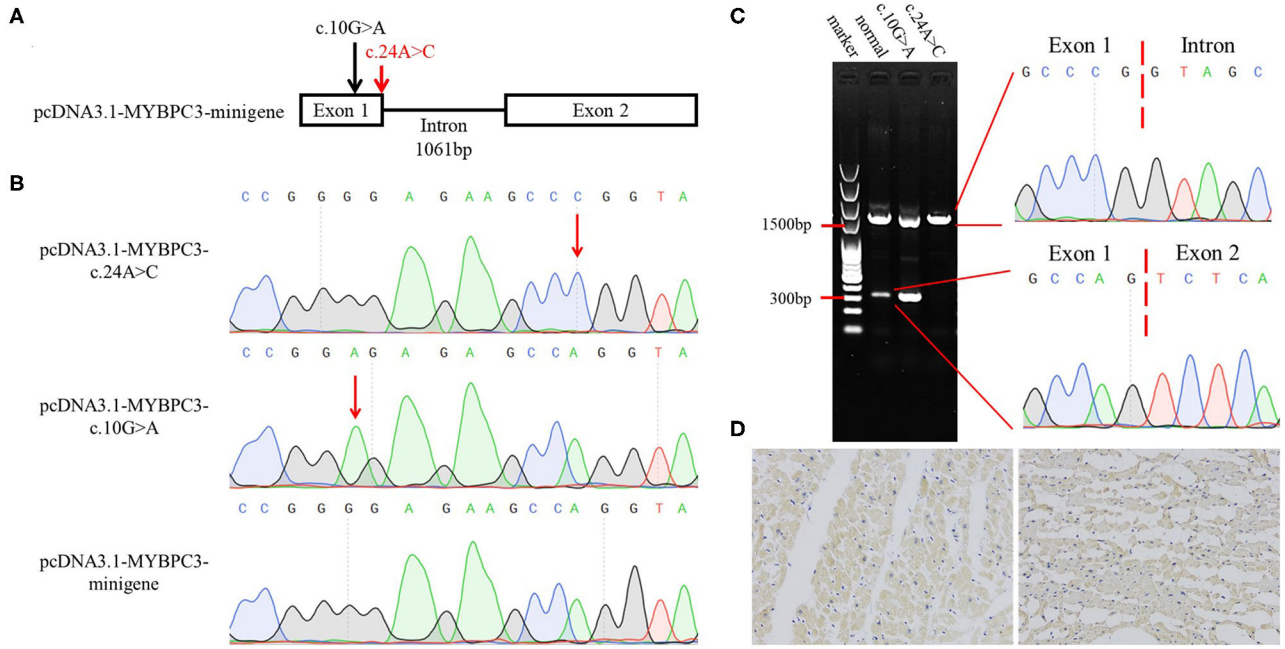

FIGURE 2 | Verification of the pathogenicity of the *MYBPC3* variant (c.24A>C, p.P8P). **(A)** The schematic diagram of minigene models. Arrows indicate variant sites and red represents the variant detected in this study. **(B)** Identification of minigene models by Sanger sequencing. **(C)** Agarose gel electrophoresis and Sanger sequencing showing that c.24A>C results in the splicing alteration. **(D)** Immunohistochemistry staining of MYBPC3. Left represents the left ventricle section of the deceased with natural death, and right represents II:1.

splicing, reduced *MYBPC3*, and was one genetic precipitating factor of her DCM and SCD.

DISCUSSION

Sudden cardiac death (SCD) is defined as "sudden and unexpected death occurring within an hour of the onset of symptoms, or occurring in patients found dead within 24 h of being asymptomatic, presumably due to a cardiac arrhythmia or hemodynamic catastrophe" (12). In the study, through postmortem and disease history talking, we confirmed that the deceased had DCM through negative pathological and toxicological assessment, without other fatal defects. The DCM could have triggered the hemodynamic anomaly and had threatened her life. Hence, we postulated that SCD was her cause of death. In addition, her father had a sudden death despite a momently struggle, supporting our speculation that the father also died of SCD.

Dilated cardiomyopathy (DCM) is one of the most common causes of heart failure and accounts for around 60% of childhood cardiomyopathies (6). Common causes of DCM include infection, inflammation, autoimmunity, chemical and toxin exposure, and genetic variants (13). Genetic causes are important at all ages as approximately 2% of family DCM harbor *MYBPC3* variants (6). In the study, the deceased carried a synonymous variant of *MYBPC3* (c.24A>C, p.P8P). In this variant, the penultimate base of exon 1, A, was substituted by C, which was predicted to change the splicing site. Her mother and sister, without the *MYBPC3* variant, was not found to have a DCM or other cardiovascular diseases.

According to the ACMG guideline, we listed the following evidence and determined that the synonymous variant of *MYBPC3* was "Likely pathogenic." (1) We performed a minigene modeling and an immunohistochemistry staining and verified the damaging effect of the variant (PS3). (2) The variant was absent from controls in GnomAD and CMDB (PM2). (3) The variant was not identified in the unaffected family members (PP1). (4) MutationTaster predicted the synonymous variant to be disease-causing as a result of splice site alteration (PP4) (10). The *MYBPC3* splicing variants (c.24 + 1G>A and c.24 + 3A>C) and our variant (c.24A>C) impacted on the same splicing site. Notably, these two splicing variants were associated with HCM (14, 15). Therefore, we considered that the synonymous variant was the genetic etiology of the deceased.

To confirm the pathogenicity of our variant, we established minigene models. Generally, minigene should be constituted by the affected exon and the adjacent introns and exons at its upstream and downstream (16). In the present case, the synonymous variant was located in the first coding exon. Thus, we constructed the minigene lack of upstream sequences as it may reduce the splicing efficiency. The minigene full-length band was prominently brighter than the spliceosome band in the pcDNA3.1-MYBPC3-minigene model. In the pcDNA3.1-MYBPC3-c.24A>C model, the spliceosome band was absent, suggesting that the variant damaged the RNA splicing. We constructed the pcDNA3.1-MYBPC3-c.10G>A model to be a negative control, while variant c.10G>A promoted

TABLE 1 | Variants identified in the deceased by whole-exome sequencing (WES) in combination with the filtration of cardiopathy-related genes.

Gene	Variant	MutationTaster	PolyPhen-2	SIFT	GnomAD	CMDB	OMIM clinical phenotype	American college of medical genetics classification
LDB3	NM_007078.2: c.2131T>C, p.S711P	D	D	D	-	-	AD, Cardiomyopathy, dilated, 1C, with or without LVNC; AD, Cardiomyopathy, hypertrophic, 24; AD, Left ventricular non-compaction 3; AD, Myopathy, myofibrillar, 4.	Uncertain significance (PM2, PP3, PP5, BP5)
MYBPC3	NM_000256.3: c.24A>C, p.P8P	D	-	-	-	-	AD, Cardiomyopathy, dilated, 1MM; AD/AR, Cardiomyopathy, hypertrophic, 4; AD, Left ventricular non-compaction 10.	Likely pathogenic (PS3, PM2, PP1, PP3)
BBS2	NM_031885.3: c.422A>G, p.N141S	D	D	T	0.00014	0.00091	AR, Bardet-Biedl syndrome 2; AR, Retinitis pigmentosa 74.	Likely benign (PM2, PP3, BS4, BP5)
EVC2	NM_147127.4: c.2643G>C, p.Q881H	D	B	D	0.00007	-	AR, Ellis-van Creveld syndrome; AD, Weyers acrofacial dysostosis.	Likely benign (PM2, PP3, BS4, BP5)
BBS4	NM_033028.4: c.1548_1549del, p.I516Mfs*8	D	-	-	0.00037	-	AR, Bardet-Biedl syndrome 4.	Likely benign (PM2, PP3, BS4, BP5)

D, disease causing; T, tolerant; B, benign; AR, recessive dominant; AD, autosomal dominant.

the splicing capacity. Mutant models exhibited the different influences of the exonic variants on the splicing and verified the pathogenicity of variant c.24A>C. The variant c.24A>C caused intron retention and frame shift, which may lead to a premature termination of translation and/or protein degradation. As per our expectation, *MYBPC3* expression was decreased in the left ventricle tissue of the deceased. Although Ito et. al. predicted and summarized the *MYBPC3* variants that alter RNA splicing, which included several missense variants, the variant (c.24A>C, p.P8P) may be the first known synonymous variant in *MYBPC3* that causes disease. This, therefore, reminded us of the significance of synonymous variants (16).

The *MYBPC3* is mapped to 11p11.2, spans more than 21 kb, and contains 35 exons (17, 18). *MYBPC3* is transversely arrayed in sarcomere A-bands, binds myosin heavy chain in thick filaments, binds titin in elastic filaments, and modulates contraction. An *MYBPC3* defect may affect the actin-myosin interactions, break sarcomere stabilities, alter calcium handling in myocardial cells, and cause DCM, HCM, or left ventricular non-compaction (8). In the study, the *MYBPC3* variant (c.24A>C, p.P8P) reduced the *MYBPC3* expression and was associated with DCM and SCD.

Sudden cardiac death (SCD) is a major public health problem worldwide. It is responsible for approximately 540,000 deaths per year in China and 170,000 to 450,000 deaths per year in the United States (12). Nearly 80% of patients with SCD had preexisting heart disease. Notably, patients presented SCD at the first clinical manifestation (19). Genetic screening of cardiopathy-related genes, such as *MYBPC3*, can contribute to assessing the risk of cardiopathy and SCD and help prevent and treat related diseases. Ehlermann et al. suggested that *MYBPC3* variants are not generally associated with a good prognosis and might cause sudden death even in asymptomatic individuals (20).

CONCLUSIONS

In summary, we reported a young woman who died of SCD. Using WES, we identified a novel variant of *MYBPC3* (NM_000256.3: c.24A>C, p.P8P) in the deceased, which may be the first known synonymous variant of *MYBPC3* that can cause disease. It damaged the splicing and resulted in the reduced *MYBPC3* expression. Our findings expanded the genetic spectrum of SCD, confirmed the pathogenicity of the *MYBPC3* variant (c.24A>C, p.P8P), emphasized the significance of synonymous variants, and contributed to the clinical diagnosis of cardiomyopathy and SCD.

DATA AVAILABILITY STATEMENT

The original contributions presented in the study are included in the article/**Supplementary Material**, further inquiries can be directed to the corresponding author/s.

ETHICS STATEMENT

Written informed consent was obtained from the deceased's legal guardian/next of kin for the publication of any potentially identifiable images or data included in this article.

AUTHOR CONTRIBUTIONS

J-YJ contributed to conception and design and carried out the analysis and interpretation of data. JX performed acquisition and analysis and interpretation of data. YD and YS assisted in the analysis and interpretation of data. Y-DG contributed to conception and design and wrote the original draft. RX revised

the draft and approved the revisions. All authors contributed to the article and approved the submitted version.

FUNDING

This work was supported by the National Science and Technology Major Project of the Ministry of Science and Technology of China (2017ZX10103005-006) and the National Natural Science Foundation of China (81970403, 82072114, and 82170598).

SUPPLEMENTARY MATERIAL

The Supplementary Material for this article can be found online at: https://www.frontiersin.org/articles/10.3389/fcvm.2022.806977/full#supplementary-material

REFERENCES

1. Kuriachan VP, Sumner GL, Mitchell LB. Sudden cardiac death. *Curr Probl Cardiol.* (2015) 40:133–200. doi: 10.1016/j.cpcardiol.2015.01.002
2. Masarone D, Limongelli G, Ammendola E, Verrengia M, Gravino R, Pacileo G. Risk stratification of sudden cardiac death in patients with heart failure: an update. *J Clin Med.* (2018) 7:436. doi: 10.3390/jcm7110436
3. Fernandez-Falgueras A, Sarquella-Brugada G, Brugada J, Brugada R, Campuzano O. Cardiac channelopathies and sudden death: recent clinical and genetic advances. *Biology (Basel).* (2017) 6. doi: 10.3390/biology6010007
4. McKenna WJ, Maron BJ, Thiene G. Classification, epidemiology, and global burden of cardiomyopathies. *Circ Res.* (2017) 121:722–30. doi: 10.1161/CIRCRESAHA.117.309711
5. McKenna WJ, Judge DP. Epidemiology of the inherited cardiomyopathies. *Nat Rev Cardiol.* (2021) 18:22–36. doi: 10.1038/s41569-020-0428-2
6. Weintraub RG, Semsarian C, Macdonald P. Dilated cardiomyopathy. *Lancet.* (2017) 390:400–14. doi: 10.1016/S0140-6736(16)31713-5
7. Seeger T, Shrestha R, Lam CK, Chen C, McKeithan WL, Lau E, et al. A premature termination codon mutation in MYBPC3 causes hypertrophic cardiomyopathy via chronic activation of nonsense-mediated decay. *Circulation.* (2019) 139:799–811. doi: 10.1161/CIRCULATIONAHA.118.034624
8. Toepfer CN, Wakimoto H, Garfinkel AC, McDonough B, Liao D, Jiang J, et al. Hypertrophic cardiomyopathy mutations in MYBPC3 dysregulate myosin. *Sci Transl Med.* (2019) 11:eaat1199. doi: 10.1126/scitranslmed.aat1199
9. Guo BB, Jin JY, Yuan ZZ, Zeng L, Xiang R. A novel COMP mutated allele identified in a Chinese family with pseudoachondroplasia. *Biomed Res Int.* (2021) 2021:6678531. doi: 10.1155/2021/6678531
10. Richards S, Aziz N, Bale S, Bick D, Das S, Gastier-Foster J, et al. Standards and guidelines for the interpretation of sequence variants: a joint consensus recommendation of the American College of Medical Genetics and Genomics and the Association for Molecular Pathology. *Genet Med.* (2015) 17:405–24. doi: 10.1038/gim.2015.30
11. Xiang R, Fan LL, Huang H, Chen YQ, He W, Guo S, et al. Increased Reticulon 3 (RTN3) Leads to Obesity and Hypertriglyceridemia by Interacting With Heat Shock Protein Family A (Hsp70) Member 5 (HSPA5). *Circulation.* (2018) 138:1828–38. doi: 10.1161/CIRCULATIONAHA.117.030718
12. Jazayeri MA, Emert MP. Sudden cardiac death: who is at risk? *Med Clin North Am.* (2019) 103:913–30. doi: 10.1016/j.mcna.2019.04.006
13. Schultheiss HP, Fairweather D, Caforio AL, Escher F, Hershberger RE, Lipshultz SE. Dilated cardiomyopathy. *Nat Rev Dis Primers.* (2019) 5:33. doi: 10.1038/s41572-019-0084-1
14. Berge KE, Leren TP. Genetics of hypertrophic cardiomyopathy in Norway. *Clin Genet.* (2014) 86:355–60. doi: 10.1111/cge.12286
15. Walsh R, Thomson KL, Ware JS, Funke BH, Woodley J, McGuire KJ, et al. Reassessment of Mendelian gene pathogenicity using 7,855 cardiomyopathy cases and 60,706 reference samples. *Genet Med.* (2017) 19:192–203. doi: 10.1038/gim.2016.90
16. Ito K, Patel PN, Gorham JM, McDonough B, DePalma SR, Adler EE, et al. Identification of pathogenic gene mutations in LMNA and MYBPC3 that alter RNA splicing. *Proc Natl Acad Sci U S A.* (2017) 114:7689–94. doi: 10.1073/pnas.1707741114
17. Gautel M, Zuffardi O, Freiburg A, Labeit S. Phosphorylation switches specific for the cardiac isoform of myosin binding protein-C: a modulator of cardiac contraction? *EMBO J.* (1995) 14:1952–60. doi: 10.1002/j.1460-2075.1995.tb07187.x
18. Carrier L, Bonne G, Bahrend E, Yu B, Richard P, Niel F, et al. Organization and sequence of human cardiac myosin binding protein C gene (MYBPC3) and identification of mutations predicted to produce truncated proteins in familial hypertrophic cardiomyopathy. *Circ Res.* (1997) 80:427–34. doi: 10.1161/01.res.0000435859.24609.b3
19. Junttila MJ, Hookana E, Kaikkonen KS, Kortelainen ML, Myerburg RJ, Huikuri HV. Temporal trends in the clinical and pathological characteristics of victims of sudden cardiac death in the absence of previously identified heart disease. *Circ Arrhythm Electrophysiol.* (2016) 9:e003723. doi: 10.1161/CIRCEP.115.003723
20. Ehlermann P, Weichenhan D, Zehelein J, Steen H, Pribe R, Zeller R, et al. Adverse events in families with hypertrophic or dilated cardiomyopathy and mutations in the *MYBPC3* gene. *BMC Med Genet.* (2008) 9:95. doi: 10.1186/1471-2350-9-95

Conflict of Interest: The authors declare that the research was conducted in the absence of any commercial or financial relationships that could be construed as a potential conflict of interest.

Publisher's Note: All claims expressed in this article are solely those of the authors and do not necessarily represent those of their affiliated organizations, or those of the publisher, the editors and the reviewers. Any product that may be evaluated in this article, or claim that may be made by its manufacturer, is not guaranteed or endorsed by the publisher.

frontiers | Frontiers in Cardiovascular Medicine

CASE REPORT
published: 26 April 2022
doi: 10.3389/fcvm.2022.887618

Clinical and Genetic Analysis of a Family With Sitosterolemia Caused by a Novel ATP-Binding Cassette Subfamily G Member 5 Compound Heterozygous Mutation

Ming-fang Shen[1,2†], Ya-nan Hu[1†], Wei-xiang Chen[1,2†], Li-sheng Liao[1,3†], Min Wu[1], Qiu-yan Wu[1], Jian-hui Zhang[1], Yan-ping Zhang[1], Jie-wei Luo[1,4] and Xin-fu Lin[1,2*]*

[1] Fujian Provincial Hospital, Shengli Clinical Medical College of Fujian Medical University, Fuzhou, China, [2] Pediatrics Department, Fujian Provincial Hospital, Fuzhou, China, [3] Department of Hematology, Fujian Provincial Hospital, Fuzhou, China, [4] Department of Traditional Chinese Medicine, Fujian Provincial Hospital, Fuzhou, China

OPEN ACCESS

Edited by:
Hayato Tada,
Kanazawa University, Japan

Reviewed by:
Hirofumi Okada,
Kanazawa University, Japan
Shailendra Patel,
University of Cincinnati, United States

***Correspondence:**
Jie-wei Luo
docluo0421@aliyun.com
Xin-fu Lin
418665840@qq.com

† These authors have contributed equally to this work

Specialty section:
This article was submitted to Cardiovascular Genetics and Systems Medicine, a section of the journal Frontiers in Cardiovascular Medicine

Received: 01 March 2022
Accepted: 05 April 2022
Published: 26 April 2022

Citation:
Shen M-f, Hu Y-n, Chen W-x, Liao L-s, Wu M, Wu Q-y, Zhang J-h, Zhang Y-p, Luo J-w and Lin X-f (2022) Clinical and Genetic Analysis of a Family With Sitosterolemia Caused by a Novel ATP-Binding Cassette Subfamily G Member 5 Compound Heterozygous Mutation. Front. Cardiovasc. Med. 9:887618. doi: 10.3389/fcvm.2022.887618

Sitosterolemia (OMIM ##210250), also known as phytosterolemia, is a rare autosomal recessive disorder caused by mutations in the ATP-binding cassette subfamily G member 5 (*ABCG5*) or member 8 (*ABCG8*) genes. This leads to abnormal functions of the transporter sterolin-1 protein encoded by *ABC*G5 and sterolin-2 protein encoded by *ABC*G8, respectively, which can hinder the formation of stable *ABCG5/G8* heterodimers, decreasing its ability to transport sterols. As a result, phytosterols in tissue or plasma are significantly increased, leading to early onset atherosclerosis-related diseases and xanthelasma of tendons and skin. In this study, whole exome sequencing was performed on a Chinese Han proband with sitosterolemia to capture the target gene and screen for suspected pathogenic mutations. Sanger sequencing of the family members was performed to verify the relationship between family genetics and phenotypes. The structural and functional changes in the transporter sterolin-1 protein after the responsible mutation were predicted using bioinformatics analysis. A novel compound heterozygous mutation in the *ABCG5* gene (NM_022436) was identified in a proband with sitosterolemia, one of which was inherited from the father: c.296T >G (p.M99R), and one from the mother: c.−76 C >T. SIFT, Polyphen2, and Mutation Taster software predicted that p.M99R may be the responsible variant and a novel variant. RNAFold software predicts that c.−76 C >T may affect the transcriptional information or the binding of RNA binding proteins by regulating the structure of RNA, and ultimately affect gene transcription or RNA stability and translation. Swiss model software predicts that the amino acid sequence around p.M99R is highly conserved, and p.M99R leads to instability of the tertiary structure of the *ABCG5/ABCG8* heterodimer. GPS 5.0 predicted that M99R affects the phosphorylation of nearby amino acid sequences, and DUET and VarSite software predicted that M99R affects the stability of sterolin-1 and cause

disease. The p.M99R and c.−76 C >T mutations led to the formation of unstable heterodimers, which disturbed sterol absorption and excretion *in vivo*. The compound heterozygous variants c.296 T >G (p.m99r) and C.−76 C >T on exon 3 of *ABCG5* in this family may be the molecular genetic basis of sitosterolemia.

Keywords: sitosterolemia, sterolin-1 protein, *ABCG5*, mutation, bioinformatics analysis

INTRODUCTION

Sterols are important natural active substances that are widely present in many living things, but the type of sterol used can be different- thus fungi use ergosterol, plants use phytosterols and mammals use cholesterol (1). Cholesterol is a sterol, can be synthesized internally, but phytosterols are not synthesized in the human body and can only be obtained through the diet. Phytosterols are components of plant cell membranes, existing mainly in vegetable oil, grains, fruits, vegetables, and nuts, with cereal sterol being the most abundant (2). Under normal conditions, the absorption of cholesterol by the human body is approximately 50%, while only a negligible proportion of phytosterols (especially xenosterols) are absorbed (<5%); they are almost discharged into the intestinal cavity and bile, and are kept at a very low levels by the action of ABCG5/ABCG8.

Sitosterolemia (OMIM ##210250), also known as phytosterolemia, is a rare autosomal recessive disorder. The clinical manifestations are similar to those of familial hypercholesterolemia, immune thrombocytopenia, and Evans syndrome. Phytosterols in the blood of normal individuals account for only 0.2%. As the plasma sitosterol content cannot be detected by routine examination, sitosterolemia can be easily misdiagnosed or missed (3, 4). Sitosterolemia is caused by mutations in ATP-binding cassette subfamily G member 5b (*ABCG5*) or *ABCG8* (5). According to the Exome Aggregation Consortium (ExAC), a public gene bank, there may be 1 in every 220 people in the general population. Individuals develop gene loss-of-function (LOF) mutations in *ABCG5* or *ABCG8* (6).

MATERIALS AND METHODS

Subjects

The proband was a 7-year-old male of Han nationality from Fujian, China. The main clinical manifestations were several raised nodules of different sizes on the elbow joints, finger joints, and ankle joints, with the largest being approximately 1 × 1.5 cm, pale yellow with borders clear, firm, and non-tender. A routine biochemical full set was re-examined in external hospitals several times, which indicated that blood lipid indicators, such as cholesterol and low-density lipoprotein, were significantly increased. The parents were not consanguineous, and there was no family history of coronary heart disease or increased blood lipid levels. The blood phytosterols spectrum and gene sequencing of the family members were investigated based on clinical manifestations, examination results, and family history of the child. This study was approved by the Ethics Committee of Fujian Provincial Hospital, and all family members or guardians who participated in this study signed an informed consent form.

Determination of Plasma Phytosterols by Gas Chromatography—Mass Spectrometry

Next, 0.1 ml of plasma was placed in a 10 ml centrifuge tube, 0.1 ml of mixed standard solution (including the following standards: squalene, cholestanol, desmosterol, lathosterol, campesterol, stigmasterol, stiosterol) was added, then 1 ml 1 mol/L Potassium hydroxide ethanol solution were also added, vortexed and mixed, sealed with a stopper, and saponified at 60°C for 60 min. After saponification, the solution was cooled to room temperature, 1 ml of deionized water and 3 ml of n-hexane were added, vortexed for 2 min, centrifuged at 3000 r/min for 10 min, and the supernatant (n-hexane layer) was transferred to a 10 mL centrifuge tube. 3 ml of n-hexane was added to the lower aqueous phase, vortexed and mixed, and centrifuged at 3000 r/m for 10 min. The supernatant was taken out and combined, and air dried with high-purity nitrogen at 40°C. 0.1 ml of derivatization reagent (BSTFA-TMCS = 99:1) was added to the residue and placed in a 60°C oven for 60 min. After the derivatization reaction, 1 μl of the sample was directly taken for analysis by gas chromatography—mass spectrometry (GC-MS) (GCMS-QP2010Plus, Shimadzu Corporation, Japan; Beijing Fu-you-Long-hui Genetic Disease Clinic assists in completing GC-MS).

Mapping and Screening of Mutant Genes in Proband and Family Members

Next-generation sequencing of the proband was performed, and DNA capture chip with multiple genes was used to enrich multiple gene fragments, comprising the target genes *ABCG5*, *XYLT2*, *NBAS*, *SLC6A19*, *ERCC6*, *ATP7B*, and *BMP1*. Protein function prediction was performed using SIFT, Polyphen2, and MutationTaster software. Sanger sequencing was used for verification, and primers for target sequences were designed using Primer Premier 5.0. The amplified fragment length of the target sequence where the suspected mutation point *ABCG5*(NM_022436) c.296T >G (p.M99R) was 492 bp. The following primers were used: forward, GAAGGAATGGGCAAGCGTAGG; reverse, TCATGCCTGCACAGAGGGGTCT. The annealing temperature was set to 58°C. The amplified fragment of the target sequence where another suspicious mutation, c.-76 C >T, was located was 369 bp. The following primers were used: forward, ACAAACGTGTGTGTTCTGCC; reverse,

TGCCTTACCTGACGCTGTAG. The annealing temperature was set to 57°C. The primers were synthesized by Wuhan Kangshengda Medical Laboratory and the PCR products were sequenced according to the standard procedure of BigDye Terminator v3.1 kit.

Biological Information Analysis Method

Swiss model and Chimera were used to predict the effect of M99R mutation on protein tertiary structure;Sift and Polyphen software were used to analyze the conservation of amino acid sequence near M99R; GPS 5.0 was used to predict the effect of M99R mutation on phosphorylation modification of nearby amino acid sequence. DUET software was used to predict the effect of M99R mutant on the stability of ABCG5 protein. The pathogenicity of M99R mutant was predicted by VarSite software. RNAFold software was used to predict the binding of transcription factors at ABCG5 c.-76C site and analyze the conservatism.

RESULTS

Evaluation of the Clinical Data of the Probands and Family Members

The family consisted of 12 members, comprising seven males and five females, wherein only one proband had sitosterolemia (**Figure 1A**). A 7-year-old proband (III1) was found to have several xanthomas of various sizes in the elbow, knuckle, and ankle joints (**Figure 1B**). Physical examination showed that several protuberant nodules of different sizes could be found in the elbow, finger and ankle of the child, with a maximum of about 1 × 1.5 cm, light yellow, clear boundary, hard, and no tenderness. After admission, the results of routine blood examination including platelet count and volume, liver and kidney electrolytes, and blood glucose tests were all normal. Tests for autoantibodies and anti-O antibodies were negative. The immune panel, blood cell sedimentation rate, and C-reactive protein level were also normal. Thyroid function tests showed no abnormalities in TSH, T3, and T4 levels. The electrocardiogram (ECG) findings were unremarkable. Full set of blood lipids: Serum total cholesterol (TC) 15.22 mmol/l (normal is <5.18 mmol/l), triglyceride (TG) 1.68 mmol/l (normal is <1.7 mmol/l), low density lipoprotein cholesterol (LDL-C) 13.28 mmol/l (normal is 1.56–3.37 mmol/L), high-density lipoprotein cholesterol (HDL-C) 1.18 mmol/l (normal is 1.29–1.55 mmol/l), apoprotein A (apoA) 1.02 g/l (normal is 1.2–1.6 g/l), apoprotein B (apoB) 3.57 g/l (normal is 0.6–1.1 g/l). Phytosterols spectrum report: squalene 0.41 μmol/L (normal 0.30–4.00 μmol/L), Cholesterol 23.48 μmol/L (normal 0.01–10.00 μmol/L), Desmosterol 2.83 μmol/L (normal 0.30–5.00 μmol/L), Lathosterol 0.64 μmol/L (normal 0.01–12.50 μmol/L), Campesterol 34.79 μmol/L (normal 0.01–10.00 μmol/L), Stigmasterol 5.74 μmol/L (normal 0.10–8.50 μmol/L), Sitosterol 280.29 μmol/L (normal 1.00–15.00 μmol/L) (**Table 1**). Therefore, the proband was diagnosed with sitosterolemia in combination with clinical manifestations, laboratory tests, exclusion of familial hypercholesterolemia and cerebral tendon xanthoma, and subsequent genetic sequencing.

The child was treated with ezetimibe 5mg QD for 2 months after diagnosis, and had a low phytosterols diet at the same time. Re-examination of phytosterol spectrum showed: Sitosterol spectrum report: squalene 0.48 μmol/L (normal 0.30–4.00 μmol/L), Cholesterol 12.77 μmol/L (normal 0.01–10.00 μmol/L), Desmosterol 2.90 μmol/L (normal 0.30–5.00 μmol/L), Lathosterol 0.70 μmol/L (normal 0.01–12.50 μmol/L), Campesterol 95.17 μmol/L (normal 0.01–10.00 μmol/L), Stigmasterol 6.58 μmol/L (normal 0.10–8.50 μmol/L), Sitosterol 93.18 μmol/L (normal 1.00–15.00 μmol/L). The cholestanol and stiosterol were significantly lower than before, but campesterol was increased. Blood lipid reexamination: Serum TC 4.86 mmol/l (normal is <5.18 mmol/l), TG 0.83 mmol/l (normal is <1.7 mmol/l), LDL-C 2.24 mmol/l (normal is 1.56–3.37 mmol/l) L), HDL-C 1.78 mmol/l (normal is 1.29–1.55 mmol/l), apoprotein A 1.5 g/l (normal is 1.2–1.6 g/l), apoprotein B 0.87 g/l (normal is 0.6–1.1 g/l). The previously elevated TC and LDL-C decreased to normal. The treatment of ezetimibe and low phytosterols diet has a significant effect on the improvement of the child's condition.

Except for the slightly higher serum TC and TG levels of I2, I4, and II5, the lipid metabolism-related indicators of other family members, sitosterol test spectrum, routine blood examination including platelet count and volume, liver and kidney electrolytes, cardiac function, and blood glucose tests were normal. Tests for autoantibodies and anti-O antibodies were negative. Blood cell sedimentation rate and C-reactive protein levels were normal. Thyroid function and ECG findings were normal.

Gene Mutation Analysis of the Probands and Family Members

Next-generation sequencing analysis showed that two heterozygous mutations were found in the *ABCG5* gene (NM_022436) in the proband, forming a compound heterozygous mutation. The two mutation points were from the parents, one of which was inherited from the father: c.296T >G (p.M99R), and the other from the mother, and the reference nucleotide sequence hg19, in which thymine (T) at c.296 of exon 3 is replaced by guanine (G), resulting in the replacement of amino acid methionine at position 99 of the coding region by arginine. This mutation was not included in the Human Gene Mutation Database (HGMD), Clinvar Database, MAF population frequency (MAF is the maximum value of ExACALL, esp6500, 1000G frequency), or gnomAD population in East Asia. The predicted scores of SIFT, polyphen2 and mutation taster were 0.006, 0.777, and 0.956, respectively. Referring to the interpretation guide of ACMG gene mutation, this locus meets four requirements (PM1, PM2, PP3, and PP4) and can be graded as a possible pathogenic mutation. The c.-76 C >T mutation in the mother was located in the vicinity of exon 3, and the cytosine (C) of c.-76 was replaced by thymine (T). This variant was not included in the HGMD, Clinvar, and East Asian gnomAD populations. The population frequency of MAFs for this locus was 0.0002. Referring to the interpretation guide of ACMG gene mutations, this locus meets two requirements (PM2, PP4), whose grading evaluation

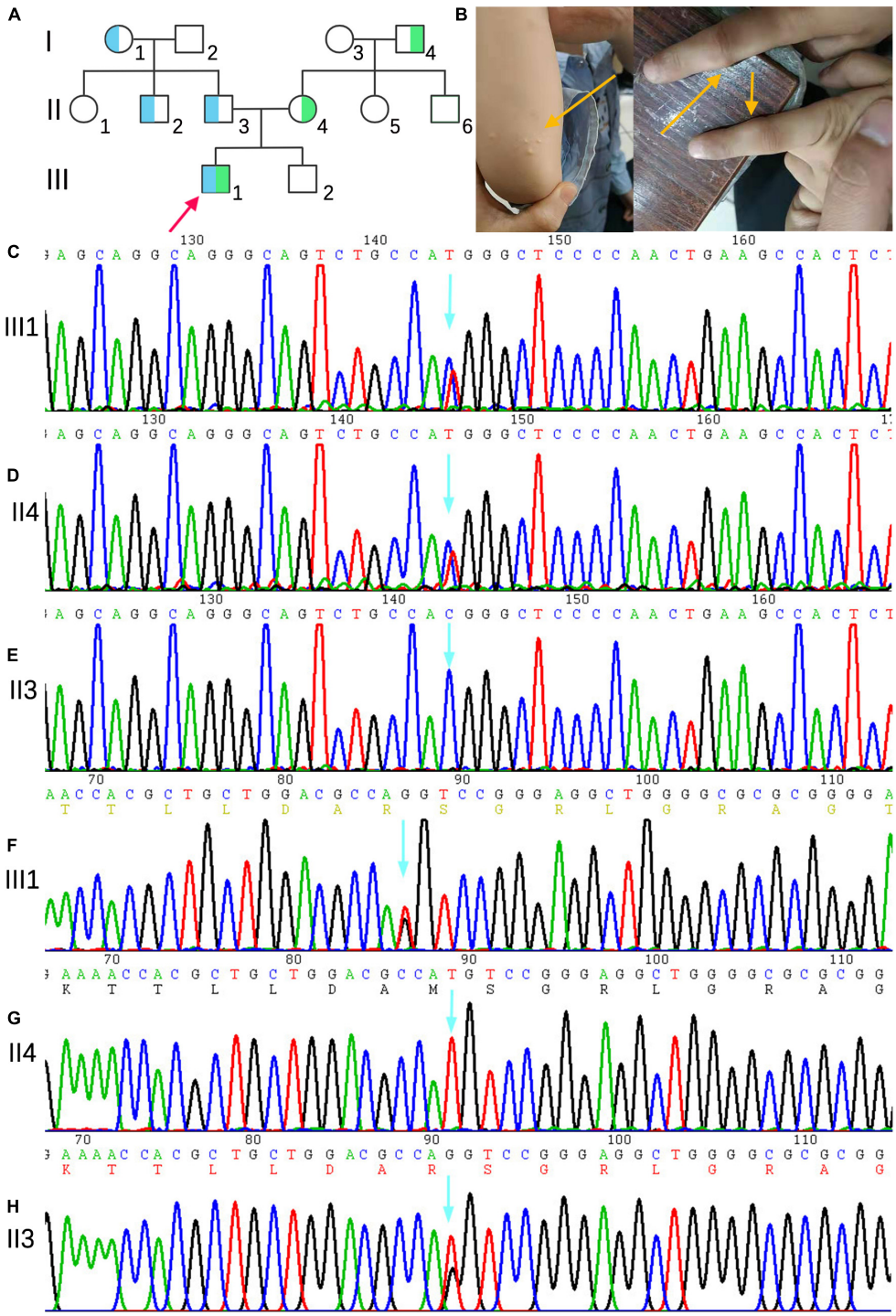

FIGURE 1 | (A) Family genetic pedigrees map for sitosterolemia. Blue indicates a carrier of the mutation of *ABCG5*(NM_022436) c.296 T >G (p.M99R) and green indicates a carrier of the mutation of *ABCG5* c.-76 C >T. the arrow indicates the proband, the square indicates males, and circle indicates female. **(B)** The proband's joint skin xanthoma. **(D–E)** Sanger sequencing showed that proband III1 carried the c.-76 C >T heterozygous variant inherited from mother (II4). **(F–H)** Sanger sequencing map showing that proband III1 carried the c.296T >G (p.M99R) heterozygous variant inherited from father (II3).

was of unknown significance. The proband's mother (II4) and grandfather (I4) carried C.-76 >T heterozygotes, whereas the proband's grandmother (I1), uncle (II2), and father (II3) carried c.296 T >G (p.M99R) heterozygotes (**Figures 1C–H**). III2, I2, II1, II5, and II6 were wild-type, without carrying the above two heterozygotes.

TABLE 1 | Biochemical indicators of family members with sitosterolemia.

Item		III1	II3	II4	II2	Reference value
Blood lipid	Triglyceride, mmol/L	1.18	1.16	1.14	1.11	0–1.7
	Total cholesterol, mmol/L	15.22↑	4.02	3.43	3.23	0–5.17
	High-density lipoprotein, 5mmol/L	1.18	1.16	1.41	1.21	1.16–1.5
	Low-density lipoprotein, mmol/L	13.28↑	2.55	1,76	1.55	1.56–3.37
	Apolipoprotein A1, g/L	1.02	1.47	1.59	1.38	1.2–1.6
	Apolipoprotein B, g/L	3.57 ↑	0.68	0.82	0.98	0.8–1.05
	APO-A1/APO-B	3.5	0.46	0.51	0.71	0.43–0.83
phytosterol spectrum	Squalene, μmol/L	0.41	2.12	1.65	0.65	0.30–4.0
	Cholesterol, μmol/L	23.48↑	7.21	4.32	1.32	0.01–10.0
	Desmosterol, μmol/L	2.83	3.23	4.33	2.21	0.30–5.00
	Lathosterol, μmol/L	0.64	5.67	7.54	1.23	0.01–12.50
	Campesterol, μmol/L	34.79↑	5.67	6.54	2.43	0.01–10.00
	Stigmasterol, μmol/L	5.74	4.32	6.43	5.43	0.10–8.50
	Sitosterol, μmol/L	280.2↑	10.23	11.2	3.4	1.00–15.00
Liver function of blood biochemistry	Total protein, g/L	75.6	78.4	67.2	72.3	60–80
	Albumin, g/L	41.5	50.4	39.5	44.3	35–55
	Globulin, g/L	34.1	28	26	22	20–30
	A/G	1.22	1.8	1.5	2.0	1.2 –2.4
	Total bilirubin, μmol/L	5.7	11.08	10.2	7.9	5.1–19
	Direct bilirubin, μmol/L	1.9	8.1	6.8	2.2	1.7–6.8
	Indirect bilirubin, μmol/L	3.8	3.01	3.3	3.8	0–12
	Alanine aminotransferase, U/L	16.1	43.9	30.3	23.2	5–40
	Aspartate transferase, U/L	27.4	25.5	29.3	23.4	8–40
Renal function of blood biochemistry	Blood urea nitrogen, mmol/L	2.39	4.22	3.34	2.58	2.86–8.2
	Creatinine, μmol/L	42.7	73.3	63.4	60.2	62–116
	Uric acid, μmol/L	281.4	234.3	278.4	244.5	208–428
Heart function of blood biochemistry	Creatine kinase, U/L	128.6	78.1	99.5	60.1	50–310
	Creatine kinase isoenzyme, U/L	27.3	22.1	15.6	21.1	0–25
	Erythrocyte sedimentation rate, mm/h	11	9	13	7	0–15
Routine blood examination	White blood cell × 10^9/L	6.05	4.21	7.23	2.34	4–10
	Hemoglobin,g/L	130	126	133	130	120–140
	Platelet count × 10^9/L	264	241	272	243	125–350
	Platelet volume,fl	10.4	9.8	10.0	7.9	7–11

APO-A1/B, Apolipoprotein A1/B; A/G, Ratio of albumin to globulin.

Biological Information Analysis

The tertiary structure of the protein after the c.296 T > G p.M99R mutation of the *ABCG5* gene (NM_022436) was predicted by Swiss model software[1] (**Figure 2A**)[2] (**Figure 2B**),[3] (**Figure 2C**). As a result, the spatial structure of the p.M99R position was found to change after the mutation. Aligning the same sequence of multiple mammalian species, it was observed that Met99 of the sterolin-1 protein encoded by the *ABCG5* gene was highly conserved in multiple species (**Figure 2D**). M99R affected the phosphorylation modification function of the CAMK pathway adjacent to T94, S100, and T108 (**Figure 2E**),[4] which may have reduced the stability of the sterolin-1 protein structure exhibited a predicted increase in ΔΔG at M99R (2.21 Kcal/mol) (**Figure 2F**).[5] The pink areas are all pathogenic mutations, and the higher the score of the number of variants, the stronger the pathogenicity. M99R was predicted to be pathogenic by VarSite (**Figure 2G**).[6] The c.−76C >T mutation significantly weakens the matching possibility of the stem-loop structure, leading to the apparent loosening of the RNA at the initiation codon, which frees the initiation codon and improves the translation efficiency. This is similar to the translation regulation mode of riboswitch, suggesting that C. − 76 C >t affects the binding of transcriptional information or RNA binding proteins by regulating the structure of RNA, and ultimately affects gene transcription or RNA stability and translation (**Figure 3**).[7]

DISCUSSION

In Patel et al. mapped the sitosterolemia disease gene to two adjacent homologous genes on chromosome 2p21: *ABCG5* and *ABCG8*. Mutations in one of these two genes can lead to sitosterolemia, which is supported by *in vitro* data (7–9).

[1]https://swissmodel.expasy.org/repository/uniprot/Q9H222?template=5do7

[2]https://community.chocolatey.org/packages/chimera/1.15

[3]http://smart.embl-heidelberg.de/

[4]http://gps.biocuckoo.cn/

[5]http://structure.bioc.cam.ac.uk/duet

[6]https://www.ebi.ac.uk/thornton-srv/databases/VarSite

[7]https://genome.ucsc.edu/cgi-bin/hgTracks?db=hg19

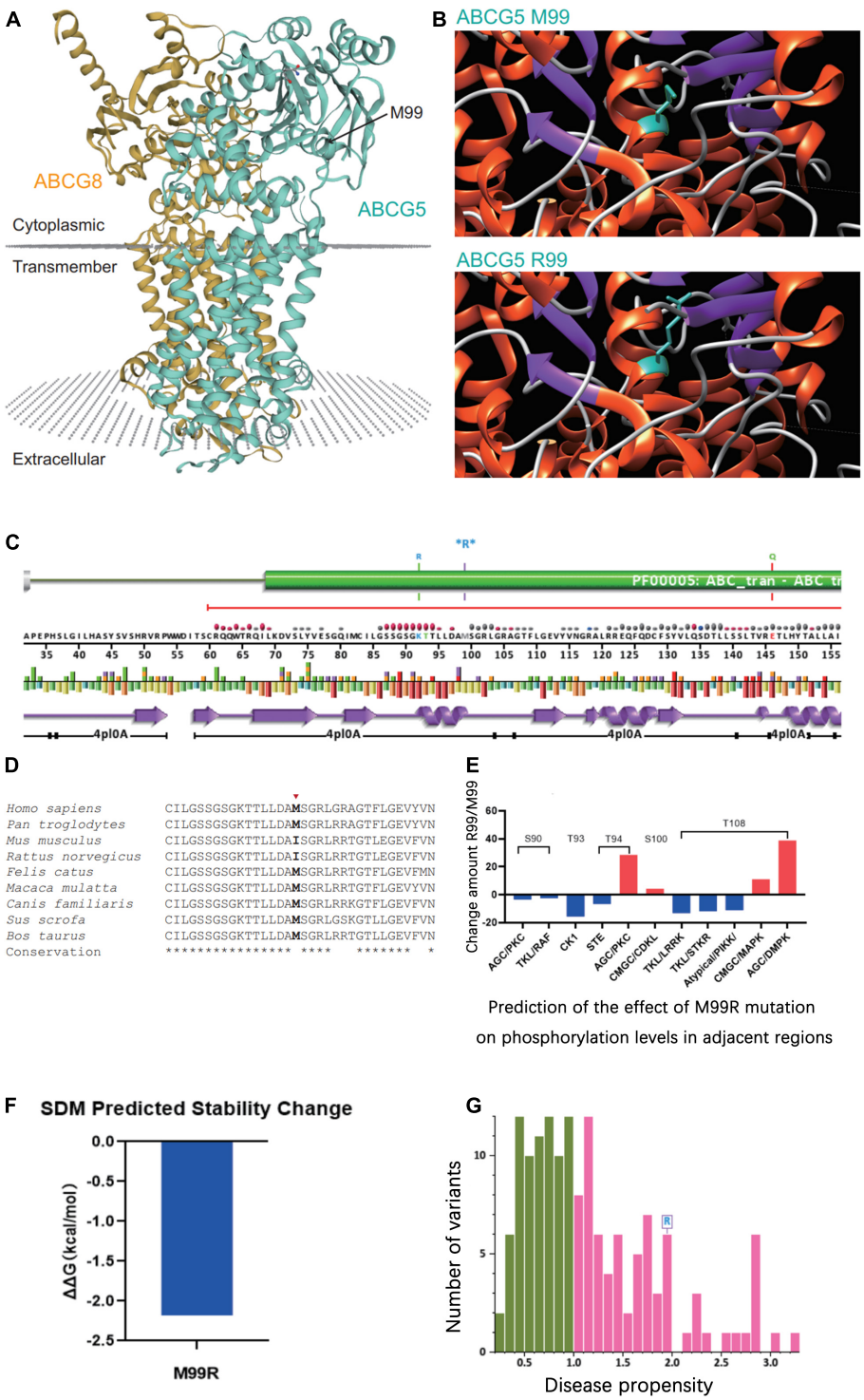

FIGURE 2 | Prediction of the effect of the *ABCG5* (NM_022436) c.296 T >G (p.M99R) variant on the tertiary structure of *ABCG5*. **(A)** Tertiary structure of the *ABCG5/ABCG8* heterodimer (https://swissmodel.expasy.org/repository/uniprot/Q9H222?template=5do7). Green indicates *ABCG5* and orange indicates *ABCG8*. The position marked by the arrow indicates *ABCG5* p.M99R. **(B)** Prediction of changes in the tertiary structure of *ABCG5* after p.M99R mutation (green) by Chimera (https://community.chocolatey.org/packages/chimera/1.15). **(C)** Protein structural information at the p.M99R site. Functional prediction of the *ABCG5* M99R mutation (http://smart.embl-heidelberg.de/). **(D)** Conservation analysis of amino acid sequences near *ABCG5* M99R. **(E)** GPS 5.0 predicts the effect of M99R on phosphorylation modifications of nearby amino acid sequences (http://gps.biocuckoo.cn/). **(F)** DUET predicts the stability effect of M99R on *ABCG5* (http://structure.bioc.cam.ac.uk/duet). **(G)** Prediction of the pathogenicity of *ABCG5* M99R by VarSite (https://www.ebi.ac.uk/thornton-srv/databases/VarSite). The pink areas are all pathogenic mutations, and the higher the score of the number of variants, the stronger the pathogenicity.

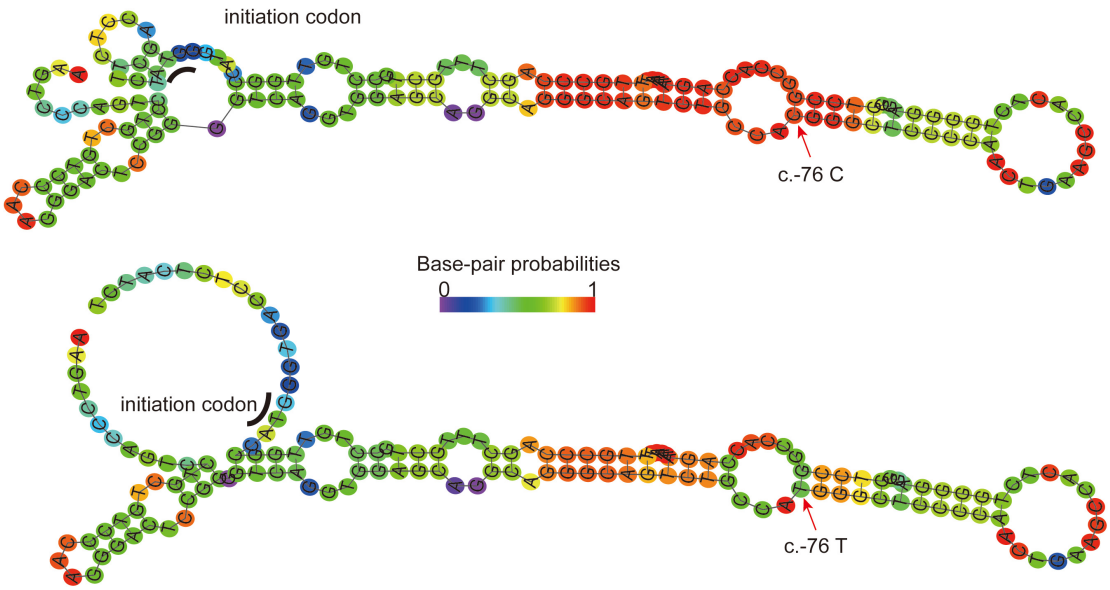

FIGURE 3 | RNAFold (http://rna.tbi.univie.ac.at//cgi-bin/RNAWebSuite/RNAfold) predicts the secondary structure of ABCG mRNA fragments (−140 to + 17) in normal wild-type **(Top)** and C. − 76C >T mutations **(Bottom)**. Arrow, mutation site; Underline, translation initiation codon; Ruler color, possibility of matching. The c.−76C >T mutation significantly weakens the matching possibility of the stem-loop structure, leading to the apparent loosening of the RNA at the initiation codon, which frees the initiation codon and improves the translation efficiency. This is similar to the translation regulation mode of riboswitch.

To verify that the expression of *ABCG5* and *ABCG8* limits sterol absorption and promotes cholesterol excretion, Yu et al. established transgenic mice containing human *ABCG5* and *ABCG8* genes (10). Wild-type (*WT*) mice and *ABCG5* and *ABCG8* knockout mice ($G5G8^{-/-}$ mice) were fed grain-based rodent chow containing 0.02% cholesterol and 4% fat *ad libitum*. The content of phytosterols in the plasma of wild-type mice was almost undetectable, whereas the absorption fraction of phytosterols in $G5G8^{-/-}$ mice increased by 2-3 times, and phytosterols accumulated in the plasma and liver. The sitosterol content in the liver of $G5G8^{-/-}$ mice increased significantly, and its plasma sitosterol level was approximately 30-fold higher than that of wild-type mice (11). In addition, Yu et al. fed *WT* mice and $G5G8^{-/-}$ mice a powdered diet containing 0.02% cholesterol or 2% cholesterol, respectively, and determined the lipid content in plasma and liver by gas chromatography. The results showed that the plasma cholesterol level of *WT* mice did not increase significantly after a high cholesterol diet, while the liver cholesterol level increased by 3-fold. After a high cholesterol diet in $G5G8^{-/-}$ mice, the plasma cholesterol increased by about 2.4-fold, while liver cholesterol levels increased by 18-fold (11). Thus, the overexpression of *ABCG5* and *ABCG8* resulted in a decrease in plasma phytosterol levels and an increase in bile cholesterol secretion. After blocking the pair of genes, the sterol levels in the plasma and liver increased significantly. Transgenic mice with increased ABCG5 and ABCG8 expression showed a 50% reduction in dietary sterol absorption, a significant increase in cholesterol bile secretion, and a significant reduction in plasma phytosterol levels. The overexpression or blockade of sterols in mice leads to changes in sterol content *in vivo*, confirming that *ABCG5* and *ABCG8* are related to the absorption and excretion of sterols.

Both *ABCG5* and *ABCG8* contain 13 exons and 12 introns, and are approximately 60 kb in size. Although the two genes are only 374 base pairs apart, they are transcribed in opposite directions and share a bidirectional promoter and regulatory elements (7). The proteins encoded by *ABCG5* and *ABCG8* are members of the ATP-binding cassette (ABC) transporter family. However, they are different from other transporters in the family because the transporters they encode are semi-transporters, sterolin-1 (encoded by *ABCG5*), and sterolin-2 protein (encoded by *ABCG8*). They contain six transmembrane structures and an ATP-binding site and form a heterodimer in the endoplasmic reticulum to become a complete ABC transporter. This is then transported to the apical membrane of hepatocytes and the apical membrane of intestinal brush border intestinal epithelial cells and is regulated by N-glycosylation and cAMP signaling during transport. It supplies energy through ATP at the apical membrane to regulate the absorption and excretion of phytosterols and cholesterol, especially sitosterol in phytosterols (12). Intestinal epithelial cells promote the excretion of phytosterols into the intestine, maintain the absorption rate of phytosterols at a low level of <5%, and promote the excretion of cholesterol to a certain extent. In liver cells, they promote the excretion of phytosterols and cholesterol into the bile, thereby reducing retention in the body (12–14).

Sitosterolemia, a genetic disease with autosomal mutations, has been confirmed to be caused by mutations in the *ABCG5* or *ABCG8* genes. The *ABCG8* mutation gene is mainly found in Caucasians, especially in Northern Europeans, while *ABCG5* gene mutations are mainly found in Asians, namely Chinese and

Japanese (15). These two genes are located in close proximity and are homologous; however, the mutation of *ABCG8* is more polymorphic than that of *ABCG5* (16). As of April 2022, there were 44 (115) and 48 (119) related mutations in *ABCG5* or *ABCG8* genes included in HGMD, mainly missense mutations, while some were splicing mutations and base deletion frameshift mutations. Monkol Lek et al. analyzed the exon sequences of 60,706 people and found that more than 110 cases of *ABCG5* and *ABCG8* carried loss-of-function alleles, of which only 37 had been described as sitosterolemia. At the same time, nearly 1990 missense variants were found; however, the pathogenicity of these missense mutations was uncertain and had not been tested or clinically verified (6). The potentially pathogenic c.296T >G (p.M99R) variant, identified in the sitosterolemia family, was a novel variant. It has been reported that *ABCG5* c.293c >G (p.Ala98Gly) (CM169032) has a disease spectrum of congenital giant thrombocytopenia with moderate thrombocytopenia (17). It can be seen that *ABCG5* or *ABCG8* gene mutations can lead to a group of highly heterogeneous disease spectrum with different phenotypes. As far as the currently confirmed mutations disease spectrum is concerned, sitosterolemia, phytosterolemia, macrothrombocytopaenia, cholelithiasis, coronary artery disease, increased risk, hypercholesterolemia, increased serum cholesterol, in low-cholesterol consumers, reduced serum non-cholesterol sterols, and smaller decline in cholesterol synthesis after weight loss, among others, are the most common, followed by phytosterolemia.

Mutations in *ABCG5* or *ABCG8* cause proteins encoding the transporters sterolin-1 and sterolin-2 to fail to form stable heterodimers, resulting in hypersteroidemia. The levels of phytosterols in the plasma, lipoprotein, red blood cells, adipose tissue, and skin surface are increased in patients with sitosterolemia. The main clinical manifestations are tendon and skin xanthoma (18). This can occur when the patient is very young, such as during the first year after birth (19). The main mechanism of xanthoma appears to be similar to the early developmental stage of atherosclerosis, that is, the formation of foam cell populations, especially in areas prone to friction (14, 20). According to statistical analysis of familial hypercholesterolemia patients, patients with xanthoma are 3.2-fold more likely to develop cardiovascular disease than patients without xanthoma (21). Furthermore, the accumulation of phytosterols in plasma lipoproteins can increase tissue sterols by affecting the stability of lipoprotein cholesterol and phytosterols. This triggers an inflammatory response, promotes the formation of foam cells and plaques, and induces premature atherosclerosis and coronary heart disease (22). In addition, patients with sitosterolemia may also have anemia and hemolysis. The lifespan of erythrocytes is closely related to lipid metabolism in the plasma, which is related to the abnormal morphology of erythrocytes and the increase in osmotic fragility caused by the appearance of phytosterols in erythrocytes (23). Patients with sitosterolemia also experience abnormal bleeding and thrombocytopenia. This is related to the direct entry of phytosterols into the platelet membrane, resulting in decreased αIIbβ3 expression on the membrane surface, which in turn leads to the loss of GPIba-FlnA linkages, the formation of microparticles, and platelet dysfunction (24), making them more susceptible to deformity and rupture. In addition, this can also be related to joint pain, arthritis, splenomegaly, adrenal dysfunction, and other clinical manifestations.

Hayato Tada suggested that sitosterolemia can be diagnosed if the following conditions are all met at the same time (25): (1) clinical manifestations (xanthoma of skin or tendon); (2) laboratory tests (serum sitosterol ≥1 mg/dl); (3) familial hypercholesterolemia and cerebrotendinous xanthomatosis are excluded; (4) pathogenic mutations *ABCG5* or *ABCG8*. But the clinical manifestations of sitosterolemia are highly heterogeneous, although the genotype and phenotype lack an obvious correlation, and most laboratories lack conditions for phytosterol determination (26). Thus, at present, the diagnosis of this disease remains very difficult. Some patients with sitosterolemia have no xanthoma and only show blood system changes, such as hemolytic anemia and thrombocytopenia. This is often misdiagnosed as idiopathic thrombocytopenia and EVANS syndrome, or even splenectomy (27). Therefore, for the diagnosis of sitosterolemia, it is not only necessary to proceed from clinical manifestations but also to improve the detection of plasma phytosterols, the morphological analysis of blood cells, and genetic diagnosis (27). And based on the pathophysiology of sitosterolemia,ezetimibe and low phytosterols diet are currently effective methods for the treatment of sitosterolemia. Ezetimibe, a Niemann-Pick C1 Like 1 inhibitor, can effectively reduce plasma phytosterols and cholesterol in patients with sitosterolemia by affecting the absorption of various sterols in the intestine (25, 28–30).

DATA AVAILABILITY STATEMENT

The original contributions presented in the study are included in the article/supplementary materials, further inquiries can be directed to the corresponding authors.

ETHICS STATEMENT

The studies involving human participants were reviewed and approved by the Ethics Committee of Fujian Provincial Hospital. Written informed consent to participate in this study was provided by the participants' legal guardian/next of kin. Written informed consent was obtained from the individual(s), and minor(s)' legal guardian/next of kin, for the publication of any potentially identifiable images or data included in this article.

AUTHOR CONTRIBUTIONS

J-WL and X-FL designed the study. M-FS, Y-NH, W-XC, and MW performed the data collection. Q-YW, J-HZ, and Y-PZ performed the data analysis and interpretation of results. M-FS wrote the original draft. J-WL and L-SL reviewed and provided critical comments on the manuscript. All authors read and approved the final version of the manuscript.

FUNDING

This work was supported by Natural Science Foundation of Fujian Province (2020J011064), Fujian Province Medical Innovation Foundation (2019-CXB-4, 2021-CXB001), Outstanding Youth Project of Fujian Provincial Hospital (2014YNQN31), and the Special Research Foundation of Fujian Provincial Department of Finance (2020-500#), P.R. China.

REFERENCES

1. Valitova JN, Sulkarnayeva AG, Minibayeva FV. Plant sterols: diversity, biosynthesis, and physiological functions. *Biochemistry (Mosc).* (2016) 81:819–34. doi: 10.1134/S0006297916080046
2. Othman RA, Myrie SB, Jones PJ. Non-cholesterol sterols and cholesterol metabolism in sitosterolemia. *Atherosclerosis.* (2013) 231:291–9. doi: 10.1016/j.atherosclerosis.2013.09.038
3. Bastida JM, Benito R, Janusz K, Díez-Campelo M, Hernández-Sánchez JM, Marcellini S, et al. Two novel variants of the Abcg5 gene cause xanthelasmas and macrothrombocytopenia: a brief review of hematologic abnormalities of sitosterolemia. *J Thromb Haemost.* (2017) 15:1859–66. doi: 10.1111/jth.13777
4. Tada H, Okada H, Nomura A, Yashiro S, Nohara A, Ishigaki Y, et al. Rare and deleterious mutations in Abcg5/Abcg8 genes contribute to mimicking and worsening of familial hypercholesterolemia phenotype. *Circ J.* (2019) 83:1917–24. doi: 10.1253/circj.CJ-19-0317
5. Bardawil T, Rebeiz A, Chaabouni M, El Halabi J, Kambris Z, Abbas O, et al. Mutations in the Abcg8 gene are associated with sitosterolaemia in the homozygous form and xanthelasmas in the heterozygous form. *Eur J Dermatol.* (2017) 27:519–23. doi: 10.1684/ejd.2017.3087
6. Lek M, Karczewski KJ, Minikel EV, Samocha KE, Banks E, Fennell T, et al. Analysis of protein-coding genetic variation in 60,706 humans. *Nature.* (2016) 536:285–91. doi: 10.1038/nature19057
7. Berge KE, Tian H, Graf GA, Yu L, Grishin NV, Schultz J, et al. Accumulation of dietary cholesterol in sitosterolemia caused by mutations in adjacent Abc transporters. *Science.* (2000) 290:1771–5. doi: 10.1126/science.290.5497.1771
8. Lee MH, Lu K, Hazard S, Yu H, Shulenin S, Hidaka H, et al. Identification of a gene, Abcg5, important in the regulation of dietary cholesterol absorption. *Nat Genet.* (2001) 27:79–83. doi: 10.1038/83799
9. Patel SB, Salen G, Hidaka H, Kwiterovich PO, Stalenhoef AF, Miettinen TA, et al. Mapping a gene involved in regulating dietary cholesterol absorption. The sitosterolemia locus is found at chromosome 2p21. *J Clin Invest.* (1998) 102:1041–4. doi: 10.1172/jci3963
10. Yu L, Li-Hawkins J, Hammer RE, Berge KE, Horton JD, Cohen JC, et al. Overexpression of Abcg5 and Abcg8 promotes biliary cholesterol secretion and reduces fractional absorption of dietary cholesterol. *J Clin Invest.* (2002) 110:671–80. doi: 10.1172/JCI16001
11. Yu L, Hammer RE, Li-Hawkins J, Von Bergmann K, Lutjohann D, Cohen JC, et al. Disruption of Abcg5 and Abcg8 in mice reveals their crucial role in biliary cholesterol secretion. *Proc Natl Acad Sci USA.* (2002) 99:16237–42. doi: 10.1073/pnas.252582399
12. Cao LJ, Yu ZJ, Jiang M, Bai X, Su J, Dai L, et al. [Clinical features of 20 patients with phytosterolemia causing hematologic abnormalities]. *Zhonghua Yi Xue Za Zhi.* (2019) 99:1226–31. doi: 10.3760/cma.j.issn.0376-2491.2019.16.007
13. Kidambi S, Patel SB. Sitosterolaemia: pathophysiology, clinical presentation and laboratory diagnosis. *J Clin Pathol.* (2008) 61:588–94. doi: 10.1136/jcp.2007.049775
14. Yoo EG. Sitosterolemia: a review and update of pathophysiology, clinical spectrum, diagnosis, and management. *Ann Pediatr Endocrinol Metab.* (2016) 21:7–14. doi: 10.6065/apem.2016.21.1.7
15. Ono S, Matsuda J, Saito A, Yamamoto T, Fujimoto W, Shimizu H, et al. A case of sitosterolemia due to compound heterozygous mutations in Abcg5: clinical features and treatment outcomes obtained with colestimide and ezetimibe. *Clin Pediatr Endocrinol.* (2017) 26:17–23. doi: 10.1297/cpe.26.17
16. Hazard SE, Patel SB. Sterolins Abcg5 and Abcg8: regulators of whole body dietary sterols. *Pflugers Arch.* (2007) 453:745–52. doi: 10.1007/s00424-005-0040-7
17. Ali S, Ghosh K, Daly ME, Hampshire DJ, Makris M, Ghosh M, et al. Congenital macrothrombocytopenia is a heterogeneous disorder in India. *Haemophilia.* (2016) 22:570–82. doi: 10.1111/hae.12917
18. Salen G, Shefer S, Nguyen L, Ness GC, Tint GS, Shore V. Sitosterolemia. *J Lipid Res.* (1992) 33:945–55.
19. Park JH, Chung IH, Kim DH, Choi MH, Garg A, Yoo EG. Sitosterolemia presenting with severe hypercholesterolemia and intertriginous xanthomas in a breastfed infant: case report and brief review. *J Clin Endocrinol Metab.* (2014) 99:1512–8. doi: 10.1210/jc.2013-3274
20. Zak A, Zeman M, Slaby A, Vecka M. Xanthomas: clinical and pathophysiological relations. *Biomed Pap Med Fac Univ Palacky Olomouc Czech Repub.* (2014) 158:181–8. doi: 10.5507/bp.2014.016
21. Oosterveer DM, Versmissen J, Yazdanpanah M, Hamza TH, Sijbrands EJ. Differences in characteristics and risk of cardiovascular disease in familial hypercholesterolemia patients with and without tendon xanthomas: a systematic review and meta-analysis. *Atherosclerosis.* (2009) 207:311–7. doi: 10.1016/j.atherosclerosis.2009.04.009
22. Salen G, Horak I, Rothkopf M, Cohen JL, Speck J, Tint GS, et al. Lethal atherosclerosis associated with abnormal plasma and tissue sterol composition in sitosterolemia with xanthomatosis. *J Lipid Res.* (1985) 26:1126–33. doi: 10.1016/s0022-2275(20)34286-3
23. Suda T, Akamatsu A, Nakaya Y, Masuda Y, Desaki J. Alterations in erythrocyte membrane lipid and its fragility in a patient with familial lecithin: cholesterol acyltrasferase (Lcat) deficiency. *J Med Invest.* (2002) 49:147–55.
24. Kanaji T, Kanaji S, Montgomery RR, Patel SB, Newman PJ. Platelet hyperreactivity explains the bleeding abnormality and macrothrombocytopenia in a murine model of sitosterolemia. *Blood.* (2013) 122:2732–42. doi: 10.1182/blood-2013-06-510461
25. Tada H, Nomura A, Ogura M, Ikewaki K, Ishigaki Y, Inagaki K, et al. Diagnosis and management of sitosterolemia 2021. *J Atheroscler Thromb.* (2021) 28:791–801. doi: 10.5551/jat.RV17052
26. Williams K, Segard A, Graf GA. Sitosterolemia: twenty years of discovery of the function of Abcg5abcg8. *Int J Mol Sci.* (2021) 22:2641. doi: 10.3390/ijms22052641
27. Sun W, Zhang T, Zhang X, Wang J, Chen Y, Long Y, et al. Compound heterozygous mutations in Abcg5 or Abcg8 causing Chinese familial sitosterolemia. *J Gene Med.* (2020) 22:e3185. doi: 10.1002/jgm.3185
28. Othman RA, Myrie SB, Mymin D, Merkens LS, Roullet JB, Steiner RD, et al. Ezetimibe reduces plant sterol accumulation and favorably increases platelet count in sitosterolemia. *J Pediatr.* (2015) 166:125–31. doi: 10.1016/j.jpeds.2014.08.069
29. Salen G, von Bergmann K, Lutjohann D, Kwiterovich P, Kane J, Patel SB, et al. Ezetimibe effectively reduces plasma plant sterols in patients with sitosterolemia. *Circulation.* (2004) 109:966–71. doi: 10.1161/01.CIR.0000116766.31036.03
30. Yu L. The structure and function of niemann-pick C1-like 1 protein. *Curr Opin Lipidol.* (2008) 19:263–9. doi: 10.1097/MOL.0b013e3282f9b563

Conflict of Interest: The authors declare that the research was conducted in the absence of any commercial or financial relationships that could be construed as a potential conflict of interest.

Publisher's Note: All claims expressed in this article are solely those of the authors and do not necessarily represent those of their affiliated organizations, or those of the publisher, the editors and the reviewers. Any product that may be evaluated in this article, or claim that may be made by its manufacturer, is not guaranteed or endorsed by the publisher.

frontiers | Frontiers in Cardiovascular Medicine

CASE REPORT
published: 06 July 2022
doi: 10.3389/fcvm.2022.939551

A Phenotype and Genotype Case Report of a Neonate With Congenital Bilateral Coronary Artery Fistulas and Multiple Collateral Arteries

Shixin Su[1,2†], *Shuliang Xia*[2,3†], *Ye He*[2,4], *Jianbin Li*[2,5], *Li Ma*[2,3], *Xinxin Chen*[2,3*†] *and Jia Li*[1,2*†]

[1] *Clinical Physiology Laboratory, Institute of Pediatrics, Guangzhou Women and Children's Medical Center, Guangzhou Medical University, Guangdong, China,* [2] *Guangdong Provincial Key Laboratory of Research in Structural Birth Defect Disease, Guangzhou Women and Children's Medical Center, Guangzhou Medical University, Guangdong, China,* [3] *Cardiovascular Surgery, Heart Center, Guangzhou Women and Children's Medical Center, Guangzhou Medical University, Guangdong, China,* [4] *Department of Pediatric Surgery, Institute of Pediatrics, Guangzhou Women and Children's Medical Center, Guangzhou Medical University, Guangdong, China,* [5] *Cardiac Intensive Care Unit, Heart Center, Guangzhou Women and Children's Medical Center, Guangzhou Medical University, Guangdong, China*

We report a unique case of an 18-day-old girl with three coronary artery fistulas to the right atrium and right ventricle, respectively: three collateral arteries arising from the descending aorta and one from the right subclavian artery draining through a sac to the top of the right atrium, patent ductus arteriosus, and atrial septal defect. She presented symptoms of acute congestive heart failure. Cardiac catheterization and surgical interventions were performed to repair the defects. The patient recovered uneventfully and grew up well at 3 years of follow-up. Whole-genome sequencing (WES) in the patient, compared to her parents, showed 17 variants within 11 genes. Among these, only compound heterozygous mutation, c.T470G (p.L157R) and c.A1622G (p.D541G), in the *DRC1* gene have been reportedly related to congenital heart disease and are the most likely causative in our patient.

Keywords: congenital heart defect, coronary artery fistula, multiple collateral arteries, *DRC1*, whole-exome sequencing

OPEN ACCESS

Edited by:
Neil Morgan,
University of Birmingham,
United Kingdom

Reviewed by:
Gaser Abdelmohsen,
Cairo University, Egypt
Yashwant Agrawal,
Banner Desert Medical Center,
United States

***Correspondence:**
Xinxin Chen
zingerchen@163.com
Jia Li
jiali_beijing@126.com

[†] These authors have contributed equally to this work

Specialty section:
This article was submitted to Cardiovascular Genetics and Systems Medicine, a section of the journal Frontiers in Cardiovascular Medicine

Received: *09 May 2022*
Accepted: *13 June 2022*
Published: *06 July 2022*

Citation:
Su S, Xia S, He Y, Li J, Ma L, Chen X and Li J (2022) A Phenotype and Genotype Case Report of a Neonate With Congenital Bilateral Coronary Artery Fistulas and Multiple Collateral Arteries. Front. Cardiovasc. Med. 9:939551. doi: 10.3389/fcvm.2022.939551

INTRODUCTION

Congenital coronary artery fistulas account for 0.4% of congenital heart defects (CHD) (1). Coronary artery fistulas arising from the right coronary artery are present in 50–60% of cases, from the left anterior descending coronary artery in 25–40%, and both coronary arteries in 5% (2–4). Coronary artery fistulas terminate most frequently in the right ventricle, followed by the right atrium, coronary sinus, and pulmonary arterial trunk (2, 5, 6). Children with such a defect are generally asymptomatic, but congestive heart failure may happen in those with a substantial left to right shunt (7). About 55–80% of coronary arterial fistulas are isolated and 20–45% are associated with other CHD, such as patent ductus arteriosus, atrial, and ventricular septal defects (3).

Major collateral arteries are usually a component of cyanotic congenital heart defects that are embryologically linked with pulmonary valve atresia or near atresia (8, 9), clinically called MAPCAs, i.e., major aortopulmonary collateral arteries. These collateral arteries regress normally with the formation and development of pulmonary arteries but may persist in pulmonary atresia or hypoplasia (10). Congenital collateral arteries are rare. To our knowledge, there has been only one report of an association of coronary arterial fistula with an arteriovenous collateral artery to the superior vena cava (11).

The etiology of CHD remains largely unknown, likely involving genetics, epigenetics, and environmental etiologies (12). The identification of gene mutation underlying CHD may improve our understanding of cardiovascular development. With WES, the list of known CHD genes is rapidly expanding. For example, Zaidi et al. (13) analyzed the 362 parent-offspring trios with the patient affected by CHD and found that *de novo* mutations in ∼400 genes could account for about 10% of the CHD cases.

In this report, we described a unique phenotype and genotype case of congenital bilateral coronary artery fistulas with multiple collateral arteries from the aorta to the right atrium, patent ductus arteriosus, and atrial septal defect with genetic findings from the child and her parents.

CASE REPORT

The report was approved by the institutional Research Ethics Board at the Guangzhou Women and Children's Medical Center (No. 24801) and written informed consent was obtained.

Clinical Details

An 18-day-old girl who presented with tachypnea, tachycardia, and poor feeding was admitted to the Cardiac Intensive Care Unit. She was delivered by caesarian section at 39-week gestation with a birth weight of 2.9 kg. She was the only child in the family. Her parents, as well as family and relatives, have been unaffected by CHD or other congenital abnormalities (**Supplementary Table S1**). At a physical examination, she had a heart rate of 145 beats /min, respiratory rate of 45 times /min, and blood pressure of 74/40 mmHg. An electrocardiograph showed sinus tachycardia and right ventricular hypertrophy. Using transthoracic echocardiography, she was diagnosed with bilateral coronary artery fistulas, multiple collateral arteries from the descending aorta, patent ductus arteriosus, atrial septal defect, and moderate mitral regurgitation and mild-moderate tricuspid regurgitation.

At the age of 5 weeks old, cardiac catheterization was performed for hemodynamic assessment and interventions. The pulmonary to systemic blood flow ratio was 4.29 with pulmonary vascular resistance 1.7 Wood unit $*m^2$. A selective angiography revealed four collateral arteries draining into the right atrium. No. 1 (4.3 mm in diameter) of the collateral arteries was originating from the right subclavian artery (**Figures 1A,C**). No. 2 was seen at the level of the 6th thoracic vertebra and twisted to the right atrium (**Figures 1B,D**). No. 3 was a tortuous collateral artery (2.7 mm at the proximal and 1.7 mm at the minimal), located between the 6th and the 7th thoracic vertebra (**Figures 1B,E**). No. 4 was a very tortuous collateral artery between the descending aorta and the right atrium (**Figures 1B,F**). No. 1 and No. 3 collaterals were occluded with coils. Coronary arterial angiography also revealed a right coronary arterial fistula to the right ventricle and another to the right atrium (**Figures 1A**, **2A**), and a fistula branching from the left anterior descending coronary artery to the right atrium (**Figures 1A**, **2B**). Pulmonary arterial pressure was 43/22 mmHg.

More details were found at cardiac surgery at the age of 6 weeks old. A 15-mm sac was found an opening to the top of the right atrium (**Figures 1A,G**). Three collateral arteries originated from the anterior and posterior walls of the descending aorta and another from the right subclavian artery coursed into the sac and then the right atrium. The patent ductus arteriosus (4 mm) was ligated and cut down. Subsequently, a cardiopulmonary bypass was performed to suture the openings of the sac and the coronary arterial fistulas. The remaining two collateral arteries were clipped.

She had a smooth postoperative recovery and was discharged from the hospital on the 22nd postoperative day. At the 3rd year follow-up, the girl did not have any symptoms of congestive failure and grew up well.

Genetic Analysis

Whole-exome sequencing (WES) was performed on the patient and her parents to screen for potentially causative mutations. Genomic DNA (gDNA) was extracted from peripheral blood samples. Exons were captured by the Agilent SureSelect Human All Exon V6 kit (Agilent, Santa Clara, CA), followed by high-throughput sequencing on the Illumina Hiseq 2500 platform to generate 150-bp paired-end reads. The average sequencing depth for the targeted region achieved 121x, and ∼98% of targeted regions were covered at >20x. The sequencing of raw data was analyzed with Genome Analysis Toolkit (GATK) for removing low-quality, including adapter contaminated reads, N-contaminated reads with more than 10% bases, and reads with more than 55% low-quality bases (<5), and then, were aligned to the reference human genome (GRCh37/hg19) with Burrows-Wheeler Aligner (BWA). Sambamba was used to mark and remove duplicate reads. Single nucleotide variants (SNVs) and deletion/ insertions (indels) were called with SAMtools. The raw calls of SNVs and indels were filtered further with the following inclusion thresholds: (1) read depth > 5; (2) Root-Mean-Square mapping quality of covering reads > 30; and (3) the variant quality score of > 20. Finally, the variants were annotated with ANNOVAR. Annotations included minor allele frequencies (MAF ≤ 1%) from public control data sets, as well as deleteriousness and conservation scores, enabling further filtering and assessment of the likely pathogenicity of variants.

A total of 175,380 variants, including 155,400 SNVs and 19,970 indels, were detected and analyzed by several filtering methods (**Figure 3A**). Firstly, we filtered for rare variants by excluding variants with minor allele frequencies of >1% in all the three databases, including 1,000 genomic data, ESP5600, and gnomAD data (gnomAD_ALL and gnomAD_EAS), and 5,728 variants remained. A total of 891 variants were found

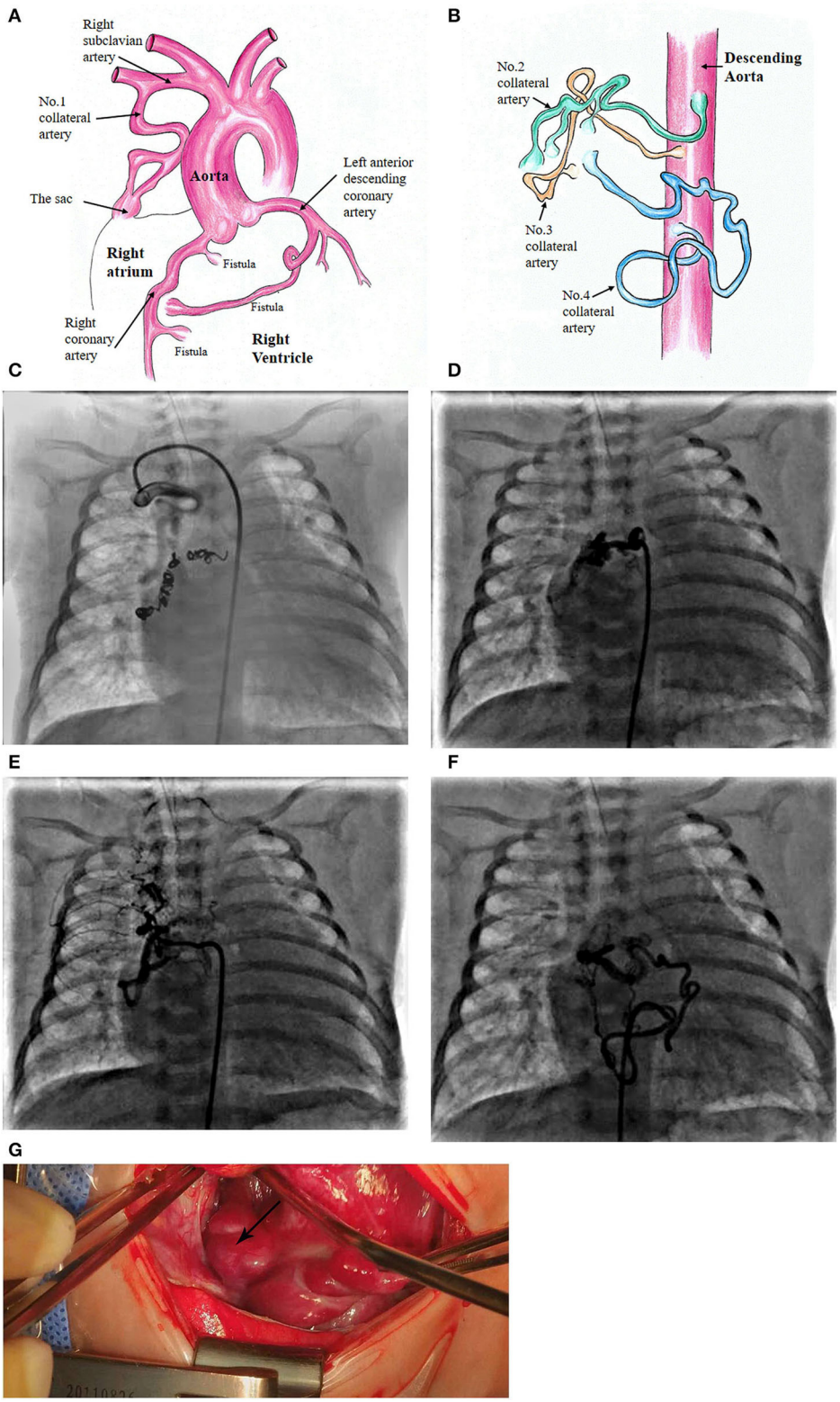

FIGURE 1 | Schematic diagram of the patient's diagnosis of 3 coronary artery fistulas to the right atrium and right ventricle, respectively **(A)**. Four collateral arteries draining through a sac to the top of the right atrium **(A,B)**. Super-selective angiogram shows the following collaterals terminating to the sac and then to the right atrium. No. 1 collateral artery originating from the right subclavian artery **(C)**. No. 2 at the level of the 6th thoracic vertebra **(D)**. No. 3 originating from the descending aorta **(E)**. No. 4 located at the lower edge of the 9th thoracic vertebra **(F)**. Surgical image of the sac at the top of the right atrium **(G)**.

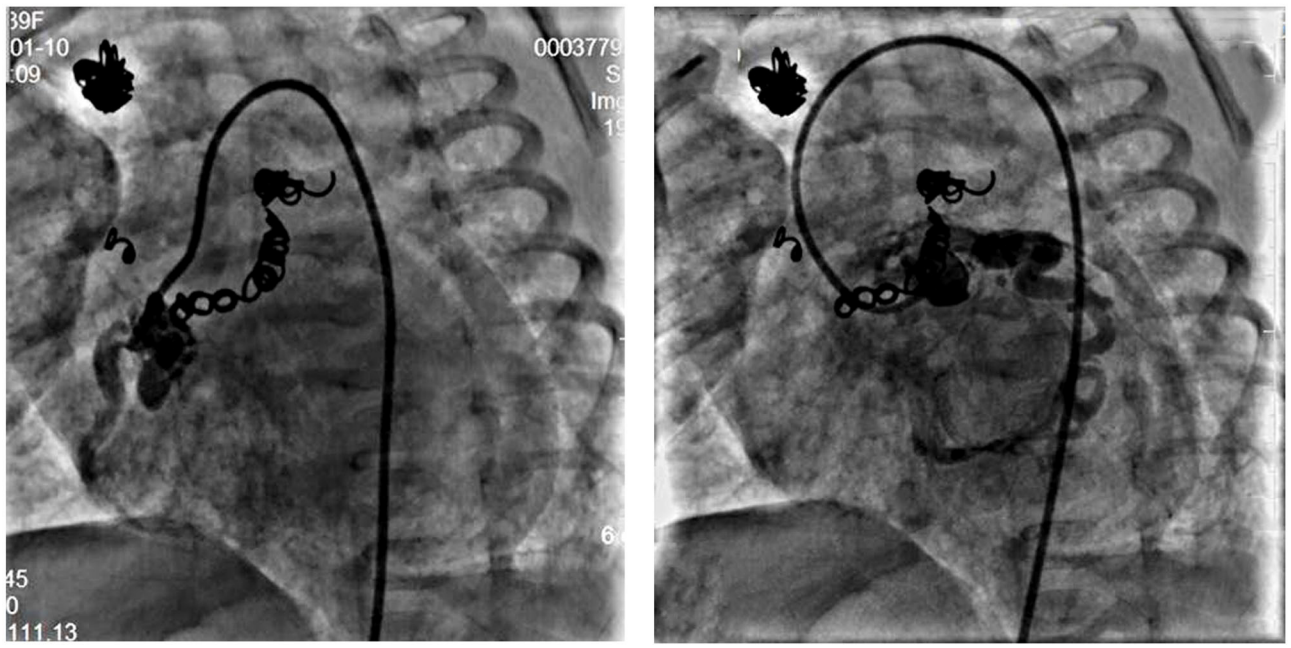

FIGURE 2 | Right coronary angiogram from left anterior oblique 45° view shows the dilated right coronary artery fistula with a proximal fistula to the right atrium and a distal fistula into the right ventricle **(A)**. Left coronary angiogram shows a fistula from the left anterior descending coronary artery to the right atrium **(B)**.

in the exon or splice site, of which 594 were non-synonymous variations leading to amino acid alternation. Then, we applied four prediction algorithms (SIFT, Poly-Phen-2, Mutation Taster, CADD) to identify candidate deleterious variants. A total of 402 variants, predicted to be damaging by at least two algorithms, were included for further downstream analysis. Given the characteristics of the pedigree, homozygous, compound heterozygous, and *de novo* variants were considered to be a candidate for causal variations. As a next step, we prioritized candidate genes among these variants. Eleven candidate genes were determined in our patient, of which three belonged to recessive mutation, 5 compound heterozygous mutations, and 3 *de novo* mutations (**Supplementary Table S2**). Among the candidate genes, *DRC1* was reportedly associated with CHD (14). In our patient, the compound heterozygous variations, c.T470G (p.L157R) adopted from her father and c.A1622G (p.D541G) adopted from her mother, in the *DRC1* gene were considered as diseased causal mutations (**Figure 3B**).

The paternally inherited c.T470G variant, located within the exon 4 of the DRC1 gene, was found to result in substituting leucine for arginine at position 157 of the encoded protein, while the maternally inherited c.A1622G variant within the exon 13 result in substituting aspartic for glycine at position 541 of the encoded protein. The pathogenicity effect of these mutations was confirmed by prediction tools (Mutation taster, SIFT, PolyPhen-2, CADD) and both the variants were predicted to be deleterious (**Table 1**). Furthermore, homology analysis indicated that leucine at position 157 and aspartic at position 41 are highly conserved among various species (**Figure 3C**).

DISCUSSION

A hemodynamic shunt always occurs in the presence of coronary artery fistula/fistulas, whereby the blood flows from the high-pressure fistula into the low-pressure chamber. Most patients with one coronary artery fistula are asymptomatic early in life because of the small fistula with the insignificant shunt (15, 16). However, some patients who presented with large fistula/fistulas and substantial left to right shunt may have symptoms of congestive heart failure with a cardiac enlargement (7, 17–20). The latter was the case in our patient with a pulmonary to systemic blood flow ratio of 4.29, which was uniquely compounded with 4 collateral arteries to the right atrium, patent ductus arteriosus, and atrial septal defect. Congenital collateral arteries have been rarely reported (11).

Interventional treatment, catheterizations, or/ and surgery, should be considered in the case of substantial shunt, significant aneurysmal formation, or presence of other cardiac malformations (21, 22). Cardiac catheterization was firstly performed on our patient to coil-occlude two of the collateral arteries. Considering the patient's severe condition and potential contrast media overdose, together with the indications of surgery, the catheterization was stopped. Cardiac surgery was subsequently performed to repair the remaining malformations. The patient recovered well from the interventions and grew well at 3 years of follow-up.

To explore the genetic pathogenesis, WES was performed on our patient and her parents. Eleven candidate genes, including three genes with recessive variants, five genes with compound heterozygous variants, and three genes with *de novo* variants

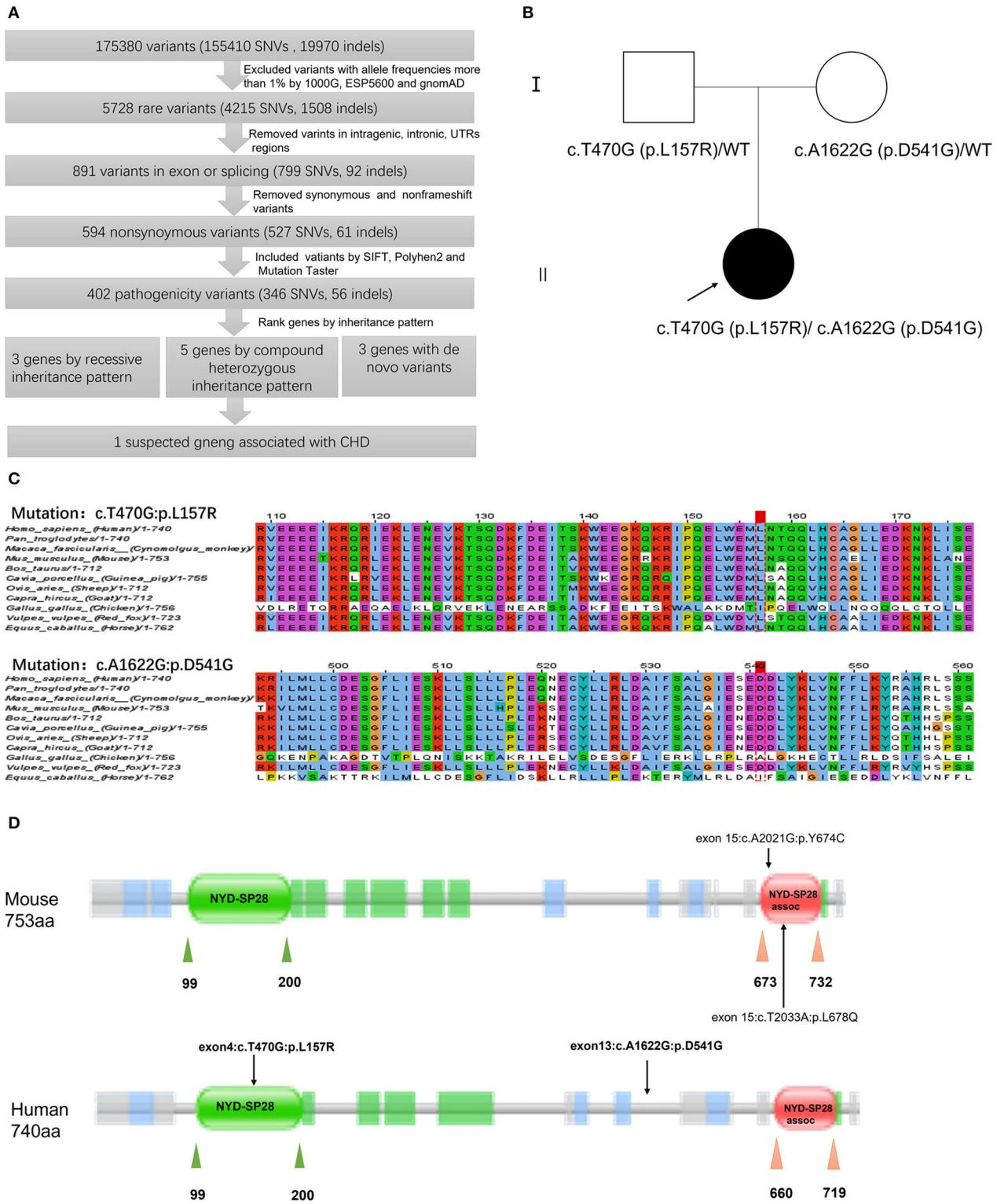

FIGURE 3 | Schematic diagram of filtering strategies in our report. Several variant filtering processes and candidate gene prioritization were applied. Only one candidate gene was associated with CHD **(A)**. Pedigrees of the patient's family. The filled and unfilled symbols represent subjects with and without CHD, respectively. Arrow indicates the proband of the family. DRC1 genotypes are shown near each symbol, WT represents wide type **(B)**. Multiple sequence alignment of the DRC1 protein sequences indicates the Leu157 residue and Asp541 residue are highly conserved among various species **(C)**. Schematic of domains within DRC1 protein. Rare variants p.L678Q and p.Y674C in DRC1 had been identified in CHD mouse by Li et al. (14), while compound heterozygous variant, c.T470G (p.L157R) and c.A1622G (p.D541G), in DRC1 was identified in our patient of which c.T470G (p.L157R) variant was lined in NYD-SP28 domain **(D)**.

TABLE 1 | Compound heterozygous mutation in DRC1 gene was predicted in our patient by whole-exome sequencing (WES).

Gene name	DRC1	
Genomic	2:26647252	2:26673482
Base change	T>G	A>G
Amino acid	L157R	D541G
ESP6500	.	.
1000G	.	.
GnomAD_ALL	0.00005779	0.00010593
GnomAD_EAS	0.00084836	0.00152243
SIFT	D	D
PolyPhen2	D	P
Mutation Taster	D	N
CADD	25.2	25.2
PhyloP	3.93	3.3471
PhastCons	1	1

SIFT: D, Deleterious; T, Tolerated.
Poly Phen2, D-Probably damaging; P, Possibly damaging; B, Benign.
Mytation Taster: A, Disease_causing_automatic; D, Disease_causing; N- Polymorphism.
CADD: CADD Phred of >15 mean indicates the mutation is predicted to be damaging.
PhyloP: (values between −14 and +6) measures both slower evolution and acceleration of evolution under neutral drift; sites predicted to be conserved are assigned positive scores, while sites predicted to be fast-evolving are assigned negative scores.
Phastcons: Phastcons is a tool to calculate conservation score and identify conserved DNA elements with a maximum score of 1 indicating a highly conserved location on the DNA.
"."Indicates the mutation cannot be predicted in the database.

were identified in our patient. To date, about 400 genes with the causative mutation have been determined in patients or mice with CHD (13, 14, 23, 24). The genetic analysis of our patient mainly concentrated on the possibility of these known genes. Among the 11 candidate genes, the *DRC1* gene with compound heterozygous variants has been associated with CHD.

The DRC1 gene is located on chromosome 2p23.3 and contains 17 exons. It encodes dynein regulatory complex protein 1 consisting of 740 amino acids. *DRC1* is a key component of the nexin-dynein regulatory complex (N-DRC) and plays an important role in ciliary movement (25). Previous studies have reported that mutations in *DRC1* largely result in primary ciliary dyskinesia (26, 27), morphological abnormalities of the sperm flagella, and male infertility (28). Notably, a study revealed the central role of cilium and cilia transduced-cell signaling in the pathogenesis of CHD by the recessive forward genetic screen in mice. *DRC1* variants have been observed in several types of CHD in mouse models. The mouse model with recessive c.A2021G (p.Y674C) variant was presented with cardiac malformation, such as dextrocardia, atrial septal defect, ventricular septal defect, and malformation of large arteries, including interrupted aortic arch and transposition of great arteries, while mouse model with recessive c.T2033A (p.L678Q) variant was also presented with dextrocardia (14). We found both variants lined in SYD-28 assoc domain through analysis of domain by Pfam with Uniprot code Q3USS3. SYD-28 assoc is the C-terminal domain of *DRC1*. Interestingly, the c.T470G (p.L157R) variant in our patient was located at the SYD-28 domain of *DRC1*, thus, may impair the function of this domain (**Figure 3D**). SYD-28 is the N-terminal domain of *DRC1*. The NYD-SP28 assoc is a short region found at the very C-terminus of family members of NYD-SP28. NYD-SP28, a human sperm tail protein, is expressed in a development-dependent manner and plays a significant role in sperm capacitation (29). Presently, reports regarding the function of NYD-SP28 remain limited. Therefore, we proposed an assumption that these two domains may be partly responsible for the influence of *DRC1* on cardiovascular development. Although another damaging variant, c.A1622G(p. D541G), was located at neither the SYD-28 domain nor the SYD-28 assoc domain, it may have contributed to the functional or structural alteration of *DRC1*.

Heterogeneity is one of the major characteristics of CHD in general. A specific gene with different variants may result in different phenotypes. For example, different variants in *NOTCH1* have been observed in several types of CHD, such as pulmonary stenosis (PS) (30), left ventricular outflow tract obstructive (31), and ventricular septal defect (32). Taken together, the compound heterozygous variants, c.T470G (p. L157R), and c.A1622G (p. D541G), in *DRC1* is the most probable cause of CHD in the patient. Our study indicates the first novel variants in *DRC1* identified in humans with CHD.

The limitations of our study should be noted. WES may miss the intronic variants that are likely to have a significant role in the pathogenesis of CHD. Sanger sequencing and the animal experiment would confirm our hypothesis that the identified genetic variants contribute to the unique CHD phenotypes in our patients.

DATA AVAILABILITY STATEMENT

The datasets for this article are not publicly available due to concerns regarding participant/patient anonymity. Requests to access the datasets should be directed to the corresponding author.

ETHICS STATEMENT

Written informed consent was obtained from the minor(s)' legal guardian/next of kin for the publication of any potentially identifiable images or data included in this article.

AUTHOR CONTRIBUTIONS

SS and SX has contributed to the conducting and reporting of the work described in the article. YH, JianL, and LM has contributed to the conducting of the work. XC has contributed to the planning and conducting of the research. JiaL has contributed to the planning, conducting, and reporting of the research. All authors contributed to the article and approved the submitted version.

SUPPLEMENTARY MATERIAL

The Supplementary Material for this article can be found online at: https://www.frontiersin.org/articles/10.3389/fcvm.2022.939551/full#supplementary-material

REFERENCES

1. Burch GH, Sahn DJ. Congenital coronary artery anomalies: the pediatric perspective. *Coron Artery Dis.* (2001) 12:605–16. doi: 10.1097/00019501-200112000-00003
2. Mangukia CV. Coronary artery fistula. *Ann Thorac Surg.* (2012) 93:2084–92. doi: 10.1016/j.athoracsur.2012.01.114
3. Dodge-Khatami A, Mavroudis C, Backer CL. Congenital heart surgery nomenclature and database project: anomalies of the coronary arteries. *Ann Thorac Surg.* (2000) 69:S270–97. doi: 10.1016/S0003-4975(99)01248-5
4. Nepal S, Annamaraju P. *Coronary Arteriovenous Fistula*. Treasure Island, FL: StatPearls (2022).
5. Challoumas D, Pericleous A, Dimitrakaki IA, Danelatos C, Dimitrakakis G. Coronary arteriovenous fistulae: a review. *Int J Angiol.* (2014) 23:1–10. doi: 10.1055/s-0033-1349162
6. Zenooz NA, Habibi R, Mammen L, Finn JP, Gilkeson RC. Coronary artery fistulas: CT findings. *Radiographics.* (2009) 29:781–9. doi: 10.1148/rg.293085120
7. Gowda RM, Vasavada BC, Khan IA. Coronary artery fistulas: clinical and therapeutic considerations. *Int J Cardiol.* (2006) 107:7–10. doi: 10.1016/j.ijcard.2005.01.067
8. Griselli M, McGuirk SP, Winlaw DS, Stumper O, de Giovanni JV, Miller P, et al. The influence of pulmonary artery morphology on the results of operations for major aortopulmonary collateral arteries and complex congenital heart defects. *J Thorac Cardiovasc Surg.* (2004) 127:251–8. doi: 10.1016/j.jtcvs.2003.08.052
9. Mainwaring RD, Punn R, Reddy VM, Hanley FL. Surgical reconstruction of pulmonary stenosis with ventricular septal defect and major aortopulmonary collaterals. *Ann Thorac Surg.* (2013) 95:1417–21. doi: 10.1016/j.athoracsur.2013.01.007
10. Boshoff D, Gewillig M. A review of the options for treatment of major aortopulmonary collateral arteries in the setting of tetralogy of Fallot with pulmonary atresia. *Cardiol Young.* (2006) 16:212–20. doi: 10.1017/S1047951106000606
11. Cayre RO, Bayol AP, Obregon R, Alday LE, A. unique aortic arterial meshwork with a major aortopulmonary collateral artery, a major arteriovenous collateral artery, and a coronary arteriovenous fistula in a young man with a bicuspid aortic valve. *Pediatr Cardiol.* (2013) 34:2017–20. doi: 10.1007/s00246-012-0567-2
12. Chung IM, Rajakumar G. Genetics of congenital heart defects: the NKX2-5 gene, a key player. *Genes*. (2016) 7:6. doi: 10.3390/genes7020006
13. Zaidi S, Choi M, Wakimoto H, Ma L, Jiang J, Overton JD, et al. *De novo* mutations in histone-modifying genes in congenital heart disease. *Nature.* (2013) 498:220–3. doi: 10.1038/nature12141
14. Li Y, Klena NT, Gabriel GC, Liu X, Kim AJ, Lemke K, et al. Global genetic analysis in mice unveils central role for cilia in congenital heart disease. *Nature.* (2015) 521:520–4. doi: 10.1038/nature14269
15. Ando G, Ascenti G, Saporito F, Trio O, Racchiusa S, Cerrito M, et al. Multislice computed tomography demonstration of a coronary-to-pulmonary artery fistula. *J Cardiovasc Med.* (2011) 12:212–4. doi: 10.2459/JCM.0b013e32833b9724
16. Liberthson RR, Sagar K, Berkoben JP, Weintraub RM, Levine FH. Congenital coronary arteriovenous fistula. Report of 13 patients, review of the literature and delineation of management. *Circulation.* (1979) 59:849–54. doi: 10.1161/01.CIR.59.5.849
17. Aggarwal V, Mulukutla V, Qureshi AM, Justino H. Congenital coronary artery fistula: presentation in the neonatal period and transcatheter closure. *Congenit Heart Dis.* (2018) 13:782–7. doi: 10.1111/chd.12653
18. Kaneko Y, Okabe H, Nagata N, Kobayashi J, Murakami A, Takamoto S. Pulmonary atresia, ventricular septal defect, and coronary-pulmonary artery fistula. *Ann Thorac Surg.* (2001) 71:355–6. doi: 10.1016/S0003-4975(00)02143-3
19. Sathanandam SK, Loomba RS, Ilbawi MN, Van Bergen AH. Coronary artery-to-pulmonary artery fistula in a case of pulmonary atresia with ventricular septal defect. *Pediatr Cardiol.* (2011) 32:1017–22. doi: 10.1007/s00246-011-0043-4
20. Okwuosa TM, Gundeck EL, Ward RP. Coronary to pulmonary artery fistula–diagnosis by transesophageal echocardiography. *Echocardiography.* (2006) 23:62–4. doi: 10.1111/j.1540-8175.2006.00116.x
21. Said SA, van der Werf T. Dutch survey of congenital coronary artery fistulas in adults. *Neth Heart J.* (2006) 14:5–13.
22. Schicchi N, Fogante M, Oliva M, Schicchi F, Giovagnoni A. Bilateral coronary-to-pulmonary artery fistulas associated with giant aneurysm in an elderly woman: case report and literature review. *Radiol Case Rep.* (2019) 14:911–6. doi: 10.1016/j.radcr.2019.04.020
23. Homsy J, Zaidi S, Shen Y, Ware JS, Samocha KE, Karczewski KJ, et al. *De novo* mutations in congenital heart disease with neurodevelopmental and other congenital anomalies. *Science.* (2015) 350:1262–6. doi: 10.1126/science.aac9396
24. Jin SC, Homsy J, Zaidi S, Lu Q, Morton S, DePalma SR, et al. Contribution of rare inherited and de novo variants in 2,871 congenital heart disease probands. *Nat Genet.* (2017) 49:1593–601. doi: 10.1038/ng.3970
25. Wirschell M, Olbrich H, Werner C, Tritschler D, Bower R, Sale WS, et al. The nexin-dynein regulatory complex subunit DRC1 is essential for motile cilia function in algae and humans. *Nat Genet.* (2013) 45:262–8. doi: 10.1038/ng.2533
26. Morimoto K, Hijikata M, Zariwala MA, Nykamp K, Inaba A, Guo TC, et al. Recurring large deletion in DRC1 (CCDC164) identified as causing primary ciliary dyskinesia in two Asian patients. *Mol Genet Genomic Med.* (2019) 7:e838. doi: 10.1002/mgg3.838
27. Lei C, Yang D, Wang R, Ding S, Wang L, Guo T, et al. DRC1 deficiency caused primary ciliary dyskinesia and MMAF in a Chinese patient. *J Hum Genet.* (2021) 67:197–201. doi: 10.1038/s10038-021-00985-z
28. Zhang J, He X, Wu H, Zhang X, Yang S, Liu C, et al. Loss of DRC1 function leads to multiple morphological abnormalities of the sperm flagella and male infertility in human and mouse. *Hum Mol Genet.* (2021) 30:1996–2011. doi: 10.1093/hmg/ddab171
29. Zheng Y, Zhang J, Wang L, Zhou Z, Xu M, Li J, et al. Cloning and characterization of a novel sperm tail protein, NYD-SP28. *Int J Mol Med.* (2006) 18:1119–25. doi: 10.3892/ijmm.18.6.1119
30. Pulignani S, Vecoli C, Borghini A, Foffa I, Ait-Ali L, Andreassi MG. Targeted next-generation sequencing in patients with non-syndromic congenital heart disease. *Pediatr Cardiol.* (2018) 39:682–9. doi: 10.1007/s00246-018-1806-y
31. Helle E, Cordova-Palomera A, Ojala T, Saha P, Potiny P, Gustafsson S, et al. Loss of function, missense, and intronic variants in NOTCH1 confer different risks for left ventricular outflow tract obstructive heart defects in two European cohorts. *Genet Epidemiol.* (2019) 43:215–26. doi: 10.1002/gepi.22176
32. Kalayinia S, Maleki M, Mahdavi M, Mahdieh N, A. novel de novo dominant mutation of NOTCH1 gene in an Iranian family with non-syndromic congenital heart disease. *J Clin Lab Anal.* (2020) 34:e23147. doi: 10.1002/jcla.23147

Conflict of Interest: The authors declare that the research was conducted in the absence of any commercial or financial relationships that could be construed as a potential conflict of interest.

frontiers | Frontiers in Cardiovascular Medicine

CASE REPORT
published: 07 July 2022
doi: 10.3389/fcvm.2022.863650

Case Report: Tetralogy of Fallot in a Chinese Family Caused by a Novel Missense Variant of *MYOM2*

Jing Wang[1†], *Chunyan Wang*[2,3†], *Haiyang Xie*[4], *Xiaoyuan Feng*[5], *Lei Wei*[4], *Binbin Wang*[2,3], *Tengyan Li*[3], *Mingan Pi*[4*] and *Li Gong*[4*]

[1] *Department of Medical Genetics and Developmental Biology, School of Basic Medical Sciences, Capital Medical University, Beijing, China,* [2] *Graduate School of Peking Union Medical College and Chinese Academy of Medical Sciences, Beijing, China,* [3] *Center for Genetics, National Research Institute for Family Planning, Beijing, China,* [4] *Department of Cardiothoracic Surgery, Wuhan Children's Hospital (Wuhan Maternal and Child Healthcare Hospital), Tongji Medical College, Huazhong University of Science and Technology, Wuhan, China,* [5] *Department of Echocardiography, Wuhan Children's Hospital (Wuhan Maternal and Child Healthcare Hospital), Tongji Medical College, Huazhong University of Science and Technology, Wuhan, China*

OPEN ACCESS

Edited by:
Neil Morgan, University of Birmingham, United Kingdom

Reviewed by:
Hannah Titheradge, Birmingham Women's and Children's Hospital, United Kingdom
Laura Southgate, St George's University of London, United Kingdom

***Correspondence:**
Li Gong
1043324064@qq.com
Mingan Pi
pimingan@163.com

[†] *These authors have contributed equally to this work*

Specialty section:
This article was submitted to Cardiovascular Genetics and Systems Medicine, a section of the journal Frontiers in Cardiovascular Medicine

Received: *27 January 2022*
Accepted: *31 May 2022*
Published: *07 July 2022*

Citation:
Wang J, Wang C, Xie H, Feng X, Wei L, Wang B, Li T, Pi M and Gong L (2022) Case Report: Tetralogy of Fallot in a Chinese Family Caused by a Novel Missense Variant of MYOM2. Front. Cardiovasc. Med. 9:863650. doi: 10.3389/fcvm.2022.863650

Background: Rare genetic variants have been identified to be important contributors to the risk of Tetralogy of Fallot (TOF), the most common cyanotic congenital heart disease (CHD). But relatively limited familial studies with small numbers of TOF cases have been reported to date. In this study, we aimed to identify novel pathogenic genes and variants that caused TOF in a Chinese family using whole exome sequencing (WES).

Methods: A Chinese family whose twins were affected by TOF were recruited for this study. A WES was performed for the affected twins, their healthy brother, and parents to identify the potential pathogenic mutated gene(s). Heterozygous variants carried by the twins, but not the unaffected brother, were retained. Public databases were used to assess the frequencies of the selected variants, and online prediction tools were accessed to predict the influences of these variants on protein function. The final candidate variant was further confirmed by Sanger sequencing in other members of the family.

Results: After several filtering processes, a heterozygous missense variant in the *MYOM2* gene (NM_003970.4:c.3097C>T:p.R1033C) was identified and confirmed by Sanger sequencing in the affected twins and their unaffected father, suggesting an inheritance pattern with incomplete penetrance. The variant was found to be extremely rare in the public databases. Furthermore, the mutated site was highly conserved among mammals, and as shown using multiple online prediction tools, this variant was predicted to be a detrimental variant.

Conclusion: We assessed a family with TOF caused by a rare heterozygous missense variant of *MYOM2*. Our findings not only further confirm the significant role of genetics in the incidence of TOF but also expand the spectrum of the gene variants that lead to TOF.

Keywords: Tetralogy of Fallot, whole exome sequencing, heterozygous variant, *MYOM2*, incomplete penetrance

INTRODUCTION

Congenital heart diseases (CHDs) are the most common birth defects affecting approximately 1% of live births each year (1). Previous studies have shown that CHDs involve a variety of cardiac malformations including patent ductus arteriosus (PDA) and Tetralogy of Fallot (TOF) (2). The TOF, as a malformation of the cardiac outflow tract, comprises four major cardiac defects that occur together: ventricular septal defect, right ventricular hypertrophy, pulmonary stenosis, and aortic override (3). The incidence of TOF is about 0.04% worldwide (4). Researchers have suggested that the etiology of approximately 80% of patients with non-syndromic TOF is unexplained.

In recent years, increasing evidence indicates that TOF has high genetic heterogeneity and various genes involved in heart development may be responsible for the phenotype of the disease (5–7). Several previous studies have identified rare potential pathogenic variants of new candidate genes in patients with TOF using whole exome sequencing (WES) such as notch receptor 1 (*NOTCH1*) (7), GATA-binding protein 4 (*GATA4*) (8), NK2 homeobox 5 (*NKX2.5*) (9), Jagged 1 (*JAG1*) (10), forkhead box C2 (*FOXC2*) (11), T-box 5 (*TBX5*) (12), T-box 1 (*TBX1*) (13), and Fms-related tyrosine kinase 4 (*FLT4*) (7). These findings provide insights into the complex genetic variants responsible for TOF; however, the specific etiology of most TOF cases remains unknown. Therefore, further studies on the genetic etiology of TOF were needed to better understand its pathogenesis. In addition, most studies focused on sporadic cases of TOF, and reports on families with TOF patients were relatively limited (14–19).

In this study, we performed a WES analysis on a Chinese family with two TOF affected children to identify novel genetic causes of TOF. Through focused analysis of shared, likely deleterious variants, we found a heterozygous missense variant of Myomesin2 (*MYOM2*) (NM_003970.4:c.3097C>T:p.R1033C) in the affected twins. Two previous reports have described rare *MYOM2* variants in patients with TOF (20, 21). This study independently validates *MYOM2* variants in the Chinese population and provides further evidence of the importance of this gene in the incidence of TOF.

MATERIALS AND METHODS

Subjects

A Chinese family with two affected fraternal twins was recruited from the Wuhan Children's Hospital. All family members were clinically evaluated by reviewing patient history, performing physical examinations, and consulting medical records. The parents and elder brother were healthy. The affected twins and their unaffected parents and elder brother were enrolled in the study. The probands of this family were the 9-month-old twins (II-2 and II-3). They were hospitalized due to hypoxia after birth and diagnosed with TOF using a Philips Epiq5 ultrasonic diagnostic instrument (S8-3 probe, frequency 3.0–8.0 MHz) according to American Society of Echocardiography criteria. The father took an echocardiogram as well. Peripheral blood samples were collected from the patients and their family members. This study was approved by the Ethics Committee of Wuhan Children's Hospital, and informed consent was obtained from the parents of this family.

Whole Exome Sequencing

Genomic DNA was extracted from the peripheral blood of the family members using a QIAamp DNA Blood Mini Kit (Qiagen, GER) according to the manufacturer's instructions. The quality of the DNA samples was then measured by NanoDrop2000 (Thermo Scientific, United States).

Exome sequencing was performed on the five members of this family. In brief, the subjects' exomes were captured using an Agilent SureSelect Human All Exon V6 Enrichment kit (Agilent, Santa Clara, CA, United States) and then sequenced on a NovaSeq platform (Illumina, San Diego, CA, United States) according to the manufacturer's guides, generating 150-bp paired-end reads. All reads were mapped to the NCBI human reference genome (hg19) using Burrows-Wheeler Alignment version 0.7.9a (http://bio-bwa.sourceforge.net). Single nucleotide variants (SNVs) and indels were detected using Genome Analysis Toolkit version 3.5 (https://gatk.broadinstitute.org/hc/en-us) and annotated using ANNOVAR (https://annovar.openbioinformatics.org/en/latest/user-guide/download/) based on splice site, intronic, exonic, 5' UTR, 3' UTR, intergenic, upstream, or downstream locations. For prioritization, missense, non–sense, frameshift, non-frameshift, or splicing site variants with a minimum allele frequency (MAF) of more than 0.1% in the East Asians and the total population in the gnomAD (https://gnomad.broadinstitute.org) database were removed.

In silico Analysis

The pathogenicity of the variants was predicted using online software programs: Sorting Intolerant From Tolerant (SIFT; http://sift-dna.org), PolyPhen-2 (http://genetics.bwh.harvard.edu/pph2/), and MutationTaster (http://www.mutationtaster.org). The missense variants predicted to be deleterious by at least two of the above tools were selected for future confirmation and analyses. *In silico* prediction studies were then carried out for the selected variant using other different online available tools to further illustrate the effect on the protein function. We also used CLC Sequence Viewer 8 software to analyze the conservation of the mutated site in various species.

Sanger Sequencing Validation

A suspected disease-causing variant of the *MYOM2* gene, c.3097C > T, was validated in the affected twins by standard Sanger sequencing. Primer5 software was used to design the polymerase chain reaction (PCR) primers specific to the regions of the variants in *MYOM2*. The primer sequences are shown in

TABLE 1 | *MOYM2*-specific primers used for Sanger sequencing.

ID	Sequence	Length (bp)
MYOM2- F	CTGTTGCTAATCCGAGTG	1,095
MYOM2- R	GATGGGATCTCCTTATGTT	

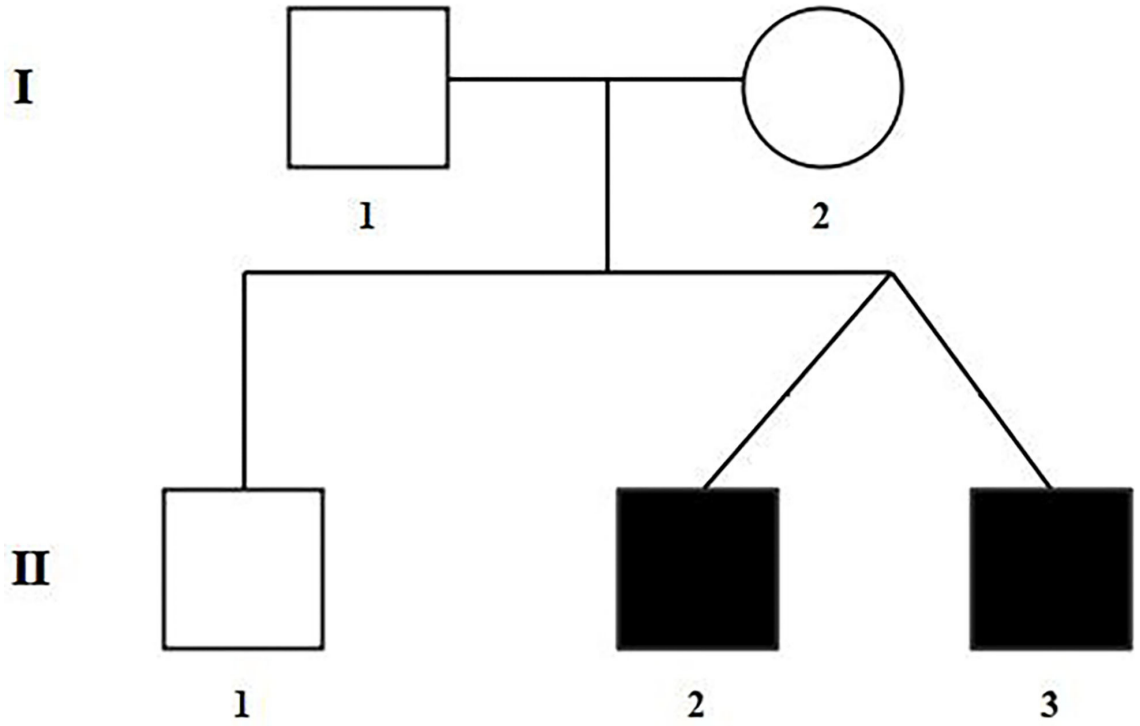

FIGURE 1 | Pedigree of the family with TOF. The filled black symbols represent the affected members.

Table 1. The healthy parents and the elder brother were then sequenced for the segregation analysis of the variant.

Protein Modeling

The amino acid sequence of human *MYOM2* was obtained from the NCBI (NP_003961.3). The wild-type and variant structures of the *MYOM2* were built using the SWISS-MODEL. PyMOL software was used to represent structural figures.

RESULTS

Clinical Descriptions

The selected Chinese family included healthy non-consanguineous parents (I-1and I-2), a healthy elder brother (II-1), and two affected male twins (II-2 and II-3) (**Figure 1**). The probands (II-2 and II-3) were diagnosed by echocardiography at 9 months and 6 days old as having TOF. No other developmental abnormalities were found during a series of examinations, including a physical examination. They had smooth breathing, no obvious cyanosis of the face and lips, and were not in any distress. As shown on the ultrasonogram for the affected elder twin (**Figure 2A**), the position of the heart, aortic ventricular connections, and aorta were normal. The aortic arch had three branches with normal initial position and arrangement. The aortic wall was smooth, the lumen was unobstructed, and the inner diameter was about 15.6 mm. However, the outflow tract of the right ventricle was narrow and about 4.0 mm wide. And interruptions occurred in interventricular septa, a few left-to-right shunt signals were detected in the lower atrial septum and a small amount of regurgitation was detected on the tricuspid valve. For his twin brother as shown on the ultrasonogram (**Figure 2B**), the position of the heart, aortic ventricular connections, and aorta were normal, and the valve morphology, structure, and opening and closing were normal. However, interruptions occurred in interventricular septa. The pulmonary artery was stenosed and the outflow tract of the right ventricle was narrow and about 4.8 mm wide. There was a localized convex posterior to the upper part of the pulmonary artery. Based on these results, the twins were diagnosed with TOF. In addition, the echo results of the father illustrated that the shape, structure, wall thickness, and function of the heart were all normal (**Supplemental Figure 1**). Furthermore, none of the other family members exhibited TOF.

Exome Sequencing and Co-Segregation Analysis

The raw data of each subject was about 12G. The mean depth of the target region was 100X and the mean coverage of the target region was 99.8%. Following rigorous filtering for rare, predicted pathogenic variants shared in the twins, and the sequencing data from the elder brother (II:1) which was used to exclude any variants that were present in the unaffected brother, we found that the affected twins did not share any homozygous or compound heterozygous mutations of previously reported genes, as well as biallelic variants of novel genes. In addition, they also did not share any de novo variants. We subsequently screened

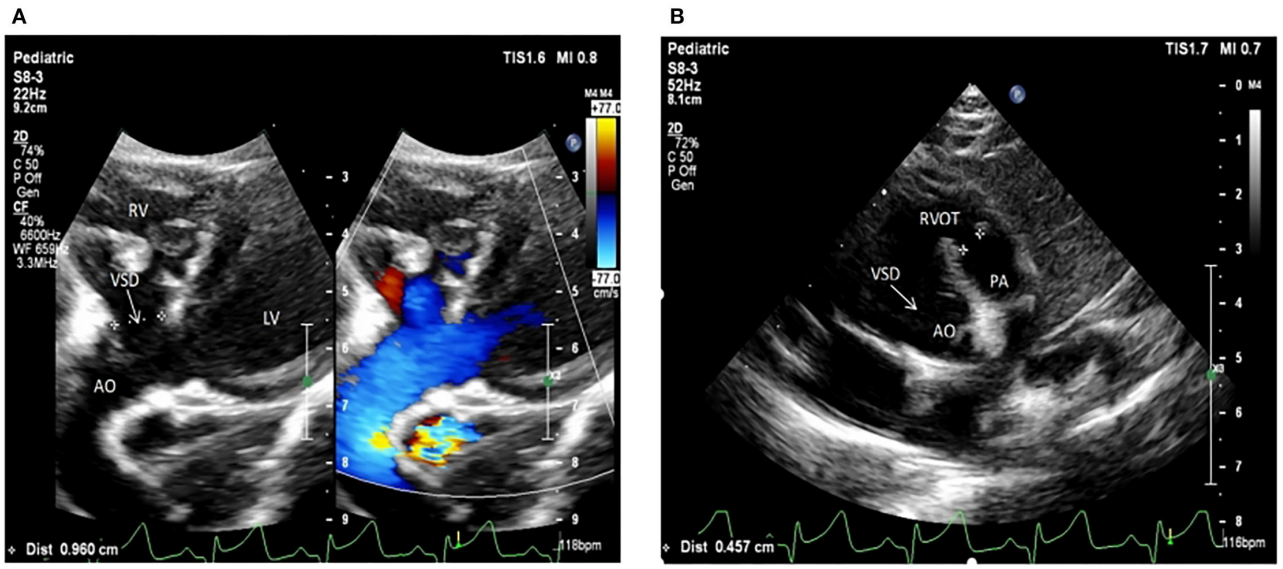

FIGURE 2 | Echocardiogram images from patients II:2 and II:3 showing the apex of the heart. **(A)** The ultrasonogram for the elder twin (II:2). **(B)** The ultrasonogram for the younger twin (II:3). LV, left ventricle; RV, right ventricle; Ao, aorta; RVOT, right ventricular out ow tract; PA, pulmonary artery.

48 heterozygous, likely deleterious variants that were shared in the twins, including 15 variants inherited from the father and 33 variants inherited from the mother (see **Supplemental Table 1**). By examining the literature for known associations related to heart diseases, for example, whether the gene variants have been reported in patients with congenital heart diseases, whether mutant mice showed abnormal cardiac development, or whether they were involved in biological processes associated with cardiac development, we finally identified a heterozygous missense variant in exon 25 of *MYOM2* gene, c.3097C>T (p.R1033C) as a possible genetic cause of TOF. The Sanger sequencing confirmed that this variant was present in the affected twins. The healthy father had a heterozygous status of this variant, however, the unaffected mother and brother did not carry this variant (**Figure 3A**).

In silico Analysis of the *MOYM2* Missense Variant

The minor allele frequency of the observed variant was assessed in East Asian and global populations using the GnomAD database and ChinaMap database (http://www.mbiobank.com/) which included deep whole genome sequencing data from 10,588 Chinese participants (22). The variant is extremely rare in both the East Asian and global populations (0.00016 and 0.000024, respectively). Furthermore, it is absent in the ChinaMap database. The missense variant of *MYOM2* was predicted to be highly damaging to the function of the *MYOM2* protein using multiple online prediction tools including SIFT, PolyPhen2, PROVEAN, MutationTaster, and CADD (**Table 2**). The variant site is near the Ig-like domain (**Figure 3B**). In addition, the alignment of *MYOM2* amino acid sequences in different species showed high conservation of arginine at position 1033 (**Figure 3C**). These results suggest that this variant is highly pathogenic, and we hypothesized that this rare heterozygous missense variant of *MYOM2* may be the cause of TOF in this affected family.

Effect of Mutation on Protein

The 3D structure of *MYOM2* protein was already created using the SWISS-MODEL program. To investigate the missense variant effect on protein, schematic structures of the WT (left) and the mutant (right) amino acids are shown in **Figure 4**. Compared with the 3D structure of WT protein, the mutant protein showed a different steric hindrance of the residue (the new residue has a smaller size), which may lead to protein misfolding, resulting in pathogenicity.

DISCUSSION

In this study, we enrolled a Chinese TOF family with two affected twins and identified a rare deleterious variant of the *MYOM2* gene, c.3097C>T (p.R1033C) in the family by whole exome and Sanger sequencing. We speculated that this variant may be the genetic cause of TOF.

As a highly heterogeneous disease, previous studies have suggested that rare potential pathogenic variants of genes related to the heart development, such as Filamin A (*FLNA*), Kinase Insert Domain Receptor (*KDR*), and *NKX2.5* are associated with the occurrence of TOF (12, 18, 19, 23). Recently, several variants in the sarcomere genes such as Myosin Heavy Chain 7 (*MYH7*) and Myosin Binding Protein C3 (*MYBPC3*) have been identified in patients with heart diseases (24–27). However, to date, the correlations between genetic variants of sarcomere genes and TOF have not been fully established.

The Myomesin gene family comprises three members including *MYOM1, MYOM2,* and *MYOM3*, and encodes the

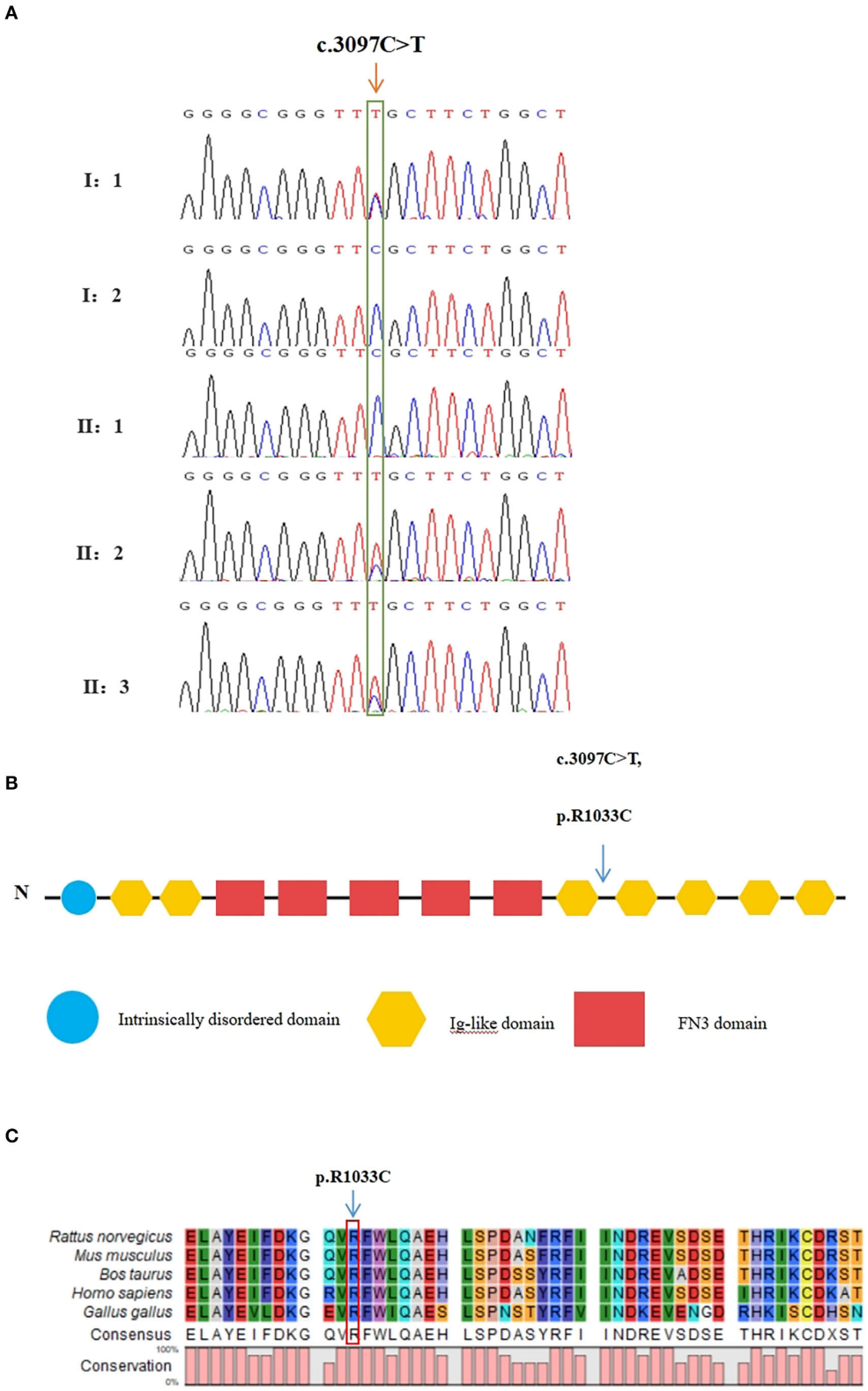

FIGURE 3 | Validation of the missense variant of *MYOM2* in the family with TOF. **(A)** Sanger sequencing results from the probands, their brothers, and their unaffected parents. The heterozygous variant in the *MYOM2* gene was identified in the twins, but not in their healthy brother. **(B)** The location of the variant in the protein structure of *MYOM2*. The arrow denotes the mutated site. **(C)** Amino acid alignment of the *MYOM2* protein from several organisms. The position of Arg1033 residue (highlighted by a red box) was highly conserved among different species.

TABLE 2 | Pathogenicity prediction of the identified mutation (c.3097C>T,p.R1033C) using multiple online *in silico* tools.

No.	*In silico* analysis tools	Prediction	Score
1	SIFT	Damaging	0.0
2	Polyphen-2	Probably_damaging	1.0
3	MutationTaster	Disease_causing	1.0
4	FATHMM-MKL	Damaging	0.986
5	CADD	Damaging	35
6	DANN	Damaging	0.999
7	PROVEAN	Damaging	−7.24
8	VEST3	Damaging	0.963
9	ClinPred	pathogenic	0.983
10	GenoCanyon	Damaging	1.00
11	INPS-MD	Stabilitychange	−0.53

proteins of sarcomere which play important roles in the development of heart and skeletal muscles (28, 29). They all include fibronectin type III (FN3) and immunoglobulin type II (Ig) like domains, acting as crosslinkers for the neighboring thick filaments of myosin in the M-band. The Ig-like domains can be found in several diverse protein families and are involved in a variety of functions, including cell-cell recognition, cell-surface receptors, muscle structure, and the immune system (30). These three myosin subtypes are also related to the contractile properties of different fiber types. While *MYOM1* is expressed in all striated muscles, *MYOM3* is expressed in skeletal muscle intermediate fiber types, and *MYOM2* is expressed in the adult heart and fast fibers (31–33). Previous studies have shown that variations in *MYOM1* and *MYOM3* could cause cardiac abnormalities, such as hypertrophic cardiomyopathy and dilated cardiomyopathy (34, 35). Moreover, Pehlivan et al. (2019) found that the loss of function of *MYOM2* can result in the termination of gestation of the affected fetus, with cardiac and arthrogryposis findings, but this does not occur with loss of function of *MYOM1* or *MYOM3* (36). Auxerre-Plantie et al. (2020) identified three heterozygous deleterious variants of *MYOM2* (c.590C > T, p.A197V; c.3320G > C, p.G1107A; and c.3904A > G, p.T1302A) which is located on the Ig-like domains and one deleterious variant of *MYOM2* (c.2119G > A, p.A707T) which was located on the FN3 domain in TOF patients (21). Furthermore, Tang et al. (2022) also identified two compound heterozygous variants of *MYOM2* in Chinese TOF patients and found the top enriched cluster of heart development contained GO terms that were related to the development of cardiac muscle and morphogenesis, including genes encoding the myomesins (*MYOM1* and *MYOM2*) by functional enrichment analysis (20). These results might provide several genetic clues to the association between *MYOM2* and heart development.

MYOM2 is located on chromosome 8p23.3, contains 37 exons, and encodes a 1,465–amino acid protein which is expressed in the human heart muscle and is a major structural component of the M-band (33, 37, 38). The sarcomere with two transverse structures, the Z-disk, and the M-band, is the Myofibrils' basic unit. Myofibrils have been reported to mediate skeletal and cardiac muscle contraction in vertebrates and invertebrates. Therefore, alterations of sarcomere proteins may influence the contractile performance of the heart and skeletal muscle (35). In addition, cardiomyocytes derived from induced pluripotent stem cells of healthy individuals and TOF patients reveal that *MYOM2* is expressed during cardiac differentiation (39). Furthermore, *MYOM2* is also expressed in embryonic and adult mouse hearts (40). Although there are no studies that mention the mammalian animal model for exploring the exact role of *MYOM2* in the heart development, given the advantages of the fly model for studying the genetics of human disease mechanisms (41), Auxerre-Plantie et al. (2020) aimed to clarify the potential cardiac function of *MYOM2* using *Drosophila* (21). They found that its partial loss of function or moderate cardiac knockdown resulted in cardiac dilation, whereas severely reduced function caused an increase in sarcomere myosin protein, which is clearly involved in the development of the heart. In addition, as it was shown that *MYOM2* physically interacts with *MYH7*, which is known to be associated with the development of CHDs in *vitro*, the CG14964, the fly ortholog for *MYOM2*, and Mhc, the fly ortholog for *MYH7*, could also interact at the genetic level *in vivo* (25, 26, 42). Furthermore, they also identified some heterozygous missense variants of *MYOM2* in TOF patients. The above findings indicate that *MYOM2* might be a candidate gene for TOF.

In this study, we performed WES on all five members of a TOF-affected family to identify novel potential pathogenic variants and genes based on rigorous bioinformatic analyses. By applying several filtering processes, we identified a heterozygous missense variant, c.3097C > T (p.R1033C), in *MYOM2* in the affected twins. Furthermore, Sanger sequencing confirmed that, while the variant was present in the affected twins and the proband's father, who did not have any abnormal cardiac phenotypes, the proband's healthy brother did not carry the variant. These results showed that this variant was transmitted from an unaffected father indicating incomplete penetrance. A previous study has reported rare heterozygous variants of *MYOM2* in TOF patients without co-segregation analysis (21). Some rare heterozygous missense variants in *NOTCH1*, a known disease-causing gene, have also been reported in the TOF patients and some of these variants are inherited from their unaffected parents (7). The incomplete penetrance is in keeping with the complex genetic etiology of non-syndromic TOF, in which families segregating the condition in a Mendelian fashion are rarely encountered and genetic background, except for the environmental factors, can be inferred to play significant roles. In addition, the missense variant identified in *MYOM2* is extremely rare in East Asian populations and the overall human population, based on the genome database archived in gnomAD and is absent in the ChinaMap database (www.mBiobank.com). Furthermore, the mutated site is highly conserved among mammals, and the variant was predicted to be deleterious by multiple online software programs. Interestingly, this mutated site is near to the previously reported rare deleterious variant of *MYOM2*. Therefore, the heterozygous missense variant that we found may have caused the TOF by affecting *MYOM2* protein function in this family.

In summary, we identified a novel heterozygous missense variant of *MYOM2* (NM_003970.4:c.3097C>T:p.R1033C) as a possible genetic contributor to familial TOF in a Chinese population. This finding increases our knowledge of the etiology

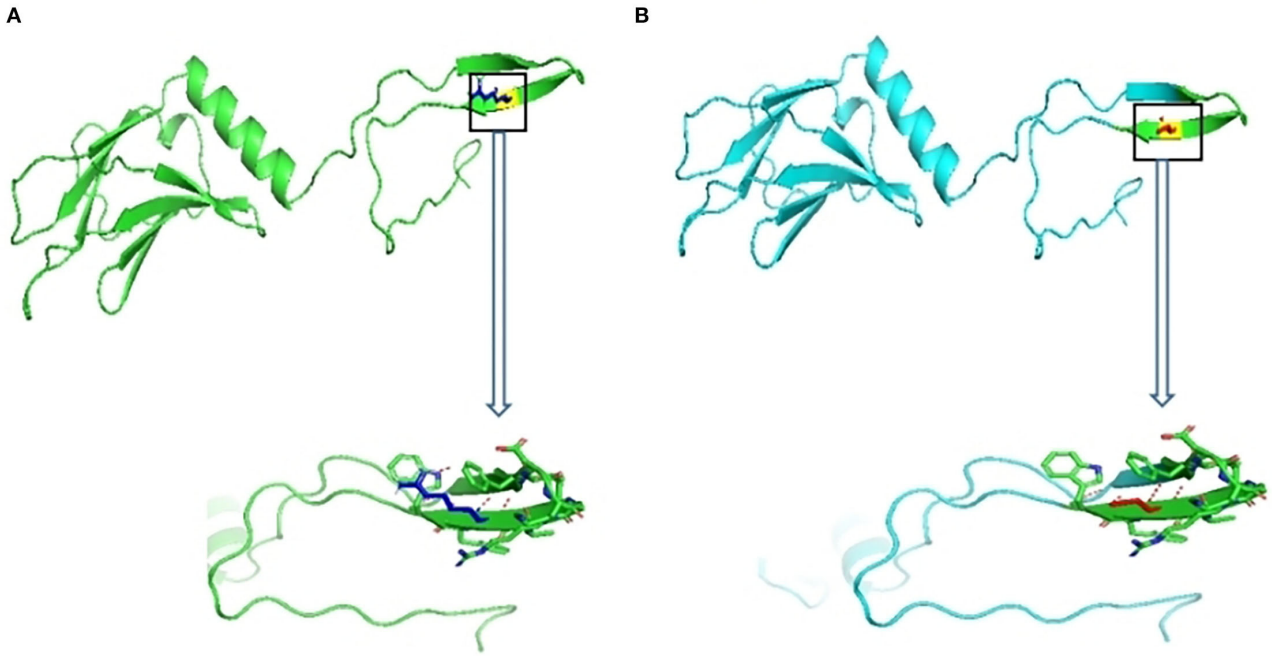

FIGURE 4 | Wild-type and variant structure of *MYOM2* protein. **(A)** Wild-type *MYOM2* predicted 3D structure. **(B)** Mutation *MYOM2* predicted 3D structure.
Supplemental Figure 1 Echo images from the twins' father. The above 4 figures were taken from Cardiac ultrasound results. These figures illustrate the shape, structure, wall thickness, and function of the heart were all normal.

of TOF by identifying a possible causative gene variant, which should be considered when diagnosing this disease. However, the exact role of this variant for TOF has not been clearly explained. Therefore, further studies are required to elucidate the exact mechanism of the association between the missense *MYOM2* variant and TOF by performing functional experiments *in vitro* and *in vivo*, and studies with larger sample sizes are needed to identify more variants of *MYOM2* in different populations.

DATA AVAILABILITY STATEMENT

The original contributions presented in the study are included in the article/**Supplementary Material**, further inquiries can be directed to the corresponding authors.

ETHICS STATEMENT

The studies involving human participants were reviewed and approved by the Ethics Committee of Wuhan Children's Hospital. Written informed consent to participate in this study was provided by the participants' legal guardian/next of kin. Written informed consent was obtained from the minor(s)' legal guardian/next of kin for the publication of any potentially identifiable images or data included in this article.

AUTHOR CONTRIBUTIONS

All authors contributed to the study conception and design. The research was designed by JW, LG, and MP. Ultrasound images were provided by HX, LW, and XF. Data analysis and interpretation were performed by JW, CW, and BW. The validation experiment was performed by TL. The first draft of the manuscript was written by CW and JW. All authors commented on early versions of the manuscript, contributed to the article, and read and approved the submitted version.

FUNDING

This work was supported by the project of the Elevate Project of Medical Basis, School of Basic Medical Sciences, Capital Medical University, 2021; Basic Science Promotion Project of Capital Medical University; the Central Government to Guide Local Scientific and Technological Development (2018ZYYD063); and the Science and Technology Project of Wuhan Health Commission (EX20E06).

ACKNOWLEDGMENTS

We would like to acknowledge all the patients who participated in our study.

SUPPLEMENTARY MATERIAL

The Supplementary Material for this article can be found online at: https://www.frontiersin.org/articles/10.3389/fcvm.2022.863650/full#supplementary-material

REFERENCES

1. Dolbec K, Mick NW. Congenital Heart Disease. *Emergency medicine clinics of* North America. (2011):29:811–27. *vii*. doi: 10.1016/j.emc.2011.08.005
2. Sun R, Liu M, Lu L, Zheng Y, Zhang P. Congenital heart disease: causes, d.iagnosis, symptoms, and treatments. *Cell biochemistry and biophysics.* (2015) 72:857–60. doi: 10.1007/s12013-015-0551-6
3. Diaz-Frias J, Guillaume M. *Tetralogy of Fallot*. Treasure Island (FL): Statpearls Publishing. (2021).
4. Apitz C, Webb GD, Redington AN. Tetralogy of fallot. *Lancet.* (2009) 374:1462–71. doi: 10.1016/S0140-6736(09)60657-7
5. Karl TR, Stocker C. Tetralogy of fallot and its Variants. *Pediatr Crit Care Med.* (2016) 17(8 Suppl. 1):*S*330–6. doi: 10.1097/PCC.0000000000000831
6. Manshaei R, Merico D, Reuter MS, Engchuan W, Mojarad BA, Chaturvedi R, et al. Genes and pathways implicated in tetralogy of fallot revealed by ultra-rare variant burden analysis in 231 Genome sequences. *Front Genet.* (2020) 11:957. doi: 10.3389/fgene.2020.00957
7. Page DJ, Miossec MJ, Williams SG, Monaghan RM, Fotiou E, Cordell HJ., et al. Whole exome sequencing reveals the major genetic contributors to nonsyndromic tetralogy of fallot. *Cir Res.* (2019) 124:553–63. doi: 10.1136/heartjnl-2019-BCS.136
8. Dixit R, Narasimhan C, Balekundri VI, Agrawal D, Kumar A, Mohapatra B. Functionally significant novel gata4 variants are frequently associated with tetralogy of fallot. *Hum mutat.* (2018) 39:1957–72. doi: 10.1002/humu.23620
9. Kheirollahi M, Khosravi F, Ashouri S, Ahmadi A. Existence of mutations in the homeodomain-encoding region of Nkx2.5 gene in iranian patients with tetralogy of fallot. *J Res Med Sci.* (2016) 21:24. doi: 10.4103/1735-1995.179893
10. Safari-Arababadi A, Behjati-Ardakani M, Kalantar SM, Jaafarinia M. Silencing mutations in Jag1 gene may play crucial roles in the pathogenesis of tetralogy of fallot. *CellMol Biol.* (2018) 64:103–7. doi: 10.14715/cmb/2018.64.4.17
11. Topf A, Griffin HR, Glen E, Soemedi R, Brown DL, Hall D, et al. functionally significant rare transcription factor variants in tetralogy of fallot. PLoS *ONE.* (2014) 9:*e*95453. doi: 10.1371/journal.pone.0095453
12. Behiry EG, Al-Azzouny MA, Sabry D, Behairy OG, Salem NE. Association of Nkx2-5, Gata4, and Tbx5 polymorphisms with congenital heart disease in egyptian children. *Mol Genomic Med.* (2019) 7:*e*612. doi: 10.1002/mgg3.612
13. Aguayo-Gomez A, Arteaga-Vazquez J, Svyryd Y, Calderon-Colmenero J, Zamora-Gonzalez C, Vargas-Alarcon G, et al. Identification of copy number variations in isolated tetralogy of fallot. *Pediatr Cardiol.* (2015) 36:1642–6. doi: 10.1007/s00246-015-1210-9
14. Eldadah ZA, Hamosh A, Biery NJ, Montgomery RA, Duke M, Elkins R., et al. Familial tetralogy of fallot caused by mutation in the jagged1 gene. *Hum Mol Genet.* (2001) 10:163–9. doi: 10.1093/hmg/10.2.163
15. Chen J, Qi B, Zhao J, Liu W, Duan R, Zhang M. A novel mutation of gata4 (K300t) associated with familial atrial septal defect. *Gene*. (2016) 575:473–7. doi: 10.1016/j.gene.2015.09.021
16. LaHaye S, Corsmeier D, Basu, M, Bowman JL, et al. Utilization of whole exome sequencing to identify causative mutations in familial congenital heart disease. *Circ Cardiovas Genet*. (2016) 9:320–9. doi: 10.1161/CIRCGENETICS.115.001324
17. Liu L, Wang HD, Cui CY, Qin YY, Fan TB, Peng BT, et al. Whole exome sequencing identifies novel mutation in eight chinese children with isolated tetralogy of fallot. *Oncotarget.* (2017) 8:106976–88. doi: 10.18632/oncotarget.22202
18. Kalayinia S, Maleki M, Mahdavi M, Mahdieh N. Whole-exome sequencing reveals a novel mutation of Flna gene in an iranian family with nonsyndromic tetralogy of fallot. *Lab Med.* (2021) 52:614–8. doi: 10.1093/labmed/lmab018
19. Skoric-Milosavljevic D, Lahrouchi N, Bosada FM, Dombrowsky G, Williams SG, Lesurf R, et al. Rare variants in KDR, encoding Vegf receptor 2, are associated with tetralogy of fallot. *Genet Med*. (2021) 23:1952–60. doi: 10.1038/s41436-021-01212-y
20. Tang CSM, Mononen M, Lam WY, Jin SC, Zhuang X, Garcia-Barcelo MM, et al. Sequencing of a Chinese tetralogy of fallot cohort reveals clustering mutations in myogenic heart progenitors. *JCI Insight.* (2022) 7:e152198. doi: 10.1172/jci.insight.152198
21. Auxerre-Plantie E, Nielsen T, Grunert M, Olejniczak O, Perrot A, Ozcelik C, et al. Identification of Myom2 as a candidate gene in hypertrophic cardiomyopathy and tetralogy of fallot and its functional evaluation in the drosophila heart. *Dis Model Mech*. (2020) 13:dmm045377. doi: 10.1242/dmm.045377
22. Cao Y, Li L, Xu M, Feng Z, Sun X, Lu J, et al. The chinamap analytics of deep whole genome sequences in 10,588 individuals. *Cell Res.* (2020) 30:717–31. doi: 10.1038/s41422-020-0322-9
23. Goldmuntz E, Geiger E, Benson DW. Nkx2.5 mutations in patients with tetralogy of fallot. *Circulation.* (2001) 104:2565–8. doi: 10.1161/hc4601.098427
24. Helms AS, Tang VT, O'Leary TS, Friedline S, Wauchope M, Arora A, et al. Effects of Mybpc3 loss-of-function mutations preceding hypertrophic cardiomyopathy. *JCI insight*. (2020) 5:e133782. doi: 10.1172/jci.insight.133782
25. Basu R, Hazra S, Shanks M, Paterson DI, Oudit GY. Novel mutation in Exon 14 of the sarcomere gene myh7 in familial left ventricular noncompaction with bicuspid aortic valve. *Cir Heart Fail.* (2014) 7:1059–62. doi: 10.1161/CIRCHEARTFAILURE.114.001666
26. van der Linde IHM, Hiemstra YL, Bokenkamp R, van Mil AM, Breuning MH, Ruivenkamp C, et al. A Dutch Myh7 founder mutation P.(Asn1918lys), is associated with early onset cardiomyopathy and congenital heart defects. *Neth heart J*. (2017) 25:675–81. doi: 10.1007/s12471-017-1037-5
27. Tharp CA, Haywood ME, Sbaizero O, Taylor MRG, Mestroni L. The giant protein titin's role in cardiomyopathy: genetic transcriptional and post-translational modifications of ttn and their contribution to cardiac disease. *Front Physiol.* (2019) 10:1436. doi: 10.3389/fphys.2019.01436
28. Grove BK, Cerny L, Perriard JC, Eppenberger HM, Myomesin and M.-,protein: expression of two m-band proteins in pectoral muscle and heart during development. *J Cell Biol.* (1985) 101:1413–21. doi: 10.1083/jcb.101.4.1413
29. Van Der Ven PF, Obermann WM, Weber K, Furst DO, Myomesin m-protein and the structure of the sarcomeric m-band. *Adv Biophys.* (1996) 33:91–9. doi: 10.1016/0065-227X(96)81666-2
30. Hu LY, Ackermann MA, Kontrogianni-Konstantopoulos A. The sarcomeric m-region:a and molecular command center for diverse cellular processes. *BioMed Res Inter.* (2015) 2015:714197. doi: 10.1155/2015/714197
31. Schoenauer R, Lange S, Hirschy A, Ehler E, Perriard JC, Agarkova I. Myomesin 3, a novel structural component of the m- and band in striated muscle. *J Mol Biol.* (2008) 376:338–51. doi: 10.1016/j.jmb.2007.11.048
32. Schoenauer R, Bertoncini P, Machaidze G, Aebi U, Perriard JC, Hegner M, et al. Myomesin is a molecular spring with adaptable elasticity. *J Mol Biol.* (2005) 349:367–79. doi: 10.1016/j.jmb.2005.03.055
33. Agarkova I, Ehler E, Lange S, Schoenauer R, Perriard JCM- and Band:a safeguard for sarcomere stability? *J Muscle Res Cell Motil.* (2003) 24:191–203. doi: 10.1023/A:1026094924677
34. Shakeel M, Irfan M, Khan IA. Rare genetic mutations in Pakistani patients with dilated cardiomyopathy. *Gene.* (2018) 673:134–9. doi: 10.1016/j.gene.2018.06.019
35. Siegert R, Perrot A, Keller S, Behlke J, Michalewska-Wludarczyk A, Wycisk A, et al. A myomesin mutation associated with hypertrophic cardiomyopathy deteriorates dimerisation properties. *Biochem Biophys Res commun.* (2011) 405:473–9. doi: 10.1016/j.bbrc.2011.01.056
36. Pehlivan D, Bayram Y, Gunes N, Coban Akdemir Z, Shukla A, Bierhals T, et al. The genomics of arthrogryposis a complex trait: candidate genes and further evidence for oligogenic inheritance. *Am J Hum Genet.* (2019) 105:132–50. doi: 10.1016/j.ajhg.2019.05.015
37. Lange S, Pinotsis N, Agarkova I, Ehler E. The m- band: the underestimated part of the sarcomere. *Biochem Biophys Actao–Mol Cell Res.* (2020) 1867:118440. doi: 10.1016/j.bbamcr.2019.02.003
38. Agarkova I, Perriard JC. The m- band: an elastic web that crosslinks thick filaments in the center of the sarcomere. *Trends Cell Biol.* (2005) 15:477–85. doi: 10.1016/j.tcb.2005.07.001
39. Grunert M, Appelt S, Schonhals S, Mika K, Cui H, Cooper A, et al. Induced pluripotent stem cells of patients with tetralogy of fallot reveal transcriptional alterations in cardiomyocyte, d.ifferentiation. *Scri Rep.* (2020) 10:10921. doi: 10.1038/s41598-020-67872-z
40. Grunert M, Dorn C, Schueler M, Dunkel I, Schlesinger J, Mebus S, et al. Rare and private variations in neural, c.rest, apoptosis and sarcomere genes define the polygenic background of isolated tetralogy

of fallot. *Hum Mol Genet.* (2014) 23:3115–28. doi: 10.1093/hmg/ddu021
41. Piazza N, Wessells RJ, Drosophila. Models of cardiac disease. *Prog Mol Biol Transl Sci.* (2011) 100:155–210. doi: 10.1016/B978-0-12-384878-9.00005-4
42. Bettinelli AL, Mulder TJ, Funke BH, Lafferty KA, Longo SA, Niyazov DM. Familial ebstein a nomaly left ventricular hypertrabeculation and ventricular septal defect associated with a Myh7 mutation. *Am J Med Genet A.* (2013) 161A:3187–90. doi: 10.1002/ajmg.a.36182

Conflict of Interest: The authors declare that the research was conducted in the absence of any commercial or financial relationships that could be construed as a potential conflict of interest.

Publisher's Note: All claims expressed in this article are solely those of the authors and do not necessarily represent those of their affiliated organizations, or those of the publisher, the editors and the reviewers. Any product that may be evaluated in this article, or claim that may be made by its manufacturer, is not guaranteed or endorsed by the publisher.

frontiers | Frontiers in Cardiovascular Medicine

TYPE Case Report
PUBLISHED 25 August 2022
DOI 10.3389/fcvm.2022.982607

OPEN ACCESS

EDITED BY
Neil Morgan,
University of Birmingham,
United Kingdom

REVIEWED BY
Radoslaw Debiec,
University of Leicester,
United Kingdom
Jose Krieger,
University of São Paulo, Brazil

*CORRESPONDENCE
Anastasia V. Blokhina
blokhina0310@gmail.com

SPECIALTY SECTION
This article was submitted to Cardiovascular Genetics and Systems Medicine,
a section of the journal
Frontiers in Cardiovascular Medicine

RECEIVED 30 June 2022
ACCEPTED 08 August 2022
PUBLISHED 25 August 2022

CITATION
Blokhina AV, Ershova AI, Meshkov AN, Kiseleva AV, Klimushina MV, Zharikova AA, Sotnikova EA, Ramensky VE and Drapkina OM (2022) Phenotypic vs. genetic cascade screening for familial hypercholesterolemia: A case report. *Front. Cardiovasc. Med.* 9:982607. doi: 10.3389/fcvm.2022.982607

Phenotypic vs. genetic cascade screening for familial hypercholesterolemia: A case report

Anastasia V. Blokhina[1]*, Alexandra I. Ershova[1], Alexey N. Meshkov[2], Anna V. Kiseleva[2], Marina V. Klimushina[3], Anastasia A. Zharikova[2,4], Evgeniia A. Sotnikova[2], Vasily E. Ramensky[4,5] and Oxana M. Drapkina[6]

[1]Laboratory of Clinomics, National Medical Research Center for Therapy and Preventive Medicine of the Ministry of Healthcare of the Russian Federation, Moscow, Russia, [2]Laboratory of Molecular Genetics, National Medical Research Center for Therapy and Preventive Medicine of the Ministry of Healthcare of the Russian Federation, Moscow, Russia, [3]Department for the Study of Biochemical Risk Markers of Chronic Noncommunicable Diseases, National Medical Research Center for Therapy and Preventive Medicine of the Ministry of Healthcare of the Russian Federation, Moscow, Russia, [4]Faculty of Bioengineering and Bioinformatics, Lomonosov Moscow State University, Moscow, Russia, [5]Laboratory of Genomic and Medical Bioinformatics, National Medical Research Center for Therapy and Preventive Medicine of the Ministry of Healthcare of the Russian Federation, Moscow, Russia, [6]Department of Fundamental and Applied Aspects of Obesity, National Medical Research Center for Therapy and Preventive Medicine of the Ministry of Healthcare of the Russian Federation, Moscow, Russia

One of the most common autosomal dominant disorders is familial hypercholesterolemia (FH), causing premature atherosclerotic cardiovascular diseases and a high risk of death due to lifelong exposure to elevated low-density lipoprotein cholesterol (LDL-C) levels. FH has a proven arsenal of treatments and the opportunity for genetic diagnosis. Despite this, FH remains largely underdiagnosed worldwide. Cascade screening is a cost-effective method for the identification of new patients with FH and the prevention of cardiovascular diseases. It is usually based only on clinical data. We describe a 48-year-old index patient with a very high LDL-C level without controlled guidelines-based medication, premature atherosclerosis, and a rare variant in the low-density lipoprotein receptor (*LDLR*) gene. Phenotypic cascade screening identified three additional FH relatives, namely the proband's daughter, and two young grandsons. The genetic screening made it possible to rule out FH in the proband's younger grandson. This clinical case demonstrates that genetic cascade screening is the most effective way of identifying new FH cases. We also first described in detail the phenotype of patients with a likely pathogenic variant *LDLR*-p.K223_D227dup.

KEYWORDS

familial hypercholesterolemia, cascade screening, phenotypic screening, genetic screening, molecular genetic testing, LDLR, duplication

Introduction

One of the most common autosomal dominant disorders is familial hypercholesterolemia (FH) (1–3), causing premature atherosclerotic cardiovascular diseases and a high risk of death due to lifelong exposure to elevated low-density lipoprotein cholesterol (LDL-C) levels (4). The genetic basis of FH is well understood and in the vast majority of cases are variants in one of the three genes: low-density lipoprotein receptor gene (*LDLR*), apolipoprotein B gene (*APOB*), and proprotein convertase subtilisin/kexin type 9 gene (*PCSK9*) (1). Highly effective lipid-lowering therapy (LLT) and extracorporeal methods of FH treatment (apheresis) are currently available (4). Despite this, FH remains largely underdiagnosed worldwide (5).

Cascade screening is a mechanism for identifying people with a genetic condition by the process of systematic family members examination using phenotypic or genetic strategy (6). It is a cost-effective method for the identification of new patients with FH and the prevention of cardiovascular disease, as highlighted in the major international guidelines (4–7). Genetic testing is recommended in international guidelines to confirm the FH, but it is not obligated and the diagnosis of FH is usually based only on clinical data (the phenotypic strategy) (4–8). However, if the FH can be diagnosed by clinical data, what are the benefits of genetic testing?

Here, we demonstrate the role of genetic screening for FH in real clinical practice and describe a case of a 48-year-old index patient with premature atherosclerosis and a very high LDL-C level without controlled guidelines-based medication. Genetic testing identified a rare likely pathogenic *LDLR* variant. Phenotypic and then genetic cascade screening confirmed heterozygous FH (HeFH) in proband's daughter with the same *LDLR* variant. Phenotypic screening suggested HeFH in two proband's grandsons, whereas the genetic screening made it possible to rule out FH in the younger grandson. We also first described in detail the phenotype of patients with a likely pathogenic variant *LDLR*: hg19::chr19:11216249_11216263dup, or NM_000527.5:c.667_681dup, NP_000518.1:p.K223_D227dup at the protein level. We observed segregation of this variant in three generations.

Case description

Materials and methods

Subjects

Three-generation family (a 48-year-old woman (the index patient), the proband's pregnant 30-year-old daughter (gestational age −3.5 weeks), and two grandsons (ten and four-year-old) presented to the Lipid Clinic (National Medical Research Center for Therapy and Preventive Medicine, Moscow, Russia) in October 2020.

Genetic analyses

Using the QIAamp DNA Blood Mini Kit (Qiagen, Hilden, Germany), DNA extraction was performed. DNA concentration was measured on a Qubit 4.0 (Thermo Fisher Scientific, Waltham, MA, USA). The libraries for the NGS custom panel were done with the SeqCap EZ Prime Choice Library kit (Roche, Basel, Switzerland). This panel included exon sequences of the *LDLR, APOB, PCSK9,* and *LDLRAP1* genes, as well as other genes, associated with lipid metabolism disorders (*ABCA1, ABCG5, ABCG8, ANGPTL3, APOA1, APOA5, APOC2, APOC3, APOE, CETP, GPD1, GPIHBP1, LCAT, LIPC, LIPI, LMF1, LPL, MTTP, SAR1B, STAP1, USF1*). Next-generation sequencing (NGS) was performed on the Nextseq 550 (Illumina, San Diego, CA, USA). All stages of sequencing were carried out according to the manufacturer's protocols.

After the bioinformatic analysis .bam and .vcf files were generated. For clinical interpretation only variants with minor allele frequency (MAF) <0.01% in the Genome Aggregation Database (gnomAD; http://gnomad.broadinstitute.org) were analyzed according to the American College of Medical Genetics and Genomics/Association for Molecular Pathology (ACMG/AMP2015) guidelines and according to the Clinical Genome Resource (ClinGen) guidelines for *LDLR* variant classification (9, 10).

The validation of variants was done by Sanger sequencing on the Applied Biosystem 3,500 Genetic Analyzer (Thermo Fisher Scientific, Waltham, MA, USA).

Results

Phenotypic cascade screening of the proband and first-degree relatives

A 48-year-old woman presented to the Lipid Clinic in October 2020 with severe hypercholesterolemia. The first blood test for total cholesterol (TC) was done in 2014 (the TC value was about 10 mmol/L) and irregular LLT (rosuvastatin 20 mg daily) was started. In February 2020 TC was 11.46 mmol/L (without LLT). The patient continued rosuvastatin 20 mg daily (LDL-C was 7.81 mmol/L). At the time of the visit, the patient's medications included rosuvastatin 20 mg daily and evolocumab 140 mg per 2 weeks (LDL-C was 3.92 mmol/L).

The patient had been smoking for 5 years and also had a history of early menopause. At a physical examination, she had obesity (height 164 cm, weight 84 kg, and body mass index 31.2 kg/m^2), bilateral Achilles tendons xanthomas, and xanthelasmas, but not corneal arcus. She also had carotid (duplex ultrasound showed 25–30% stenoses of both carotid bifurcations), femoral (20–25% stenoses of left common femoral

and left popliteal arteries), and coronary atherosclerosis (the Agatston score was 252.83). The echocardiography showed aortic valve calcification.

The patient's father had two strokes, with the first event occurring at the age of 55, and died of myocardial infarction at the age of 70. Father's TC levels are unknown. Proband's mother is 69-year-old. According to oral communication provided by the proband, her TC is not high, although the lipid profile is not available. TC levels had also not been measured in the patient's 30-year-old daughter and two grandsons (ten and four-year-old).

Given severe hypercholesterolemia, family history, and examination, the proband has a "definite" diagnosis of HeFH (14 points according to the Dutch Lipid Clinic Network (DLCN)) (11). Thus, HeFH was diagnosed in the proband by clinical data. The presence of FH in a proband indicates the need for phenotypic cascade screening in first-degree relatives. We invited the patient's 30-year-old daughter for examination. She had no xanthomas, xanthelasmas, or corneal arcus, but she had already had peripheral atherosclerosis (duplex ultrasound showed 15–20% stenosis of the right common femoral artery). She also had a high LDL-C level (9.81 mmol/L) but had never taken a LLT (Figure 1A). Therefore, proband's daughter also had a "definite" diagnosis of HeFH (10 points according to the DLCN).

Genetic cascade screening of the proband and the proband's daughter

According to the 2019 European Society of Cardiology/European Atherosclerosis Society guidelines for the management of dyslipidaemias, a patient with a clinical FH diagnosis is recommended to undergo molecular genetic testing (recommendations class I, evidence level C) to identify pathogenic or likely pathogenic variants in the *LDLR*, *APOB*, or *PCSK9* (4).

In the index patient, a total of 89 variants were identified. Of these, only two variants (duplication and missense) had MAF <0.01% and changed the gene amino acid sequence (Table 1).

One of the variants is a heterozygous missense variant in *ABCG5*: hg19:chr2:44059195G>C, NM_022436.3:c.293C>G, NP_071881.1:p.A98G, rs145164937. According to the ACMG/AMP2015 guidelines, this variant has two evidences of pathogenicity: MAF <0.01% in gnomAD (PM2) and multiple *in silico* predictions as deleterious (PP3). Thus, this variant can be classified as uncertain significance.

At the same time, the proband had a heterozygous likely pathogenic duplication in *LDLR*: chr19:11216249_11216263dup, NM_000527.5:c.667_681dup, NP_000518.1:p.K223_D227dup. The validation of this variant was done by Sanger sequencing (Figure 2). This variant was also confirmed in the proband's daughter by Sanger sequencing. The observed criteria of pathogenicity according to the ACMG/AMP2015 are PM4, PM2, PP1, and PP5 (9).

Phenotypic cascade screening of the second-degree relatives

Considering the presence of HeFH in the proband's daughter, we analyzed the proband's grandson's lipid profile (Figure 1A).

For the diagnosis of FH in the proband's grandsons, the pediatric diagnostic criteria should be used (13). The eldest grandson has a very high LDL-C level and FH can be diagnosed by clinical data (LDL-C level and family history). The younger grandson's LDL-C level is not very high, but the positive genetic testing of his mother may suggest HeFH (LDL-C level ≥3.5 mmol/L).

Genetic cascade screening of the second-degree relatives

The same *LDLR* variant was verified in elder proband's grandson by Sanger sequencing. Despite that phenotypic screening suggested HeFH in two proband's grandsons, the genetic screening made it possible to rule out FH in the younger grandson (Figure 1B).

Personalized treatment and recommendations

Considering HeFH and additional risk factors, the proband has a very high cardiovascular risk. The LDL-C target level is less than 1.4 mmol/L. After 1 month of high-intensity statin therapy (rosuvastatin 40 mg daily) with ezetimibe 10 mg daily and the injection of evolocumab (140 mg per 2 weeks), she achieved the LDL-C target level (LDL-C 1.29 mmol/L).

The proband's daughter needs high-intensity statin therapy and her LDL-C target level is less than 1.8 mmol/L. However, she is currently pregnant. LLT should not be given during pregnancy or during the breastfeeding period (4). Therefore, we are going to initiate the LLT after the end of breastfeeding.

The proband's elder grandson was sent for further examination to a specialized pediatric department. He should be educated to adopt a proper diet and treated with a statin. His LDL-C target should be <3.5 mmol/L (4, 13).

We recommended a lipid-lowering diet and dynamic monitoring of LDL-C level for the proband's younger grandson. For future perspectives, NGS of the lipid metabolism disorder genes and determination of polygenic risk scores for LDL-C level may be considered. Finally, we recommended screening for HeFH of the future child of the proband's daughter after his birth.

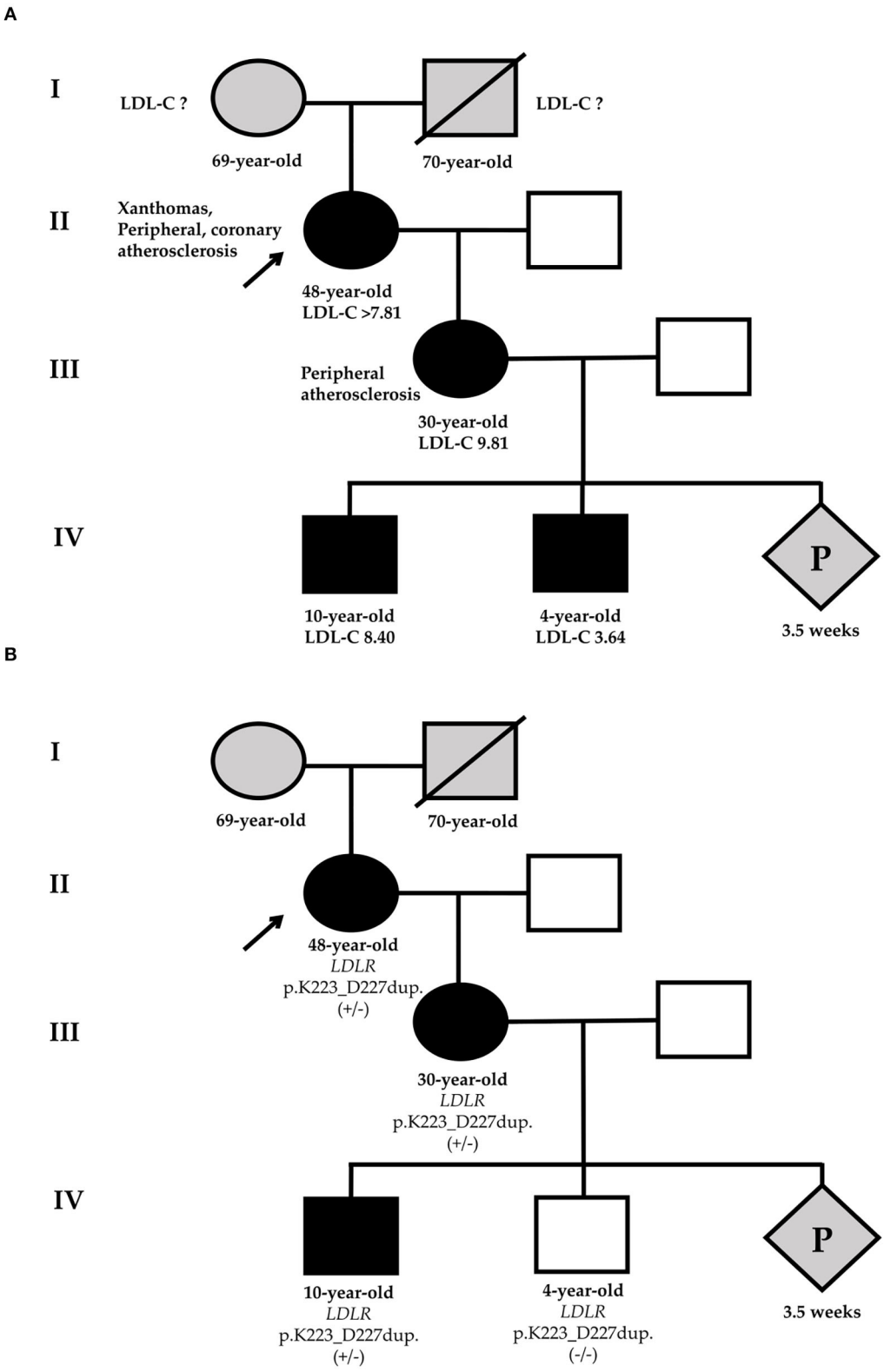

FIGURE 1
Phenotypic **(A)** and genetic **(B)** cascade screening. According to phenotypic screening, the younger grandson has HeFH [black-filled square **(A)**], in relation to genetic screening, he is healthy [white square **(B)**]. Circles represent females, squares indicate males, and diamond is pregnancy (unknown gender). Black-filled symbols show FH phenotype, gray symbols point to members with an unknown phenotype, and white symbols are healthy family members. Slashes indicate deceased members. +/− or -/- represent heterozygous or wild-type of *LDLR*-p.K223_D227dup variant. The index patient (II-1) is marked with an arrow. LDL-C, low-density lipoprotein cholesterol; P, pregnancy.

TABLE 1 Two Two rare variants with MAF < 0.01% identified in the proband.

Gene	Genomic coordinates (hg19)	Transcript; DNA change; Protein change	dbSNP ID	gnomAD MAF (v. 2.1.1)	ACMG interpretation
LDLR	chr19:11216249_11216263dup	NM_000527.5; c.667_681dup; p.K223_D227dup	-	-	Likely pathogenic (PM4, PM2, PP1, PP5)
ABCG5	chr2:44059195G>C	NM_022436.3; c.293C>G; p.A98G	rs145164937	0.002253	Variant of uncertain significance (PM2, PP3)

ACMG, American College of Medical Genetics and Genomics; gnomAD, Genome Aggregation Database; MAF, minor allele frequency.

Discussion

Familial hypercholesterolemia is one of the most common monogenic disorders with underestimated real prevalence. The meta-analyses of 2020 showed that the prevalence of HeFH in the general population is one in 313 (14). A recent population study in Russia showed the prevalence of HeFH is one in 173 (15).

In patients with FH cumulative LDL-C exposure is the leading cause of premature cardiovascular events (16). Hence, early identification of FH and its treatment with highly effective and safe LLT is necessary. Nevertheless, despite the high prevalence, the presence of diagnostic criteria, as well as the availability of NGS, and effective methods for reducing LDL-C levels, FH remains underdiagnosed and undertreated worldwide (5).

Here, we presented a three-generation family, where we identified HeFH by both phenotypic and genetic cascade screening in the proband's family members.

Using phenotypic cascade screening we confirmed HeFH by clinical data at the proband, the proband's daughter, and grandsons. The younger grandson's LDL-C level is not very high, but based on the positive genetic testing of his mother we may suggest HeFH. However, the genetic screening allowed to rule out FH in the younger grandson. Given FH at the proband's daughter, her future child also has a 50% probability of inheriting FH.

Using NGS we identified a rare *LDLR* duplication variant p.K223_D227dup with segregation in two proband's relatives. According to the ClinGen 2021 guidelines for *LDLR* variant classification, the duplication meets two moderate criteria, such as absence in the gnomAD (PM2) and segregation with phenotype in three informative meioses (PP1_Moderate). Besides, this variant was found in two unrelated FH cases (PS4_Supporting) (17) and also identified in a patient with FH diagnosis based on validated clinical criteria, after alternative causes of high cholesterol, were excluded (PP4). Therefore, p.K223_D227dup can be classified as likely pathogenic. This variant has not been previously described in patients with FH in the European population (18). The identification and interpretation of pathogenicity of new or rare FH-associated variants supplement the knowledge about the spectrum of FH variants. We also first described in detail the phenotype of patients with p.K223_D227dup based on segregation in three generations. This made it possible to increase the segregation level of pathogenicity from supporting to moderate.

Cascade screening is the step-by-step identification of patients with a monogenic disease among the proband's first-, second-, and, when possible, third-degree relatives. There are two strategies for cascade screening of the proband's relatives: phenotypic and genetic (6).

Considering a phenotypic strategy, FH can be based on clinical data, using the DLCN criteria (11), the Simon Broome Register Diagnostic Criteria (19), the biochemical criteria for diagnosis of the proband's relatives (8), and the criteria of FH in children (13). Genetic testing is also recommended in international guidelines to confirm the FH and conduct cascade screening (4–8). However, if the FH can be diagnosed by clinical data, what are the benefits of genetic testing?

Firstly, genetic testing helps to confirm the genetic basis of the disease and clarify the cardiovascular risk stratification. In this case, the positive genetic testing results for the proband, the proband's daughter, and especially for the proband's elder grandson may suggest a greater risk of developing cardiovascular events compared with a clinical FH phenotype without an established monogenic etiology. This statement has been noted in a number of studies (20, 21). Furthermore, the gene type and even the pathogenic variant type can affect an individual's LDL-C level and consequently the risk of developing premature coronary and peripheral atherosclerosis (7). In a number of studies, it has been noted that *LDLR* pathogenic variants carriers have a greater level of LDL-C compared to *APOB* or *PCSK9* variants (22). In this case, all positive *LDLR* variant patients had a very high LDL-C level. The LDL-C

FIGURE 2
Genetic analysis of the index patient. **(A)** Integrated genome view of *LDLR*-p.K223_D227dup with IGV (12). **(B, C)** Electropherograms of *LDLR*-p.K223_D227dup: **(B)** sequence from the forward primer, **(C)** sequence from the reverse primer (reverse complement).

level of the 10-year-old male was almost comparable to his 30-year-old mother.

Besides this, cardiovascular risk in patients with FH is considered manageable. Using genetic testing not only does not decrease perceptions of control over FH, cholesterol levels, or cardiovascular diseases but on the contrary, leads to more positive patient perceptions of FH (23, 24). It means that patients feel personally responsible for managing their health. Patients consider that FH genetic testing is very important and, regardless of the result, are ready to recommend genetic

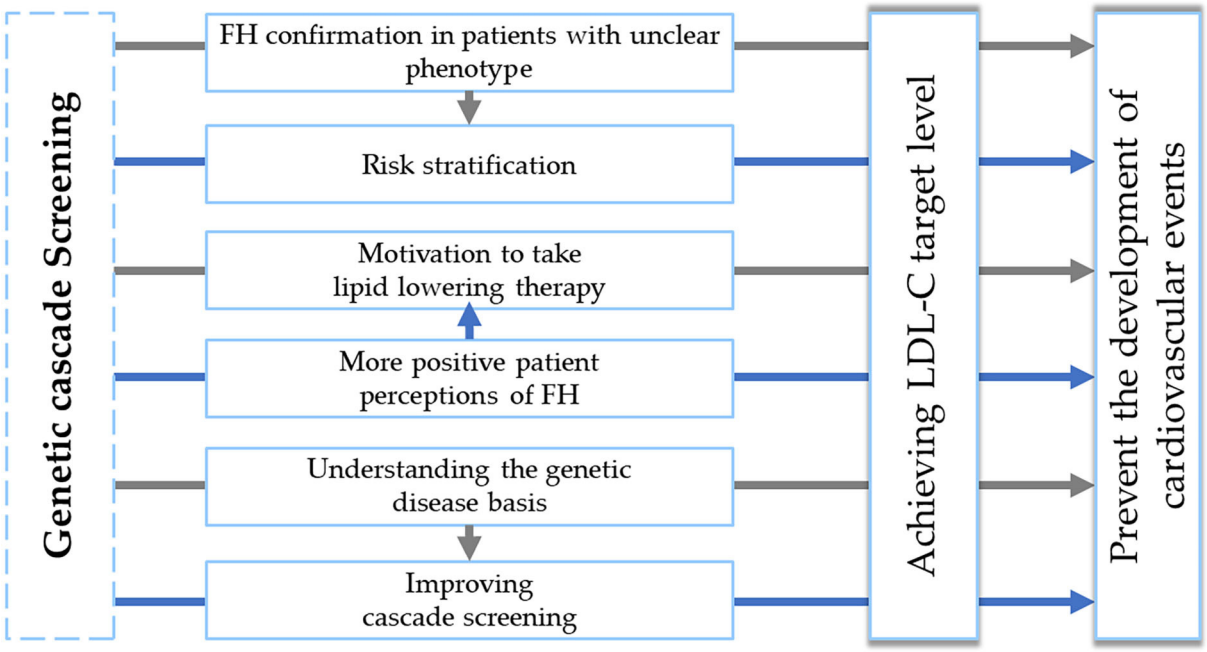

FIGURE 3
Genetic cascade screening benefits. FH, familial hypercholesterolemia. LDL-C, low-density lipoprotein cholesterol.

screening to their family members, which, in turn, can help to improve FH diagnosis (24). In this case, all available proband's relatives underwent genetic screening.

A meta-analysis of 17 studies performed in 2016 did not show any significant behavioral changes in smoking, physical activity, or dietary intake before and after the genetic testing. However, only one study of patients with FH was included in this meta-analysis (25). On the other hand, several studies of patients with FH showed other behavioral changes, such as changes in the perception of the most effective way to achieve LDL-C level. The patients with pathogenic variants consider their disease more accurately, with increased motivation to take LLT (23, 24). In this work after the positive genetic testing results, the proband began to take all prescribed LLT and achieved LDL-C targets. The early diagnosis is associated with appropriate treatment, lifestyle modifications, and in turn better prognosis. However, children have a silent presentation of FH and phenotypic screening alone is not enough. For examination of children and adolescents, it is not often possible to identify such phenotypic markers as xanthomas, corneal arcus, arteries atherosclerotic changes, or premature cardiovascular events (13, 26).

Genetic testing in childhood and adolescence, in a period of the formation of healthy lifestyle habits, is essential for ensuring long-term adherence and can contribute to the primary prevention of cardiovascular diseases. Starting FH treatment from a young age, and being surrounded by other family members during treatment, facilitates adherence and has particular importance in the treatment of FH (27). Children with FH variant are more understanding of their genetic disease basis. Furthermore, FH carrier children demonstrate high feelings of control over their disease (28).

Characterization of genetic cascade screening benefits is presented in Figure 3.

It is important to note that FH variants are verified only in 20–80% of patients with HeFH phenotype and at the same time the negative genetic testing results do not rule out a diagnosis of FH (29, 30). In this case, the genetic screening allowed to exclude the presence of *LDLR* variant p.K223_D227dup in the younger grandson. It is likely that his elevated LDL-C level is due to diet. Even with a negative FH genetic analysis, it is always necessary to remember about other lipid metabolism genetic disorders or that some patients with the typical FH phenotype may have a polygenic etiology of hypercholesterolemia (31). Targeted, exome or even genome sequencing, as well as genetic risk scores, may help to establish the reason for hypercholesterolemia. This highlights the unique role of genetic testing in the personalized medicine era.

Conclusion

In summary, given the high FH prevalence, the availability of NGS, and effective methods for reducing LDL-C levels, genetic cascade screening is the most

reliable, effective, and expedient method of personalized medicine for identifying new FH cases, including children and adolescents at the preclinical stage. This helps to clarify the cardiovascular risk stratification, and carry out targeted preventive measures, including lifestyle, cardiovascular risk factors correction, and early initiation of intensive LLT to achieve LDL-C targets and prevent the development of cardiovascular events. In unclear phenotypes, especially in children, genetic screening may help to rule out FH.

Data availability statement

The datasets presented in this study can be found in online repositories. The names of the repository/repositories and accession number(s) can be found below: https://www.ncbi.nlm.nih.gov/, SRR19880502.

Ethics statement

Ethical review and approval was not required for the study on human participants in accordance with the local legislation and institutional requirements. The patients/participants provided their written informed consent to participate in this study. Written informed consent was obtained from the individual(s), and minor(s)' legal guardian/next of kin, for the publication of any potentially identifiable images or data included in this article.

Author contributions

AB was treating the patients, performing their follow-ups, carrying out the interpretation of NGS data, and writing this case. AE was treating the patients, supervising all parts of this article's preparation, and editing the article. AM supervised the genetic testing of the patient and provided valuable comments on this case. AK performed the NGS and edited this article. MK performed the Sanger sequencing. AZ carried out the bioinformatic analyses of NGS data. ES performed the NGS. VR supervised the bioinformatic analyses of NGS data and edited this article. OD is the chief of the center who provided valuable comments on this case. All authors contributed to the article and approved the submitted version.

Conflict of interest

The authors declare that the research was conducted in the absence of any commercial or financial relationships that could be construed as a potential conflict of interest.

Publisher's note

All claims expressed in this article are solely those of the authors and do not necessarily represent those of their affiliated organizations, or those of the publisher, the editors and the reviewers. Any product that may be evaluated in this article, or claim that may be made by its manufacturer, is not guaranteed or endorsed by the publisher.

References

1. Berberich AJ, Hegele RA. The complex molecular genetics of familial hypercholesterolaemia. *Nat Rev Cardiol.* (2019) 16:9–20. doi: 10.1038/s41569-018-0052-6

2. Hu P, Dharmayat KI, Stevens CA, Sharabiani MT, Jones RS, Watts GF, et al. Prevalence of familial hypercholesterolemia among the general population and patients with atherosclerotic cardiovascular disease: a systematic review and meta-analysis. *Circulation.* (2020) 141:1742–59. doi: 10.1161/CIRCULATIONAHA.119.044795

3. Toft-Nielsen F, Emanuelsson F, Benn M. Familial hypercholesterolemia prevalence among ethnicities-systematic review and meta-analysis. *Front Genet.* (2022) 13:840797–840797. doi: 10.3389/fgene.2022.840797

4. Mach F, Baigent C, Catapano AL, Koskinas KC, Casula M, Badimon L, et al. 2019 ESC/EAS guidelines for the management of dyslipidaemias: lipid modification to reduce cardiovascular risk: the task force for the management of dyslipidaemias of the European Society of Cardiology (ESC) and European Atherosclerosis Society (EAS). *Eur Heart J.* (2020) 41:111–88. doi: 10.1093/eurheartj/ehz455

5. Nordestgaard BG, Chapman JM, Humphries SE, Ginsberg HN, Masana L, Descamps OS, et al. Familial hypercholesterolaemia is underdiagnosed and undertreated in the general population: guidance for clinicians to prevent coronary heart disease: consensus statement of the European Atherosclerosis Society. *Eur Heart J.* (2013) 34:3478–3490. doi: 10.1093/eurheartj/eht273

6. Harada-Shiba M, Arai H, Ishigaki Y, Ishibashi S, Okamura T, Ogura M, et al. Guidelines for diagnosis and treatment of familial hypercholesterolemia 2017. *J Atheroscler Thromb.* (2018) 25:751–70. doi: 10.5551/jat.CR003

7. Sturm AC, Knowles JW, Gidding SS, Ahmad ZS, Ahmed CD, Ballantyne CM, et al. Clinical genetic testing for familial hypercholesterolemia: JACC scientific expert panel. *J Am Coll Cardiol.* (2018) 72:662–80. doi: 10.1016/j.jacc.2018.05.044

8. DeMott K, Nherera L, Shaw EJ, Minhas R, Humphries SE, Kathoria M, et al. *Clinical Guidelines and Evidence Review for Familial Hypercholesterolaemia: the Identification and Management of Adults and Children with Familial Hypercholesterolaemia.* London: National Collaborating Centre for Primary Care and Royal College of General Practitioners (2008). 14 p.

9. Richards S, Aziz N, Bale S, Bick D, Das S, Gastier-Foster J, et al. Standards and guidelines for the interpretation of sequence variants: a joint consensus recommendation of the American College of Medical Genetics and Genomics and the Association for Molecular Pathology. *Genet Med.* (2015) 17:405–23. doi: 10.1038/gim.2015.30

10. Chora JR, Iacocca MA, Tichy L, Wand H, Kurtz CL, Zimmermann H, et al. The clinical genome resource (ClinGen) familial hypercholesterolemia variant curation expert panel consensus guidelines for LDLR variant classification. *Genet Med.* (2022) 24:293–306. doi: 10.1016/j.gim.2021.09.012

11. Civeira F. Guidelines for the diagnosis and management of heterozygous familial hypercholesterolemia. *Atherosclerosis.* (2004) 173:55–68. doi: 10.1016/j.atherosclerosis.2003.11.010

12. Robinson JT, Thorvaldsdóttir H, Wenger AM, Zehir A, Mesirov JP. Variant review with the integrative genomics viewer. *Cancer Res.* (2017) 77:e31–4. doi: 10.1158/0008-5472.CAN-17-0337

13. Wiegman A, Gidding SS, Watts GF, Chapman JM, Ginsberg HN, Cuchel M, et al. Familial hypercholesterolaemia in children and adolescents: gaining decades of life by optimizing detection and treatment. *Eur Heart J.* (2015) 36:2425–2437. doi: 10.1093/eurheartj/ehv157

14. Beheshti SO, Madsen CM, Varbo A, Nordestgaard BG. Worldwide prevalence of familial hypercholesterolemia: meta-analyses of 11 million subjects. *J Am Coll Cardiol.* (2020) 75:2553–2566. doi: 10.1016/j.jacc.2020.03.057

15. Meshkov AN, Ershova AI, Kiseleva AV, Shalnova SA, Drapkina OM, Boytsov SA, et al. The prevalence of heterozygous familial hypercholesterolemia in selected regions of the Russian federation: the FH-ESSE-RF study. *J Pers Med.* (2021) 11:464. doi: 10.3390/jpm11060464

16. Tada H, Okada H, Nohara A, Yamagishi M, Takamura M, Kawashiri MA. Effect of cumulative exposure to low-density lipoprotein-cholesterol on cardiovascular events in patients with familial hypercholesterolemia. *Circ J.* (2021) 28:CJ-21. doi: 10.1093/eurheartj/ehab724.2555

17. Miyake Y, Yamamura T, Sakai N, Miyata T, Kokubo Y, Yamamoto A. Update of Japanese common LDLR gene mutations and their phenotypes: mild type mutation L547V might predominate in the Japanese population. *Atherosclerosis.* (2009) 203:153–60. doi: 10.1016/j.atherosclerosis.2008.07.005

18. Meshkov A, Ershova A, Kiseleva A, Zotova E, Sotnikova E, Petukhova A, et al. The LDLR, APOB, and PCSK9 variants of index patients with familial hypercholesterolemia in Russia. *Genes.* (2021) 12:66. doi: 10.3390/genes12010066

19. Simon Broome Register Group. Risk of fatal coronary heart disease in familial hypercholesterolaemia. *BMJ.* (1991) 303:893–6.

20. Khera AV, Won HH, Peloso GM, Lawson KS, Bartz TM, Deng X, et al. Diagnostic yield and clinical utility of sequencing familial hypercholesterolemia genes in patients with severe hypercholesterolemia. *J Am Coll Cardiol.* (2016) 67:2578–89. doi: 10.1016/j.jacc.2016.03.520

21. Tada H, Kawashiri MA, Nohara A, Inazu A, Mabuchi H, Yamagishi M. Impact of clinical signs and genetic diagnosis of familial hypercholesterolaemia on the prevalence of coronary artery disease in patients with severe hypercholesterolaemia. *Eur Heart J.* (2017) 38:1573–9. doi: 10.1093/eurheartj/ehx004

22. Doi T, Hori M, Harada-Shiba M, Kataoka Y, Onozuka D, Nishimura K, et al. Patients with LDLR and PCSK9 gene variants experienced higher incidence of cardiovascular outcomes in heterozygous familial hypercholesterolemia. *J Am Heart Assoc.* (2021) 10:e018263. doi: 10.1161/JAHA.120.018263

23. Marteau T, Senior V, Humphries SE, Bobrow M, Cranston T, Crook MA, et al. Psychological impact of genetic testing for familial hypercholesterolemia within a previously aware population: a randomized controlled trial. *A J Med Genet A.* (2004) 128:285–93. doi: 10.1002/ajmg.a.30102

24. Marchand M, Chen V, Trinder M, Cermakova L, Brunham LR. Patient perspectives regarding genetic testing for familial hypercholesterolemia. *CJC Open.* (2021) 3:557–64. doi: 10.1016/j.cjco.2020.12.006

25. Holland GJ, French DP, Griffin SJ, Prevost AT, Sutton S, King S, et al. The impact of communicating genetic risks of disease on risk-reducing health behaviour: systematic review with meta-analysis. *BMJ.* (2016) 352:i1102. doi: 10.1136/bmj.i1102

26. Tada H, Takamura M, Kawashiri MA. Familial hypercholesterolemia: a narrative review on diagnosis and management strategies for children and adolescents. *Vascul Health Risk Manag.* (2021) 17:59. doi: 10.2147/VHRM.S266249

27. Kinnear FJ, Wainwright E, Perry R, Lithander FE, Bayly G, Huntley A, et al. Enablers and barriers to treatment adherence in heterozygous familial hypercholesterolaemia: a qualitative evidence synthesis. *BMJ Open.* (2019) 9:e030290. doi: 10.1136/bmjopen-2019-030290

28. Meulenkamp TM, Tibben A, Mollema ED, Van Langen IM, Wiegman A, De Wert GM, et al. Predictive genetic testing for cardiovascular diseases: impact on carrier children. *A J Med Genet A.* (2008) 146:3136–46. doi: 10.1002/ajmg.a.32592

29. Talmud PJ, Shah S, Whittall R, Futema M, Howard P, Cooper JA, et al. Use of low-density lipoprotein cholesterol gene score to distinguish patients with polygenic and monogenic familial hypercholesterolaemia: a case-control study. *Lancet.* (2013) 381:1293–301. doi: 10.1016/S0140-6736(12)62127-8

30. Trinder M, Li X, DeCastro ML, Cermakova L, Sadananda S, Jackson LM, et al. Risk of premature atherosclerotic disease in patients with monogenic versus polygenic familial hypercholesterolemia. *J Am Coll Cardiol.* (2019) 74:512–22. doi: 10.1016/j.jacc.2019.05.043

31. Vrablik M, Tichý L, Freiberger T, Blaha V, Satny M, Hubacek JA. Genetics of familial hypercholesterolemia: new insights. *Front Genet.* (2020) 11:574474. doi: 10.3389/fgene.2020.574474

frontiers | Frontiers in Cardiovascular Medicine

TYPE Case Report
PUBLISHED 25 August 2022
DOI 10.3389/fcvm.2022.992185

OPEN ACCESS

EDITED BY
Neil Morgan,
University of Birmingham,
United Kingdom

REVIEWED BY
Hidenori Tani,
Keio University School of Medicine, Japan
Florentina Pluteanu,
University of Bucharest, Romania

*CORRESPONDENCE
Ping Zhang
zhpdoc@126.com

SPECIALTY SECTION
This article was submitted to Cardiovascular Genetics and Systems Medicine,
a section of the journal
Frontiers in Cardiovascular Medicine

RECEIVED 12 July 2022
ACCEPTED 05 August 2022
PUBLISHED 25 August 2022

CITATION
Yang J, Li K, Lv T, Xie Y, Liu F and Zhang P (2022) Case report: Mexiletine suppresses ventricular arrhythmias in Andersen-Tawil syndrome.
Front. Cardiovasc. Med. 9:992185.
doi: 10.3389/fcvm.2022.992185

Case report: Mexiletine suppresses ventricular arrhythmias in Andersen-Tawil syndrome

Jing Yang[1,2], Kun Li[2], Tingting Lv[2], Ying Xie[2], Fang Liu[2] and Ping Zhang[1,2]*

[1]School of Clinical Medicine, Tsinghua University, Beijing, China, [2]Department of Cardiology, Beijing Tsinghua Changgung Hospital, School of Clinical Medicine, Tsinghua University, Beijing, China

It is arduous to determine clinical solutions for Andersen-Tawil syndrome (ATS) in patients intolerant of β-blocker. Here, we present the case of a 7-year-old boy with periodic paralysis and dysmorphic features who experienced syncope four times during exercise. His ECG revealed enlarged U waves and QU-prolongation associated with ATS-specific U wave patterns, frequent PVCs, and non-sustained bidirectional or polymorphic ventricular tachycardia. The genetic test showed a *de novo* missense R218W mutation of *KCNJ2*. With the diagnosis of ATS and intolerance of β-blocker, the patient was prescribed oral medications of mexiletine 450 mg/day without severe adverse effects. The repeat ECG showed decreased PVC burden from 38 to 3% and absence of ventricular tachycardia. He remained symptom-free during over 2 years of outpatient follow-up. This case demonstrates a new anti-arrhythmic therapy with mexiletine for prevention of life-threatening cardiac events in patients with ATS who are intolerant of β-blocker treatment.

KEYWORDS

mexiletine, ventricular arrhythmias, Andersen-Tawil syndrome, case report, KCNJ2

Introduction

Andersen-Tawil syndrome (ATS) is a rare hereditary arrhythmia disease also classified as long QT syndrome type 7 (LQT7) and is manifested as ventricular arrhythmias (VAs), periodic paralysis, and dysmorphic features. In patients diagnosed with ATS, β-blockers and/or flecainide is primarily recommended according to a Heart Rhythm Society (HRS) expert consensus statement (1). However, it is arduous to determine clinical solutions for patients intolerant of β-blocker considering the lack of access to flecainide in China. Recently, several studies reported that patients with LQT types 1–3 were responsive to anti-arrhythmic mexiletine. However, the efficacy of mexiletine in patients with ATS (LQT7) with *KCNJ2* mutation was rarely reported. Here, we present the effective treatment of a boy who suffered from ATS and recurrent syncope with oral mexiletine for complex ventricular arrhythmias.

Case description

A 7-year-old boy was brought to the local hospital with a main complaint of experiencing syncope four times. The first episode happened during a tug-of-war at the kindergarten about 2 years ago before the visit to our hospital; the boy reported palpitation with amaurosis followed by loss of consciousness without limb convulsions, tongue bites, or incontinence. The boy regained consciousness spontaneously after 20 s and experienced palpitations for the following 10 min. The patient experienced three additional episodes during exercising, climbing stairs, and lifting heavy objects. A 24-h ambulatory electrocardiogram (ECG) demonstrated frequent premature ventricular contractions (PVCs) in bigeminy and non-sustained bidirectional ventricular tachycardia (VT). His serum potassium was 3.9 mmol/L, and the echocardiograms revealed normal cardiac structure and function. Both head computer tomography and electroencephalogram (EEG) appeared to be normal. The local doctors then considered the diagnosis of catecholaminergic polymorphic ventricular tachycardia (CPVT) and prescribed metoprolol 11.25 mg twice per day. He manifested apparent fatigue and cold extremities after taking the pill just for 2 days. Successive electrocardiograms showed sinus bradycardia, and he stopped taking the medication. Two months later, the boy lost consciousness repeatedly after climbing stairs. Therefore, he was transferred to our institution, a university-affiliated teaching hospital, for further evaluation and treatment.

Upon admission, his neurology examination was unremarkable. The physical examination revealed dysmorphology, including mandibular hypoplasia, single palmar crease, and long bone over hyperextension (Figure 1A). His medical history revealed lower limb myasthenia with hypokalemia, but it recovered after potassium supplement. The patient was of normal stature (height of 125 cm) with no family history of sudden cardiac death (SCD).

The patient's surface electrocardiograms (ECGs) taken in the local hospital demonstrated sinus rhythm with frequent PVCs. Enlarged U waves (U wave is defined as an early diastolic deflection after the end of the T wave and is considered enlarged if its amplitude is $\geq$ 0.15 mV and its duration is $\geq$ 210 ms, indicated by red arrows in Figure 2) (2) in leads II, III, aVF, V1-V2, and wide T-U junction (T peak-U peak 240 ms) were shown in ECGs. He had a QTc interval of 380 ms and a QUc interval of 671 ms (QU interval is defined as from onset of QRS to the end of the U wave, and QT and QU intervals are corrected (QTc and QUc) using Bazett's formula for comparison with different heart rates).

A series of electrocardiograms conducted in our hospital revealed frequent PVCs with right bundle branch block (RBBB) morphology and bidirectional PVCs, with QTc of 420 ms and QUc of 680 ms (Supplementary Figure 1). Furthermore,

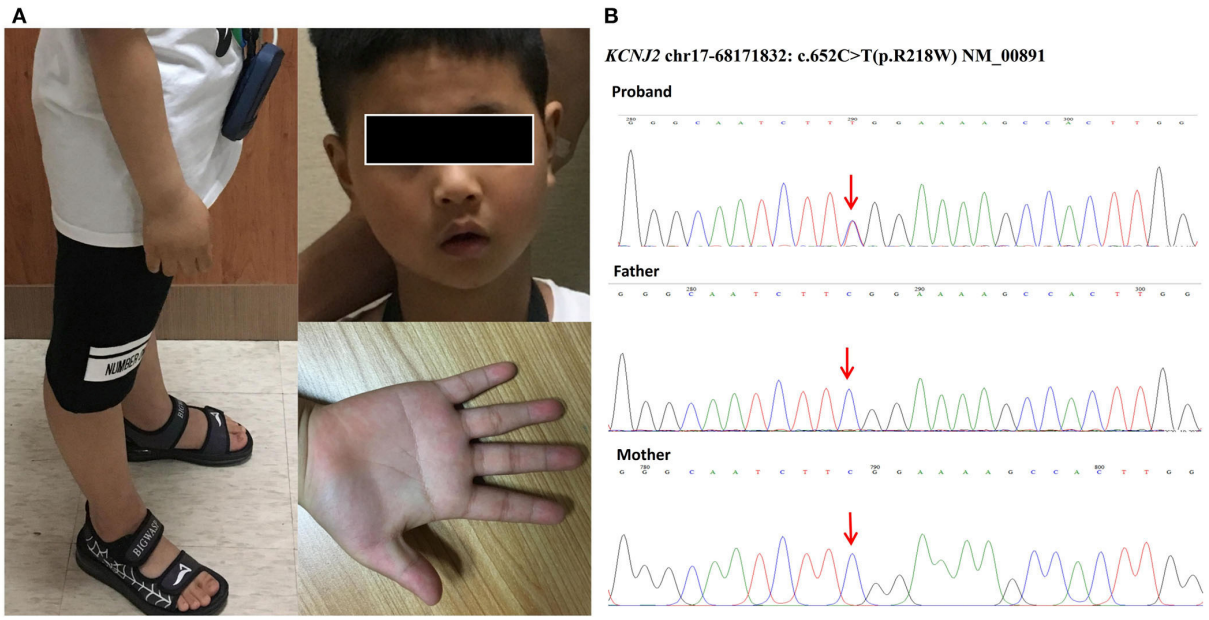

FIGURE 1
(A) Dysmorphology pictures of the boy included mandibular hypoplasia, single palmar crease, and long bone over hyperextension. **(B)** Genetic testing of our patient identified a heterozygous missense mutation named c.652C > T (p.R218W) in the coding region of *KCNJ2*. His parents were tested as wild types without mutations, so our patient carried a *de novo* mutation.

frequent PVCs (38% of total beats) in bigeminy and recurrent asymptomatic non-sustained bidirectional or polymorphic ventricular tachycardia (bVT/pVT, 2,659 times VT) were shown in 24-h Holter recording (GE MARS) (Supplementary Figure 2). Atrial electrical abnormalities were not detected during careful rhythm monitoring. *U* wave was more prominent at a slow heart rate.

The clinical diagnosis of congenital ATS was made based on the typical prolonged QUc interval and enlarged U waves, dysmorphology, and history of paroxysmal hypokalemia. The recurrent syncope was most likely due to sustained VT or ventricular fibrillation (VF). With the diagnosis of ATS and intolerance to β-blocker, the patient was prescribed an oral medication of mexiletine. Considering the high risk of gastrointestinal side effects, a low dose of 300 mg/day (10 mg/kg/day every 8 h) was initially prescribed. Then, the prescribed dosage was gradually increased to 450 mg/day (15 mg/kg/day every 8 h), for which the patient reported occurrence of mild side effects including nausea and loss of appetite. Three days after taking mexiletine, continuous electrocardiograph monitoring showed suppressed ventricular arrhythmias. A 24-h Holter was performed after the treatment showed decreased PVC burden from 38 to 3% of total beats (Figure 3) and absence of ventricular tachycardia. We also measured the patient's electrocardiographic indexes of SCD prediction including heart rate turbulence (turbulence onset and turbulence slope, TO and TS) and T wave alternans, TWA). The result showed a significant difference before and after the treatment (TO 1.84 vs.−1.24%, TS 3.44 vs. 14.17 ms/RR, and TWA 98 uV vs. 77 uV in lead V1). Additionally, the patient was given an exercise stress test (Bruce protocol). The test results revealed a QUc 730 ms at the baseline heart rate 78 bpm and 590 ms during exercise with a heart rate of 121 bpm, a *U* wave infusion with the *P* wave, and a "U on P" sign (*U*-wave masquerading *P*-wave) at peak heart rate 144 bpm (Supplementary Figure 3). Neither ventricular nor atrial arrhythmia was induced during exercise after taking mexiletine.

Considering the genetic characteristics, we screened the ECGs of his 1st-degree blood relatives. The QT interval was completely normal without a U wave in his parents. The genetic testing of our patient identified a heterozygous missense mutation named c.652C > T (p.R218W, NM_00891, Figure 1B) in the C-terminal interaction domain of *KCNJ2*. The mutation

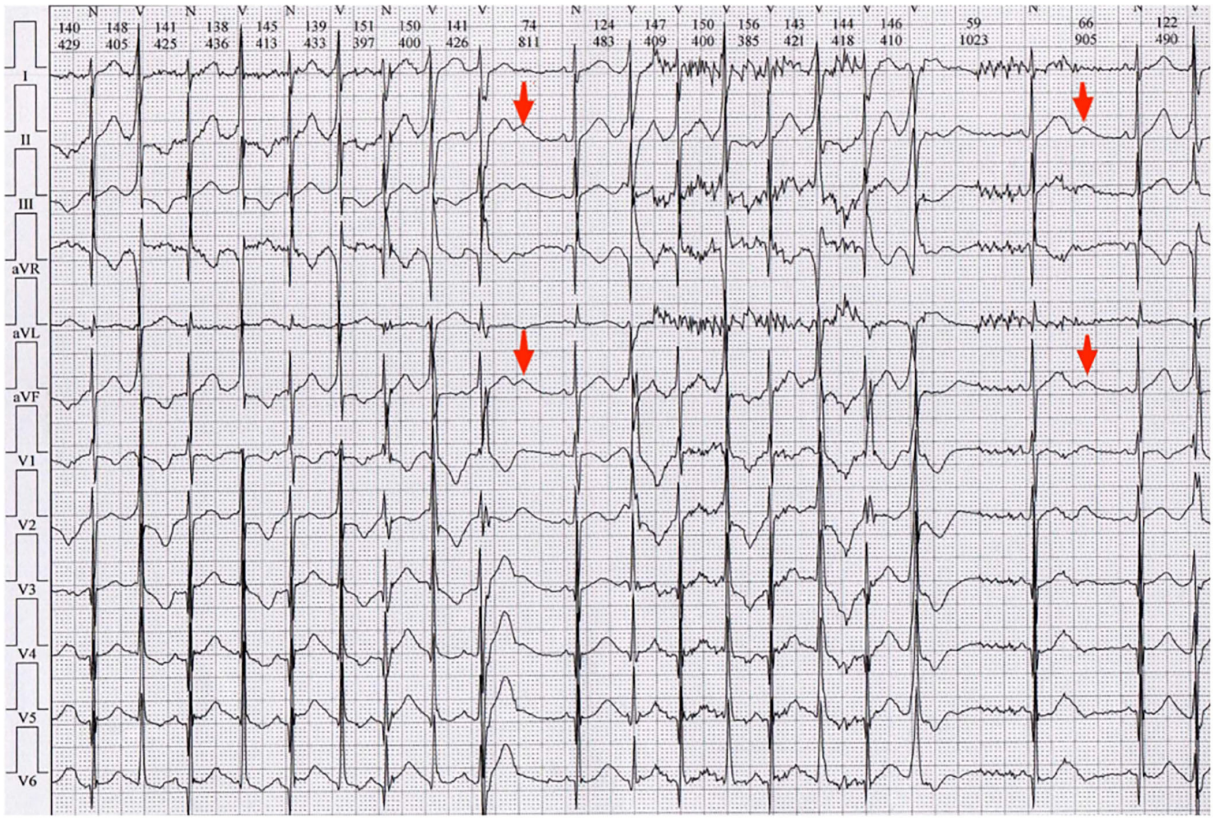

FIGURE 2
Electrocardiogram (ECG) of the local hospital demonstrated sinus rhythm with frequent PVCs. Enlarged *U* waves (*U* wave is considered enlarged if its amplitude is ≥ 0.15 mV and its duration is ≥ 210 ms, indicated by red arrows) in leads II, III, aVF, V1-V2, and wide T-U junction (Tp-Up, 240 ms) were shown in ECGs. He had QTc of 380 ms and QUc of 671 ms.

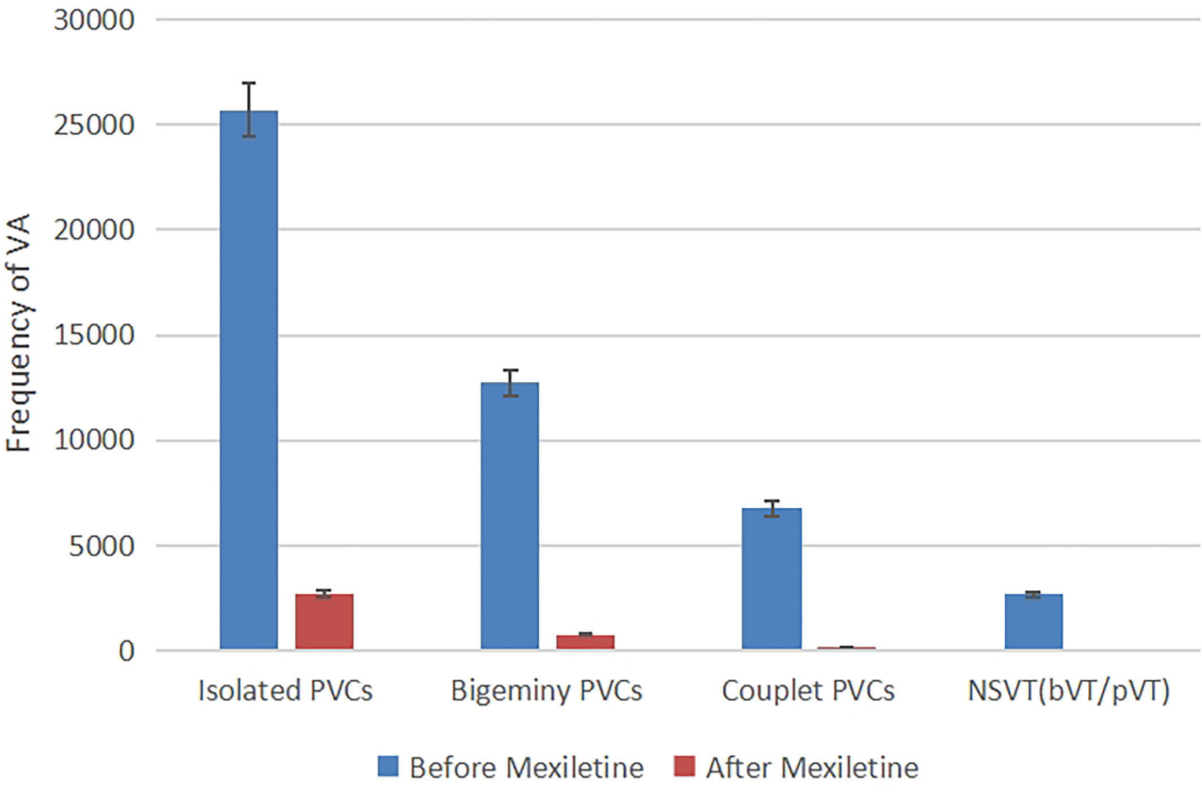

FIGURE 3
Frequency of ventricular arrhythmia in 24-h Holter recording before and after taking mexiletine 3 days, kinds of ventricular arrhythmias (isolated PVCs, bigeminy PVCs, couplet PVCs, and non-sustained ventricular tachycardia) were suppressed.

was a hot spot that caused loss of function and resulted in a dominant-negative effect on Kir2.1 (3). His parents were tested as wild types without mutations (Figure 1B). Therefore, the result showed that our patient carried a *de novo* mutation.

The patient was discharged from our hospital with a prescription of mexiletine (15 mg/kg/day every 8 h). The patient reported no further experience of severe adverse effects. For over 2 years of outpatient follow-up, he remained symptom-free. A repeat 24-h Holter showed < 0.1% PVC burden. The QUc interval was shortened from 680 to 610 ms with no change in U wave amplitude (Supplementary Figure 4).

Discussion

Andersen-Tawil syndrome (ATS) is a rare inherited disease characterized by specific ventricular arrhythmias including bidirectional or polymorphic ventricular tachycardia (bVT/pVT), periodic paralysis, and dysmorphic features (2). BVT/pVT has been popularly described in ATS excluding digitalis toxicity and catecholaminergic polymorphic ventricular tachycardia (CPVT). Since both ATS and CPVT are rare inherited arrhythmic disorders, there are some clinical similarities between patients with ATS and those with CPVT. Careful differential diagnosis between ATS and CPVT is important before treatment. First, typical QUc prolongation is obvious in widespread limb and/or precordial leads of baseline electrocardiograms in ATS. Second, frequent premature ventricular contractions (PVCs) with right bundle branch block (RBBB) morphology are popular in patients with ATS, while those with left bundle branch block (LBBB) morphology are dominant in patients with CPVT. Third, ventricular arrhythmias are induced during exercise stress test even on effective medication in patients with CPVT while suppressed at peak exercise in patients with ATS (4).

There are two types of ATS based on gene mutation. Type 1 ATS, in which a mutation in the *KCNJ2* gene can be identified, accounts for about 60–70% of all patients with ATS, while type 2 (ATS2), of which the genetic cause is still unknown, accounts for the remaining 30–40% of ATS cases. The *KCNJ2* gene encodes the Kir2.1 inward rectifier potassium channel protein, which mainly causes prolongation of phase 3 of the action potential with reduced inward rectifier potassium current (I_{K1}) resulting from *KCNJ2* mutations (3). Cardiac repolarization duration prolongation leads to distinctive T-U wave morphology and a variety of ventricular arrhythmias. According to the latest ATS-iPS cell-derived cardiomyocytes, the mechanism of ventricular arrhythmia is associated with intracellular calcium overload and sodium/calcium exchanger (NCX) mediated triggered activity (5).

In the expert consensus on the treatment of ATS, the β-adrenergic blocker is a primary option including metoprolol or propranolol in China. However, treatment response varies in patients with the type of arrhythmia. Proportional LQT2 patients and a majority of LQT3 patients showed QT interval prolongation in slow heart rate after taking β-blocker. And the efficacy of β-blockers was controversial for counteracting VAs in patients with ATS (6). In our case, the boy experienced apparent fatigue and bradycardia after receiving metoprolol 11.25 mg twice a day for only 2 days. Flecainide is an alternative anti-arrhythmic agent for patients' intolerant of β-blocker. It can significantly suppress ventricular arrhythmia by directly blocking NCX and irregular calcium release besides blocking the fast-inward sodium channel. Additionally, flecainide may activate I_{K1} in ventricular myocytes (7). Unfortunately, flecainide is not yet available in China.

Therefore, the class Ib anti-arrhythmic drug mexiletine was proposed as an alternative therapy for patients with partial LQT2, LQT3, and LQT8 (Timothy Syndrome). To date, mexiletine treatment efficacy in ATS (LQT7) with *KCNJ2* mutations has rarely been reported. The mechanism underlying the suppression of VAs by mexiletine in ATS has not been fully understood. One possible explanation is that mexiletine inhibits the late Na current (I_{Na-L}), thereby reducing NCX and intracellular calcium during the repolarization phase. The physiologic I_{Na-L} is intensified by loss of potassium channel function including I_{KS} and I_{K1}. Additionally, the increased I_{Na-L} at lower heart rate was named as reverse use-dependence (8), which explains the treatment failure of beta-blocker in patients with ATS. It is important to note that the ratio of the inhibitory concentration at 50% block (IC50) for I_{Na-L} block by mexiletine falls within the therapeutic concentration range (9). There are no studies on the effect of mexiletine on the I_{K1} current. Another interpretation is that mexiletine shortens the action potential duration (APD) of ventricular muscles by activation of the ATP-sensitive potassium channel (K_{ATP}) (10), as the QUc interval is shortened by 70 ms in our patient. The most popular adverse effects associated with mexiletine are minor gastrointestinal or neurological effects, which can be tolerated.

In summary, our case demonstrates a new anti-arrhythmic therapy with mexiletine for prevention of life-threatening cardiac events in patients with ATS who are intolerant of β-blocker. Future studies are needed to provide empirical supports for the aforementioned treatment and to further examine the underlying mechanism of its efficacy.

Data availability statement

The original contributions presented in the study are included in the article/Supplementary materials, further inquiries can be directed to the corresponding author.

Ethics statement

The studies involving human participants were reviewed and approved by Ethics Committee of Beijing Tsinghua Changgung Hospital. Written informed consent to participate in this study was provided by the participants' legal guardian/next of kin.

Author contributions

The study was designed by JY and PZ. ECG data collection was performed by KL. The *KCNJ2* gene mutation was identified by TL by Sanger sequencing. The clinical care and treatment follow-up of the patient were performed by YX and FL. All authors contributed to the article, conception of the study, and approved the submitted version.

Funding

This study was funded by Beijing Municipal Administration of Hospitals Clinical Medicine Development of Special Funding (No. ZYLX201831).

Acknowledgments

We would like to acknowledge the patient who participated in our study.

Conflict of interest

The authors declare that the research was conducted in the absence of any commercial or financial relationships that could be construed as a potential conflict of interest.

Publisher's note

Supplementary material

The Supplementary Material for this article can be found online at: https://www.frontiersin.org/articles/10.3389/fcvm.2022.992185/full#supplementary-material

References

1. Priori SG, Wilde AA, Horie M, Cho Y, Behr ER, Berul C, et al. HRS/EHRA/APHRS expert consensus statement on the diagnosis and management of patients with inherited primary arrhythmia syndromes: document endorsed by HRS, EHRA, and APHRS in May 2013 and by ACCF, AHA, PACES, and AEPC in June 2013. *Heart Rhythm.* (2013) 10:1932–63. doi: 10.1016/j.hrthm.2013.05.014

2. Zhang L, Benson DW, Tristani-Firouzi M, Ptacek LJ, Tawil R, Schwartz PJ, et al. Electrocardiographic features in Andersen-Tawil syndrome patients with KCNJ2 mutations: characteristic T-U-wave patterns predict the KCNJ2 genotype. *Circulation.* (2005) 111:2720–6. doi: 10.1161/CIRCULATIONAHA.104.472498

3. Plaster NM, Tawil R, Tristani-Firouzi M, Canún S, Bendahhou S, Tsunoda A, et al. Mutations in Kir21 cause the developmental and episodic electrical phenotypes of Andersen's syndrome. *Cell.* (2001) 105:511–9. doi: 10.1016/S0092-8674(01)00342-7

4. Inoue YY, Aiba T, Kawata H, Sakaguchi T, Mitsuma W, Morita H, et al. Different responses to exercise between Andersen-Tawil syndrome and catecholaminergic polymorphic ventricular tachycardia. *Europace.* (2018) 20:1675–82. doi: 10.1093/europace/eux351

5. Nguyen H L, Pieper G H, Wilders R. Andersen-Tawil syndrome: clinical and molecular aspects. *Int J Cardiol.* (2013) 170:1–16. doi: 10.1016/j.ijcard.2013.10.010

6. Bökenkamp R, Wilde AA, Schalij MJ, Blom NA. Flecainide for recurrent malignant ventricular arrhythmias in two siblings with Andersen-Tawil syndrome. *Heart Rhythm.* (2007) 4:508–11. doi: 10.1016/j.hrthm.2006.12.031

7. Miyamoto K, Aiba T, Kimura H, Hayashi H, Ohno S, Yasuoka C, et al. Efficacy and safety of flecainide for ventricular arrhythmias in patients with Andersen-Tawil syndrome with KCNJ2 mutations. *Heart Rhythm.* (2015) 12:596–603. doi: 10.1016/j.hrthm.2014.12.009

8. Yu S, Li G, Huang CL, Lei M, Wu L. Late sodium current associated cardiac electrophysiological and mechanical dysfunction. *Pflugers Arch.* (2018) 470:461–9. doi: 10.1007/s00424-017-2079-7

9. Makielski JC. Late sodium current: a mechanism for angina, heart failure, and arrhythmia. *Trends Cardiovasc Med.* (2016) 26:115–22. doi: 10.1016/j.tcm.2015.05.006

10. Sato T, Shigematsu S, Arita M. Mexiletine-induced shortening of the action potential duration of ventricular muscles by activation of ATP-sensitive K+ channels. *Br J Pharmacol.* (1995) 115:381–2. doi: 10.1111/j.1476-5381.1995.tb16342.x

frontiers | Frontiers in Cardiovascular Medicine

TYPE Case Report
PUBLISHED 14 September 2022
DOI 10.3389/fcvm.2022.974842

OPEN ACCESS

EDITED BY
Olivier M. Vanakker,
Ghent University, Belgium

REVIEWED BY
Zizhong Hu,
Nanjing Medical University, China
D. Ch. Zhang,
Pizhou Chinese Hospital, China
Yaowen Song,
Shanxi Eye Hospital, China

*CORRESPONDENCE
Bangtao Yao
yaobamtao_njmu@163.com
Gang Liu
lg1974329@163.com
Xiaogui Zhao
zhaoxiaogui_jsph@163.com

SPECIALTY SECTION
This article was submitted to Cardiovascular Genetics and Systems Medicine,
a section of the journal
Frontiers in Cardiovascular Medicine

RECEIVED 21 June 2022
ACCEPTED 23 August 2022
PUBLISHED 14 September 2022

CITATION
Yao B, Chen X, Liu G and Zhao X (2022) Case report: Spontaneous bilateral intraocular lens dislocation in a patient with homocystinuria.
Front. Cardiovasc. Med. 9:974842.
doi: 10.3389/fcvm.2022.974842

Case report: Spontaneous bilateral intraocular lens dislocation in a patient with homocystinuria

Bangtao Yao[1]*, Xujian Chen[2], Gang Liu[1]* and Xiaogui Zhao[1]*

[1]Department of Ophthalmology, Nanjing Lishui People's Hospital, Zhongda Hospital Lishui Branch, Southeast University, Nanjing, China, [2]Department of Ophthalmology, Nanjing Lishui District Hospital of Traditional Chinese Medicine, Nanjing, China

Background: Spontaneous bilateral intraocular lens dislocation of the vitreous cavity is a rare ocular disorder. This article aims to comprehensively describe bilateral spontaneous intraocular lens dislocation with unilateral lamellar macular hole and retinoschisis in a Chinese woman with homocystinuria.

Case presentation: A 72-year-old Chinese woman with homocystinuria presented with a painless bilateral blurring of vision. The slit lamp showed the absence of lenses in both eyes. B-ultrasound and orbital computed tomography (CT) demonstrated bilateral posterior dislocation of the crystalline lenses, and spectral-domain optical coherence tomography (SD-OCT) revealed a lamellar macular hole and retinoschisis in the right eye. Biochemical examination demonstrated that the total homocysteine level was moderately elevated.

Conclusion: This report is the first to present an extensive and valuable description of bilateral intraocular lens dislocation with unilateral lamellar macular hole and retinoschisis secondary to homocystinuria. We have demonstrated that this case was spontaneous and chronic. CT is an effective diagnostic tool for patients with ectopia lentis. Early diagnosis and suitable management of patients with homocystinuria are essential to prevent these complications.

KEYWORDS

ectopia lentis, homocystinuria, spontaneous, high myopia, lamellar macular hole, osteoporosis, CT

Introduction

Homocystinuria is a rare autosomal recessive disease mainly caused by the absence of cystathionine-β-synthase, which is involved in the methionine metabolism pathway, affecting 0.82 in 100,000 the population worldwide (1, 2). Untreated cases result in multisystemic disorders, including ocular diseases, skeletal abnormalities, developmental delay, and thromboembolic events (3).

Ectopia lentis, also known as lens subluxation or dislocation, is the most significant ocular complication in patients with homocystinuria (4). Previous reports have documented that cystathionine-β-synthase deficiency could influence the nutritional metabolism of the lens zonule, leading to their degeneration and disruption (5). A completely dislocated lens can move freely from the original position into the anterior chamber or vitreous cavity, which may result in acute angle-closure glaucoma and uveitis (1, 6).

To our knowledge, complete lens dislocation into the vitreous cavity associated with a lamellar macular hole and retinoschisis in homocystinuria has not been reported.

Case description

A 72-year-old Chinese woman with homocystinuria presented with a bilateral painless blurring of vision for several decades. She said that the problem had occurred since childhood; however, it had remained untreated. The patient did not complain of metamorphopsia or recent vision deterioration. The patient did not also complain of any other systemic symptoms, such as chest tightness, palpitation, dizziness, or headache. The patient had no history of trauma or surgery, high blood pressure, diabetes mellitus, hyperlipidemia, coronary atherosclerotic heart disease, Marfan syndrome, or Marchesani syndrome. The patient's parents were close relatives.

On examination, her height and weight were 165 cm and 66.2 kg, respectively. The best-corrected visual acuity was 20/300 OD and 20/250 OS, with a refractive status of +5.25/−2.75 × 25 OD and +5.75/−3.25 × 154 OS. The anterior segment showed the absence of lenses in both eyes. Fundus examination revealed optic atrophy, staphyloma, and chorioretinal atrophy. The initial intraocular pressure was 16 mm Hg OD and 17 mm Hg OS, and the axial length was 31.11 mm OD and 29.33 mm OS. B-ultrasound showed that the lenses were located in the vitreous cavity in both eyes (red arrows, **Figure 1**). Orbital computed tomography (CT) demonstrated free-floating lenses in the posterior poles (yellow arrows, **Figure 2**), and spectral-domain optical coherence tomography (SD-OCT) revealed a lamellar macular hole and retinoschisis in the right eye (**Figure 3**).

The plasma total homocysteine concentration was 49.1 μmol/L (normal 0–15). The X-ray bone density test showed osteoporosis (−2.9 g/cm^2), and a slender appearance with arachnodactyly was not observed. All other investigations were normal.

The patient was diagnosed with homocystinuria, osteoporosis, ectopia lentis, lamellar macular hole, and retinoschisis. The patient was treated with vitamin B6 and folic acid. She chose to defer surgery and was advised to undergo physical and ophthalmic examinations every 6 months. During the 3-year follow period, her condition remained stable. The patient did not provide any other chief complaints. Her intraocular pressure was normal, and SD-OCT images remained unchanged.

Discussion

Homocystinuria is a rare autosomal recessive metabolic disease caused by cystathionine-β-synthase deficiency (1). It is diagnosed by elevated plasma total homocysteine concentration (7). Clinically, it is characterized by ocular disorders, skeletal abnormalities, developmental delays, and thromboembolic events (3).

Ocular complications secondary to homocystinuria include ectopic lentis, high myopia, secondary pupillary block glaucoma, optic atrophy, and retinal detachment. Ectopia lentis (lens subluxation or dislocation) is the most significant manifestation of these complications and was first described by Dr. Karl Stellwag in 1856 (1, 4).

Ectopia lentis is typically inferonasal and has been observed in more than 90% of untreated patients with homocysteinemia in their third decade of life (1). Age has been reported as a predictor of zonular instability and disruption, and complete dislocation is frequently observed in older patients (1). The lens can move significantly either into the anterior chamber or the vitreous cavity with or without angle-closure glaucoma. However, bilateral posterior lens luxation is rare.

The biochemical mechanism of ectopia lentis in homocystinuria is not yet fully understood. Defects in fibril disulfide bridges may provide a biochemical basis for lens dislocation (5). Previous reports have shown that the deficiency of cystathionine-β-synthase could influence the nutritional metabolism of the lens zonule, which causes their degeneration and rupture. Furthermore, elevated homocysteine levels may interfere with the cross-linking of sulfhydryl groups in elastin (8).

Myopia is secondary to lens instability and axial elongation in patients with homocysteinemia. Previous reports have documented that high myopia is related to pathological changes in weak scleral connective tissue, and it was present in almost 45% of homocystinuria cases (4). Hsia et al. suggested that a lamellar macular hole in association with retinoschisis is specific to myopic tractional maculopathy (9). In the present case, a lamellar macular hole and retinoschisis secondary to high myopia were observed on SD-OCT images. A lamellar macular hole is a common macular structural defect in high myopia tractional maculopathy; however, its formation is complicated. Lamellar hole-associated epiretinal proliferation and posterior vitreous adhesion occur more frequently in eyes with high myopia (10).

In the present case, homocystinuria presented with ophthalmic manifestations of osteoporosis. Other complications, such as developmental delay and thromboembolism, were not present, possibly due to the well-controlled homocysteine concentration for decades.

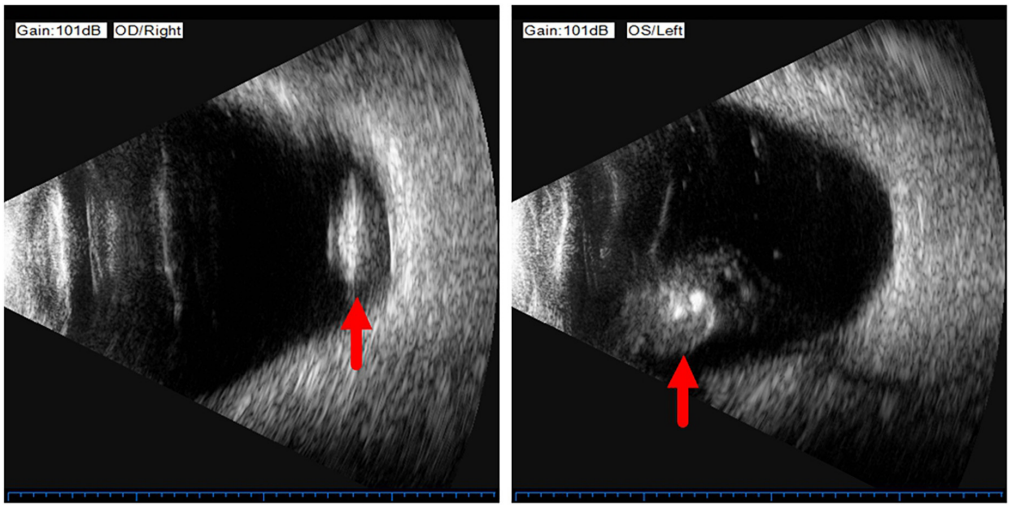

FIGURE 1
B-ultrasound showed that the lenses were located in the vitreous cavity in both eyes (red arrows).

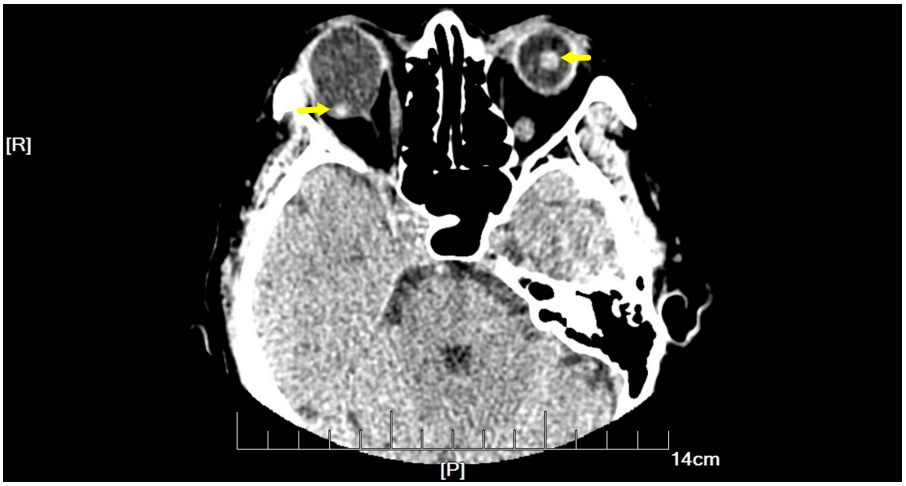

FIGURE 2
Orbital computed tomography (CT) demonstrated free-floating lenses in the posterior poles (yellow arrows).

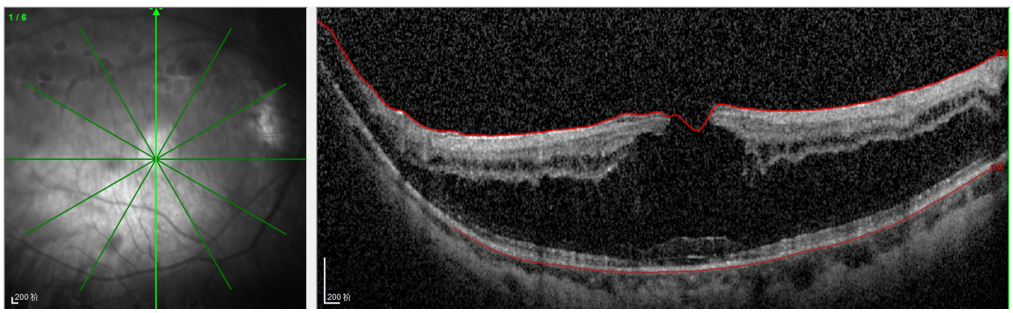

FIGURE 3
Spectral-domain optical coherence tomography (SD-OCT) revealed the lamellar macular hole and retinoschisis in her right eye.

Bilateral ectopia lentis is closely associated with several systemic disorders (6). Therefore, differential diagnoses, such as Marfan syndrome, should be carefully addressed. Patients with Marfan syndrome typically have arachnodactyly and a tall slender appearance, and ectopia lentis is commonly subluxated and superior temporal (11).

Clinically, vitamin B6 and folic acid have proven effective for homocystinuria, reducing the incidence of complications (1). However, the treatment of ectopia lentis remains controversial. Surgical intervention in patients with anterior lens dislocation with or without secondary acute glaucoma is recommended. Surgical decisions must be made with caution in cases, where the lens is dislocated into the vitreous cavity, as postoperative retinal detachment and vitreal prolapse have been reported (12). In the present case, the patient chose to defer surgery and was treated with vitamin B6 and folic acid. During the 3-year follow-up period, her condition remained stable.

However, the present study has some limitations. First, the sample size of this study was small. Second, the enzyme activity assay was not performed.

In conclusion, we described the first case of bilateral intraocular lens dislocation with a lamellar macular hole and retinoschisis in a patient with homocystinuria. We have demonstrated that this case was spontaneous and chronic. Neonatal screening and early diagnosis are essential for preventing these complications.

Data availability statement

The original contributions presented in this study are included in the article/**Supplementary material**, further inquiries can be directed to the corresponding authors.

Ethics statement

The studies involving human participants were reviewed and approved by the Nanjing Lishui People's Hospital. The patient/participant provided their written informed consent to participate in this study and for the publication of this case report.

Author contributions

BY wrote the manuscript, established the diagnosis, and reviewed the manuscript. XC dealt with the figures and consulted the literature. GL edited the manuscript. XZ reviewed the manuscript. All authors have read and approved the final manuscript.

Conflict of interest

The authors declare that the research was conducted in the absence of any commercial or financial relationships that could be construed as a potential conflict of interest.

Publisher's note

Supplementary material

The Supplementary Material for this article can be found online at: https://www.frontiersin.org/articles/10.3389/fcvm.2022.974842/full#supplementary-material

References

1. Harrison DA, Mullaney PB, Mesfer SA, Awad AH, Dhindsa H. Management of ophthalmic complications of homocystinuria. *Ophthalmology.* (1998) 105:1886–90. doi: doi.org/10.1016/S0161-6420(98)91035-1

2. Weber Hoss GR, Sperb-Ludwig F, Schwartz IVD, Blom HJ. Classical homocystinuria: a common inborn error of metabolism? An epidemiological study based on genetic databases. *Mol Genet Genomic Med.* (2020) 8:e1214. doi: doi.org/10.1002/mgg3.1214

3. Sellos-Moura M, Glavin F, Lapidus D, Evans K, Lew CR, Irwin DE. Prevalence, characteristics, and costs of diagnosed homocystinuria, elevated homocysteine, and phenylketonuria in the United States: a retrospective claims-based comparison. *BMC Health Serv Res.* (2020) 20:183. doi: 10.1186/s12913-020-5054-5

4. Gus PI, Donis KC, Marinho D, Martins TF, de Souza CFM, Carloto RB, et al. Ocular manifestations in classic homocystinuria. *Ophthal Genet.* (2021) 42:71–4. doi: doi.org/10.1080/13816810.2020.1821384

5. Gerding H. Ocular complications and a new surgical approach to lens dislocation in homocystinuria due to cystathionine-beta-synthetase deficiency. *Eur J Pediatr.* (1998) 157(Suppl. 2):S94–101. doi: 10.1007/pl00014312

6. Miraftabi A, Zand A, Abri Aghdam K. Unilateral and spontaneous complete anterior dislocation of the crystalline lens in a patient with homocystinuria. *Cureus.* (2021) 13:e14655. doi: 10.7759/cureus.14655

7. Garland J, Prasad A, Vardy C, Prasad C. Homocystinuria: challenges in diagnosis and management. *Paediatr Child Health.* (1999) 4:557–62.

8. Hua N, Ning Y, Zheng H, Zhao L, Qian X, Wormington C, et al. Recurrent dislocation of binocular crystal lenses in a patient with cystathionine beta-synthase deficiency. *BMC Ophthalmol.* (2021) 21:212. doi: 10.1186/s12886-021-01974-8

9. Hsia Y, Ho TC, Yang CH, Hsieh YT, Lai TT, Yang CM. Clinical characteristics and long-term evolution of lamellar macular hole in high myopia. *PLoS One.* (2020) 15:e0232852. doi: 10.1371/journal.pone.0232852

10. Lai TT, Yang CM. Lamellar hole-associated epiretinal proliferation in lamellar macular hole and full-thickness macular hole in high myopia. *Retina.* (2018) 38:1316–23. doi: doi.org/10.1097/IAE.0000000000001708

11. Morris AA, Kožich V, Santra S, Andria G, Ben-Omran TI, Chakrapani AB, et al. Guidelines for the diagnosis and management of cystathionine beta-synthase deficiency. *J Inherit Metab Dis.* (2017) 40:49–74. doi: doi.org/10.1007/s10545-016-9979-0

12. Monera Lucas CE, Escolano Serrano J, Romero Valero D, Fernández Martínez C, Navarro Navarro A, Martínez Toldos JJ. Posterior bilateral lens luxation in an agitated patient: cause or consequence? *Arch Soc Esp Oftalmol.* (2021) 96:93–6. doi: doi.org/10.1016/j.oftale.2020.07.015

frontiers | Frontiers in Cardiovascular Medicine

TYPE Case Report
PUBLISHED 16 September 2022
DOI 10.3389/fcvm.2022.899283

OPEN ACCESS

EDITED BY
Neil Morgan,
University of Birmingham,
United Kingdom

REVIEWED BY
Kazuma Sugie,
Nara Medical University, Japan
Friederike Zunke,
University Hospital Erlangen, Germany

*CORRESPONDENCE
Hong Wang
alextowh@163.com

†These authors have contributed equally to this work

SPECIALTY SECTION
This article was submitted to Cardiovascular Genetics and Systems Medicine,
a section of the journal
Frontiers in Cardiovascular Medicine

RECEIVED 18 March 2022
ACCEPTED 20 June 2022
PUBLISHED 16 September 2022

CITATION
Wang JJ, Yu B, Song X and Wang H (2022) *De novo LAMP2* insertion mutation causes cardiac-only Danon disease: A case report.
Front. Cardiovasc. Med. 9:899283.
doi: 10.3389/fcvm.2022.899283

De novo LAMP2 insertion mutation causes cardiac-only Danon disease: A case report

James Jiqi Wang[1,2†], Bo Yu[1,2†], Xiuli Song[1,2] and Hong Wang[2,3*]

[1]Division of Cardiology, Department of Internal Medicine, Tongji Medical College, Tongji Hospital, Huazhong University of Science and Technology, Wuhan, China, [2]Hubei Key Laboratory of Genetics and Molecular Mechanism of Cardiological Disorders, Tongji Medical College, Tongji Hospital, Huazhong University of Science and Technology, Wuhan, China, [3]Genetic Diagnostics Center, Tongji Medical College, Tongji Hospital, Huazhong University of Science and Technology, Wuhan, China

Danon disease is a rare disease caused by glycogen storage lysosomal disorder. It is related to the pathogenic mutation of the *LAMP2* gene. In this case report, we present a patient with a novel pathogenic mutation (c.764_765insGA) with cardiac-only symptoms. Her family members do not carry the same mutation she does, suggesting this is a *de novo* mutation. Further tests revealed vacuoles and glycogen disposition in the patient's heart tissue and a significant decrease in LAMP2 protein expression. Protein structure remodeling of LAMP2 predicted that the mutant protein has conformational change lacking an important transmembrane domain, subsequently causing protein destabilization.

KEYWORDS

Danon disease, Sanger sequencing, genetic diagnosis, *LAMP2*, hypertrophy

Introduction

Danon disease (OMIM: 300257) is an X-linked dominant disorder caused by a defect of the lysosome-associated membrane protein 2 (LAMP2) gene (1). LAMP2 is essential in the progress of the autophagosome maturation (2). Mutations of *LAMP2* identified in Danon disease lead to splicing defects or protein truncation, which underlies LAPM2 deficiency in skeletal and cardiac muscles (1). Defect of *LAMP2* caused impaired autophagosome-lysosome fusion and degradation, which leads to failure of cellular autophagy and accumulation of glycogen granules and autophagic vacuoles (3).

Danon disease is clinically characterized by a triad of skeletal myopathy, intellectual disability, and cardiomyopathy (4). Due to haploinsufficiency, male patients are usually more severely affected than female patients and are often the proband of this disease (5). The impact on the skeletal muscle manifests as myalgia, poor exercise tolerance, and fatigue (1). Serum creatine kinase (CK) levels are often elevated in male patients with skeletal muscle involvement and in female patients, serum CK levels are usually normal or mildly elevated (1). Mild to moderate intellectual disabilities are found in 70%-100% of male patients and 50% of female patients exhibit mild mental disorder (6, 7). Patients with Danon disease mainly manifest conduction abnormalities and cardiomyopathy. Wolf-Parkinson-White syndrome predominates in electrocardiograph (ECG) abnormalities (69% of patients) and others include supraventricular tachycardia, delta waves, high precordial voltage, and

complete ventricular block (AVB) (8). Cardiomyopathy is the predominant and most life-threatening manifestation for a patient with Danon disease, including dilated cardiomyopathy and hypertrophic cardiomyopathy (HCM). Cardiac syndromes include chest tightness, heart murmur, fatigue, or palpation. In male patients, cardiac symptoms usually began in infancy/childhood or adolescence, while females present with slower progression and later onset of the disease. In some female patients, the cardiac disease may act as an isolated clinical feature (73%) (2).

The exact prevalence of Danon disease is not clear. The diagnosis of Danon disease is gradually increasing with the development of gene testing. Unfortunately, cardiac transplantation and implantable cardioverter defibrillator (ICD) are the only therapeutic interventions for Danon disease (9, 10). According to a study, without heart transplantation, the mean age of death in males is 19.0 ± 8.0 and 34.6 ± 15.5 in females (6). Thus, an early diagnosis and clinical intervention are essential to prevent the lethal prognosis of this disease.

Herein we report a Danon disease case carrying a novel frameshift (c.764_765insGA) *LAMP2* variant who only manifested cardiac symptoms. Her family members did not share her mutation or phenotype, suggesting that this was a *de novo* mutation.

Materials and methods

Whole exome sequencing

The proband and her family members' genome DNA were extracted from their peripheral blood *via* QIAamp DNA Mini Kit (Qiagen, Germany) and quantified with the Nanodrop 2000 (Life Technology, USA).

To thoroughly identify the potentially pathogenic gene, whole exome sequencing was carried out using the proband's DNA. Qualified samples were exome sequenced using the SureSelect Human All Exon library kit (Agilent, USA) and Novaseq 6000 or Hiseq Xten platform in the paired-end mode of 150 base pairs (Illumina, California, USA). The whole exome sequencing (WES) data were processed in accordance with the best practice of The Genome Analysis Toolkit. The resulting variants were annotated using ANNVAR. Rare variants were defined as those with a minor allele frequency of < 0.001 in East Asian databases from ExAC, The 1000 Genomes Project, and gnomAD.

Sanger sequencing

Potentially identified mutation and low coverage regions (<20 folds) were verified *via* Sanger sequencing with specific primers. Validated mutations were also Sanger sequenced in the patient's relatives and extra 800 unrelated Chinese health controls.

Pathological analysis and immunohistochemistry analysis

Biopsy specimens were obtained from the patient's left ventricle. Hematoxylin-eosin (HE) and Periodic acid-Schiff (PAS) staining were performed to investigate the patient's myocardial structure and glycogen disposition. For immunohistochemistry, a primary antibody against LAMP2 (1:100 dilution) was obtained from Abclonal (China, A14017) and a secondary antibody (goat anti-rabbit, 1:2000 dilution) was obtained from Abcam (England, ab205718).

Proteome expression analysis

We performed proteomic analysis to further investigate protein expression caused by this mutation using white blood cells from the patient's peripheral blood. Workflow of blood samples prepared before the proteomic measurement is described elsewhere (11). Samples were measured using an LC-MS instrument consisting of an EASY-nLC 1200 ultra-high-pressure system (Thermo Fisher Scientific) coupled *via* a nano-electrospray ion source to Fusion Lumos Orbitrap (Thermo Fisher Scientific). The mass spectrometry proteomics data have been deposited to the ProteomeXchange Consortium (http://proteomecentral.proteomexchange.org) *via* the iProX partner repository with the dataset identifier PXD034265. LAMP2/ACTB ratio was used to compare the expression of LAMP2 between the patient and healthy controls.

Protein structure remodeling

We predicted the structure of the mutant protein using a deep learning technique. The specific protein structural modeling open-source code using AlphaFold Protein Structure Database is available at (https://github.com/deepmind/alphafold) (DeepMind Technologies, USA). Figures were presented *via* UCSF ChimeraX (RBVI, USE) (12).

Results

Case report

The proband was a 25-year-old female who complained of intermittent chest distress and shortness of breath for half

a month before being admitted to our hospital. Symptoms were relieved automatically after a few minutes. According to the patient, she had experienced similar cardiac symptoms in the past few years with no significant inducement. The patient had mild myopia which can be corrected with glasses. Intelligence Quotient (IQ) test showed normal results (IQ: 111). She denied having symptoms of skeletal muscle and the electromyogram did not show abnormal electrical activity. Her parents (father, 52 y, and mother, 50 y) did not show any cardiac, skeletal muscle, or mental disorder and neither did her 6-year-old brother. On admission, her body temperature was 36.3°C, pulse 60 bpm, respiratory rate 20/min, and blood pressure 90/61 mmHg. Blood biochemistry tests indicated slightly elevated aspartate aminotransferase (AST, 42 U/L, normal range: 0–32 U/L), alanine aminotransferase (ALT, 38 U/L, normal range: 0–33 U/L), and normal level of creatine kinase (CK, 75 U/L, normal range: 0–170 U/L). Blood routine examination revealed elevated white blood cells (WBC, 16.35*10∧9/L) and neutrophils (12.45*10∧9/L). Myocardial markers showed significantly elevated amino terminal brain natriuretic peptide precursor (NT-proBNP, 2,276 pg/ml) and hypersensitive cardiac troponin I (hscTNI, 3,171.7 pg/ml). Respiratory pathogen antibody test showed positive influenza A virus IgM, mycoplasma pneumonia IgG, and chlamydia IgG. The patient was first diagnosed with acute myocarditis and was treated with mechanical circulatory support measurement (intra-aortic balloon counterpulsation) in accordance with the procedures previously reported because of shock (13). The patient's vital signs stabilized after 8 days. However, during hospitalization, her echocardiogram (Figure 1) indicated a thickness of the interventricular septum (basal segment: 9 mm; middle segment: 14 mm; apical segment: 14 mm), left ventricular posterior wall (14 mm), and apical segment of the anterolateral wall (11 mm). Holter monitor and ECG (Supplementary Figure 1) showed a short PR interval (76 ms), "delta wave," and lowered ST segment (V4–V6), suggesting preexcitation of the ventricle. In order to differentiate from myocardial edema which also presents a transient thickness of cardiac muscle, another echocardiogram was performed before discharge and the result still showed a thickened interventricular septum (basal segment: 9 mm; middle segment: 16 mm) and left ventricular posterior wall (11 mm). For genetic testing, genomics was extracted from the patient's peripheral blood and genetic sequencing revealed a novel frameshift heterozygous mutation (c.764_765insGA) of *LAMP2*. However, her mother, father, uncle, and aunt did not have the same mutation (Figure 2A). Her 6-year-old younger brother had normal development and did not experience chest distress, shortness of breath, palpitation, or exhibit other cardiac symptoms. The patient's family refused echocardiogram and genetic testing for the patient's brother (Figure 2A).

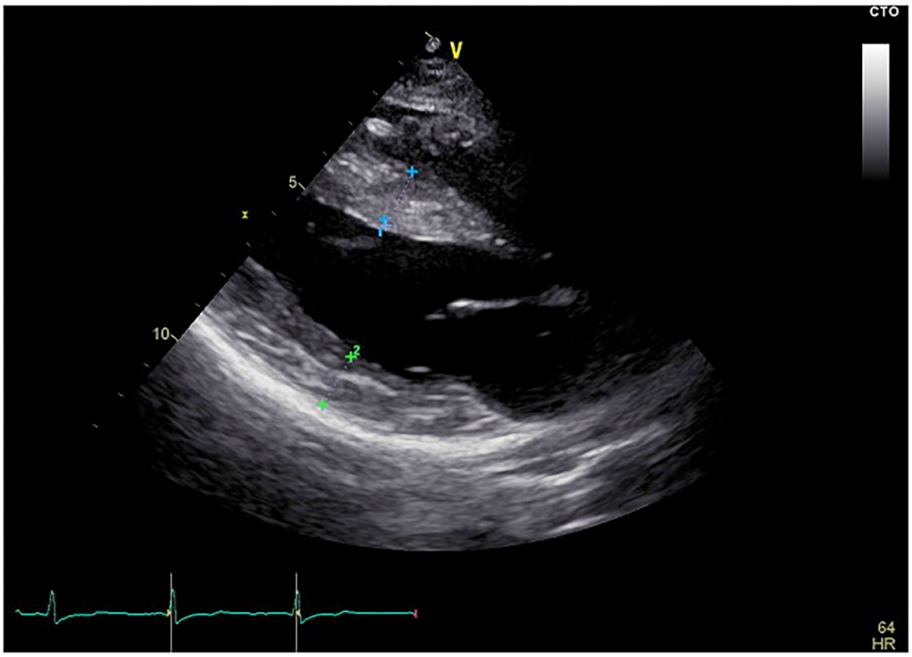

FIGURE 1
Echocardiogram of the patient. The echocardiogram showed thickened interventricular septum and left ventricular posterior wall. Blue cross marked part: interventricular septum, thickness was 1.4 cm; Green cross marked part: posterior wall of left ventricle, thickness was 1.4 cm; Yellow scale bar shows length in cm.

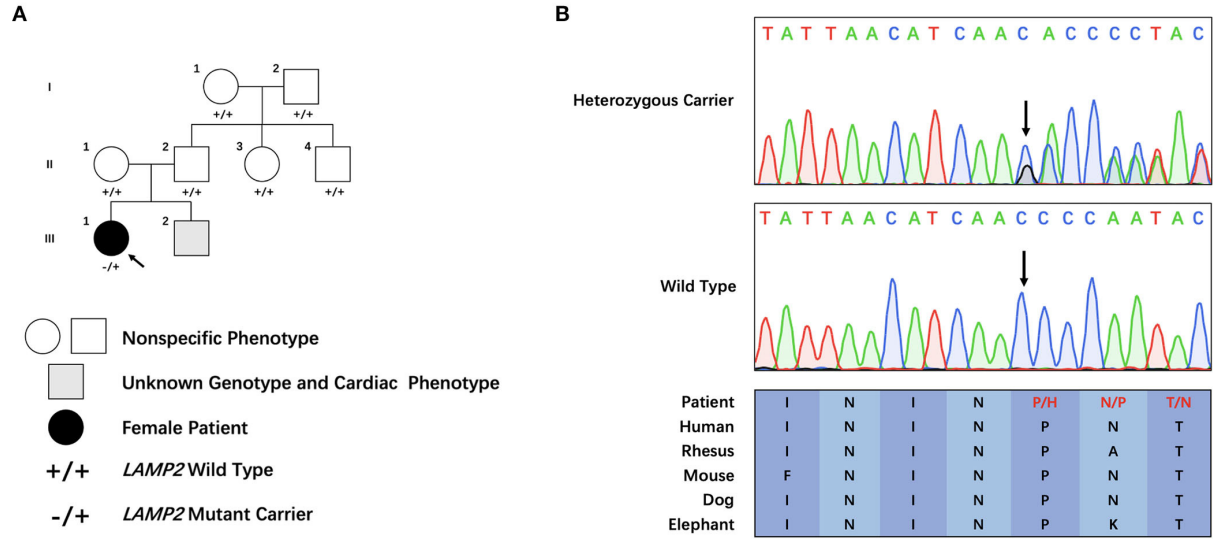

FIGURE 2
Clinical and genetic characteristics of the pedigree. **(A)** Family tree of the cardiac-only Danon disease pedigree. **(B)** Sanger sequencing of the family. Colored blocks indicate evolutionary conservation of the cluster across multiple species.

Genetic analysis

Through filtering and Sanger sequencing, we found a pathogenic heterozygous frameshift mutation, c.764_765insGA, following the ACMG guideline (14). We did not identify any other potentially pathogenic variant of CNVs of known ion channelopathy or hypertrophic cardiomyopathy-related genes. Neither was it found in the extra 800 unrelated Chinese healthy controls. Moreover, this mutation was absent in public databases (Clinvar: https://www.ncbi.nlm.nih.gov/clinvar/, ExAC: http://exac.broadinstitute.org/ and HGMD: http://www.hgmd.cf.ac.uk/ac/search.php) is evolutionary, and highly conserved across multiple species (Figure 2B). The mutation was not identified in her parents or other family members, which suggested this novel frameshift mutation was a *de novo* one.

Pathological and immunohistochemical analysis

HE staining of the endocardial biopsy sample section revealed ambiguous cell boundary, and karyopyknosis of the cell nucleus (Figures 3A,B), indicating destruction of myocardiocytes. The PAS staining showed abnormal cell structure, small vacuoles, and glycogen disposition within muscle fibers (Figures 3A,B), which is consistent with the canonical histological feature of Danon disease. Immunohistochemical (IHC) staining of the patient's myocardial slice against LAMP2 showed high and low expressing patches (Figure 4C).

Proteome expression analysis

Proteomic analysis revealed a decreased expression of the patient's LAMP2 compared with other healthy controls. LAMP2 was normalized by internal reference (ACTB). LAMP2 Expression of the patient was significantly lower than healthy controls (Figure 4D, Supplementary Table 1). On average, healthy controls express 26.83 ± 12.87 times more LAMP2 than patients carrying c.764_765insGA mutation.

Protein structure remodeling

The c.764_765insGA inserting mutation causes a mistranslation in the downstream and premature termination to 281-amino-acid residues. Significant differences were found between the mutant and wild-type LAMP2 (Figures 4A,B); i.e., the truncated mutant protein lacks transmembrane helical domain and cytoplasmic domain, leading to abnormal protein function.

Discussion

To date, more than 200 pathogenic mutations have been reported, covering exon 1 to exon 9. Through genetic sequencing, we identified a novel *LAMP2* frameshift (c.764_765insGA) mutation. The frameshift mutation in our patient caused premature termination of protein translation 46 amino acids forward. Unlike most other cases, the proband

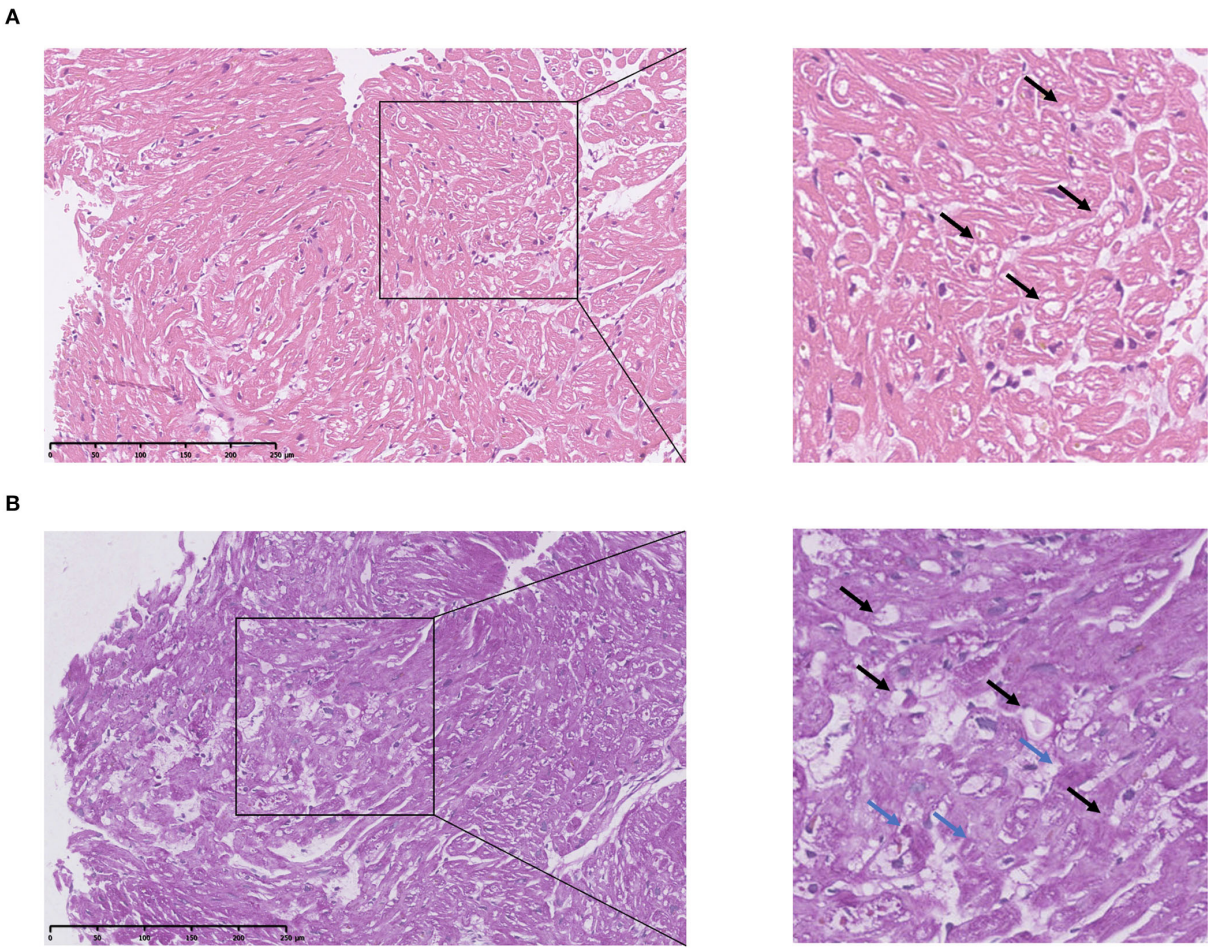

FIGURE 3
Pathological analysis of patient's cardiac muscle specimen. **(A)** HE staining of patient's heart tissue. The square shows destructed cardiac cell structure. Arrows indicate small vacuoles within cells. **(B)** PAS staining of patient's heart tissue. Blue arrows indicate glycogen disposition within the muscle fiber. Black arrows indicate small vacuoles within cells.

of this case is female. Her parents and relatives, however, who are all over 50 years old, did not share the same mutation or symptom with her, and neither did her 6-year-old brother. These findings suggest that this is a *de novo* pathogenic mutation. The mutation we revealed was absent in the unrelated 800 healthy controls, the Exome Aggregation Consortium (ExAc), ClinVar, and HGMD databases. According to the ACMG guideline and standard, this mutation should be categorized as a pathogenic mutation (PVS1+PS2+PM2). What is worth noting is that she was first presented with myocarditis, and we wondered if there was a potential correlation between Danon disease and myocarditis. However, we did not find any cases of Danon diseases combined with myocarditis. Thus, to the best of our knowledge, this is the first Danon disease case that presented first with myocarditis. Whether there is a connection between the susceptibility of myocarditis and the destruction of heart structure requires further investigation. What caught our attention is that the primary diagnosis of the patient was not Danon disease. If a gene diagnosis test was not taken into consideration, her pathogenic mutation may not have been revealed and may pass on to her offspring, which would cause a huge emotional and economic burden to this family. This reflects the important role genetic test plays in the diagnosis of patients.

As the main components of the lysosomal membrane LAMP2 are thought to protect the lysosomal membrane from hydrolytic enzymes, studies have proven a more crucial role of LAMP2 compared to LAMP1 (15). To further investigate the impact of this mutation, a heart biopsy was obtained from her left ventricle. HE staining of the section revealed unstructured cardiac cells (Figure 3A). PAS staining showed small vacuoles and glycogen disposition within cardiac muscle fibers (Figure 3B), which was similar to previously reported pathological features of the Danon disease (2). IHC staining of the heart tissue showed high and low expressing patches of LAMP2 (Figure 4C). Protein structure

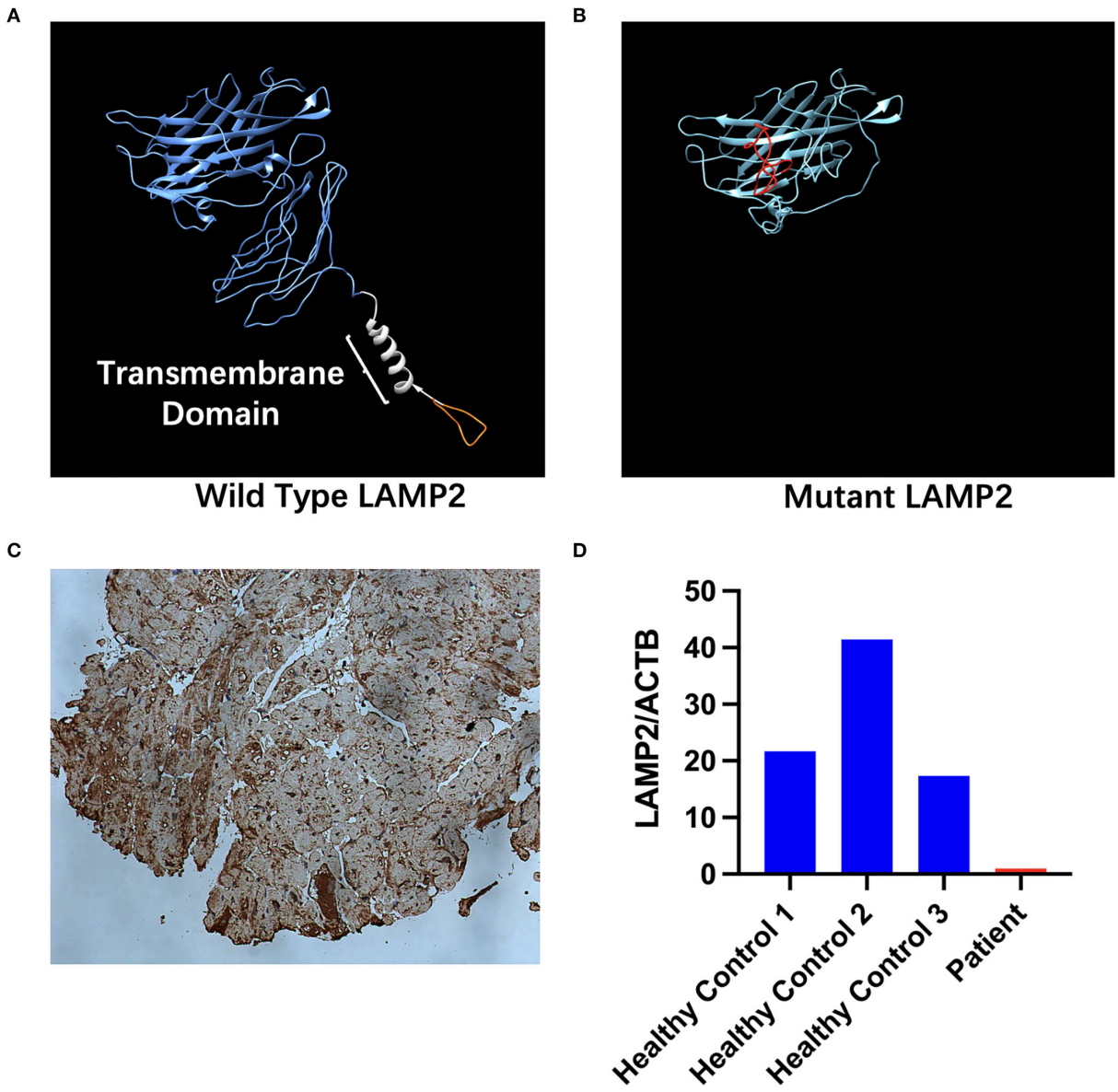

FIGURE 4
Structure and expression changes caused by mutant *LAMP2*. **(A)** *in-silico* structural modeling of wild-type LAMP2. The orange part shows the part that is truncated in the mutant LAMP2. The blue segment indicates the lumenal part of LAMP2. The white segment indicates the transmembrane part of LAMP2. The orange segment indicates the cytoplasmic part of LAMP2. **(B)** *In-silico* structural modeling of mutant LAMP2. The red segment indicates the mistranslated segment caused by the insertion mutation. The transmembrane helical domain is missing. **(C)** Immunohistochemical analyses for LAMP2. **(D)** Relative expression of LAMP2 in patient's and healthy controls' peripheral blood measured *via* proteomic analysis.

remodeling *via* deep learning technique predicted that the mutation lacks the vital cross membrane domain which may lead to an unstabilized protein structure. Further proteomic analysis revealed a considerable decrease in the patient's *LAMP2* expression (Figure 4D), which is in accordance with protein structure prediction, contributing to the deficiency of functioning LAMP2. Unlike most cases, the proband of this case is female. Her symptoms did not cover all the classical clinical triad mentioned above, but only presented with cardiac hypertrophy and preexcitation of the ventricle. This is probably due to the haploinsufficiency of her heterozygous mutation. This is in accordance with previously reported female Danon disease patients, where only one-third of female patients had skeletal myopathy and 50% had cognitive disorders (1). Haploinsufficiency is a very important finding regarding the pathophysiology of female Danon disease patients.

Sugie et al. reported a female Danon disease patient whose LAMP2 was significantly decreased (only 1/6 compared to control) and had severe cardiomyopathy but no skeletal myopathy while her son had both heart and skeletal muscle involvement (16). In 2016 they reported another Danon disease female patient whose LAMP2 decreased by 50% (LAMP2-haploinsufficiency) (17). These female Danon disease patients with heterozygous pathogenic *LAMP2* mutation shared similar LAMP2 expression features and symptoms with the patient in this report.

To date, the ClinVar database included 29 frameshift mutations of the *LAMP2* gene. Compared with missense mutations, frameshift mutations generally cause more severe damage to the protein's length and structure. Thus, all the reported 29 frameshift mutations are categorized as "likely pathogenic" or "pathogenic."

In conclusion, we identified a *de novo* frameshift mutation in a Danon disease female patient that only presented with cardiac hypertrophy and preexcitation. To the best of our knowledge, this mutation has not been reported earlier. This finding enriches the pathogenic gene spectrum of *LAMP2* and facilitates future genetic counseling and genetic diagnosis.

Data availability statement

The datasets presented in this study can be found in online repositories. Proteomic data presented in this study can be found *via* the link at: http://proteomecentral.proteomexchange.org/cgi/GetDataset?ID=PXD034265. Exome sequencing in this study can be found *via* the following link: https://ngdc.cncb.ac.cn/gsa-human/browse/HRA002525.

Ethics statement

The studies involving human participants were reviewed and approved by Ethics Committee of Tongji Hospital, Tongji Medical College, Huazhong University of Science and Technology. The patients/participants provided their written informed consent to participate in this study. Written informed consent was obtained from the individual(s) for the publication of any potentially identifiable images or data included in this article.

Author contributions

HW designed and conceptualized this study. JW wrote this manuscript and conducted the pathological analysis of the patient's left ventricle tissue. BY conducted DNA isolation, whole exome sequencing, and revised the manuscript. XS participated in the clinical sample and data collection. All authors read and approved this manuscript.

Funding

This study was supported by the National Natural Science Foundation of China (82100526).

Acknowledgments

We thank the patient and her family members and the healthy control subjects who provided their samples and clinical data for this study. We also thank the medical workers who participated in the diagnosis and treatment of the patient.

Conflict of interest

The authors declare that the research was conducted in the absence of any commercial or financial relationships that could be construed as a potential conflict of interest.

Publisher's note

Supplementary material

The Supplementary Material for this article can be found online at: https://www.frontiersin.org/articles/10.3389/fcvm.2022.899283/full#supplementary-material

References

1. Endo Y, Furuta A, Nishino I. Danon disease: a phenotypic expression of LAMP-2 deficiency. *Acta Neuropathol.* (2015) 129:391–8. doi: 10.1007/s00401-015-1385-4

2. Xu J, Li Z, Liu Y, Zhang X, Niu F, Zheng H, et al. Danon disease: a case report and literature review. *Diagn Pathol.* (2021) 16:39. doi: 10.1186/s13000-021-01100-8

3. Nascimbeni AC, Fanin M, Angelini C, Sandri M. Autophagy dysregulation in Danon disease. *Cell Death Dis.* (2017) 8:e2565. doi: 10.1038/cddis.2016.475

4. Cheng Z, Fang Q. Danon disease: focusing on heart. *J Hum Genet.* (2012) 57:407–10. doi: 10.1038/jhg.2012.72

5. Liu X, Lu S, Guo W, Xi B, Wang W. Antibiotics in the aquatic environments: a review of lakes, China. *Sci Total Environ.* (2018) 627:1195–208. doi: 10.1016/j.scitotenv.2018.01.271

6. Boucek D, Jirikowic J, Taylor M. Natural history of Danon disease. *Genet Med.* (2011) 13:563–8. doi: 10.1097/GIM.0b013e31820ad795

7. Sugie K, Yamamoto A, Murayama K, Oh SJ, Takahashi M, Mora M, et al. Clinicopathological features of genetically confirmed Danon disease. *Neurology.* (2002) 58:1773–8. doi: 10.1212/WNL.58.12.1773

8. D'Souza RS, Levandowski C, Slavov D, Graw SL, Allen LA, et al. Danon disease: clinical features, evaluation, and management. *Circ Heart Fail.* (2014) 7:843–9. doi: 10.1161/CIRCHEARTFAILURE.114.001105

9. Zhang Y, Ren H, Zhou S. A case report of delayed diagnosis of danon disease: caused by a newly recognized mutation in the lysosome-associated membrane protein-2 gene. *Medicine.* (2020) 99:e22640. doi: 10.1097/MD.0000000000022640

10. Stokes MB, Taylor AJ, Mclean CA, D'arcy CE, Mariani JA. Severe left ventricular hypertrophy and marked cardiac fibrosis in Danon disease. *Int J Cardiol.* (2016) 221:14–6. doi: 10.1016/j.ijcard.2016.06.311

11. Chen YM, Zheng Y, Yu Y, Wang Y, Huang Q, Qian F, et al. Blood molecular markers associated with COVID-19 immunopathology and multi-organ damage. *EMBO J.* (2020) 39:e105896. doi: 10.15252/embj.2020105896

12. Goddard TD, Huang CC, Meng EC, Pettersen EF, Couch GS, Morris JH, et al. UCSF ChimeraX: meeting modern challenges in visualization and analysis. *Protein Sci.* (2018) 27:14–25. doi: 10.1002/pro.3235

13. Li S, Xu S, Li C, Ran X, Cui G, He M, et al. A life support-based comprehensive treatment regimen dramatically lowers the in-hospital mortality of patients with fulminant myocarditis: a multiple center study. *Sci China Life Sci.* (2019) 62:369–80. doi: 10.1007/s11427-018-9501-9

14. Richards S, Aziz N, Bale S, Bick D, Das S, Gastier-Foster J, et al. Standards and guidelines for the interpretation of sequence variants: a joint consensus recommendation of the American college of medical genetics and genomics and the association for molecular pathology. *Genet Med.* (2015) 17:405–24. doi: 10.1038/gim.2015.30

15. Eskelinen EL. Roles of LAMP-1 and LAMP-2 in lysosome biogenesis and autophagy. *Mol Aspects Med.* (2006) 27:495–502. doi: 10.1016/j.mam.2006.08.005

16. Sugie K, Koori T, Yamamoto A, Ogawa M, Hirano M, Inoue K, et al. Characterization of Danon disease in a male patient and his affected mother. *Neuromuscul Disord.* (2003) 13:708–11. doi: 10.1016/S0960-8966(03)00105-6

17. Sugie K, Yoshizawa H, Onoue K, Nakanishi Y, Eura N, Ogawa M, et al. Early onset of cardiomyopathy and intellectual disability in a girl with Danon disease associated with a *de novo* novel mutation of the LAMP2 gene. *Neuropathology.* (2016) 36:561–5. doi: 10.1111/neup.12307

frontiers | Frontiers in Cardiovascular Medicine

TYPE Case Report
PUBLISHED 04 October 2022
DOI 10.3389/fcvm.2022.971501

OPEN ACCESS

EDITED BY
Neil Morgan,
University of Birmingham,
United Kingdom

REVIEWED BY
Andreas Brodehl,
Heart and Diabetes Center North Rhine-Westphalia, Germany
Raj Sewduth,
VIB KU Leuven Center for Cancer Biology, Belgium

*CORRESPONDENCE
Liang-Liang Fan
swfanliangliang@csu.edu.cn
Yao Deng
619065374@qq.com

†These authors have contributed equally to this work

SPECIALTY SECTION
This article was submitted to Cardiovascular Genetics and Systems Medicine,
a section of the journal
Frontiers in Cardiovascular Medicine

RECEIVED 17 June 2022
ACCEPTED 05 September 2022
PUBLISHED 04 October 2022

CITATION
Liu Y-X, Yu R, Sheng Y, Fan L-L and Deng Y (2022) Case report: Whole-exome sequencing identifies a novel *DES* mutation (p. E434K) in a Chinese family with cardiomyopathy and sudden cardiac death.
Front. Cardiovasc. Med. 9:971501.
doi: 10.3389/fcvm.2022.971501

Case report: Whole-exome sequencing identifies a novel *DES* mutation (p. E434K) in a Chinese family with cardiomyopathy and sudden cardiac death

Yu-Xing Liu[1,2,3†], Rong Yu[4†], Yue Sheng[2,3], Liang-Liang Fan[1,2,3*] and Yao Deng[1*]

[1]Department of Cardiovascular Surgery, National Clinical Research Center for Geriatric Disorders, Xiangya Hospital, Central South University, Changsha, China, [2]Department of Cell Biology, School of Life Sciences, Central South University, Changsha, China, [3]Hunan Key Laboratory of Animal Models for Human Disease, School of Life Sciences, Central South University, Changsha, China, [4]Department of Anesthesiology, The Second Xiangya Hospital, Central South University, Changsha, China

Background: Desmin is an intermediate filament protein that plays a critical role in the stabilization of the sarcomeres and cell contacts in the cardiac intercalated disk. Mutated *DES* gene can cause hereditary cardiomyopathy with heterogeneous phenotypes, while the underlying molecular mechanisms requires further investigation.

Methods: We described a Chinese family present with cardiomyopathy and sudden cardiac death (SCD). Whole-exome sequencing (WES) and bioinformatics strategies were employed to explore the genetic entity of this family.

Results: An unknown heterozygote missense variant (c.1300G > A; p. E434K) of *DES* gene was identified. The mutation cosegregates in this family. The mutation was predicted as pathogenic and was absent in our 200 healthy controls.

Conclusion: We identified a novel *DES* mutation (p. E434K) in a Chinese family with cardiomyopathy and SCD. Our study not only provided a new case for the study of the relationship between *DES* mutations and hereditary cardiomyopathy but also broadened the spectrum of *DES* mutations.

KEYWORDS

hereditary cardiomyopathy, SCD, *DES*, mutation, whole-exome sequencing

Introduction

Hereditary cardiomyopathy is defined as a primary cardiac disease caused by genetic deficiencies of cardiac muscle (1). Highly heritable but genetically diversely, hereditary cardiomyopathies represent multiple clinical phenotypes, including dilated cardiomyopathy (DCM), hypertrophic cardiomyopathy (HCM), restrictive cardiomyopathy (RCM), arrhythmogenic cardiomyopathy (ACM), non-compaction cardiomyopathy (NCM), and other or mixed phenotypes (2). To date, mutations in over 50 genes have been identified as the causative factor for different forms of cardiomyopathies (3). Proteins encoded by these pathogenic genes, such as sarcomere proteins, nuclear envelope proteins, cytoskeletal proteins, desmosomal proteins, and calcium/sodium-handling proteins of sodium channel, voltage-gated, are strongly linked with the occurrence of cardiomyopathy (4). However, there is no clear genotype–phenotype correlations of cardiomyopathy yet, which poses challenges to clinical diagnosis.

Desmin is an important intermediate filament (IF) protein principally expressed in cardiac, skeletal, and smooth muscle tissue (5). Encoded by the gene *DES*, desmin plays a key role in the mechanical stabilization of the striated muscle sarcomeres and cell contacts within the cardiac intercalated disk (ID) (5). Mutations in *DES* gene have been reported to be associated with skeletal myopathy and different hereditary cardiomyopathies (6). Nevertheless, the exact molecular mechanism of how *DES* mutations lead to these diseases, especially in cardiomyopathies, is not fully understood.

In this study, we described a Chinese family with cardiomyopathy and sudden cardiac death (SCD). Employing whole-exome sequencing (WES) technology and bioinformatics strategies, we identified a novel heterozygous mutation in *DES* gene which may be responsible for the genetic entity of this family.

Case description

Clinical features

A Chinese family with cardiomyopathy and SCD was encountered. The proband (II-5) was a 50-year-old woman from the central south region of China (Hunan Province) (**Figure 1A**). For more than a decade, she suffered from intermittent chest tightness and palpitation with two syncope episodes experience. According to her medical history, the proband was suspected to be Brugada syndrome in the previous treatment; however, she refused to be further hospitalized for testing and treatment then. During 1 week before her admission, she had increased chest tightness and brief syncope at work, and therefore, she was admitted to our hospital. Physical examination at admission showed high blood pressure (180/130 mmHg). The electrocardiogram (ECG) records showed sinus rhythm, over-load volume of the left ventricle (**Figure 1B**), but this is not typical for Brugada. The results of ambulatory ECG (AECG) have been shown in **Supplementary Figure 1**. An echocardiographic assessment revealed the enlargement of left ventricle (LV) and left atrium (LA) (56 and 40 mm, respectively; normal values: <50 and <28 mm, respectively), accompanied by a significant decrease in LV compliance (LVC). Coronary angiography suggested a myocardial bridge and mild stenosis of the left anterior descending artery (**Supplementary Figure 2**). No myopathies, neurological or bone abnormalities, were found in the proband. Further family history investigation found hypertension in her father (I-1), who died of possible coronary heart disease at age of fifty-two. Her eldest brother (II-1) also suffered from repeated attacks of syncope. Both her eldest brother (II-1) and her third brother (II-3) had SCD. Her sister (II-4) had a history of hypertension. The rest of her family members were healthy and no other malformations were observed in this family (**Table 1** and **Figure 1A**). Given the family history of SCD, the proband received an implantable cardioverter-defibrillator (ICD) and returned for scheduled visits. On the other hand, 200 healthy subjects as described in our previous study were enrolled in this study to exclude polymorphisms (7).

Genetic analysis

Whole-exome sequencing yielded 11.7 Gb of data with 99.5% coverage of the target region and 99.1% of the target covered over 10 ×. Data quality control steps, co-segregation, and bioinformatics analysis were performed following the published literature and our previous published studies (8–11). After preliminary screening, variants were further filtered by cardiomyopathy-related genes list as described in our previous study (12). A set of eight variants in eight genes were detected and were further analyzed. Bioinformatics annotations of the eight variants are shown in **Table 2**. Sanger sequencing was performed on all available family members and showed that a novel heterozygous mutation (c.1300G > A; p. E434K) of the *DES* gene (NM_001927.4) may underlie the genetic factor of this family (**Figure 1C**). Sanger sequencing confirmed that all living affected members in this family, including the proband (II-5) and her sister (II-4), harbored this heterozygous missense mutation in *DES*. DNA samples of other affected family members (I-1, II-1, and II-3) were unavailable. This mutation was neither identified in the unaffected living family members (II-2 and III-1) (**Table 2**), nor in our 200 healthy controls. Alignment of desmin amino acid sequences revealed that E434 is conserved in different species (**Figure 1D**). Modeling of

10.3389/fcvm.2022.971501

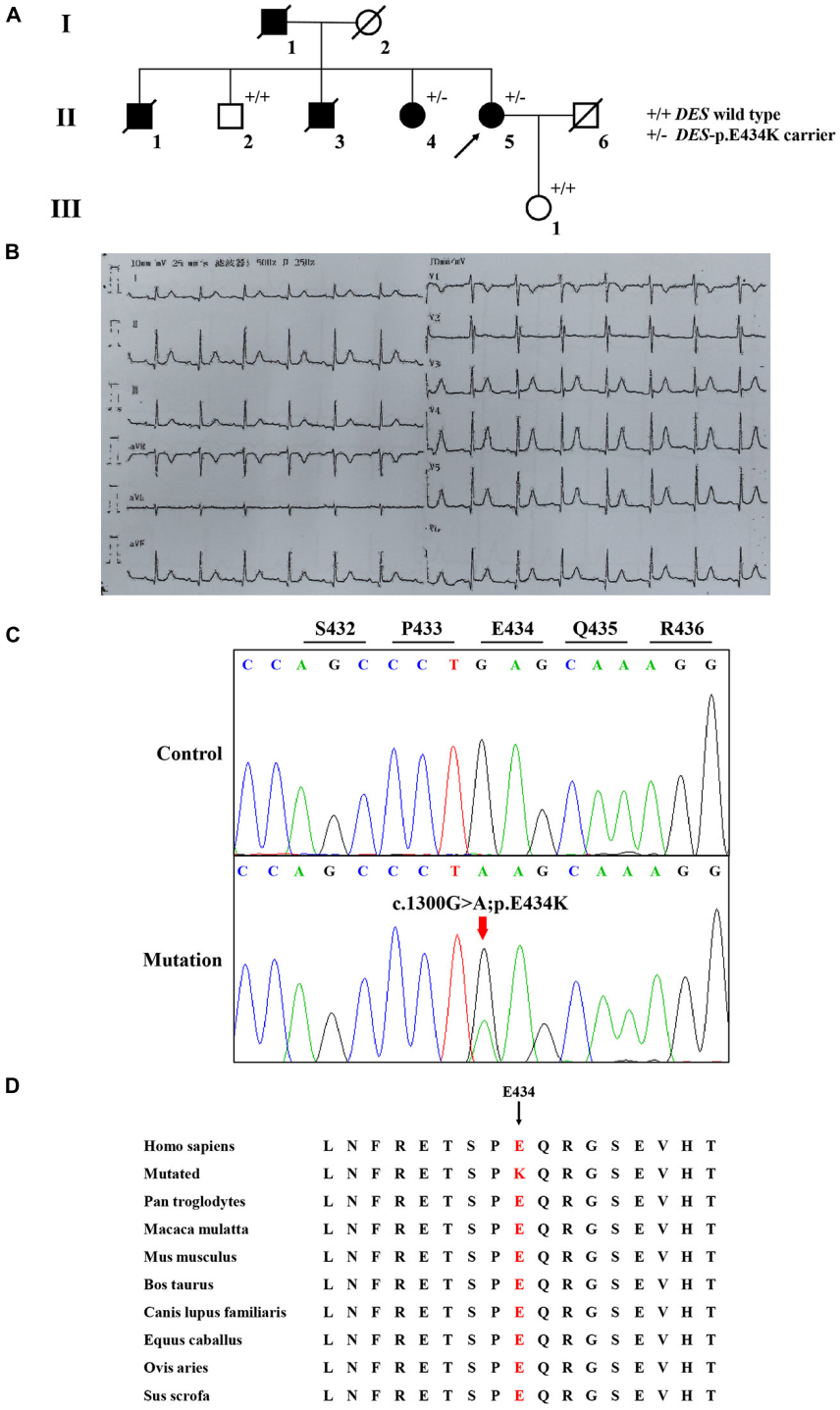

FIGURE 1
The clinical and sequencing data of this family. **(A)** The genealogy of this family. Squares indicate male family members and circles indicate female members. The black symbols represent the clinically affected members. The white symbols represent unaffected and healthy members. The arrow shows the proband. Crossed-out symbols stand for deceased relatives. ± represents heterozygous *DES*-p. E434K variant. + / + represents a wild type. **(B)** ECG of the proband. **(C)** Sanger DNA sequencing chromatogram detected a heterozygous mutation (c.1300G > A; p. E434K) of *DES* gene in the proband. **(D)** Alignment of multiple DES protein sequences across species. Letters in red show the E434 site is evolutionarily conserved.

TABLE 1 Clinical data of patients in this family.

Subjects	I-1	II-1	II-3	II-4	II-5 (proband)
Sex	M	M	M	F	F
Age (years)	52	48	44	52	50
Hypertension	+	−	−	+	+
Syncope	−	+	−	−	+
SCD	+	+	+	−	−
Sinus rhythm	NA	NA	NA	NA	+
Myocardial bridge	NA	NA	NA	NA	+

F, female; M, male; SCD, sudden cardiac death; NA, not available.

proteins before and after missense mutation was performed by the SWISS-MODEL.[1] Results revealed that the missense mutation at E434K may lead to the changing of protein surface charge as marked by red arrow in **Figure 2A**. In the WT desmin protein, E434 is hydrophobic with S432 and R436. In the mutated desmin protein, the hydrophobic effect with S432 disappeared after E434K mutation, while the hydrophobic effect with R436 remained (**Figure 2A**). Furthermore, MetaDome software[2] indicated that the affected residue, E434, is located in an intolerant region of desmin (**Figure 2B**).

Discussion

In this case report, we reported a Chinese family with cardiomyopathy and SCD. The proband suffered from hypertension and recurrent syncope. Employing WES combined with cardiomyopathy-related gene-filtering, an unknown heterozygous mutation (c.1300G > A; p. E434K) of *DES* gene was detected and might be the pathogenic genetic factor in this family. Of note, the case history investigation of proband's sister (II-4) revealed that she had hypertension with occasional chest tightness while without a history of syncope. Since recent studies have pointed out that mutations in *DES* gene may cause cardiac myopathies with a broad spectrum of pathological phenotypes within the same family (13). The same is suspected in this family of the present study. Unfortunately, the proband's sister (II-4) refused to cooperate with further tests because of financial reasons.

Desmin is an IF protein that is prominently expressed in cardiac, skeletal, and smooth muscle tissue (5). As a kind of typical IF proteins, desmin consists of a head domain, a central homologous rod domain, and a tail domain (14). The structure of desmin is related to the assembly mechanism of IF. Different disease-causing *DES* mutations interfere at different stages within this assembly process (15, 16). In our study, the missense mutation (p. E434K) locates in the tail domain that alters the acidic glutamic acid at position 434 to a basic lysine acid. This missense mutation at E434 site may lead to the charged change in desmin protein. The hydrophobic effect of amino acid residues near the mutant site may also be affected (**Figure 2A**). Although the exact molecular function of the desmin tail domain is not well understood, it is suggested that the tail domain participates in width control of unit length filaments and mediates Ca^{2+}- or Mg^{2+}-dependent cross-linking (17, 18). Moreover, changes in hydrophobicity of amino acid residues may also affect the formation of a hydrophobic seam, which further leads to filament formation defects (6). Thus, we suggested that the missense mutation (p. E434K) detected in *DES* gene may be disease-causing, in line with the previous studies.

According to published literature, mutations in *DES* gene can cause myopathies or cardiomyopathies with heterogeneous phenotypes (19). Some patients with *DES* mutations may also present a combined skeletal and cardiac myopathy. For cases with cardiomyopathies, the spectrum of cardiac phenotypes associated with *DES* mutations ranges from DCM, HCM, RCM, arrhythmogenic right ventricular cardiomyopathy (ARVC), and left ventricular cardiomyopathy (LVNC). Most of the *DES* mutations were detected in DCM. The associated clinical phenotypes of some mutations overlap significantly. For example, *DES*-p. K144* has been reported in both DCM and HCM. Moreover, *DES*-p. P419S and *DES*-p. R454W have been reported in different cardiomyopathies, including DCM, HCM, ARVC, and RCM (6). These *DES* mutations may be associated with an incomplete penetrance and diverse expressivity. Recent studies have pointed out that mutations in *DES* gene may cause cardiac myopathies with a broad spectrum of pathological phenotypes within the same family (20–24). Some complex or mixed phenotypes had been also reported in rare cases with atypical or unknown cardiomyopathy (6). Nevertheless, it is still not clear why phenotypes caused by *DES* mutations are diverse. A brief review of these reported phenotypes according to the Human Gene Mutation Database (HGMD)[3] is shown in **Figure 2C**, which may help the diagnosis of diseases associated with *DES* mutations. It is worth noting that less than 1% of cases reported cardiomyopathy as coexists with SCD, which suggested that the family reported in our study is relatively rare. Of note, the mutation (c.1300G > A; p. E434K) of *DES* gene identified in the present study has not been published, therefore, is considered novel.

1 https://swissmodel.expasy.org/

2 https://stuart.radboudumc.nl/metadome/dashboard

3 http://www.hgmd.cf.ac.uk/docs/login.html

TABLE 2 Variants identified by WES in this family.

POS	Gene name	Transcript variant	Protein variant	SIFT	Polyphen-2	Mutationtaster	OMIM clinical phenotype	ToppGene function	American college of medical genetics classification	Carrier
Chr11: 46880739-46880739	*LRP4*	NM_002334 c.5513G > A	p. R1838Q	D	D	D	AR, Myasthenic syndrome, congenital	Apolipoprotein binding	PM2; PP3	*II-2*; II-5
Chr2: 220290396-220290396	*DES*	NM_001927 c.1300G > A	p. E434K	T	D	D	AD, Cardiomyopathy or myopathy	Structural constituent of cytoskeleton	PM2; PP1; PP3	II-4; II-5
Chr2: 21255276-21255276	*APOB*	NM_000384 c.1302G > T	p. R434S	D	B	P	AD, Familial hypercholesterolemia	Low-density lipoprotein particle receptor binding	PM2	*II-2*; II-5
Chr2: 71591296-71591296	*ZNF638*	NM_001014972 c.1631G > C	p. R544P	D	D	D	Mu, Autism	RNA splicing	PM2; PP3	*II-2*; II-5
Chr5: 127595212-127595212	*FBN2*	NM_001999 c.8674G > T	p. D2892Y	D	B	D	AD, Contractural arachnodactyly, congenital	Calcium ion binding	PM2; PP3	*II-2*; *III-1*; II-4; II-5
Chr4: 5800368-5800368	*EVC*	NM_153717 c.2153G > A	p. R718Q	T	D	P	AD, Weyers acrofacial dysostosis	Endochondral bone growth	PM2	*III-1*; II-5
Chr17: 78063651-78063651	*CCDC40*	NM_001243342 c.2800C > T	p. R934W	D	D	D	AR, Ciliary dyskinesia, primary	Epithelial cilium movement involved in determination of left/right asymmetry	PM2; PP3	*III-1*; II-4; II-5
Chr10: 60580135-60580135	*BICC1*	NM_001080512 c.2701C > T	p. L901F	D	D	D	AD, Renal dysplasia, cystic	Determination of left/right symmetry	PM2; PP3	*II-2*; II-5

B, begin; D, disease-causing; P, polymorphism; POS, position; T, tolerated; AD, autosomal dominant; AR, autosomal recessive; PP, pathogenic supporting; PM, pathogenic moderate. Italic text represents healthy family members.

10.3389/fcvm.2022.971501

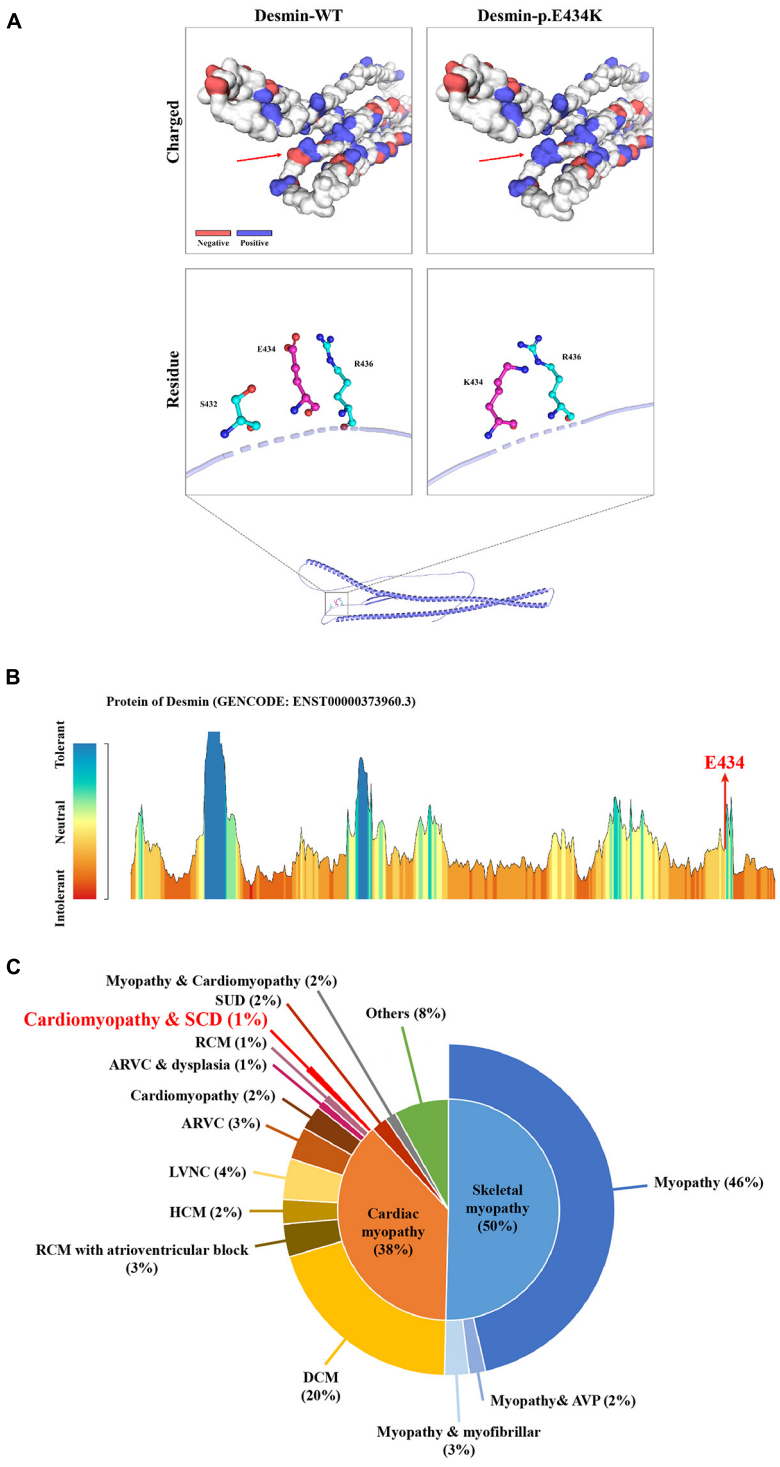

FIGURE 2
The bioinformatics analysis of mutations. Structure prediction of the mutant protein. The wild-type DES (DES-WT) protein structure and the p. E434K mutant DES (DES-p. E434K) protein structure were predicted by SWISS-MODEL online software. **(A)** Red arrow shows the charged change of desmin protein. In the DES-WT protein, E434 is hydrophobic with S432 and R436. In the DES-p.E434K protein, the hydrophobic effect with S432 disappeared after E434K mutation, while the hydrophobic effect with R436 remained **(B)** MetaDome server was used to identify the intolerant regions in DES. As depicted, the affected nucleotide/residue is located in an intolerant region. **(C)** Overview of all reported phenotypes caused by *DES* mutations. ARVC, arrhythmogenic right ventricular cardiomyopathy; AVP, autophagic vacuolar pathology; DCM, dilated cardiomyopathy; HCM, hypertrophic cardiomyopathy; LVNC, left ventricular non-compaction; RCM, restrictive cardiomyopathy; SCD, sudden cardiac death; SUD, sudden unexplained death.

Conclusion

We used WES to explore the genetic entity in a Chinese family with cardiomyopathy and SCD. A novel heterozygous missense mutation (c.1300G > A; p. E434K) of *DES* gene was detected. Our study not only provided a new case for the study of the relationship between *DES* mutations and hereditary cardiomyopathy but also broadened the spectrum of *DES* mutations.

Data availability statement

The original contributions are included in the **Supplementary material** and the following database: GSE-Human repository, accession number: HRA002969 (https://ngdc.cncb.ac.cn/gsa-human/browse/HRA002969).

Ethics statement

The studies involving human participants were reviewed and approved by the Review Board of the Xiangya Hospital of the Central South University in China. The patients/participants provided their written informed consent to participate in this case study. Written informed consent was obtained from the individual(s) for the publication of this care report and any potentially identifiable images or data included in this article.

Author contributions

RY enrolled the family members. YS performed DNA isolation and sanger sequencing. Y-XL and L-LF performed genetic analysis. Y-XL wrote the manuscript. L-LF and YD supported the project. All authors reviewed the manuscript.

Funding

This study was supported by National Natural Science Foundation of China (81800220), National Natural Science Foundation of Hunan province (2019JJ50890), Research Project of Hunan Provincial Health Commission (202103012102), the Fundamental Research Funds for the Central Universities of Central South University (2021zzts0079), and Hunan Provincial Innovation Foundation for Postgraduate (CX20210177).

Acknowledgments

We thank all subjects for participating in this study. We also thank Shuai Guo from the University of Texas, MD Anderson Cancer Center for the help with language editing.

Conflict of interest

The authors declare that the research was conducted in the absence of any commercial or financial relationships that could be construed as a potential conflict of interest.

Publisher's note

All claims expressed in this article are solely those of the authors and do not necessarily represent those of their affiliated organizations, or those of the publisher, the editors and the reviewers. Any product that may be evaluated in this article, or claim that may be made by its manufacturer, is not guaranteed or endorsed by the publisher.

Supplementary material

The Supplementary Material for this article can be found online at: https://www.frontiersin.org/articles/10.3389/fcvm.2022.971501/full#supplementary-material

References

1. Kimura A. Molecular etiology and pathogenesis of hereditary cardiomyopathy. *Circ J.* (2008) 72:A38–48. doi: 10.1253/circj.cj-08-0050

2. Yuan SM. Cardiomyopathy in the pediatric patients. *Pediatr Neonatol.* (2018) 59:120–8. doi: 10.1016/j.pedneo.2017.05.003

3. Mook OR, Haagmans MA, Soucy JF, van de Meerakker JB, Baas F, Jakobs ME, et al. Targeted sequence capture and GS-FLX titanium sequencing of 23 hypertrophic and dilated cardiomyopathy genes: implementation into diagnostics. *J Med Genet.* (2013) 50:614–26. doi: 10.1136/jmedgenet-2012-101231

4. Zhao Y, Feng Y, Zhang YM, Ding XX, Song YZ, Zhang AM, et al. Targeted next-generation sequencing of candidate genes reveals novel mutations in patients with dilated cardiomyopathy. *Int J Mol Med.* (2015) 36:1479–86. doi: 10.3892/ijmm.2015.2361

5. Hnia K, Ramspacher C, Vermot J, Laporte J. Desmin in muscle and associated diseases: beyond the structural function. *Cell Tissue Res.* (2015) 360:591–608. doi: 10.1007/s00441-014-2016-4

6. Brodehl A, Gaertner-Rommel A, Milting H. Molecular insights into cardiomyopathies associated with desmin (DES) mutations. *Biophys Rev.* (2018) 10:983–1006. doi: 10.1007/s12551-018-0429-0

7. Xiang R, Fan LL, Huang H, Cao BB, Li XP, Peng DQ, et al. A novel mutation of GATA4 (K319E) is responsible for familial atrial septal defect and pulmonary valve stenosis. *Gene.* (2014) 534:320–3.

8. Wang T, Liu YX, Luo FM, Dong Y, Li YL, Fan LL. A novel homozygous variant of TMEM231 in a case with hypoplasia of the cerebellar vermis and polydactyly. *Front Pediatr.* (2021) 9:774575. doi: 10.3389/fped.2021.774575

9. Huang H, Chen Y, Jin J, Du R, Tang K, Fan L, et al. CSRP3, p.Arg122*, is responsible for hypertrophic cardiomyopathy in a Chinese family. *J Gene Med.* (2022) 24:e3390. doi: 10.1002/jgm.3390

10. Tavasoli AR, Memar E, Ashrafi MR, Hosseini S, Haghighi R, Ghabeli H, et al. Primary and secondary microcephaly, global developmental delay, and seizure in two siblings caused by a novel missense variant in the ZNF335 gene. *J Mol Neurosci.* (2022) 2022:1955. doi: 10.1007/s12031-021-01955-y

11. Fan LL, Liu JS, Huang H, Du R, Xiang R. Whole exome sequencing identified a novel mutation (p.Ala1884Pro) of beta-spectrin in a Chinese family with hereditary spherocytosis. *J Gene Med.* (2019) 21:e3073. doi: 10.1002/jgm.3073

12. Zhang SB, Liu YX, Fan LL, Huang H, Li JJ, Jin JY, et al. A novel heterozygous variant p.(Trp538Arg) of SYNM is identified by whole-exome sequencing in a Chinese family with dilated cardiomyopathy. *Ann Hum Genet.* (2019) 83:95–9. doi: 10.1111/ahg.12287

13. Bergman JE, Veenstra-Knol HE, van Essen AJ, van Ravenswaaij CM, den Dunnen WF, van den Wijngaard A, et al. Two related dutch families with a clinically variable presentation of cardioskeletal myopathy caused by a novel S13F mutation in the desmin gene. *Eur J Med Genet.* (2007) 50:355–66. doi: 10.1016/j.ejmg.2007.06.003

14. Carlsson L, Thornell LE. Desmin-related myopathies in mice and man. *Acta Physiol Scand.* (2001) 171:341–8. doi: 10.1046/j.1365-201x.2001.00837.x

15. Brodehl A, Hedde PN, Dieding M, Fatima A, Walhorn V, Gayda S, et al. Dual color photoactivation localization microscopy of cardiomyopathy-associated desmin mutants. *J Biol Chem.* (2012) 287:16047–57. doi: 10.1074/jbc.M111.313841

16. Bar H, Mucke N, Kostareva A, Sjoberg G, Aebi U, Herrmann H. Severe muscle disease-causing desmin mutations interfere with in vitro filament assembly at distinct stages. *Proc Natl Acad Sci U.S.A.* (2005) 102:15099–104. doi: 10.1073/pnas.0504568102

17. Lin YC, Broedersz CP, Rowat AC, Wedig T, Herrmann H, Mackintosh FC, et al. Divalent cations crosslink vimentin intermediate filament tail domains to regulate network mechanics. *J Mol Biol.* (2010) 399:637–44. doi: 10.1016/j.jmb.2010.04.054

18. Herrmann H, Haner M, Brettel M, Muller SA, Goldie KN, Fedtke B, et al. Structure and assembly properties of the intermediate filament protein vimentin: the role of its head, rod and tail domains. *J Mol Biol.* (1996) 264:933–53. doi: 10.1006/jmbi.1996.0688

19. Brodehl A, Pour HS, Stanasiuk C, Ratnavadivel S, Hendig D, Gaertner A, et al. Restrictive cardiomyopathy is caused by a novel homozygous desmin (DES) mutation p.Y122H leading to a severe filament assembly defect. *Genes (Basel).* (2019) 10:918. doi: 10.3390/genes10110918

20. Klauke B, Kossmann S, Gaertner A, Brand K, Stork I, Brodehl A, et al. De novo desmin-mutation N116S is associated with arrhythmogenic right ventricular cardiomyopathy. *Hum Mol Genet.* (2010) 19:4595–607. doi: 10.1093/hmg/ddq387

21. Brodehl A, Dieding M, Biere N, Unger A, Klauke B, Walhorn V, et al. Functional characterization of the novel DES mutation p.L136P associated with dilated cardiomyopathy reveals a dominant filament assembly defect. *J Mol Cell Cardiol.* (2016) 91:207–14. doi: 10.1016/j.yjmcc.2015.12.015

22. Marakhonov AV, Brodehl A, Myasnikov RP, Sparber PA, Kiseleva AV, Kulikova OV, et al. Noncompaction cardiomyopathy is caused by a novel in-frame desmin (DES) deletion mutation within the 1A coiled-coil rod segment leading to a severe filament assembly defect. *Hum Mutat.* (2019) 40:734–41. doi: 10.1002/humu.23747

23. Bermudez-Jimenez FJ, Carriel V, Brodehl A, Alaminos M, Campos A, Schirmer I, et al. Novel desmin mutation p.Glu401Asp impairs filament formation, disrupts cell membrane integrity, and causes severe arrhythmogenic left ventricular cardiomyopathy/dysplasia. *Circulation.* (2018) 137:1595–610. doi: 10.1161/CIRCULATIONAHA.117.028719

24. Harada H, Hayashi T, Nishi H, Kusaba K, Koga Y, Koga Y, et al. Phenotypic expression of a novel desmin gene mutation: hypertrophic cardiomyopathy followed by systemic myopathy. *J Hum Genet.* (2018) 63:249–54. doi: 10.1038/s10038-017-0383-x

frontiers | Frontiers in Cardiovascular Medicine

TYPE Case Report
PUBLISHED 11 October 2022
DOI 10.3389/fcvm.2022.939013

OPEN ACCESS

EDITED BY
Georges Nemer,
Hamad Bin Khalifa University, Qatar

REVIEWED BY
Shiwei Yang,
Children's Hospital of Nanjing Medical University, China
Zhou Zhou,
Chinese Academy of Medical Sciences and Peking Union Medical College, China

*CORRESPONDENCE
Uma Kumar
kumar.umaa@gmail.com

†These authors have contributed equally to this work and share first authorship

SPECIALTY SECTION
This article was submitted to Cardiovascular Genetics and Systems Medicine, a section of the journal Frontiers in Cardiovascular Medicine

RECEIVED 08 May 2022
ACCEPTED 20 September 2022
PUBLISHED 11 October 2022

CITATION
Manhas J, Lohani LR, Seethy A, Kumar U, Gamanagatti S and Sen S (2022) Case report: Characterization of a rare pathogenic variant associated with loss of COL3A1 expression in vascular Ehlers Danlos syndrome. *Front. Cardiovasc. Med.* 9:939013. doi: 10.3389/fcvm.2022.939013

Case report: Characterization of a rare pathogenic variant associated with loss of COL3A1 expression in vascular Ehlers Danlos syndrome

Janvie Manhas[1†], Lov Raj Lohani[2†], Ashikh Seethy[1], Uma Kumar[2*], Shivanand Gamanagatti[3] and Sudip Sen[1]

[1]Department of Biochemistry, All India Institute of Medical Sciences, New Delhi, India, [2]Department of Rheumatology, All India Institute of Medical Sciences, New Delhi, India, [3]Department of Radiodiagnosis, All India Institute of Medical Sciences, New Delhi, India

The vascular subtype of Ehlers Danlos Syndrome (vEDS) is a rare connective tissue disorder characterized by spontaneous arterial, bowel or organ rupture. The diagnosis of vEDS is established in a proband by identification of a heterozygous pathogenic variant in the alpha-1 gene of type III collagen (*COL3A1*) by molecular analysis. In this report, we present a case of vEDS with life threatening, spontaneous arterial dissections in association with an uncharacterized rare variant of *COL3A1, exon19:c.1340G > A*. Primary culture of patient skin fibroblasts followed by immunofluorescence revealed a complete absence of COL3A1 protein expression as well as altered morphology. Electron microscopy of the cultured fibroblasts showed abnormal vacuoles in the cytoplasm suggestive of a secretory defect. In this study, we have performed functional characterization of the *COL3A1 exon19:c.1340G > A* variant for the first time and this may now be classified as likely pathogenic in vEDS.

KEYWORDS

vascular Ehlers Danlos syndrome, COL3A1 pathogenic variant, clinical fibroblast testing, exome sequencing, stroke, hepatic artery dissection

Introduction

Vascular Ehlers Danlos Syndrome (vEDS; OMIM130050) is a rare connective tissue disorder caused by mutations in the alpha-1 chain of type III collagen (COL3A1) polypeptide leading to serious risk of arterial or organ rupture and premature death (1). It is dominantly inherited in 50% cases and the other 50% present with *de novo* pathogenic, somatic variants in *COL3A1* (2). The most common *COL3A1* pathogenic variant is a heterozygous missense substitution for glycine in the (Gly-X-Y) repeating

sequence of collagen triple helix which disrupts the assembly of type III homotrimeric collagen (3). This leads to defective type III collagen synthesis and assembly, manifesting as loss of mechanical strength in arteries and other hollow organs. The natural course of vEDS and associated clinical phenotype of patients are both reported to be influenced by the type of *COL3A1* variant (3, 4). Therefore, establishing a diagnosis of vEDS should ideally always include molecular genetic testing for *COL3A1* pathogenic variants and biochemical analysis to ascertain the pathogenicity of unreported variants (5).

Due to limited genetic testing and unavailability of clinical fibroblast culture testing, the prevalence and burden of vEDS in India is underestimated and underreported. vEDS is defined based on one major and several minor diagnostic criteria (1) which highlight the plethora of different physical signs that may constitute the clinical phenotype and cause confusion during diagnosis. Considering the unpredictable, life threatening complications of vEDS with a low median survival of around 48 years (2), it becomes imperative to employ genetic testing early during the management of a suspected vEDS patient especially when the phenotype is indistinguishable from other inherited connective tissue disorders.

Case description

A 48-year-old male with no past history of any relevant disease presented with the sudden onset of severe headache followed by right sided hemiparesis. On examination the patient had a thin face with prominent nose and lobeless ears (**Figure 1A**) along with fragile and thin skin over the extremities suggestive of Acrogeria (**Figure 1B**). Presence of varicose veins with some ecchymotic patches were observed over the lower limbs (**Figure 1C**). Chest veins were also found to be prominent (**Figure 1A**). Hypermobility of small joints of the hands (**Figure 1D**) and clubbing of feet were observed (**Figure 1B**). However, hyper elasticity of skin and marfanoid features were not present. Bilateral pitting edema was present in the lower limbs. All other vital parameters were within normal range.

Digital Subtraction Angiography (DSA) was suggestive of dissection with sub occlusive narrowing in the left internal carotid artery in the skull base region (**Figures 1E,F**). Patient was started on anticoagulation therapy with vitamin K antagonist (VKA) and 5 mg of warfarin, dose titrated to maintain a target INR (International Normalized Ratio) of 2–3. Hemiparesis gradually subsided and warfarin was stopped.

Patient was asymptomatic for 1 year followed by the sudden onset of upper abdominal pain. Computed tomography (CT) angiography showed aneurysmal dilatation of left hepatic artery (**Figures 1G,H**) along with multiple arterial dissections involving left renal artery (**Figures 1I,J**) and multiple infarcts in right renal artery and proximal right common iliac artery (**Figures 1K,L**). The patient also developed elevated blood pressure which was a new symptom and was managed using anti-hypertensives. A rise in the level of the inflammatory marker, C-reactive protein was observed in serum. Nerve conduction study and nerve biopsy were suggestive of axonal and demyelinating neuropathy in both lower legs. Blood tests for vasculitis markers including antinuclear antibody, perinuclear and cytoplasmic antineutrophil cytoplasmic antibodies (myeloperoxidase and proteinase) were found to be negative. The patient was negative for HIV, hepatitis B and C. Within a few days our patient presented with another episode of acute abdominal pain with bilateral subcostal tenderness. He was diagnosed with hemoperitoneum due to Hepatic Artery rupture with ischemic liver changes, for which aneurysmal coiling was performed. There was no history of weight loss, fever, hemoptysis or melena. Laboratory test results are shown in **Supplementary Table 1**.

Whole exome sequencing analysis reveals a likely pathogenic *COL3A1* variant of uncertain significance

DNA was isolated from the peripheral blood sample of the patient and sent for whole exome sequencing (WES) to identify the cause of the disease. A total of 34058 variants were called after filtering for the depth of sequencing (minimum 10), of which 9257 were exonic variants, including single nucleotide variants and short indels. Exclusion of synonymous variants and filtering for minor allele frequency of <5% retained 854 variants. Once the non-pathogenic variants were removed using SIFT, Polyphen2-HDIV and Mutation Assessor predictions, 548 variants remained (**Supplementary Data 1**). After inclusion of 28 variants which affected splicing, there were 576 pathogenic variants across 392 different genes, of which 154 were found to be associated with a phenotype in OMIM.

On further evaluation based on the patient's phenotype of 'blood vessel abnormalities AND hypermobility' in OMIM, *COL3A1 exon19:c.1340G > A* [chr2:g.188994587G > A,NM_000090.3:c.1340G>A, NM_000090.3(COL3A1_i001):p.(Gly447Asp), all descriptions are based on hg38] variant leading to the substitution of Aspartic acid for Glycine at codon 447 (p.G447D) in type III collagen α1 polypeptide was identified. The variant attributes according to the American College of Medical Genetics and Genomics (ACMG) and the Association for Molecular Pathology (AMP) guidelines (6) for the interpretation of sequence variants were PM2, PP2, and PP3. Visualization of this variant in Integrative Genome Viewer (IGV) suggested heterozygosity (**Supplementary Data 1** in **Supplementary Figure 1**). This variant has been previously found to be associated with vascular subtype of Ehlers Danlos syndrome in one case report (7). Since this variant has not been reported in the 1000 genomes

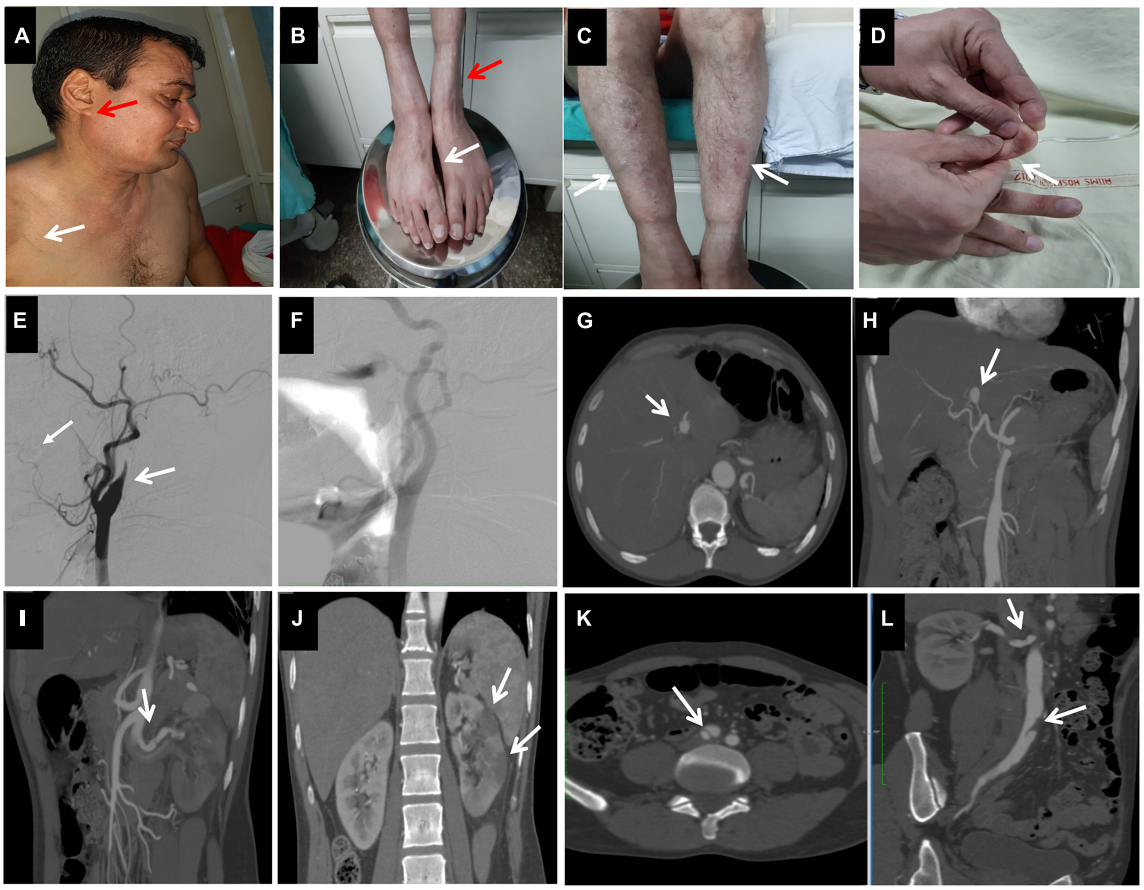

FIGURE 1
Observed clinical features of the patient, **(A):** Thin Nose, lobe less ear (red arrow), thin skin with visible chest veins (white arrow), **(B):** Acrogeria (red arrow) with club foot (white arrow), **(C):** Easy bruising and thin skin, varicose veins, **(D):** Hypermobility of small joints (shown in distal phalange of index finger). Digital subtraction angiography images of bilateral common carotid arteries showing dissection of left internal carotid artery **(E,F)**. Right internal carotid artery was normal. Axial **(G)** and coronal **(H)** maximum intensity projection (MIP) CT images showing aneurysmal dilatation of left hepatic artery. Coronal MIP images **(I,J)** of contrast enhanced CT show dissection involving left renal artery with multiple infarcts of renal parenchyma. Axial **(K)** and coronal **(L)** MIP CT images show dissection involving right renal artery and right common iliac artery.

(8), Exome Aggregation Consortium (9) (ExAC) and other databases (10) and no functional data was available regarding this variant, we further proceeded to analyze the pathogenic basis of this variant using molecular techniques.

The Exon19:c. *1340G > A* variant leads to absence of COL3A1 protein in skin fibroblasts

Patient and control fibroblasts were cultured from skin biopsy (11) (**Figures 2A,B**) and analysis of protein expression of COL3A1 was done using immunofluorescence. There was a complete absence of COL3A1 production in the patient fibroblasts compared to the control fibroblasts (**Figures 2C,D**). The morphology of patient fibroblasts was also observed to be altered as compared to the control fibroblasts. Fibroblasts derived from skin biopsy of patient with exon19:c. *1340G > A* variant were larger in size as compared to the control fibroblasts (**Figures 2C,D**). It has been previously reported that dermal fibroblasts from vEDS have defective collagen biosynthesis/processing, endoplasmic reticulum homeostasis/protein folding, disorganized ECM interactions and may acquire a myofibroblast like phenotype (12). In order to investigate the altered morphology, we performed a Transmission electron microscopy (TEM) analysis. TEM has previously been suggested to be a useful addition to the repertoire of diagnostic tests in vEDS (13). Previous studies have reported an inefficient secretion of mutant collagen molecules which can lead to altered structural anatomy of the endoplasmic reticulum and unfolded protein response (14). We observed lamellar vacuolar bodies in the cytoplasm of vEDS fibroblasts which were not present in control fibroblasts (**Figures 2E,F**). On in-depth observational analysis, these bodies appeared to be

"Amphisomes," organelles of the autophagy pathway resulting from fusion of endosomes and autophagosomes (15). This may explain the altered morphology and size of vEDS fibroblasts.

Sanger sequencing

Genomic DNA was also extracted from cultured dermal fibroblasts from patient and age-matched control and the *COL3A1 exon19:c.1340G > A* variant obtained from Whole exome sequencing was confirmed by Sanger sequencing (**Figure 2G**). All methodology provided in **Supplementary Data 2**.

Discussion

Diagnosis of vEDS based on clinical diagnostic criteria alone is often difficult due to significant overlap in clinical presentation with other connective tissue disorders and arteriopathies. vEDS diagnosis should be suspected in individuals presenting with spontaneous ruptures of arteries, uterus or bowel at a young age. Careful interpretation of genetic testing results and variant assessment according to the ACMG/AMP guidelines (6) is essential to confirm the diagnosis, as all COL3A1 variants are not pathogenic (16). Additionally, clinical fibroblast testing and functional analysis can help to accurately report pathogenicity of novel sequence variants.

Classification of *COL3A1* exon19:c.1340G > A as likely pathogenic variant

About 705 unique likely pathogenic/pathogenic *COL3A1* variants have been reported, which are listed in the *Leiden Open Variation Database* (see https://databases.lovd.nl/shared/genes/COL3A1). Missense mutation involving substitution of a glycine amino acid in the triple helix is the most common type of mutation reported in the database. The second most common type of mutation is a *COL3A1* RNA splicing mutation. Large deletions or insertions in *COL3A1* are relatively uncommon in vEDS. Most patients with vEDS develop major complications before the age of 30 years. Autosomal dominant inheritance of vEDS shows a penetrance approaching 100% but may also vary according to the age of presentation. Haploinsufficient patients have a lower penetrance of ∼50% and were observed to survive 10–15 years longer than individuals harboring RNA splicing or glycine mutations (17). Interestingly, a missense mutation with substitution of a valine or an aspartic acid for a glycine was reported to have a poorer prognosis than a substitution of a serine (17). Although the phenotype of patients with amino acid substitutions in COL3A1 may partially overlap with of some haploinsufficient patients (18), there is considerable evidence for genotype-phenotype correlation (3, 16, 17) in vEDS which may be critical for screening and lifelong management of the affected individual and family members.

Our patient presented with stroke along with cranial and abdominal visceral arteries' dissections and rupture. Patient was hypertensive, had an elevated C-reactive protein (CRP) and neuropathy which lead to an initial suspicion of Polyarteritis Nodosa (PAN) (19). However, he did not show constitutional symptoms of fever, fatigue, weight loss, muscle/joint pains, radiological findings or other features defined by American College of Rheumatology classification criteria for PAN. The clinical presentation also favored the differential diagnosis of vEDS, but the presenting age of 48 years was not consistent with this diagnosis. The presence of multiple clinical findings namely acrogeria, progeria, lobeless ear, hypermobile small joints of hands, thin fragile skin, foot clubbing and multiple arterial dissections favored the diagnosis of vEDS. Patient had renal infarcts following renal artery dissection which could have contributed to the rise in blood pressure. It has been reported that delayed clearance of thrombi as well as the vascular insult to arteries in vEDS may lead to a rise in inflammatory markers (20), as observed in this case. Presence of axonal polyneuropathy has also been reported before in vEDS (21, 22). As there was no family history of EDS or related syndromes, in order to establish the diagnosis in a proband it was imperative to perform molecular genetic testing to identify and characterize this variant (2). Corticosteroids are used in PAN to reduce inflammation but they have been reported to trigger arterial dissections by elevating blood pressure and increasing blood vessel fragility by its inhibitory effect on collagen formation and connective tissue strength (23). Therefore, the patient was managed symptomatically till the genetic testing results were obtained.

Whole exome sequencing revealed a rare, uncharacterized variant of *COL3A1* gene, exon19:c.1340G > A variant. A molecular diagnostic study was carried out to confirm if this variant was responsible for the vEDS phenotype. Dermal Fibroblast culture was established using skin biopsy from the patient and age matched control and COL3A1 protein expression was studied using immunofluorescence. The COL3A1 expression was observed to be absent in the exon19:c.1340G > A variant (**Figures 2C,D**). This suggests the expression of a mutant collagen with a dominant negative effect leading to a possible degradation after binding with the wild type collagen molecule. The presence of the variant was further confirmed by Sanger sequencing of the PCR amplicon obtained by using DNA extracted from cultured fibroblasts as the template and primers flanking the site of the variant (**Figure 2G**). We also observed 2 more non-synonymous variants of *COL3A1* (exon 30:c.2092G > A and exon 50:c.4059T > G) during the data analysis of the WES. However, based on their high minor allele frequencies, these were found to be non-deleterious (**Table 1**). Transmission

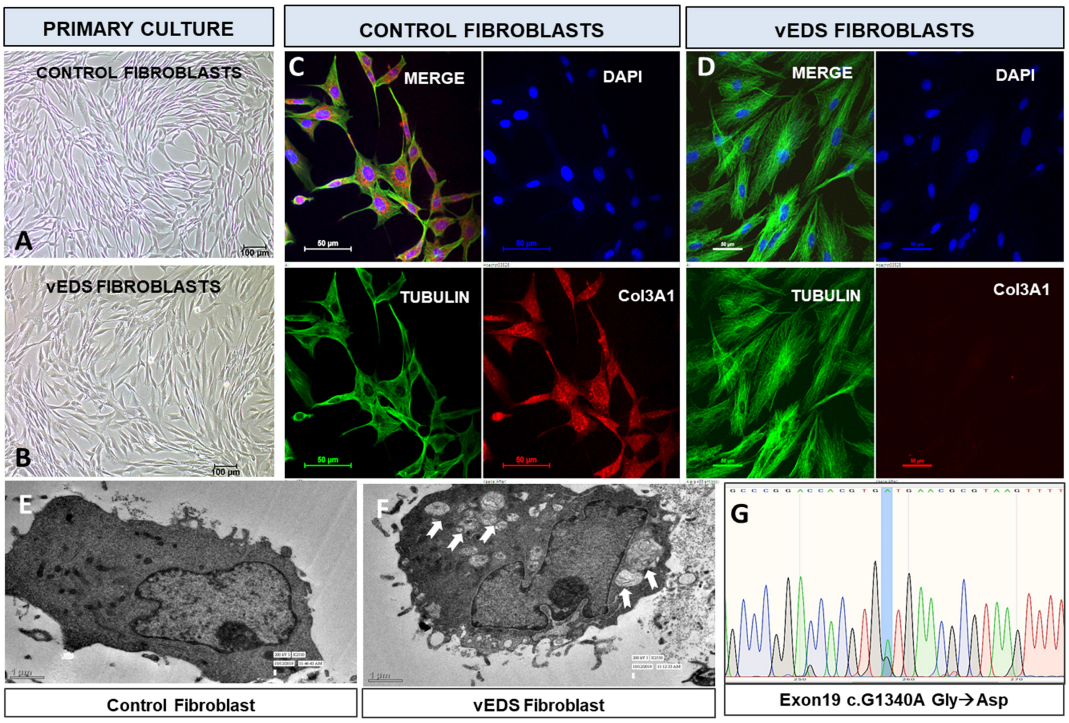

FIGURE 2
Primary culture of skin derived fibroblasts from **(A)** age matched control **(B)** suspected vEDS patient. Immunofluorescence analysis of fibroblasts show **(C)** presence of Col3A1(Red) control fibroblasts whereas **(D)** patient fibroblasts show absence of Col3A1. Transmission electron microscopy of **(E)** control fibroblasts with normal morphology, **(F)** vEDS fibroblasts with altered morphology, arrows show intracytoplasmic lamellar vacuolar bodies. **(G)** Sequences of wild-type (1340-G) and mutant (1340-A) COL3A1 cDNA derived from patient skin fibroblasts. As vEDS patient is heterozygous for COL3A1 c.1340G > A mutation, sequencing of the region harboring the mutation results in detection of both guanine and adenine at position 1340. The G > A mutation leads to an exchange from glycine to aspartic acid at the protein level.

Electron Microscopy (TEM) studies of the dermal fibroblasts suggested that exon19:c.1340G > A variant is associated with altered endoplasmic reticular morphology in vEDS which may contribute to the disease mechanism.

According to the ACMG/AMP standards and guidelines for interpretation of sequence variants (6), the following *COL3A1* variant criteria may be used to classify exon19:c. 1340G > A variant as pathogenic variant:

PS3 → functional studies supporting damaged or altered gene product, absence of COL3A1 protein expression on immunofluorescence studies on skin fibroblasts and altered morphology of fibroblasts on electron microscopy studies.

PM2 → variant not reported before in Exome sequencing project 1000 genomes and ExAC.

PP2 → missense z-scores of COL3A1 gene > 3.09, which was regarded as intolerant to missense variants.

PP3 → SIFT (Deleterious), PolyPhen (Damaging) and a CADD-Phred score of 26.1 (pathogenic) support a deleterious effect on the gene or gene product.

Using the ACMG/AMP rules for combining the above criteria (6), *COL3A1 exon19:c.1340G > A* variant classification was found to be likely pathogenic (II) (**Table 1**).

Treatment and management

Diagnosis and management of a rare, life threatening vascular disease condition in absence of any curative therapy is a difficult conundrum for both the patient and the treating physician. Besides symptomatic treatment and regular follow up, psychological therapy and family support is required to accept and live with such a condition. Clinical evaluation of vEDS patients includes regular blood pressure monitoring, non-invasive arterial screening to detect dissections and dilatations such as ultrasonography, computed tomography or magnetic resonance imaging (1, 2). Any invasive procedures like colonoscopy, angiograms or surgeries should be carefully assessed for risk and if necessary should be performed by surgeons experienced and familiar with the enhanced caution required due to tissue fragility and its associated complications (24).

After the confirmation of *COL3A1* variant by exome sequencing and biochemical analysis, diagnosis was confirmed as vEDS. Patient was explained about the disease and its prognosis and referred for genetic counseling. It has been reported that Celiprolol improves the biomechanical integrity

TABLE 1 ACMG/AMP classification criterion: Pathogenic Strong (PS3): Well-established *in vitro* or *in vivo* functional studies supportive of a damaging effect on the gene or gene product; Pathogenic moderate 2 (PM2) = Absent from controls in Exome Sequencing Project, 1000 Genomes or ExAC; Pathogenic supporting 2 (PP2) = Missense variant in a gene that has a low rate of benign missense variation and where missense variants are a common mechanism of disease; Pathogenic supporting 3 (PP3) = Multiple lines of computational evidence support a deleterious effect on the gene or gene product (conservation, evolutionary, splicing impact, etc); Benign stand-alone 1 (BA1) = Allele frequency > 5% in Exome Sequencing, 1000 Genomes or ExAC; Benign supporting 4 (BP4) = Multiple lines of computational evidence suggest no impact on gene or gene product (conservation, evolutionary, splicing impact, etc).

Details of the variant			Minor allele frequency				Pathogenicity prediction — *in silico*				ACMG attributes	Variant classification
Genomic co-ordinates	AAChange. refGene	Conseq -uence	ExAC_ ALL	1000g 2015 aug_all	gnomAD_ exome_ ALL	gnomAD_ genome_ ALL	SIFT_ pred	Polyphen2_ HDIV_pred	Mutation Taster_pred	CADD_ phred		
chr2:188994587 G > A	NM_000090.3 (COL3A1_i001): p.(Gly447Asp)	Missense	.	.	.	.	D	D	D	26.1	PS3 PM2 PP2 PP3	Likely Pathogenic (II)
chr2:188999354 G > A	NM_000090.3 (COL3A1_i001): p.(Ala698Thr)	Missense	0.3204	0.21845	0.2497	0.2118	T	B	P	22.9	BA1 BP4	Benign (I)
chr2:189010695 T > G	NM_000090.3 (COL3A1_i001): p.(His1353Gln)	Missense	0.9985	0.996605	0.9988	0.9958	T	B	P	6.799	BA1 BP4	Benign (I)

AA, Amino Acid; ExAC, Exome Aggregation Consortium; 1000g, 1000 Genomes project; gnomAD, Genome Aggregation Database; SIFT, Sorting Intolerant from Tolerant; pred, prediction software; PolyPhen2_HDIV, Polymorphism Phenotyping v2 Hum Div Model; CADD_phred, Combined Annotation Dependent Depletion_phred software; D, Deleterious; PD, Probable Damaging; VUS, Variant of uncertain significance; MAF, Minor allele frequency (z score); ACMG, American College of Medical Genetics and Genomics; AMP, Association of Molecular Pathology.

of the aorta (25) and may be an option for the prevention of complications in vEDS (26). Due to lack of Celiprolol and any other approved therapies in India and many other countries, there are not many options available for treating vEDS patient besides symptomatic and supportive therapy.

As research advances further in this field, gene therapy may be a promising option for the treatment of vEDS in the future. However, addition of the defective gene is not applicable for dominant diseases such as vEDS where the defective procollagen gene, COL3A, is a homotrimer of three identical α1 chains. As most of the patients present with a heterozygous mutation, there is a structural defect in half of the synthesized collagen α1 fibrils which results in 1/8th normal and 7/8th abnormal COL3A trimers. Interesting approaches such as siRNA mediated inhibition of the mutated allele and strategies to enhance transcriptional activation of the normal allele are being tested *in vivo* for phenotypic correction of vEDS (27, 28).

A recent study has identified PLC/IP3/PKC/ERK pathway (phospholipase C/inositol 1,4,5-triphosphate/protein kinase C/extracellular signal-regulated kinase) as major drivers of vascular pathology in vEDS based on preclinical models (29). AR101 (enzastaurin) is an orally active, small molecule, serine/threonine kinase inhibitor of the PLC/IP3/PKC/ERK pathways which has been previously studied in over 40 human trials including a range of cancers.[1] PREVEnt trial, which will assess the efficacy of enzastaurin in preventing cardiac or arterial events in patients with vEDS confirmed with *COL3A1* gene mutations is scheduled to begin next year and if successful may provide us with a new treatment for the life-threatening complications of vEDS.

Conclusion

We evaluated a rare *COL3A1* variant in vEDS using the ACMG/AMP standards and guidelines. The diagnosis was confirmed by genetic testing and pathogenicity was established by clinical fibroblast testing and functional assays. Based on our observations, *COL3A1 exon19:c.1340G > A* variant may now be classified as a likely pathogenic variant for vEDS exome analysis. Further detailed study may be required to understand the exact molecular mechanism of vEDS pathogenesis in this variant.

Data availability statement

The original contributions presented in this study are included in the article/**Supplementary material**, further inquiries can be directed to the corresponding author.

1 Prevention of Rupture with Enzastaurin in Vascular Ehlers-Danlos Syndrome (https://clinicaltrials.gov/ct2/show/NCT05463679).

Ethics statement

Ethical review and approval was not required for the study on human participants in accordance with the local legislation and institutional requirements. The patients/participants provided their written informed consent to participate in this case study. Written informed consent was obtained from the individual(s) for the publication of this case study and any potentially identifiable images or data included in this article.

Author contributions

JM, LL, and UK conceived and designed the study. LL and UK performed the clinical evaluation. JM, AS, and SS performed and analyzed the experiments related to genetic testing and biochemistry. SG analyzed the radiology findings. JM, LL, and AS wrote the article. All authors proofread the manuscript.

Funding

JM was supported by Department of Health Research (DHR)-Indian council of Medical Research (ICMR) Young Scientist Fellowship (R.12014/04/2017-HR).

Acknowledgments

We gratefully acknowledge the Electron Microscopy facility of Department of Anatomy, All India Institute of Medical Sciences, (AIIMS) New Delhi.

Conflict of interest

The authors declare that the research was conducted in the absence of any commercial or financial relationships that could be construed as a potential conflict of interest.

Publisher's note

Supplementary material

The Supplementary Material for this article can be found online at: https://www.frontiersin.org/articles/10.3389/fcvm.2022.939013/full#supplementary-material

SUPPLEMENTARY TABLE 1
Laboratory investigations.

DATASHEET 1
Supplementary Data 1 (Whole exome sequencing data analysis pipeline).

DATASHEET 2
Supplementary Data 2 (Materials and Methods).

References

1. Malfait F, Francomano C, Byers P, Belmont J, Berglund B, Black J, et al. The 2017 international classification of the ehlers-danlos syndromes. *Am J Med Genet C Semin Med Genet.* (2017) 175:8–26.

2. Byers PH. Vascular ehlers-danlos syndrome. In: Adam MP, Ardinger HH, Pagon RA, Wallace SE, Bean LJ, Stephens K editors. *GeneReviews*. Seattle (WA): University of Washington (2019).

3. Frank M, Albuisson J, Ranque B, Golmard L, Mazzella JM, Bal-Theoleyre L, et al. The type of variants at the COL3A1 gene associates with the phenotype and severity of vascular ehlers–danlos syndrome. *Eur J Hum Genet.* (2015) 23:1657–64. doi: 10.1038/ejhg.2015.32

4. The Ehlers–Danlos Syndromes, Rare Types - Brady - 2017. *American Journal of Medical Genetics Part C: Seminars in Medical Genetics - Wiley Online Library*. (2020). Available online at: https://onlinelibrary.wiley.com/doi/full/10.1002/ajmg.c.31550 (accessed July 24, 2020).

5. Cortini F, Villa C, Marinelli B, Combi R, Pesatori AC, Bassotti A. Understanding the basis of ehlers-danlos syndrome in the era of the next-generation sequencing. *Arch Dermatol Res.* (2019) 311:265–75. doi: 10.1007/s00403-019-01894-0

6. Richards S, Aziz N, Bale S, Bick D, Das S, Gastier-Foster J, et al. Standards and guidelines for the interpretation of sequence variants: a joint consensus recommendation of the american college of medical genetics and genomics and the association for molecular pathology. *Genet Med.* (2015) 17:405–24. doi: 10.1038/gim.2015.30

7. Jones K, Choong A, Canham N, Renton S, Pollitt R, Nesbitt M, et al. A combined vascular surgical and clinical genetics approach to diffuse aneurysmal disease. *Ann R Coll Surg Engl.* (2015) 97:e73–6. doi: 10.1308/003588415X14181254790121

8. 1000 Genomes Project Consortium, Auton A, Brooks LD, Durbin RM, Garrison EP, Kang HM, et al. A global reference for human genetic variation. *Nature.* (2015) 526:68–74.

9. Karczewski KJ, Weisburd B, Thomas B, Solomonson M, Ruderfer DM, Kavanagh D, et al. The ExAC browser: displaying reference data information from over 60 000 exomes. *Nucleic Acids Res.* (2017) 45:D840–5. doi: 10.1093/nar/gkw971

10. gnomAD. (2020). Available online at: https://gnomad.broadinstitute.org/ (accessed July 24, 2020).

11. Vangipuram M, Ting D, Kim S, Diaz R, Schüle B. Skin punch biopsy explant culture for derivation of primary human fibroblasts. *J Vis Exp.* (2013) 77:1437. doi: 10.3791/3779

12. Chiarelli N, Carini G, Zoppi N, Ritelli M, Colombi M. Molecular insights in the pathogenesis of classical ehlers-danlos syndrome from transcriptome-wide expression profiling of patients' skin fibroblasts. *PLoS One.* (2019) 14:e0211647. doi: 10.1371/journal.pone.0211647

13. Angwin C, Ghali N, Baker D, Brady AF, Pope FM, Vandersteen A, et al. Electron microscopy in the diagnosis of ehlers–danlos syndromes: correlation with clinical and genetic investigations. *Br J Dermatol.* (2020) 182:698–707. doi: 10.1111/bjd.18165

14. Chiarelli N, Ritelli M, Zoppi N, Colombi M. Cellular and molecular mechanisms in the pathogenesis of classical, vascular, and hypermobile ehlers–danlos syndromes. *Genes.* (2019) 10:3307. doi: 10.3390/genes10080609

15. Meijer AJ, Codogno P. Autophagy: regulation and role in disease. *Crit Rev Clin Lab Sci.* (2009) 46:210–40. doi: 10.1080/10408360903044068

16. Kuivaniemi H, Tromp G. Type III collagen (COL3A1): gene and protein structure, tissue distribution, and associated diseases. *Gene.* (2019) 707:151–71. doi: 10.1016/j.gene.2019.05.003

17. Pepin MG, Schwarze U, Rice KM, Liu M, Leistritz D, Byers PH. Survival is affected by mutation type and molecular mechanism in vascular ehlers-danlos syndrome (EDS type IV). *Genet Med.* (2014) 16:881–8. doi: 10.1038/gim.2014.72

18. Schwarze U, Schievink WI, Petty E, Jaff MR, Babovic-Vuksanovic D, Cherry KJ, et al. Haploinsufficiency for one COL3A1 allele of type III procollagen results in a phenotype similar to the vascular form of ehlers-danlos syndrome. ehlers-danlos syndrome type IV. *Am J Hum Genet.* (2001) 69:989–1001. doi: 10.1086/324123

19. Lightfoot RW, Michel BA, Bloch DA, Hunder GG, Zvaifler NJ, McShane DJ, et al. The american college of rheumatology 1990 criteria for the classification of polyarteritis nodosa. *Arthr Rheum.* (1990) 33:1088–93. doi: 10.1002/art.1780330805

20. Milewicz DM, Reid A, Cecchi A. Vascular ehlers danlos syndrome: exploring the role of inflammation in arterial disease. *Circ Cardiovasc Genet.* (2014) 7:5–7. doi: 10.1161/CIRCGENETICS.114.000507

21. Voermans NC, Drost G, van Kampen A, Gabreëls-Festen AA, Lammens M, Hamel BC, et al. Recurrent neuropathy associated with ehlers-danlos syndrome. *J Neurol.* (2006) 253:670–1. doi: 10.1007/s00415-005-0056-0

22. Castori M, Voermans N. Neurological manifestations of ehlers-danlos syndrome(s): a review. *Iran J Neurol.* (2014) 13:190–208.

23. Ohara N, Miyata T, Sato O, Oshiro H, Shigematsu H. Aortic aneurysm in patients with autoimmune diseases treated with corticosteroids. *Int Angiol.* (2000) 19:270–5. doi: 10.1053/ejvs.1999.0982

24. Eagleton MJ. Arterial complications of vascular ehlers-danlos syndrome. *J Vasc Surg.* (2016) 64:1869–80. doi: 10.1016/j.jvs.2016.06.120

25. Dubacher N, Münger J, Gorosabel MC, Crabb J, Ksiazek AA, Caspar SM, et al. Celiprolol but not losartan improves the biomechanical integrity of the aorta in a mouse model of vascular ehlers-danlos syndrome. *Cardiovasc Res.* (2020) 116:457–65. doi: 10.1093/cvr/cvz095

26. Frank M, Adham S, Seigle S, Legrand A, Mirault T, Henneton P, et al. Vascular ehlers-danlos syndrome: long-term observational study. *J Am Coll Cardiol.* (2019) 73:1948–57. doi: 10.1016/j.jacc.2019.01.058

27. Müller GA, Hansen U, Xu Z, Griswold B, Talan MI, McDonnell NB, et al. Allele-specific siRNA knockdown as a personalized treatment strategy for vascular ehlers-danlos syndrome in human fibroblasts. *FASEB J.* (2012) 26:668–77. doi: 10.1096/fj.11-182162

28. Watanabe A, Wada T, Tei K, Hata R, Fukushima Y, Shimada T. 618. a novel gene therapy strategy for vascular ehlers-danlos syndrome by the combination with RNAi mediated inhibition of a mutant allele and transcriptional activation of a normal allele. *Mol Ther.* (2005) 11:S240. doi: 10.1016/j.ymthe.2005.07.158

29. Bowen CJ, Calderón Giadrosic JF, Burger Z, Rykiel G, Davis EC, Helmers MR, et al. Targetable cellular signaling events mediate vascular pathology in vascular ehlers-danlos syndrome. *J Clin Invest.* (2020) 130:686–98. doi: 10.1172/JCI130730

frontiers | Frontiers in Cardiovascular Medicine

TYPE Case Report
PUBLISHED 08 November 2022
DOI 10.3389/fcvm.2022.1037370

OPEN ACCESS

EDITED BY
Neil Morgan,
University of Birmingham,
United Kingdom

REVIEWED BY
Silvia Favilli,
Meyer Children's Hospital, Italy
Emanuele Micaglio,
IRCCS San Donato Polyclinic, Italy

*CORRESPONDENCE
Ana Karina Zambrano
anazambrano17@hotmail.com

†These authors have contributed equally to this work and share first authorship

SPECIALTY SECTION
This article was submitted to Cardiovascular Genetics and Systems Medicine,
a section of the journal
Frontiers in Cardiovascular Medicine

RECEIVED 05 September 2022
ACCEPTED 19 October 2022
PUBLISHED 08 November 2022

CITATION
Cadena-Ullauri S, Guevara-Ramirez P, Ruiz-Pozo V, Tamayo-Trujillo R, Paz-Cruz E, Sánchez Insuasty T, Doménech N, Ibarra-Rodríguez AA and Zambrano AK (2022) Case report: Genomic screening for inherited cardiac conditions in Ecuadorian mestizo relatives: Improving familial diagnose.
Front. Cardiovasc. Med. 9:1037370.
doi: 10.3389/fcvm.2022.1037370

Case report: Genomic screening for inherited cardiac conditions in Ecuadorian mestizo relatives: Improving familial diagnose

Santiago Cadena-Ullauri[1†], Patricia Guevara-Ramirez[1], Viviana Ruiz-Pozo[1], Rafael Tamayo-Trujillo[1], Elius Paz-Cruz[1], Tatiana Sánchez Insuasty[2], Nieves Doménech[3], Adriana Alexandra Ibarra-Rodríguez[4] and Ana Karina Zambrano[1*†]

[1]Centro de Investigación Genética y Genómica, Facultad de Ciencias de la Salud Eugenio Espejo, Universidad UTE, Quito, Ecuador, [2]Cardióloga ecocardiografísta, Centros Médicos Especializados Cruz Roja Ecuatoriana, Quito, Ecuador, [3]Instituto de Investigación Biomédica de A Coruña (INIBIC)-CIBERCV, Complexo Hospitalario Universitario A Coruña (CHUAC), Sergas, Universidad da Coruña (UDC), La Coruña, Spain, [4]Grupo de Investigación Identificación Genética-IdentiGEN, FCEN, Universidad de Antioquia, Medellín, Colombia

Introduction: Genomic screening is an informative and helpful tool for the clinical management of inherited conditions such as cardiac diseases. Cardiac-inherited diseases are a group of disorders affecting the heart, its system, function, and vasculature. Among the cardiac inherited abnormalities, one of the most common is Wolff-Parkinson-White syndrome. Similarly, hypertrophic cardiomyopathy is another common autosomal dominant inherited cardiac disease. Hypertrophic cardiomyopathy is associated with an increased incidence of Wolff-Parkinson-White syndrome; reports have suggested that it could be caused by a mutation in the protein-coding gene PRKAG2, which encodes a subunit of the AMP-activated protein kinase.

Case presentation: A 37-year-old Ecuadorian male (Subject A) with familiar history of bradycardia, cardiac pacemaker implantation, and undiagnosed cardiac conditions began with episodes of tachycardia, dizziness, shortness of breath, and a feeling of fainting. He was diagnosed with hypertrophic myocardiopathy and Wolff Parkinson White preexcitation syndrome. Furthermore, his cousin's son, an 18-year-old Ecuadorian male (Subject B), started suffering from migraine and tachycardia at any time of the day. He was diagnosed with hypertrophic myocardiopathy; his electrocardiogram showed a systolic overload. Next-generation sequencing and ancestry analyses were performed. A c.905G>A p.(Arg302Gln) mutation in the gene PRKAG2 and a mainly European composition were identified in both subjects.

Conclusion: Genetic testing is a valuable tool as it can provide important information regarding a disease, including its cause and consequences, not only for single individuals but to identify at-risk relatives. Furthermore, NGS results could guide the physician into targeted therapy. In the present case report, a missense pathogenic Arg302Gln mutation in the PRKAG2

gene has been identified in two related Ecuadorian Subjects diagnosed with hypertrophic myocardiopathy and Wolff-Parkinson-White. The variant has not been reported in Latin America; hence, this is the first report of the Arg302Gln mutation in the PRKAG2 gene in mestizo Ecuadorian subjects with mainly European ancestry components.

KEYWORDS

genomic, cardiovascular disease, case report, genetics, ancestral

Introduction

Genomic screening is an informative and helpful tool for the clinical management of inherited conditions such as cardiac diseases. Thus, the results could be essential for identifying the disease causative, starting the patient early and targeting treatment, and increasing the chances of survival since there is evidence of an increased risk of sudden death in some cardiac conditions (1).

Cardiac-inherited diseases are a group of disorders affecting the heart, its system, function, and vasculature (2). In 2015, the % of deaths caused by heart disease was 20.3% for the Hispanic ethnic group in the United States (3). In Ecuador, in 2016, the first cause of death was acute myocardial infarction which constituted 9.05% of deaths (4).

Among the cardiac inherited abnormalities, one of the most common is Wolff-Parkinson-White syndrome (WPW), an autosomal dominant disease; its prevalence fluctuates between 0.68 and 1.7/1000 (5). WPW involves an abnormal atrioventricular electrical conductive with an electrocardiogram (ECG) pattern of short PR interval and prolonged QRS (6, 7). Its associated symptoms include tachycardia, such as palpitations, syncope, dizziness, and sudden death (7).

Furthermore, hypertrophic cardiomyopathy (HCM) is one of the most common autosomal dominant inherited cardiac diseases, with an estimated prevalence of 1 per 200 to 500 people in the general population (8). Recent studies suggest that approximately 20 million people worldwide are affected by HCM (just 10% of cases are identified) (8–10). HCM diagnosis is based on the presence of a non-dilated left ventricular hypertrophy, identified by an echocardiogram or magnetic resonance (8). At a cellular level, cardiac myocytes are hypertrophied, disorganized, and separated by fibrosis areas (11).

The HCM is associated with an increased incidence of WPW syndrome; reports have suggested that it could be caused by a mutation in the protein-coding gene PRKAG2, which encodes a subunit of the AMP-activated protein kinase (AMPK). AMPK is essential in regulating cellular ATP energy metabolism since it activates energy production and inhibits energy consumption (5, 12).

Here we report a complete genomic screening for cardiac inherited conditions of two relatives to improve early diagnosis of familial cases.

Case description

Clinical phenotype

A 37-year-old Ecuadorian male (Subject A) with familiar history of bradycardia; his father, two paternal aunts, and paternal grandmother underwent cardiac pacemaker implantation because of the bradycardia. Additionally, a cousin (father of subject B) was diagnosed with hypertrophic cardiomyopathy, and a half-brother from his father's side suffers an unknown cardiac condition (Figure 1). The patient went to the physician at the first time when he was 23 years old because of symptoms such as tachycardia, dizziness, shortness of breath, and a feeling of fainting at any time of the day. He was referred to the cardiologist, and electro and echocardiogram were performed. The diagnoses of WPW and HCM were based on the electrocardiogram, which showed a sinus rhythm with a short P-R interval accompanied by a prolonged QRS complex with a delta wave. A complete right bundle branch block with a significant increase in R wave voltages in the anterior, septal, low lateral, and high lateral (DI and aVL) regions was observed. A deep T wave inversion was identified in this same plane, and a low level in the segment ST-T V3-V6 (Supplementary Figure S1). The echocardiogram confirmed a structurally normal heart. Carvedilol was initially prescribed at a dose of 6.25 mg per day. However, four months prior to the publication of this case report, the dose increased to 12.5 mg daily.

Fourteen years later after the initial diagnosis, a genomic test was performed.

Moreover, 3 years ago, his cousin's son, an 18-year-old Ecuadorian male (Subject B) with the same familiar history of cardiac conditions (Figure 1), was referred to the cardiologist after suffering from migraines and tachycardia at any time of the day, especially after a sudden movement. Subject B underwent an electrocardiogram, and the results

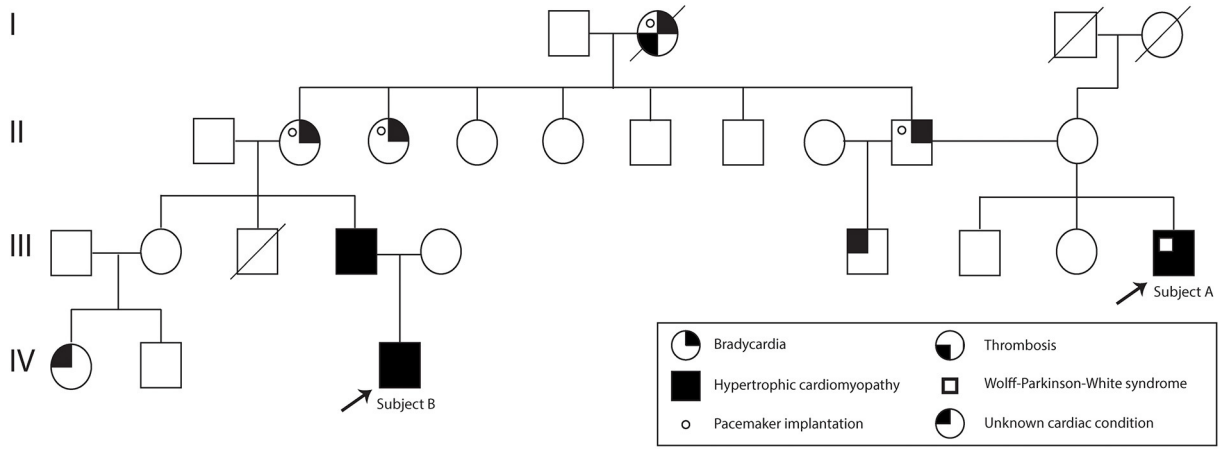

FIGURE 1
Subject A and B pedigree. Subject A and Subject B are indicated with an arrow. The family history of cardiac problems is depicted in the pedigree.

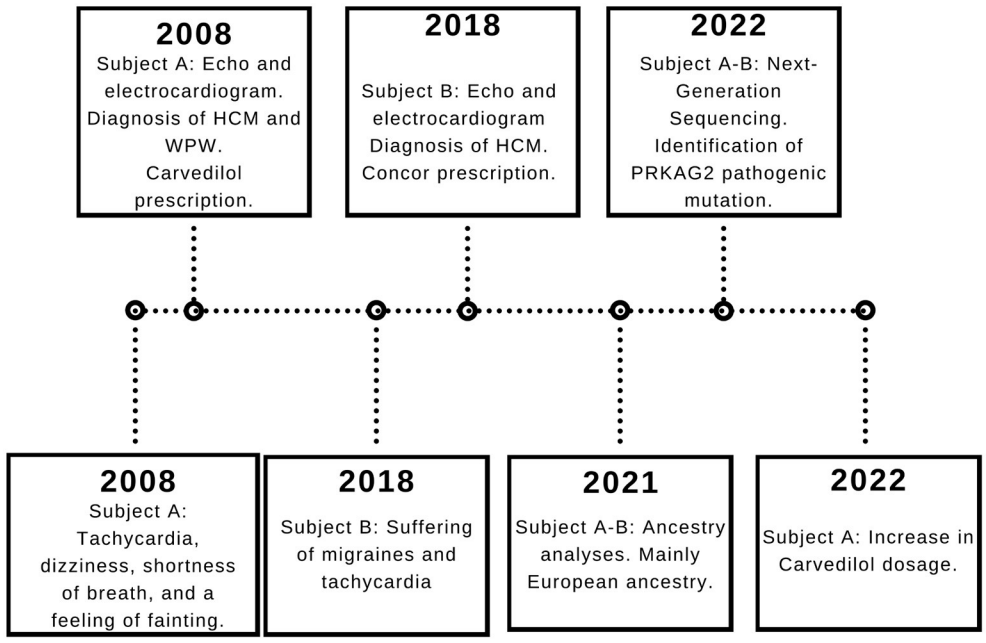

FIGURE 2
Subject A and B timeline. The relevant data is displayed in the timeline.

showed a systolic overload compatible with hypertrophic myocardiopathy, no association with WPW was found. Bisoprolol was prescribed at a dose of 1.25 mg daily, and the subject reported a significant reduction in the frequency of migraines. Similar to Subject A, a genomic screening was done. The timeline regarding subject A and B is presented in Figure 2.

Sampling and DNA extraction

Patients A and B self-identified as "mestizo" and signed the informed consent to participate in the study.

A peripheral blood sample was collected in an EDTA tube. The DNA was extracted with PureLink Genomic DNA

Mini Kit (Life Technologies) according to the manufacturer's protocol (13).

The DNA quantity and purity were measured by spectrophotometry and fluorometric methods; the quality was analyzed with an agarose gel. The sample was then diluted to 5ng/μL according to the sequencing protocol.

Next-generation sequencing (NGS)

The genomic procedure was performed at Centro de Investigación Genética y Genómica, using the commercially available kit TruSight Cardio kit (Illumina), covering 174 genes (575 kb of cumulative target region size) with known association with 17 Inherited Cardiac Conditions (47 genes for Hypertrophic Cardiomyopathy). The samples were processed according to the manufacturer's protocol (14) and run for 315 cycles in MiSeq System (Illumina).

Ancestral proportion analysis

For ancestral proportion analyses, PCR amplification was done with 46 ancestral informative INDEL markers in one multiplex reaction, according to Pereira et al. (15). Fragment separation and detection were executed on the 3,500 Genetic Analyzer (Thermo Fisher Scientific). The results were collected on Data Collection v 3.3 and analyzed in Gene Mapper v. 5 (Thermo Fisher Scientific).

Genomic and statistical data analysis

Genomic data analysis was done following the pipeline: 1) the alignment to the reference genome (hg38) and variant caller with DRAGEN Enrichment v. 3.9.5; 2) the annotation with Annotation Engine v.3.15; 3) the consequence prediction by PolyPhen and Sift; 4) the variants were filtered in the software Variant Interpreter v.2.16.1.300

The ancestral inference analysis was done with STRUCTURE v.2.3.4 using the option for an admixture model.

Diagnostic assessment

Genomic results

After applying variant filters (pass quality and association including pathogenic, likely pathogenic, and of uncertain significance), nine variants were displayed to be involved in the diagnosis of subject A; however, two intronic and two PolyPhen-predicted benign variants were discarded. The disease-relevant variants are presented in Table 1.

After applying variant filters (pass quality and association including pathogenic, likely pathogenic, and of uncertain significance) in subject B, six variants were found; however, one intronic and three predicted as benign by PolyPhen were discarded. The two diagnosis-associated variants are presented in Table 2.

Both individuals presented the same mutation c.905G>A p.(Arg302Gln) in the gene PRKAG2, which has been associated with PRKAG2 cardiac syndrome.

Ancestral characterization

Subject A has a major European (51%) composition, followed by Native American (43.9%) and African (5.1%).

Moreover, subject B also has a major European (51.1%), followed by Native American (41.6%) and African (7.3%) composition.

Data corroborates that both individuals are a population mixture, in agreement with their initial self-identification.

Discussion

Nowadays, genetic testing is increasingly recommended, as it provides helpful information for clinical management, including early diagnosis, family screening, and targeted therapy for cardiovascular diseases. Although, NGS has limitations, such as the need for bioinformatic knowledge for sample processing, interpretation of variants of unknown significance, or management of incidental findings (16). The American Heart Association has encouraged research in cardiovascular genetics to further understand the molecular aspects of these diseases (17). In the present case report, the TruSight Cardio (Illumina) kit was used; the panel of this kit consists of 174 genes that have been associated with 17 different cardiovascular diseases. By analyzing this amount of information, the chances of identifying pathogenic or likely pathogenic variants associated with the clinical diagnosis increase.

Heart diseases are the most common cause of death with no correlation with demographic or ethnic factors (5, 11). Among cardiomyopathies, HCM is the most common condition (18). Sarcomeric protein mutations have been primarily associated with familial or sporadic cases of HCM; however, non-sarcomere proteins involved in biological processes such as cellular metabolism have also been correlated to HCM (19). Moreover, regarding WPW, about 2 to 5% of patients diagnosed with HCM exhibit WPW (11, 20, 21).

The serine/threonine protein kinase AMPK regulates cellular energetic homeostasis. The enzyme is stimulated by AMP concentration and the activity of the AMPK-kinase; its principal function is to counterbalance ATP depletion. Moreover, AMPK comprises three subunits (α,

TABLE 1 Genomic variants found in Subject A.

Gene	Variant	Consequence	Association	Zygosity
PRKAG2	SNV c.905G>A p.(Arg302Gln)	Missense	Pathogenic	Heterozygous
GCKR	SNV c.307G>A p.(Val103Met)	Missense	Likely Pathogenic	Heterozygous
APOB	SNV c.9871C>T p.(Arg3291Cys)	Missense	Variant of uncertain significance	Heterozygous
TTN	SNV c.44986C>T p.(Arg14996Cys)	Missense	Variant of uncertain significance	Heterozygous
PKP2	SNV c.1726A>T p.(Met576Leu)	Missense	Variant of uncertain significance	Heterozygous

TABLE 2 Genomic variants found in Subject B.

Gene	Variant	Consequence	Association	Zygosity
PRKAG2	SNV c.905G>A p.(Arg302Gln)	Missense	Pathogenic	Heterozygous
TTN	SNV c.8056A>G p.(Ile2686Val)	Missense	Variant of uncertain significance	Heterozygous

β, γ). The Gamma 2 regulatory subunit of AMP-Activated Protein Kinase (PRKAG2) activity enhances the Alpha subunit activation by binding to AMP (21, 22). Mutations in the gene that encodes PRKAG2 have been associated with glycogen storage cardiomyopathies by disrupting AMPK's ability to bind to AMP, dysregulating the metabolic and glucidic uptake, and causing the deposition of amylopectin and glycogen (5). The symptoms of the PRKAG2 cardiac syndrome vary, ranging from asymptomatic to a phenotype that includes cardiac hypertrophy, primarily involving the left ventricle, supraventricular tachycardia (WPW), increased risk of heart failure, and sudden cardiac death (5, 22). The results of NGS identified a pathogenic missense mutation G>A at position 905, causing a change from arginine to glutamine at codon 302, exon 7 of the PRKAG2 gene, in both subjects; however, only subject A presents WPW.

Similarly, different mutations in the gene TTN were found. In subject A, a missense mutation Arg14996Cys, and in subject B, a missense mutation Ile2686Val; however, both variants are categorized as variants of uncertain significance (VUS), and mutations in the TTN gene have been primarily associated with dilated cardiomyopathy, not hypertrophic (23, 24). Moreover, three more variants were found in subject A, two VUS in the genes APOB and PKP2, and one likely pathogenic variant in the gene GCKR; this variant has been associated with a higher risk of type 2 diabetes (25).

Ancestry analyses were performed to determine the genetic background of both subjects. Subjects A and B had mainly European ancestry components. Databases such as Allele Frequency Aggregator (26), The Exome Aggregation Consortium (ExAC) (27), and The genome Aggregation Database-Exomes (gnomAD-Exomes) (28) were used for information regarding the frequency, in Latin America, of the identified variant. The mutation has not been reported in Latin American populations; hence, this is the first report of an Arg302Gln mutation in the PRKAG2 gene in Latin America.

Conclusion

Genetic testing is a useful tool as it can provide important information regarding a disease, including its cause and consequences, not only for single individuals but also to identify at-risk relatives. Furthermore, NGS results could guide the physician into targeted therapy. In the present case report, a missense pathogenic Arg302Gln mutation in the

PRKAG2 gene has been identified in two related Ecuadorian Subjects diagnosed with hypertrophic myocardiopathy and Wolff-Parkinson-White. The variant has not been reported in Latin America; hence, this is the first report of the Arg302Gln mutation in the PRKAG2 gene in mestizo Ecuadorian subjects with mainly European ancestry components.

Unfortunately, in the presented family case, the access to other family members' samples were limited due to their refusal and unavailability to participate in the study.

Data availability statement

The results are presented in the paper. Genomic Data are available in NCBI Sequence Read Archive (SRA) with the BioProject accession number PRJNA891265 (http://www.ncbi.nlm.nih.gov/bioproject/891265). For more information, please contact the corresponding author AZ (anazambrano17@hotmail.com).

Ethics statement

The studies involving human participants were reviewed and approved by Comité de Ética de Investigación en Seres Humanos—Universidad UTE. The patients/participants provided their written informed consent to participate in this study.

Author contributions

Conceptualization and formal analysis: SC-U and AZ. Resources: TS. Methodology: AZ, SC-U, PG-R, VR-P, EP-C, and RT-T. Writing—review and editing: AZ, SC-U, PG-R, VR-P, EP-C, ND, AI-R, and RT-T. Supervision, project administration, and funding acquisition: AZ. All authors contributed to the article and approved the submitted version.

Funding

The project was funded by Universidad UTE.

Acknowledgments

The authors are grateful to the patients for participating in the study and to the Cruz Roja Ecuatoriana for their collaboration.

Conflict of interest

The authors declare that the research was conducted in the absence of any commercial or financial relationships that could be construed as a potential conflict of interest.

Publisher's note

All claims expressed in this article are solely those of the authors and do not necessarily represent those of their affiliated organizations, or those of the publisher, the editors and the reviewers. Any product that may be evaluated in this article, or claim that may be made by its manufacturer, is not guaranteed or endorsed by the publisher.

Supplementary material

The Supplementary Material for this article can be found online at: https://www.frontiersin.org/articles/10.3389/fcvm.2022.1037370/full#supplementary-material

SUPPLEMENTARY FIGURE S1
Subject A electrocardiogram.

References

1. Waddell-Smith KE, Donoghue T, Oates S, Graham A, Crawford J, Stiles MK, et al. Inpatient detection of cardiac-inherited disease: the impact of improving family history taking. *Open Hear.* (2016) 3:e000329. Available online at: http://openheart.bmj.com/

2. NHS England. *NHS Standard Contract for Cardiology: Inherited Cardiac Conditions*. NHS Comm Board (2013). p. 1–22. Available online at: http://www.england.nhs.uk/wp-content/uploads/2013/06/d01-com-dis-equ-prosth.pdf

3. Centers for Disease Control and Prevention. *Underlying Cause of Death, 1999-2020 Request*. CDC WONDER Online Database (2020). Available online at: https://wonder.cdc.gov/ucd-icd10.html

4. Ministerio de Salud Pública del Ecuador. *Perfil de Mortalidad por Sexo 2016*. (2017). Available online at: https://public.tableau.com/profile/darwin5248#!/vizhome/defunciones2016/Historia1?publish=yes

5. Porto AG, Brun F, Severini GM, Losurdo P, Fabris E, Taylor MRG, et al. Clinical spectrum of PRKAG2 syndrome. *Circ Arrhythmia Electrophysiol.* (2016) 9:e003121. doi: 10.1161/CIRCEP.115.003121

6. MacRae CA, Ghaisas N, Kass S, Donnelly S, Basson CT, Watkins HC, et al. Familial hypertrophic cardiomyopathy with Wolff-Parkinson-White syndrome maps to a locus on chromosome 7q3. *J Clin Invest.* (1995) 96:1216–20.

7. Gupta A, Al-Ahmad A. Wolff parkinson white syndrome. In: *Cardiac Electrophysiology: Clinical Case Review*. StatPearls Publishing (2021). p. 267–9. Available online at: https://www.ncbi.nlm.nih.gov/books/NBK554437/

8. Antunes M de O, Scudeler TL. Hypertrophic cardiomyopathy. *IJC Hear Vasc.* (2020) 27:100503. doi: 10.1016/j.ijcha.2020.100503

9. Maron BJ. Clinical course and management of hypertrophic cardiomyopathy. *N Engl J Med.* (2018) 379:655–68. doi: 10.1056/NEJMra1710575

10. Maron BJ, Rowin EJ, Maron MS. Global burden of hypertrophic cardiomyopathy. *JACC Hear Fail.* (2018) 6:376–8. Available online at:

11. Marian AJ, Braunwald E. Hypertrophic cardiomyopathy: Genetics, pathogenesis, clinical manifestations, diagnosis, and therapy. *Circ Res.* (2017) 121:749–70. doi: 10.1161/CIRCRESAHA.117.311059

12. Blair E, Redwood C, Ashrafian H, Oliveira M, Broxholme J, Kerr B, et al. Mutations in the gamma(2) subunit of AMP-activated protein kinase cause familial hypertrophic cardiomyopathy: evidence for the central role of energy compromise in disease pathogenesis. *Hum Mol Genet.* (2001) 10:1215–20. doi: 10.1093/hmg/10.11.1215

13. Life Technologies. *PureLink ® Genomic DNA Kits for Purification of Genomic DNA*. Invitrogen by life Technologies (2013). p. 1–48. Available online at: https://tools.thermofisher.com/content/sfs/manuals/purelink_genomic_man.pdf

14. Illumina. Customize a short end-to-end workkow guide with the Custom Protocol Selector TruSight ® Cardio Sequencing Kit Reference Guide. 2016;

15. Pereira R, Phillips C, Pinto N, Santos C, dos Santos SE, Amorim A, et al. Straightforward inference of ancestry and admixture proportions through ancestry-informative insertion deletion multiplexing. *PLoS ONE.* (2012) 7:e29684. doi: 10.1371/journal.pone.0029684

16. Di Resta C, Galbiati S, Carrera P, Ferrari M. Next-generation sequencing approach for the diagnosis of human diseases: Open challenges and new opportunities. *Electron J Int Fed Clin Chem Lab Med.* (2018) 29:4–14.

17. Musunuru K, Hershberger RE, Day SM, Klinedinst NJ, Landstrom AP, Parikh VN, et al. Genetic testing for inherited cardiovascular diseases: A scientific statement from the american heart association. *Circ Genomic Precis Med.* (2020) 13:E000067. doi: 10.1161/HCG.0000000000000067

18. Heron M. *National Vital Statistics Reports Volume 68, Number 6, June 24, 2019, Deaths: Leading Causes for 2017*. (2019). Available online at: https://www.cdc.gov/nchs/products/index.htm

19. Elliot PM, Zamorano JL, Anastasakis A, Borger MA, Borggrefe M, Cecchi F, et al. 2014 ESC guidelines on diagnosis and management of hypertrophic cardiomyopathy: The task force for the diagnosis and management of hypertrophic cardiomyopathy of the European Society of Cardiology (ESC). *Eur Heart J.* (2014) 35:2733–79. doi: 10.1093/eurheartj/ehu284

20. Kelly BS, Mattu A, Brady WJ. Hypertrophic cardiomyopathy: electrocardiographic manifestations and other important considerations for the emergency physician. *Am J Emerg Med.* (2007) 25:72–9. doi: 10.1016/j.ajem.2006.04.017

21. Aggarwal V, Dobrolet N, Fishberger S, Zablah J, Jayakar P, Ammous Z. PRKAG2 mutation: An easily missed cardiac specific non-lysosomal glycogenosis. *Ann Pediatr Cardiol.* (2015) 8:153–6. doi: 10.4103/0974-2069.154149

22. Banankhah P, Fishbein GA, Dota A, Ardehali R. Cardiac manifestations of PRKAG2 mutation. *BMC Med Genet.* (2018) 19:17–20. doi: 10.1186/s12881-017-0512-6

23. Begay RL, Graw S, Sinagra G, Merlo M, Slavov D, Gowan K, et al. Role of titin missense variants in dilated cardiomyopathy. *J Am Heart Assoc.* (2015) 4:1–9. doi: 10.1161/JAHA.115.002645

24. Norton N, Duanxiang L, Rampersaud E, Morales A, Martin ER, Zuchner S, et al. Exome sequencing and genome-wide linkage analysis in 17 families illustrates the complex contribution of TTN truncating variants to dilated cardiomyopathy. *Circ Cardiovasc Genet.* (2013) 6:1–7. doi: 10.1161/CIRCGENETICS.111.000062

25. Rees MG, Ng D, Ruppert S, Turner C, Beer NL, Swift AJ, et al. Correlation of rare coding variants in the gene encoding human glucokinase regulatory protein with phenotypic, cellular, and kinetic outcomes. *J Clin Invest.* (2012) 122:205–17. doi: 10.1172/JCI46425

26. Phan L, Jin Y, Zhang H, Qiang W, Shektman E, Shao D, et al. *ALFA: Allele Frequency Aggregator*. National Center for Biotechnology Information; U.S. National Library of Medicine (2020). Available online at: http://www.ncbi.nlm.nih.gov/snp/docs/gsr/alfa

27. Karczewski KJ, Weisburd B, Thomas B, Solomonson M, Ruderfer DM, Kavanagh D, et al. The ExAC browser: Displaying reference data information from over 60 000 exomes. *Nucleic Acids Res.* (2017) 45:D840–5. doi: 10.1093/nar/gkw971

28. Karczewski KJ, Francioli LC, Tiao G, Cummings BB, Alföldi J, Wang Q, et al. The mutational constraint spectrum quantified from variation in 141,456 humans. *Nature.* (2020) 581:434–43. doi: 10.1038/s41586-020-2308-7.

frontiers | Frontiers in Cardiovascular Medicine

TYPE Case Report
PUBLISHED 10 November 2022
DOI 10.3389/fcvm.2022.1030160

OPEN ACCESS

EDITED BY
Neil Morgan,
University of Birmingham,
United Kingdom

REVIEWED BY
Yousef Shahin,
The University of Sheffield,
United Kingdom
Olga Vriz,
King Faisal Specialist Hospital &
Research Centre, Saudi Arabia

*CORRESPONDENCE
Ling Tan
dr.tanling@csu.edu.cn
Hao Tang
dr.tanghao@csu.edu.cn

SPECIALTY SECTION
This article was submitted to Cardiovascular Genetics and Systems Medicine,
a section of the journal
Frontiers in Cardiovascular Medicine

RECEIVED 28 August 2022
ACCEPTED 17 October 2022
PUBLISHED 10 November 2022

CITATION
Zeng Y, Hu Y, Jiang B, Tan L and Tang H (2022) Unusual combination of acute aortic dissection, Mayer-Rokitansky-Küster-Hauser syndrome, and 46,XX gonadal dysgenesis: A case report.
Front. Cardiovasc. Med. 9:1030160.
doi: 10.3389/fcvm.2022.1030160

Unusual combination of acute aortic dissection, Mayer-Rokitansky-Küster-Hauser syndrome, and 46,XX gonadal dysgenesis: A case report

Yifan Zeng, Yerong Hu, Bo Jiang, Ling Tan* and Hao Tang*

Department of Cardiovascular Surgery, The Second Xiangya Hospital of Central South University, Changsha, Hunan, China

Background: Acute Stanford type A aortic dissection (ATAAD) is a life-threatening disease. Elderly patients are the high-risk population for aortic dissection (AD). Young patients with AD usually have heritable connective tissue diseases such as Marfan syndrome and Loeys-Dietz syndrome. However, young AD patients without heritable connective tissue disease are relatively rare.

Case presentation: Herein, we report a case of a 25-year-old female diagnosed with ATAAD accompanied by undeveloped secondary sexual characteristics. Computed tomography angiography (CTA) showed that her AD involved the ascending and abdominal aorta. She had undergone thoracic endovascular aortic stent graft implantation in a local hospital due to acute Stanford type B aortic dissection at age 19. No uterus or ovaries were found on CTA and transabdominal ultrasonography. Sex hormone detection revealed a low estrogen level. G-banded karyotyping analyses revealed a normal 46,XX karyotype. Finally, her abnormalities in the reproductive system were diagnosed as MRKH syndrome and 46,XX gonadal dysgenesis. Whole-exome sequencing (WES) in the patient found an SNP variant of *ACTA2* c.773G>A and *MYH11* c.5081A>G. *MYH11* c.5081A>G was also found in her mother and younger brother. Copy number variations sequencing (CNV-seq) found an approximately 109.30 Kb duplication at chromosome 6p22.3 (Chr 6: g.24920238–25029535) with a copy number of 3. We performed emergent total aortic arch replacement with frozen elephant trunk surgery, and the patient recovered well after surgery. However, her abdominal AD was stilling progression during 6 months of follow-up.

Conclusion: To our knowledge, we report the world's first case of early-onset recurrent AD combined with MRKH syndrome and 46,XX gonadal dysgenesis.

KEYWORDS

aortic dissection, MRKH syndrome, 46,XX gonadal dysgenesis, total aortic arch replacement, frozen elephant trunk, whole-exome sequencing

Introduction

Aortic dissection (AD) is a disease in which the intima of the aorta tear separates the intima and media of the aortic wall and allows blood to enter the false lumen. Acute Stanford type A aortic dissection (ATAAD) is a life-threatening disease with 50% mortality in the first 48 h (1). The annual incidence of ATAAD varies between 3 and 4/100,000 (2). Female incidence is lower but of higher mortality than male incidence (3).

Primary amenorrhea is a leading cause of female infertility. Mayer-Rokitansky-Küster-Hauser (MRKH) syndrome and gonadal dysgenesis (GD) are the most common causes of primary amenorrhea. Mayer-Rokitansky-Küster-Hauser syndrome, a congenital disorder also referred to as Müllerian agenesis, is characterized by congenital aplasia of the uterus, cervix, and the upper part (2/3) of the vagina in females with typical secondary sex characteristics and a normal 46,XX karyotype (4). Chromosomal regions 1q21.1, 16p11.2, 17q12, and 22q11.21 have been identified as recurrent genetic abnormalities associated with MRKH syndrome (5). Gonadal dysgenesis with female phenotype is defined as the absence or incomplete development of ovaries. Gonadal dysgenesis is mainly associated with sex chromosome abnormalities. The 45,XO, 45,X/46,XX, 45,X/46,X, dic(X), 46,XX, and 46,XY karyotypes have been reported (6). Gonadal dysgenesis with a normal 46,XX karyotype is relatively rare. The coexistence of MRKH syndrome and 46,XX GD is very rare, and only a few cases have been reported (7–9).

This article presents the world's first case of early-onset recurrent AD accompanied with MRKH syndrome and 46,XX GD.

Case presentation

A 25-year-old female patient who presented with persistent chest pain was admitted to our institution. Undeveloped secondary sexual characteristics were found during physical examination (Figure 1A). Computed tomography angiography (CTA) showed that her AD involved the ascending (Figure 1B) and abdominal aorta (Figure 1C). She had undergone thoracic endovascular aortic stent graft implantation (Figures 1B,D, arrow) in a local hospital due to acute Stanford type B aortic dissection at age 19. No uterus or ovaries was found by CTA (Figures 1E,F, arrowhead) and transabdominal ultrasound (Figure 1G, arrowhead). Sexual hormone detection revealed hypergonadotropic hypogonadism (follicle-stimulating hormone 66.98 IU/L, luteinizing hormone 25.41 IU/L, and estradiol 0.1 pg/ml).

Her height (155 cm) and weight (55 kg) were within the normal range in the Chinese female population, and she had no hypertension or family history of genetic disorders. In early pregnancy, her parents, both working at a chemical plant, had a history of exposure to potential toxicants, including cyanide, ammonia, sulfuric acid, and nitric acid. Her 18-year-old brother had hypertension, and her mother had coronary artery atherosclerosis. She presented with primary amenorrhea at age 15, was diagnosed by a gynecologist as MRKH syndrome accompanied with congenital absence of the ovaries, and was treated with hormone replacement therapy (HRT) for only 3 months. G-banded karyotyping analysis revealed a normal 46,XX karyotype (Figure 2A). The abnormalities in her reproductive system were eventually diagnosed as MRKH syndrome with 46,XX GD.

To further explore the genetic correlation between AD and congenital dysplasia of the reproductive system, we performed whole-exome sequencing (WES) and copy number variations sequencing (CNV-seq). Whole-exome sequencing of the patient and her family members, including her mother, father, and brother, showed a single nucleotide polymorphism (SNP) in the *MYH11* gene (*MYH11*; NM_002474.2; c.5081A>G; p.Glu1694Gly) and *ACTA2* gene (*ACTA2*; NM_001613.2; c.773G>A; p.Arg258His). MYH11 c.5081A>G was carried by the patient, her mother, and her brother, and ACTA2 was only carried by the patient (Figure 2B). The WES results were validated by Sanger sequencing (Figure 2C). An approximately 109-Kb (Chr 6: g.24920238-25029535) duplication at chromosome 6p22.3 was found in the patient by CNV-seq, which has not been related to the development of the uterus and ovaries. Finally, no clear genetic link between AD and abnormalities in the female reproductive system was found.

We performed emergency total aortic arch replacement and frozen elephant trunk surgery, and the patient recovered well and was discharged on postoperative day 12.

The patient refused to receive HRT after surgery, and her abdominal aortic dissection (AAD) was progression during a 6-month follow-up (Figures 3A–F). The false lumen of AAD at intimal tears (Figures 3A–C) and maximum diameter (Figures 3D–F) both expanded slightly 7 days after surgery and rapidly expanded 6 months after surgery.

Discussion

The main feature of this patient was early-onset recurrent AD accompanied with rare dysplasia of the female reproductive system (MRKH syndrome and 46,XX GD) without heritable connective tissue disease. No significant genetic relationship between AD, MRKH syndrome, and 46,XX GD was found. Nevertheless, the reason why this patient suffered from recurrent AD at a young age remains to be determined.

Single nucleotide polymorphism mutations in *MYH11* and *ACTA2* were detected in this 25-year-old female patient, suggesting that the co-mutations in *MYH11* and *ACTA2* may be involved in the pathogenesis of AD. The *ACTA2* mutation in the patient was *de novo* in her family. Besides, *ACTA2* c.773G>A

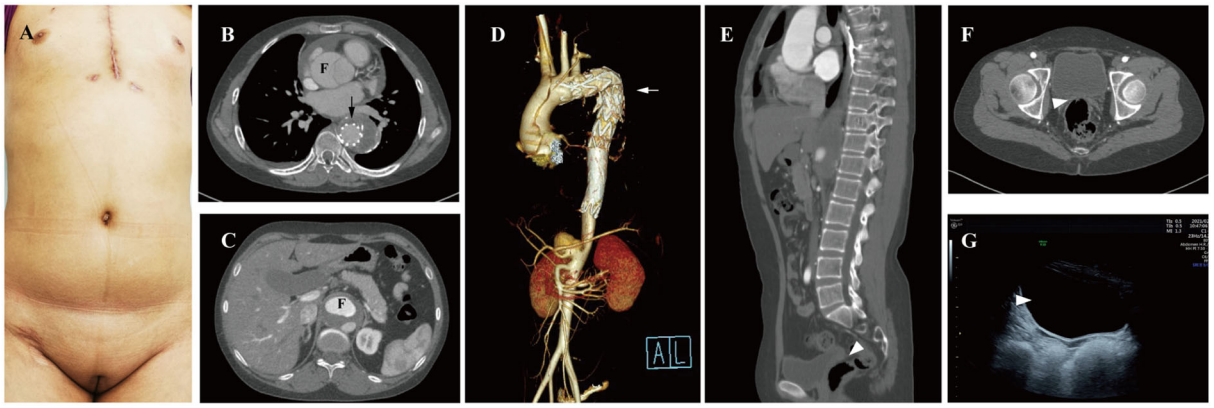

FIGURE 1
Preoperative examination of the 25-year-old female patients. **(A)** Undeveloped secondary sexual characteristics. CTA shown aortic dissection involving the ascending **(B)** and abdominal aorta **(C)**, F, false lumen. **(D)** Thoracic endovascular aortic stent was grafted (arrow); no uterus or ovaries was found between urinary bladder and rectum by CTA (**E,F**, arrowhead) and transabdominal ultrasound (**G**, arrowhead). CTA, computed tomography angiography; F, false lumen.

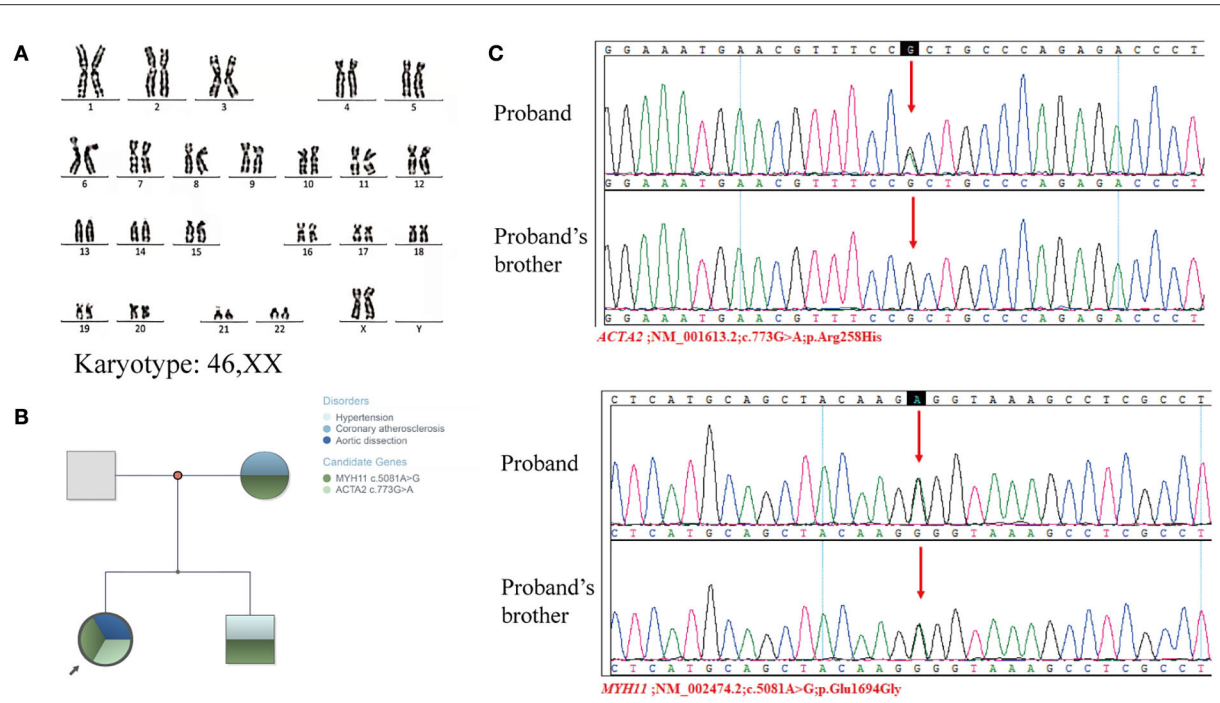

FIGURE 2
Genetic examination of the proband and proband's families. **(A)** Karyotyping analyses revealed a normal 46,XX karyotype. **(B)** Family tree. **(C)** Sanger sequencing validated the mutation of *ACTA2* c.773G>A and *MYH11* c.5081A>G in the proband and her brother.

has been reported to be associated with the pathogenesis of AD (10). According to the *European Reference Network for Rare Vascular Diseases (VASCERN) consensus*, *ACTA2* is closely related to the morbidity of cardiovascular disease, primarily seen in AD with 54% Stanford type A AD (median age 36 years) and 21% type B (median age 27 years) (11). Nevertheless, the onset age of AD in this patient was significantly earlier than the reported average age. A possible explanation is the synergistic effect of mutations in *MYH11* and *ACTA2*. A mouse experiment has shown that $Acta2^{-/-}Myh11^{R247C/R247C}$ mouse accelerates aortic enlargement and increases medial degeneration (12). However, the function of *MYH11* c.5081A>G in cardiovascular diseases remains unclear. *MYH11* c.5081A>G is carried by the patient, her mother, and her brother (Figure 2C). Furthermore,

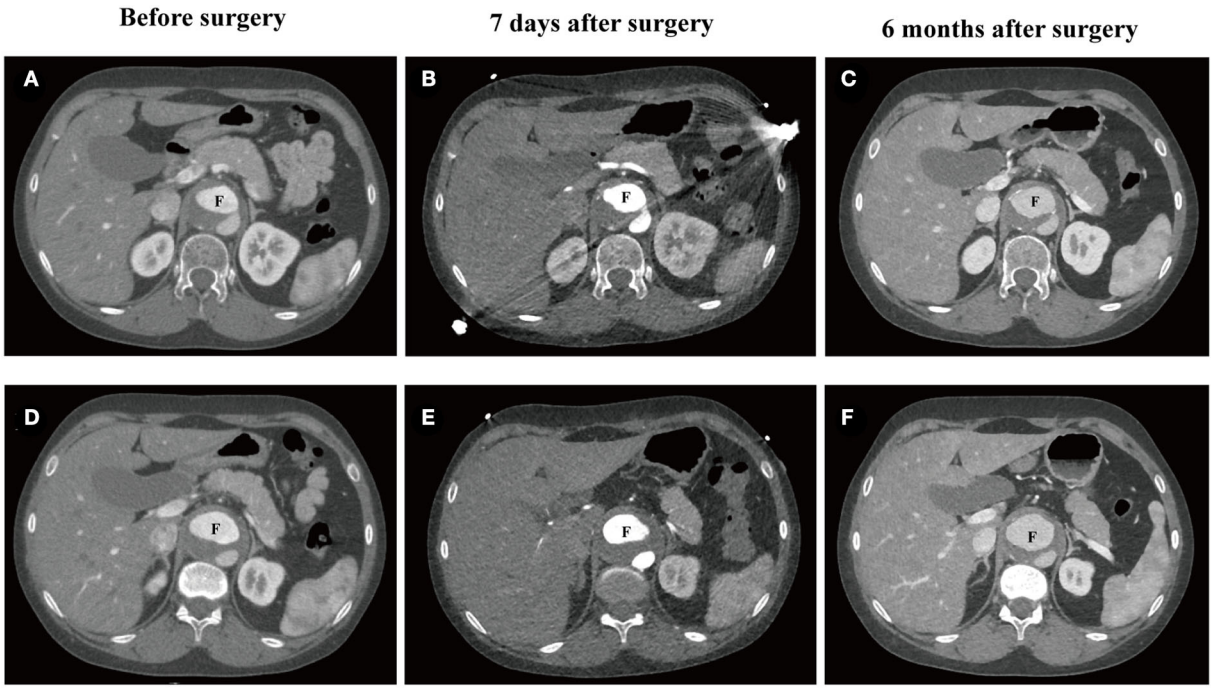

FIGURE 3
CTA of abdominal aortic dissection in the 25-year-old female patient. **(A–C)** The false lumen at the position of intimal tears before surgery (32.8 × 22.8 mm^2), 7 days after surgery (32.6 × 22.2 mm^2), and 6 months after surgery (35.9 × 26.8 mm^2). **(D–F)** Maximum diameter of the false lumen of AAD before surgery (38.9 × 23.1 mm^2), 7 days after surgery (39.3 × 24.6mm^2), and 6 months after surgery (40.9 × 29.1 mm^2). CTA, computed tomography angiography; F, false lumen.

they suffered from cardiovascular conditions. In comparison, no mutations in *MYH11* and *ACTA2* were detected in her father who had no cardiovascular diseases. Therefore, we believe that *MYH11* c.5081A>G may be essential in developing cardiovascular diseases.

Low estrogen caused by MRKH syndrome and 46,XX GD may also accelerate the progression of AD. To our knowledge, AD accompanied with gonadal anomalies is rare and mostly seen in Turner Syndrome (TS). Turner Syndrome is a genetic disorder mainly caused by complete or partial absence of one of the X chromosomes. The morbidity and mortality of TS are highly related to the presence of hypertension, aortic dilatation, aortic aneurysm, and AD (13). Hormone replacement therapy is thought to relieve aortic dilation and AD in TS patients (14). The life expectancy of TS patients after HRT is significantly prolonged, which may be related to the cardiovascular protective effects of estrogen. Besides, carotid artery intima thickness has been reported to be decreased significantly after HRT in patients with 46,XX GD and TS (15), suggesting that HRT may have a cardiovascular protective effect in patients with 46,XX GD. However, there is no clinical consensus on the necessity of using HRT in patients with AD accompanied with GD. In this case, this patient did not receive HRT after surgery, and the AAD is progressing rapidly. Therefore, we recommend using HRT for patients with estrogen deficiency. Moreover, the use of HRT in postmenopausal women with aortic aneurysm or AD still needs to be investigated.

The molecular basis of GD and MRKH syndrome is still not known. CNV-seq found a 109-Kb (Chr 6: g.24920238–25029535) duplication at chromosome 6p22.3, but no reports related to MRKH syndrome, 46,XX GD, or AD yet. We thought that the etiology of dysplasia of the female reproductive system is related to the toxicant exposure of her parents during the gestation period. A number of toxicants, such as phthalate esters (PEs), have been reported to have a direct link with GD when exposed during early pregnancy (16). Animal studies have confirmed that *utero* exposure of PEs lead to characteristics of MRKH syndrome in SD rats (17). Moreover, long-term ambient fine particles (PM2.5) exposure could induce ovarian dysfunction in mice (18). Therefore, environmental pollution plays an important role in the dysgenesis of the reproductive system, but the mechanism remains to be explored.

Data availability statement

The datasets presented in this study can be found in online repositories. The names of the repository/repositories

and accession number(s) can be found in the article/supplementary material.

Ethics statement

The studies involving human participants were reviewed and approved by the Second Xiangya Hospital, Central South University. The patients/participants provided their written informed consent to participate in this study. Written informed consent was obtained from the individual(s) for the publication of any potentially identifiable images or data included in this article.

Author contributions

YZ drafted the manuscript. HT and YH designed the study. HT and LT revised the manuscript. BJ, YZ, and HT were responsible for the collection of data or analysis. All authors contributed to the article and approved the submitted version.

Funding

This work was supported by the Key Research and Development Program of Hunan Province of China [Award number(s): 2019SK2022].

Conflict of interest

The authors declare that the research was conducted in the absence of any commercial or financial relationships that could be construed as a potential conflict of interest.

Publisher's note

References

1. Gawinecka J, Schönrath F, von Eckardstein A. Acute aortic dissection: pathogenesis, risk factors and diagnosis. *Swiss Med Wkly.* (2017) 147:w14489. doi: 10.4414/smw.2017.14489

2. LeMaire SA, Russell L. Epidemiology of thoracic aortic dissection. *Nat Rev Cardiol.* (2011) 8:103–13. doi: 10.1038/nrcardio.2010.187

3. Smedberg C, Steuer J, Leander K, Hultgren R. Sex differences and temporal trends in aortic dissection: a population-based study of incidence, treatment strategies, and outcome in Swedish patients during 15 years. *Eur Heart J.* (2020) 41:2430–8. doi: 10.1093/eurheartj/ehaa446

4. Morcel K, Camborieux L, Programme de Recherches sur les Aplasies Müllériennes (PRAM), Guerrier D. Mayer-Rokitansky-Küster-Hauser (MRKH) syndrome. *Orphanet J Rare Dis.* (2007) 2:13. doi: 10.1186/1750-1172-2-13

5. Triantafyllidi VE, Mavrogianni D, Kalampalikis A, Litos M, Roidi S, Michala L. Identification of genetic causes in Mayer-Rokitansky-Küster-Hauser (MRKH) syndrome: a systematic review of the literature. *Children (Basel).* (2022) 9:961. doi: 10.3390/children9070961

6. Acién P, Acién M. Disorders of sex development: classification, review, and impact on fertility. *J Clin Med.* (2020) 9:E3555. doi: 10.3390/jcm9113555

7. Manne S, Veeraabhinav CH, Jetti M, Himabindu Y, Donthu K, Badireddy M. A rare case of 46,XX gonadal dysgenesis and Mayer-Rokitansky-Kuster-Hauser syndrome. *J Hum Reprod Sci.* (2016) 9:263–6. doi: 10.4103/0974-1208.197694

8. Kisu I, Ono A, Iijma T, Katayama M, Iura A, Hirao N. Mayer-Rokitansky-Küster-Hauser syndrome with a uterine cervix and normal vagina associated with gonadal dysgenesis in a 46,XX female. *J Obstet Gynaecol Res.* (2019) 45:1386–90. doi: 10.1111/jog.13956

9. Opdecam L, Barudy Vasquez J, Camerlinck M, Makar A. Misdiagnosis of associated mullerian agenesis in a female with 46,XX gonadal dysgenesis: a case report and review of literature. *J Obstet Gynaecol.* (2021) 41:1164–5. doi: 10.1080/01443615.2020.1798908

10. Regalado ES, Guo D, Prakash S, Bensend TA, Flynn K, Estrera A, et al. Aortic disease presentation and outcome associated with ACTA2 mutations. *Circ Cardiovasc Genet.* (2015) 8:457–64. doi: 10.1161/CIRCGENETICS.114.000943

11. van de Laar IMBH, Arbustini E, Loeys B, Björck E, Murphy L, Groenink M, et al. European reference network for rare vascular diseases (VASCERN) consensus statement for the screening and management of patients with pathogenic ACTA2 variants. *Orphanet J Rare Dis.* (2019) 14:264. doi: 10.1186/s13023-019-1186-2

12. Kwartler CS, Gong L, Chen J, Wang S, Kulmacz R, Duan X-Y, et al. Variants of unknown significance in genes associated with heritable thoracic aortic disease can be low penetrant "risk variants." *Am J Hum Genet.* (2018) 103:138–43. doi: 10.1016/j.ajhg.2018.05.012

13. Donadille B, Christin-Maitre S. Heart and Turner syndrome. *Ann d'Endocrinol.* (2021) 82:135–40. doi: 10.1016/j.ando.2020.12.004

14. Elsheikh M, Bird R, Casadei B, Conway GS, Wass JA. The effect of hormone replacement therapy on cardiovascular hemodynamics in women with Turner's syndrome. *J Clin Endocrinol Metab.* (2000) 85:614–8.2016092613300400190

15. Ostberg JE, Storry C, Donald AE, Attar MJH, Halcox JPJ, Conway GS. A dose-response study of hormone replacement in young hypogonadal women: effects on intima media thickness and metabolism. *Clin Endocrinol (Oxf).* (2007) 66:557–64. doi: 10.1111/j.1365-2265.2007.02772.x

16. Johansson HKL, Svingen T, Fowler PA, Vinggaard AM, Boberg J. Environmental influences on ovarian dysgenesis - developmental windows sensitive to chemical exposures. *Nat Rev Endocrinol.* (2017) 13:400–14. doi: 10.1038/nrendo.2017.36

17. Hannas BR, Howdeshell KL, Furr J, Gray LE. *In utero* phthalate effects in the female rat: a model for MRKH syndrome. *Toxicol Lett.* (2013) 223:315–21. doi: 10.1016/j.toxlet.2013.03.021

18. Zhou S, Xi Y, Chen Y, Zhang Z, Wu C, Yan W, et al. Ovarian dysfunction induced by chronic whole-body PM2.5 exposure. *Small.* (2020) 16:e2000845. doi: 10.1002/smll.202000845

frontiers | Frontiers in Cardiovascular Medicine

TYPE Original Research
PUBLISHED 26 January 2023
DOI 10.3389/fcvm.2023.1091183

OPEN ACCESS

EDITED BY
Neil Morgan,
University of Birmingham, United Kingdom

REVIEWED BY
Giacomo Tini,
Sapienza University of Rome, Italy
Zhuang Tian,
Peking Union Medical College Hospital (CAMS), China

*CORRESPONDENCE
Xiaohong Pan
✉ heartpanxh@zju.edu.cn
Yu Liu
✉ liuyu@dicp.ac.cn

†These authors have contributed equally to this work

SPECIALTY SECTION
This article was submitted to Cardiovascular Genetics and Systems Medicine, a section of the journal Frontiers in Cardiovascular Medicine

RECEIVED 06 November 2022
ACCEPTED 09 January 2023
PUBLISHED 26 January 2023

CITATION
Ma Q, Wang M, Huang Y, Nie Y, Zhang X, Yang DD, Wang Z, Ding S, Qian N, Liu Y and Pan X (2023) Identification of a novel transthyretin mutation D39Y in a cardiac amyloidosis patient and its biochemical characterizations.
Front. Cardiovasc. Med. 10:1091183.
doi: 10.3389/fcvm.2023.1091183

Identification of a novel transthyretin mutation D39Y in a cardiac amyloidosis patient and its biochemical characterizations

Qunchao Ma[1†], Mengdie Wang[2,3†], Yanan Huang[2], Ying Nie[4], Xin Zhang[5,6], Dan Dan Yang[1], Zhuo Wang[1], Siyin Ding[1], Ningjing Qian[1], Yu Liu[2*] and Xiaohong Pan[1*]

[1]Department of Cardiology, The Second Affiliated Hospital, Zhejiang University School of Medicine, Hangzhou, Zhejiang, China, [2]Chinese Academy of Sciences (CAS) Key Laboratory of Separation Science for Analytical Chemistry, Dalian Institute of Chemical Physics, Chinese Academy of Sciences, Dalian, China, [3]Department of Chemistry, University of Chinese Academy of Sciences, Beijing, China, [4]Instrumentation and Service Center for Physical Sciences, Westlake University, Hangzhou, Zhejiang, China, [5]School of Science, School of Life Sciences, Westlake University, Hangzhou, China, [6]Westlake Laboratory of Life Sciences and Biomedicine, Institute of Natural Sciences, Westlake Institute for Advanced Study, Hangzhou, China

Hereditary transthyretin cardiac amyloidosis (hATTR-CA) is a rare autosomal dominantly inherited disease caused by mutations in the transthyretin (TTR) gene. TTR mutations often cause the instability of transthyretin, production of misfolded proteins, and ultimately excessive deposition of insoluble amyloid fibrils in the myocardium, thereby leading to cardiac dysfunction. Herein, we report a novel transthyretin D39Y mutation in a Chinese family. We characterized the kinetic and thermodynamic stabilities of D39Y mutant TTR, revealing that TTR D39Y mutant was less stable than WT TTR and more stable than amyloidogenic mutation TTR L55P. Meanwhile, the only FDA approved drug Tafamidis showed satisfactory inhibitory effect toward ATTR amyloid formation and strong binding affinity in test tube revealed by isothermal titration calorimetry. Finally, we measured the well-folded tetrameric TTR concentration in patient's and his descents' blood serum using a previously reported UPLC-based assay. Notably, the tetramer concentrations gradually increased from symptomatic D39Y gene carrier father, to asymptomatic D39Y gene carrier daughter, and further to wild type daughter, suggesting the decrease in functional tetrameric TTR concentration may serve as an indicator for disease age of onset in D39Y gene carriers. The study described a Chinese family with hATTR-CA due to the TTR variant D39Y with its destabilizing effect in both kinetic and thermodynamic stabilities.

KEYWORDS

cardiac amyloidosis, novel mutation, stability, transthyretin, tetramer concentration

Introduction

Transthyretin cardiac amyloidosis (ATTR-CA) is an infiltrative disease characterized by abnormal deposition of amyloid fibrils in the myocardium (1). ATTR-CA commonly presents with signs and symptoms of heart failure, and is often accompanied by various extracardiac manifestations. The disease can be divided into two categories, wild-type ATTR cardiac amyloidosis (wtATTR-CA) and hereditary transthyretin cardiac amyloidosis (hATTR-CA),

according to the presence or absence of a transthyretin (TTR) mutation. Mutations in TTR are the common cause of hATTR-CA. The majority of TTR mutations are caused by single nucleotide substitutions (2). In hATTR-CA patients, the phenotypic presentation, severity and age of onset are variable depending on the specific type of TTR mutation (3). However, ATTR-CA remains a progressive disease with dismal prognosis and poor quality of life. The median survival after diagnosis in patients with Val122Ile hATTR-CA is only 31 months (3). ATTR-CA is often accompanied with racial and geographic differences, yet the clinical and genetic features of this disease are not well elucidated.

Transthyretin consists of 127 amino acids, with a β-sheet-rich structure (3). TTR is synthesized mostly by the liver to transport thyroxine (T4) and holo-retinol binding protein (RBP) in the blood and cerebrospinal fluid (4). Due to hydrophobic and hydrogen bonding, monomeric TTR assembles into tetramer through a dimer intermediate (5). In the case of denaturing microenvironment or genetic mutations, the natural TTR loses its physiological function and conformation to form fibril aggregates that eventually deposit in different organs or tissues (6, 7). Misfolding and aggregation of TTR attract increasing attention, given its amyloidogenicity. This aggregation process occurs in two steps: folded tetrameric TTR dissociates to dimers at the weaker dimer-dimer interface and dimers further dissociate into aggregation-prone monomers; metastable monomers undergo denaturation and eventually assemble into amyloids (8). The tetramers dissociation is the biochemical rate-limiting step of the entire process because the unfolding of monomers is 5–6th orders of magnitude faster than the tetramer dissociation (9). Normally, TTR can induce amyloidosis by decreasing its thermodynamic and/or kinetic stability (10, 11). Thus, studying the biochemical properties of TTR variants is important for the precise diagnosis and choice of therapies for patients with ATTR amyloidosis, especially given their differential clinical symptoms, onset age, and responses to drug treatments.

In this study, we reported a new TTR mutation D39Y occurring in China (c.175G>T p.D39Y, numbered without the first 20 amino acids that serve as signaling peptide and are cleaved during TTR secretion). This patient was a 75-years-old male, presenting dyspnea on exertion and lower extremity edema. Through biochemical and biophysical characterizations, we observed that D39Y displayed compromised thermodynamic stability (Cm = 2.8 M) compared to wild-type TTR (WT-TTR, Cm = 3.4 M). The kinetic stability of D39Y TTR reflected by the tetramer dissociation rate (kdiss = 0.07 h-1, t1/2 = 9.9 h) significantly decreased under physiological conditions. Meanwhile, dissociation of heterotetramers consisting of wild-type and D39Y subunits was not affected by increasing the D39Y mutant subunit ratio, potentially explaining the late disease onset of this mutation. The binding affinity of small molecule drug Tafamidis with TTR-D39Y mutant measured by isothermal titration calorimetry (ITC) was comparable to WT-TTR, resulting in satisfactory inhibition of amyloid formation. Finally, we measured the tetrameric TTR concentration in three blood serum samples across a two-generation pedigree. Notably, the tetramer concentrations gradually increased from symptomatic D39Y gene carrier father, to asymptomatic D39Y gene carrier daughter, and further to wild type daughter, suggesting decrease in functional tetrameric TTR concentration may serve as an indicator for disease age of onset in D39Y gene carriers.

Materials and methods

Human samples

A 75-years-old male patient presented relapsed heart failure symptoms and was diagnosed with ATTR-CA at the Department of Cardiology, Second Affiliated Hospital of Zhejiang University College of Medicine (SAHZU). Clinical data were obtained from the medical history system at SAHZU from September 2019 to April 2022. We performed genetic sequencing to differentiate hATTR-CA from wtATTR-CA for this patient. When hATTR-CA is confirmed, we recommend genetic screening for the patient's 46-year-old daughter and 43-year-old daughter because this disease is inherited. Written Informed consent was taken from the patient and relatives before acquiring blood samples and clinical data. In parallel, blood samples and data analysis were conducted at the SAHZU, and biochemical characterization analysis was performed at Chinese Academy of Sciences (CAS) Key Laboratory of Separation Science for Analytical Chemistry. The participants agreed to the publication of clinical data and complementary examinations after the identifiable personal information was removed. This investigation was performed according to the Declaration of Helsinki and with approval by the Institutional Ethics Committee of SAHZU (Ethical Batch Number: 20220273). This was a prospective study involving retrospective clinical data.

Plasmid construction and protein purification

Wild-type transthyretin and variants were recombinantly prepared following previous literature. Genes of *E. coli* transthyretin were codon optimized, synthesized by GenScript, and sub-cloned into pET-29b (+) vectors. WT, L55P, and D39Y plasmids were transformed into BL21 DE3 *E. coli* cells. Cells were grown to OD600 at 0.6–0.8 before being induced by IPTG (0.5 mM) at 37°C for 4 h. Cultured cells were harvested and resuspended in resuspension buffer (50 mM Tris, 150 mM NaCl, pH = 7.5; 15 mL buffer/L of culture). Cells expressing recombinant proteins were thawed and lysed by sonication at 4°C. Lysed cells were centrifuged for 30 min at 16,000 rpm. Ammonium sulfate (final concentration of 242 g/L) was slowly added to the supernatant with rigorous stirring at 4°C for 20 min. The solution was centrifuged at 12,000 rpm for 15 min at 4°C. The supernatant was supplemented with additional ammonium sulfate to a final concentration of 607 g/L with rigorous stirring at 4°C for 20 min. The solution was centrifuged at 12,000 rpm for 15 min at 4°C. The pellet was resuspended in 20 mL of anion exchange buffer A (25 mM Tris, 1 mM EDTA, pH = 8.0) and dialyzed against 4 L of buffer A overnight at 4°C. After dialysis, the sample was filtered and applied to a 50 mL Source 15Q anion exchange column (GE Healthcare) equilibrated with buffer A. TTR was eluted using a linear gradient of NaCl (160 mL; 50–350 mM) followed by a NaCl wash (50 mL; 350 mM). Eluted TTR was purified using a 120 mL Superdex 200 gel filtration column (GE Healthcare) in SEC buffer (10 mM sodium phosphate, 100 mM KCl, 1 mM EDTA, pH = 7.4). The protein containing fractions were identified by SDS-PAGE gel analysis, pooled, and concentrated. No significant impurities were identified and purity was estimated to be 98% based on SDS-PAGE electrophoresis analysis.

Thermodynamic stability of TTR measured by urea-mediated tryptophan fluorescence

To quantify the thermodynamic stability of protein TTR, we denatured D39Y-TTR (3.6 μM) by urea of concentration from 0.5 to 9.0 M in phosphate buffer (10 mM sodium phosphate, 100 mM KCl, 1 mM EDTA, pH = 7.4). After 96 h, the fluorescence of tryptophan was measured from 310 to 410 nm with excitation at 295 nm. The ratio at 355 nm and 335 nm was recorded as a signal of the unfolding of TTR.

Urea-mediated TTR dissociation measured by resveratrol binding

Resveratrol increases in its fluorescence quantum yield and displays a blue shift when it selectively binds to the TTR tetramer. We quantified the dissociation of TTR by measuring the concentration of tetrameric TTR to text the equilibrium between TTR tetramers and monomers. 500 μL D39Y TTR (3.6 μM) was incubated with urea (5 M) in phosphate buffer (10 mM sodium phosphate, 100 mM KCl, 1 mM EDTA, pH = 7.4) for 96 h. In order not to disturb the equilibrium of tetramers and monomers, TTR samples were treated with resveratrol (18 μM) just before the fluorescence measurement. Excited at 320 nm, the resveratrol fluorescence spectrum was recorded from 310 to 410 nm. Fluorescence at 394 nm was reported on the concentration of tetrameric D39Y TTR.

Kinetics of monomer unfolding and tetramer dissociation measured by urea denaturation

Kinetic stability was determined by the rate-limiting dissociation of the tetramer, because monomer unfolding was much faster than tetramer dissociation. To verify this, we incubated TTR (3.6 μM) in urea at the concentration from 3 to 9 M in phosphate buffer (10 mM sodium phosphate, 100 mM KCl, 1 mM EDTA, pH = 7.4, 25°C). Tryptophan fluorescence (I355/335) was recorded at period of time. The kinetics data fit well to a single exponential function: I355/335 = I355/335N + A (1–e-kdiss t); where I355/335N is the native protein fluorescence intensity ratio (355/335 nm), A is the amplitude difference, kdiss is the tetramer dissociation rate constant and t is time in h. The lnkdiss versus urea concentration plot is linear, allowing extrapolation to 0 M urea.

Fibril formation assay

Tafamidis of various concentrations was preincubated with TTR (7.2 μM) in phosphate buffer (10 mM sodium phosphate, 100 mM KCl, 1 mM EDTA, pH = 7.4) at 37°C for 0.5 h. Acidic aggregation buffer (200 mM NaOAc, 100 mM KCl, acidified by AcOH to pH = 4.40) was added to the samples to get a final concentration of TTR of 7.2 μM, and after incubating at 37°C for 72 h, the extent of fibril formation was measured by OD at 330 nm.

Isothermal titration calorimetry (ITC)

Following the protocol reported before, dissociation constants for Tafamidis binding to wild type, L55P and D39Y TTR were determined using a MicroCal PEAQ-ITC (Malvern MAN0572-01-EN-00). A solution of Tafamidis (300 μM in 10 mM sodium phosphate, 100 mM KCl, 1 mM EDTA, 5% DMSO, 5% EtOH, pH = 7.4) was prepared and titrated into an ITC cell containing TTR (25 μM in 10 mM sodium phosphate, 100 mM KCl, 1 mM EDTA, 5% DMSO, 5% EtOH, pH = 7.4). The initial injection of 1 μL was followed by 35 injections of 1 μL each (25°C). Integration of the thermogram after subtraction of blanks yielded a binding isotherm that fit best to a model of one binding site. The data were fit by a non-linear least squares approach with one adjustable parameter, namely, Kd, using the ITC data analysis module in Microcal PEAQ-ITC analysis software.

Analysis of patients serum by ultra performance liquid separation (UPLC)

This protocol was adapted from previous work by the Kelly group. Briefly, UPLC (FLR) Waters Acquity H-Class uplc plus pro and Protein-pakTM Hi RCSQ (5 μm, 4.6 × 100 mm) were from Waters. The A2 molecule was synthesized in the laboratory. The patients' sera were incubated with A2 for covalent labeling and subjected to UPLC separation and detection of tetramer TTR. Each sample was injected onto a Waters Acquity H-Class UPLC plus pro instrument fitted with a Protein-pakTM Hi RCSQ (5 μm, 4.6 × 100 mm) from Waters. TTR was eluted from the column using the following gradient (Buffer A: 25 mM Tris–HCl, pH = 9.0, 1 mM EDTA; Buffer B: 1 M NaCl, 1 mM EDTA, 25 mM Tris–HCl, pH = 9.0).

Results

Genetic mutation identification and patient's clinical presentations

The proband presented worsening dyspnea on exertion and lower extremity edema over 1 year. The proband's ECG revealed an atrial flutter with low voltage in the limb leads, with a QS pattern in lead II, III and aVF. Laboratory investigations showed mild elevated BNP (135.7 pg/ml) and troponin T (0.027 ng/ml). Serum and urine protein electrophoresis with immunofixation and sFLC assay were negative. Echocardiography showed bi-atrial enlargement, symmetrical left ventricular hypertrophy (septal 17.4 mm and posterior wall 16.6 mm), and mild impaired left ventricular systolic function (LVEF 49.2%) (**Figure 1A**, right side). Speckle tracking echocardiography revealed severely depressed global longitudinal strain with apical sparing (GLS-8.4%) (**Figure 1A**, left side) which was a hallmark of cardiac amyloidosis. Cardiac enhanced magnetic resonance showed diffuse subendocardial late gadolinium enhancement (**Figure 1B**). Tc-99m-PYP nuclear scintigraphy showed grade 3 myocardial uptake with increased heart/contralateral lung ratio (HCL 2.38) (**Figure 1C**). Furthermore, the proband and his two asymptomatic daughters were sequenced and analyzed

10.3389/fcvm.2023.1091183

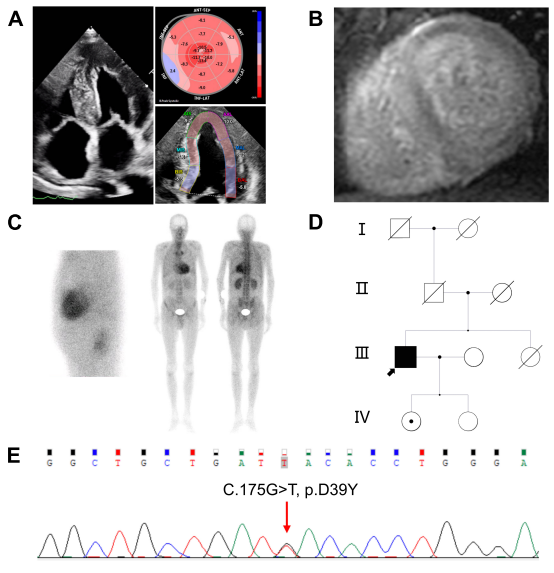

FIGURE 1
Clinical features of the proband **(A)** right, 4-chambers view of two-dimensional echocardiography; left, speckle tracking echocardiography; **(B)** short axis view of cardiac magnetic resonance imaging showed diffuse subendocardial late gadolinium enhancement in ventricular walls; **(C)** Tc-99m-PYP scintigraphy revealed grade 3 myocardial uptake, and HCL ratio was 2.38; left, planar myocardial imaging; right, planar whole-body imaging; **(D)** pedigree of the family. The black arrow represents the proband, dot in the center of the circle represent female carrier: **(E)** Sequence analysis of exon 2 of the TTR gene. The proband showed a homozygous missense variant with a G>T change at nucleotide 175. PYP: Pyrophosphate. HCL: Heart/contralateral lung ratio. TTR, Transthyretin.

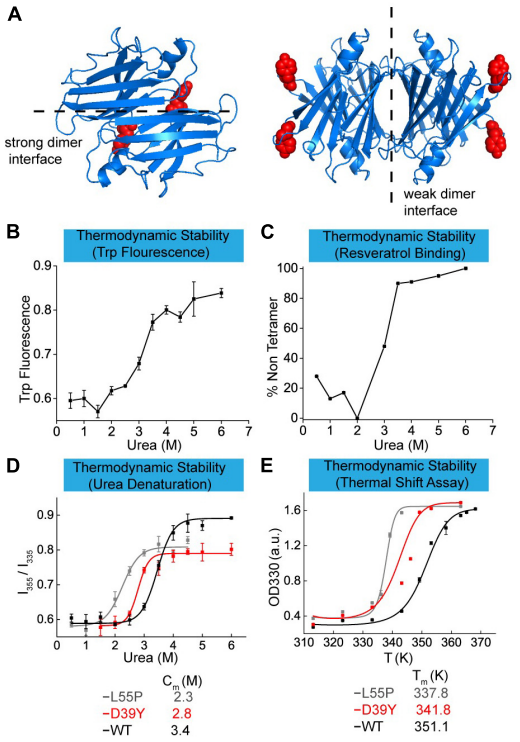

FIGURE 2
Thermodynamic stability of TTR-D39Y. **(A)** X-ray crystallographic structure of D39Y-TTR modified from WT-TTR (PDB code: 1BMZ). Y-39 was highlighted in red. **(B)** Urea-mediated unfolding of TTR-D39Y measured by tryptophan fluorescence changes (ratio at 355 nm and 335 nm). **(C)** Urea-mediated tetramer dissociation of TTR-D39Y measured by resveratrol binding fluorescence (394 nm). **(D)** Denaturation curve measured by tryptophan fluorescence. **(E)** Thermodynamic stability measured by thermal shift assay.

(Figure 1D). The proband showed a novel homozygous missense variant at base position 175 in exon 2 of the TTR gene (c.175G>T), resulting in an aspartic acid change to tyrosine (p.D39Y, numbered without the first 20 amino acids that serve as signaling peptide and are cleaved during TTR secretion) (Figure 1E). The proband's eldest daughter was identified as carrying this heterozygous variant of TTR gene c.175G>T. *In silico* analyses predicted this c.175G>T variant could be pathogenic (SIFT: affect protein function; Polyphen-2: benign; Mutation Taster: polymorphism; M-CAP: damaging).

Thermodynamic stability of the TTR variant D39Y

Point mutants on TTR protein usually affect its thermodynamic and kinetic stability leading to ATTR amyloidosis diseases. In this work, we elucidated the effect of D39Y mutation (Figure 2A) on the thermodynamic stability in three ways and compared it with the parameters of commonly studied mutation L55P and wild type TTR. First, we measured the thermodynamic stability by urea-mediated denaturation (Figure 2B), followed by resveratrol binding measurement (Figure 2C). Normally, the thermodynamic stability was quantified by urea denaturation midpoints (Cm), revealing that D39Y (Cm = 2.8 M) exhibited higher stability than L55P-TTR (Cm = 2.3 M), but lower than that of WT-TTR (Cm = 3.4 M) (Figure 2D). To further validate this result, we performed a thermal shift assay that can quantify the thermodynamic stability of TTR *via* melting temperature (Tm). TTR (7.2 μM) was heated in acid aggregation buffer (NaOAc 200 mM, KCl 100 mM, acidified by AcOH to pH = 4.4), respectively from 35 to 96°C for 5 min and measured the optical density at 330 nm. The thermal shift assay concluded the same that D39Y (Tm = 341.8 K) is more stable than L55P (Tm = 337.8 K), but less stable than WT (Tm = 351.1 K) and (Figure 2E). Overall, D39Y-TTR is thermodynamically destabilized compared to WT-TTR.

Kinetic stability of D39Y-TTR mutant protein

Some TTR mutations destabilize TTR by decreasing the tetramer dissociation kinetic barrier. To verify whether the variant D39Y reduced the kinetic stability of TTR, we quantified it using tetramers dissociation half time (t1/2) measured by urea mediated denaturation (Figures 3A, B). Kinetically, in 6 M urea, D39Y (t1/2 = 5.4 h) was less stable than WT (t1/2 = 17.1 h), but more stable compared with L55P (t1/2 = 0.6 h) (Figure 3C). Under physiological conditions (0 M urea), the conclusion still held true. Extrapolated from the urea mediated tetramer dissociation curve (Figure 3B), D39Y (t1/2 = 9.9 h, 0 M urea) was less stable compared with WT (t1/2 = 42 h), but more stable than L55P (t1/2 = 4.4 h) on kinetic stability under 0 M physiological conditions (Figure 3D).

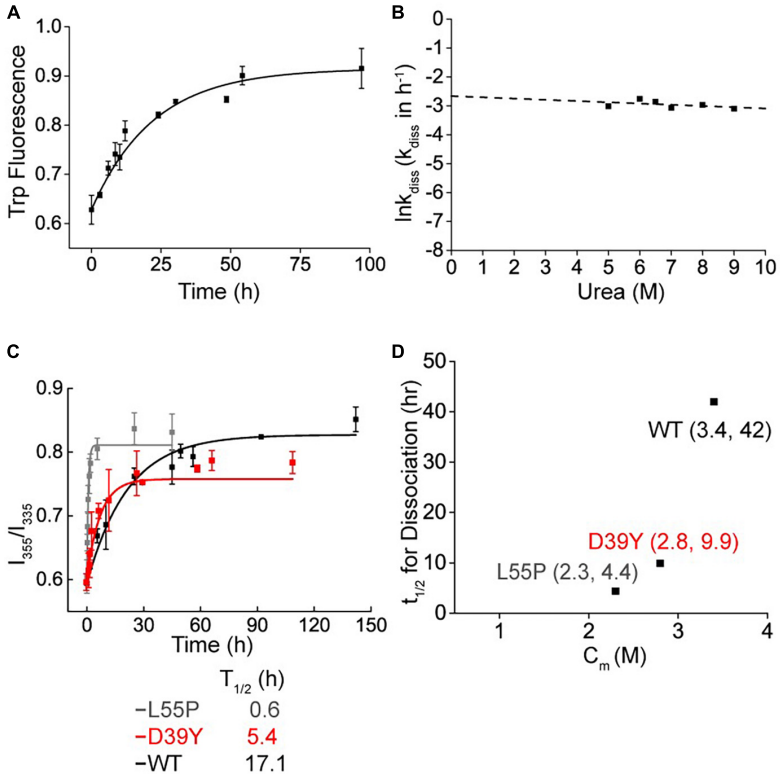

FIGURE 3
Kinetic stability of D39Y TTR. **(A)** Tetramer dissociation measured by tryptophan fluorescence in 9 M urea. **(B)** The logarithm of the rate of tetramer dissociation, lnkdiss (kdiss in h-1) plotted as a function of urea concentration. The lnkdiss vs. urea concentration plot is linear, allowing extrapolation to 0 M urea. **(C)** Kinetic stability measured by tryptophan fluorescence in 6 M urea. L55P, gray curve; D39Y, red curve; WT, black curve. **(D)** Relationship between thermodynamic (*x* Axis; Cm of denaturation curve) and kinetic (*y* Axis; t1/2 of tetramer dissociation) stability.

D39Y: WT TTR heterozygous tetramers is kinetically stable and resistant to proteolysis

Transthyretin is usually heterotetramers in patients' serum due to the subunit exchange effect. To compare the kinetic stability of heterotetramers of variant D39Y and WT, we mixed up D39Y and WT TTR and incubated them in phosphate buffer (10 mM sodium phosphate, 100 mM KCl, 1 mM EDTA, pH = 7.4) at D39Y:WT ratios from 4:0 to 0:4 at 4°C for 48 h for efficient subunit exchange. Then, the subunit exchanged samples were subjected to cross-linking reaction. Through the cross-linking reaction, glutaraldehyde crosslinked two TTR monomers into a dimer, the dimer into a tetramer, and the dimer into a tetramer, as well as octamers and multimers of larger molecular weights. Therefore, we observed these products of higher molecular weights as corresponding bands on this SDS-PAGE gel. Due to the limited resolution of the SDS-PAGE gel and the randomness of crosslinking reaction between TTR multimers, these higher molecular bands representing TTR crosslinked multimers exhibited as a smear bands cluster at the top of the gel. Fortunately, this experiment does not rely on the quantification of these smear bands of higher molecular weights. We monitored the dimeric bands that were well defined and the molecular weight of which was clearly discernible by the gel ladder. SDS-PAGE gel analysis of TTR proteins after cross-linking showed that homotetramers and heterotetramers had the same kinetic stability as the dissociated dimer bands did not change with the increasing ratio of D39Y and WT (Figure 4A). This result may explain the late disease age-of-onset for the D39Y patient reported herein.

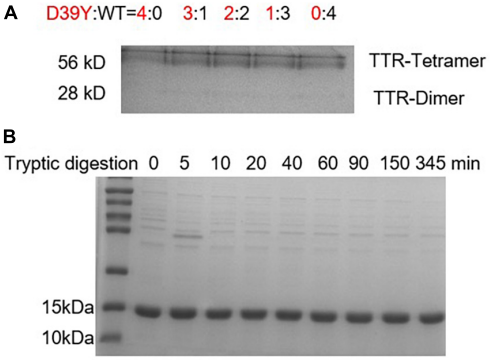

FIGURE 4
Heterozygous tetramers of D39Y: WT TTR is stable and resistant to proteolysis. **(A)** SDS-PAGE electrophoresis analysis of D39Y: WT TTR heterozygous tetramers after crosslinking revealed no increasing dimer bands upon increasing D39Y mutant protein ratio. It suggests heterozygous tetramers of D39Y: WT TTR is kinetically stable. Heterozygous tetramers were prepared at indicated molar ratios of D39Y mutant (red) to WT (black), from 4:0 (D39Y alone) to 0:4 (WT alone), as shown above the gel. **(B)** SDS-PAGE electrophoresis analysis of D39Y showed proteolytic resistance toward trypsin digestion, suggesting D39Y mutation does not generate proteolytic fragments that lead to amyloid formation.

On the other hand, besides the deposition of full-length amyloid TTR, fragment 49–127 to trigger TTR aggregation is also a pathway to form amyloid fibrils. To assess whether D39Y is capable of forming digested fragments, D39Y (3.6 μM) was incubated with trypsin (5 μg/mL) at 37°C for 0–345 min. The products were analyzed by SDS-PAGE gel, revealing no digested bands at 9 kDa. This result demonstrates that D39Y is resistant to proteolysis and does not generate amyloid-prone proteolytic fragments (**Figure 4B**). Overall, these lines of evidence may also explain D39Y late disease age-of-onset.

D39Y responses well to tafamidis stabilization

We next evaluated whether D39Y TTR exhibited a differential response to Tafamidis stabilization compared to WT and L55P-TTR. Using OD300 turbidity assay, we assessed the inhibitory effect of Tafamidis on WT-TTR and mutant TTR amyloid formation under acidic aggregation conditions (200 mM NaOAc, 100 mM KCl, acidified by AcOH to pH = 4.4). D39Y showed a similar response to Tafamidis upon one site occupation at 1:1 stoichiometry (**Figures 5A–C**). However, upon the increasing concentration of Tafamidis, we did not observe a dose-dependent inhibitory effect after 3.6 μM, indicating its negative cooperativity present in mutant TTR binding to Tafamidis. This result was supported by the ITC experiment as two binding site model was not feasible in D39Y mutant (**Figures 5D–F**). However, D39Y binds to Tafamidis as tightly as the WT TTR, indicating its potential satisfactory response to Tafamidis treatment.

Functional tetrameric TTR concentration in patient's serum indicates the disease age-of-onset

We next explored the tetramer concentration of TTR in patient' serum using UPLC method reported by the Kelly group (11) (**Figure 6A**). Stilbene A2 probe selectively reacts with the Lysine-15 at the weak dimer-dimer interface of TTR tetramer and fluoresces at 430 nm. Due to the stable covalent bonds between A2 and TTR tetramers, we can quantify the folded tetrameric TTR by UPLC (**Figure 6A**). Based on the above working principle of this assay, we established the linear correlation between the fluorescence intensity of the peak and TTR tetramer concentration spiked in serum for afterward quantification (**Figures 6B, C**). The results showed that A2 fluorescence intensity increased with the concentration of TTR, giving a wide linear range from 0.5 to 20 μM (**Figure 6C**).

It has been reported that TTR may partition into folded tetrameric, misfolded oligomeric and amyloid fibril conformations. The decrease in tetramer TTR in blood serum may manifest the disease onset of TTR amyloidosis. Toward this end, we assessed the concentration of TTR tetramer in D39Y symptomatic patient (father), asymptomatic D39Y gene carrier (daughter 1), and wild type non-D39Y gene carrier (daughter 2). Next, we quantified the TTR tetramer concentration in the sera of three subjects of the patient's family (**Figures 6D, E**). Intriguingly, the fluorescence intensity of the healthy daughter (WT, 4.8 μM) shows much higher than the symptomatic father (D39Y, 2.5 μM). Whereas the asymptomatic daughter's TTR tetramer concentration stayed in the middle (D39Y, 3.7 μM) (**Figure 6F**). In addition, the chromatographic peak shape

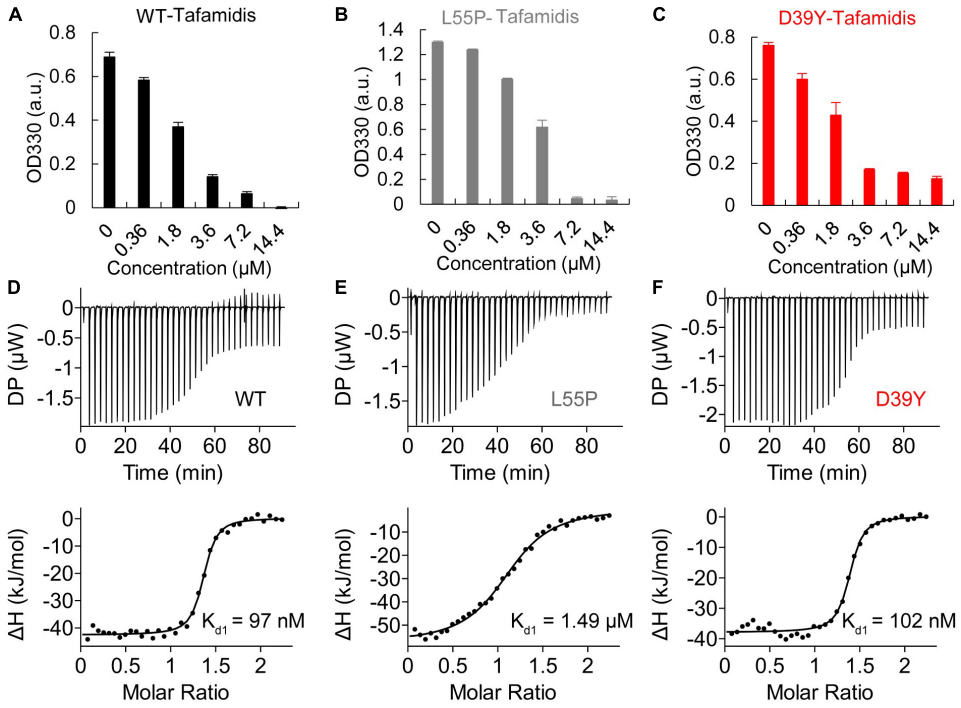

FIGURE 5
Inhibitory effect of Tafamidis on TTR amyloid formation. **(A)** WT **(B)** L55P **(C)** D39Y (3.6 μM) were incubated with increasing concentration of Tafamidis in acidic aggregation buffer (200 mM NaOAc, 100 mM KCl, acidified by AcOH to pH = 4.4) for 72 h. OD330 turbidity assay was used to monitor the formation of TTR amyloid. Isothermal titration calorimetry (ITC) of Tafamidis with wild type **(D)**, L55P **(E)** and D39Y **(F)** TTR revealed the dissociation constant of Tafamidis with TTR. TTR concentrations were 300 μM.

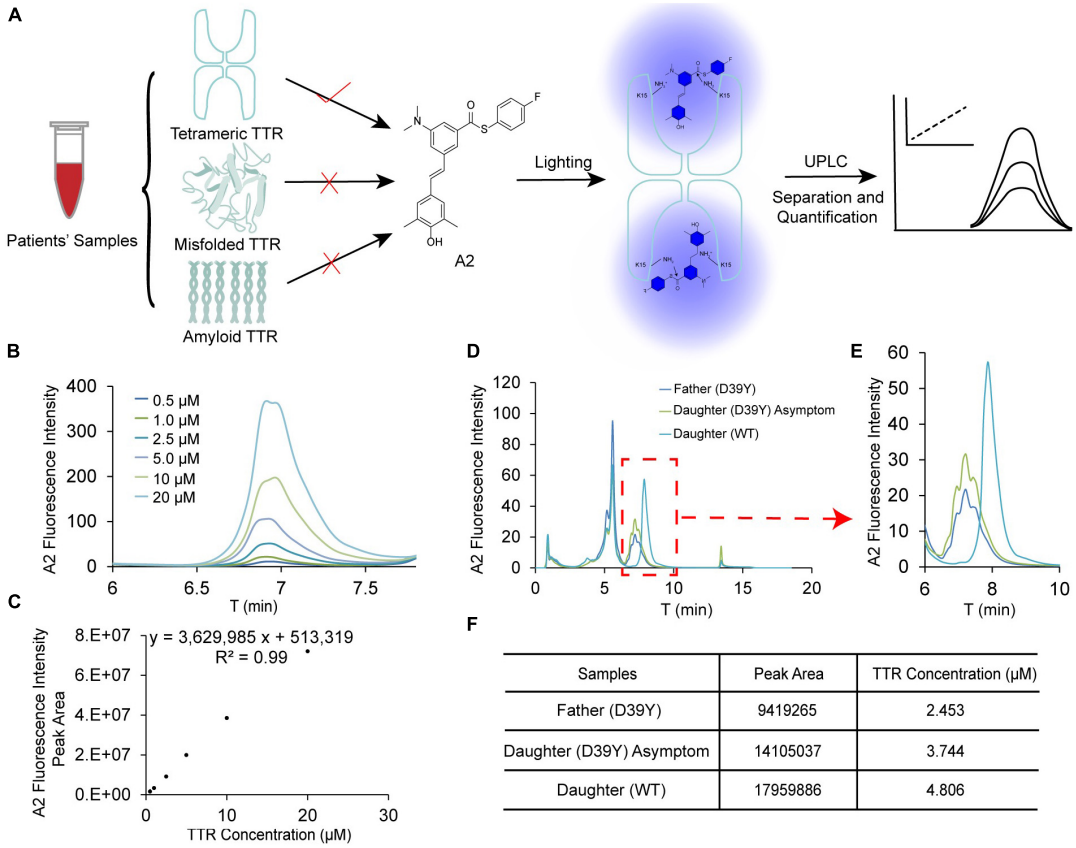

Samples	Peak Area	TTR Concentration (μM)
Father (D39Y)	9419265	2.453
Daughter (D39Y) Asymptom	14105037	3.744
Daughter (WT)	17959886	4.806

FIGURE 6
Quantification of tetramer TTR concentration in patient's blood serum. **(A)** The scheme for quantification of TTR tetramer concentration in patient's serum using by UPLC. A2 selectively reacts with TTR tetramer and reports on the concentration by its fluorescence. **(B,C)** Linear correlation between TTR concentration and fluorescence intensity of A2. **(D)** The raw chromatographic data for the symptomatic father (D39Y), asymptomatic daughter (D39Y) and healthy daughter (WT) on UPLC detected by A2 fluorescence. **(E,F)** Quantification of the peak area and TTR tetramer concentration of three samples.

of D39Y (multiplet peaks) and WT (singlet peak) TTR in this assay reflects its genotypes. These results highlighted that TTR tetramer concentration may serve as a disease onset parameter for D39Y mutation carrier and for the drug interference window time.

Discussion

Cardiac amyloidosis is a devastating and progressive infiltrative cardiomyopathy caused by the extracellular deposition of misfolded transthyretin (12). The clinical presentation and manifestations are non-specific in early stage amyloidosis, leading to massively underdiagnoses. Early diagnosis and treatment were essential for preventing disease progression and adverse cardiovascular events. Witteles et al. (13) had elaborated that under what clinic scenarios should amyloid cardiomyopathy be highly suspected and associated with "Red-flag" signs. In this study, we described the first case of hATTR-CA associated with a D39Y TTR mutation in China. The proband was admitted to our hospital with a series of "Red-flag" features, such as signs and symptoms of heart failure, limb lead low voltage on EKG and increased left ventricular wall thickness on echocardiography. Thus, we initiated screening for amyloidosis in this patient.

The amyloidogenic risk factors for a TTR mutant are usually associated with thermodynamic and kinetic stability (14–17). Thermodynamic stability and kinetic stability measurements of the TTR D39Y mutant showed that it was less stable than WT TTR and more stable than amyloidogenic mutation TTR L55P. These data indicated that instability of variant D39Y TTR is one of the fundamental causes of TTR amyloidosis. TTR are heterotetramers in patients' serum due to the subunit exchange effect. We further revealed the heterozygous tetramer is stable, implicating D39Y's late onset amyloid cardiomyopathy. Despite tetramer destabilization being generally considered to be the major step in developing amyloid fibrils, it has recently been shown that TTR proteolysis has been suggested as another mechanism mediating the amyloid formation (18, 19). The TTR fragments, particularly the 49–127°C-terminal peptide contributed to the formation of TTR amyloid fibrils (18, 19). Interestingly, we did not detect the amyloid-prone proteolytic fragments generated by D39Y variant. This might be because some amyloid variants are insensitive to this limited proteolysis *in vitro* (13, 20). In heart tissue with shear force, these variants become more susceptible to proteolytic cleavage and decomposition under shear stress, which seems to explain why our proband had the cardiac-predominant phenotypes (18, 20).

The average concentration of serum TTR ranged from 3 to 6 μmol/L in healthy adult humans (21–23). The levels of serum TTR found in previous studies are reduced in hATTR patients (24, 25). The decline in serum TTR portended worse survival in wild-type ATTR-CA patients, which was considered as an independent predictor

of OS in patients with transthyretin amyloidosis (26). A Danish cohort study including 16,967 individuals demonstrated that lower serum TTR concentrations indicated a risk of incident HF (27). Also, patients with higher tetrameric TTR tend to respond better to TTR kinetic stabilizers (28–30). Here, The A2-UPLC quantification method was established to detect the tetrameric plasma TTR under native conditions. Among family members, the proband had the lowest TTR concentration with symptoms of heart failure. His asymptomatic daughter had a mild decrease in TTR concentration compared to his non-carrier daughter. Hence, the variant destabilizes the TTR tetramer structure, contributing to amyloid deposition. However, given the small sample size, we cannot wholly exclude the influence of other factors (e.g., age, gender, and nutritional status), which might interfere with the TTR concentration. Additionally, periodic monitoring to observe dynamic changes in the TTR tetramer concentration should be considered in further studies.

More than 120 pathogenic variants have been identified in the TTR gene (2). The Val30Met is the most frequent pathogenetic variant in the Europe population and Japan (12, 31). This mutation is typically associated with familial amyloid polyneuropathy, whereas approximately 43% of patients have cardiac involvement (31). The val122Ile variant is the most common cause of hATTR-CA (2, 32). However, Damrauer et al. (33) showed that among 92 TTR val122Ile carriers with heart failure, 24 (26%) experienced neuropathy, while only 13 (14%) suffered from carpal tunnel syndrome. This finding suggested the necessity of genetic screening for TTR patients. Currently, only scattered TTR variants were found in China, and most of them were associated with familial amyloid polyneuropathy, lacking comprehensive analysis and diagnosis of cardiac amyloidosis (34–37). In this study, the proband and his asymptomatic daughter carried a novel missense variant in TTR D39Y. The proband presented with hATTR-CA demonstrated a clinical profile dominated by cardiac manifestations, largely without evidence of extracardiac manifestations (e.g., polyneuropathy, carpal tunnel syndrome, autonomic insufficiency, and gastrointestinal dysfunction). The exact age of onset and penetrance of this D39Y mutant is not fully elucidated, which could account for this heterogeneity of phenotype.

Recently, several new drugs targeting TTR stabilization and suppressing TTR production have been developed for ATTR amyloidosis therapy. Tafamidis, an oral drug that acts as a small molecule stabilizer of TTR tetramers has been approved for the treatment of familial amyloid polyneuropathy (FAP) and ATTR-CA (38–40). The Tafamidis in Transthyretin Cardiomyopathy Clinical Trial (ATTR-ACT) enrolled 441 patients with ATTR cardiomyopathy, and 106 (24%) of them were hATTR-CA patients with the most common mutations of Val122Ile, Thr60Ala, and Ile68Leu (40). This trial showed that Tafamidis treatment reduced mortality and cardiovascular-related hospitalizations, improved quality of life and relieved symptoms in patients with ATTR-CA compared to placebo controls. Of note, our study verified Tafamidis had a profound inhibition on WT-TTR and L55P TTR amyloid formation. D39Y showed a similar response upon Tafamidis treatment. Also, the ITC experiments revealed that the binding affinities of Tafamidis with D39Y are similar to WT-TTR and much stronger than L55P. Here, we demonstrated the potential benefits of Tafamidis D39Y hATTR-CA. Despite encouraging preliminary results, further studies including long term follow-up are required.

Conclusion

In conclusion, this study described a Chinese family with hATTR-CA due to the TTR variant D39Y with its destabilizing effect in both kinetic and thermodynamic stabilities. Also, a decrease in functional tetrameric TTR concentration may serve as a disease age of onset indicator for the D39Y gene carriers. Tafamidis also exhibited the potential benefits to D39Y hATTR-CA.

Data availability statement

The datasets presented in this study can be found in online repositories. The names of the repository/repositories and accession number(s) can be found below: http://doi.org/10.17632/4cpkx3c66b.1, CC BY 4.0.

Ethics statement

The studies involving human participants were reviewed and approved by Institutional Ethics Committee of Second Affiliated Hospital of Zhejiang University School of Medicine. The patients/participants provided their written informed consent to participate in this study. Written informed consent was obtained from the individual(s) for the publication of any potentially identifiable images or data included in this article.

Author contributions

XP and YL designed the experimental study and revised the manuscript. QM provided the clinical samples and analyzed clinical data. MW and YH conducted experiments and acquired data. YN and XZ acquired the ITC results. QM and MW performed the data analyses and wrote the manuscript and prepared the figures. DY and ZW compiled the imaging data collection and consultation. SD and NQ helped with patient follow-up. All authors read and approved the final manuscript.

Funding

This work was supported by the National Natural Science Foundation of China Grant (Nos. 81700424 and 21907091) and the Natural Science Foundation of Zhejiang Province, China (No. LQ20H020007).

Conflict of interest

The authors declare that the research was conducted in the absence of any commercial or financial relationships that could be construed as a potential conflict of interest.

Publisher's note

References

1. Ruberg F, Grogan M, Hanna M, Kelly J, Maurer M. Transthyretin amyloid cardiomyopathy: JACC state-of-the-art review. *J Am Coll Cardiol.* (2019) 73:2872–91. doi: 10.1016/j.jacc.2019.04.003

2. Maurer M, Hanna M, Grogan M, Dispenzieri A, Witteles R, Drachman B, et al. Genotype and phenotype of transthyretin cardiac amyloidosis: THAOS (transthyretin amyloid outcome survey). *J Am Coll Cardiol.* (2016) 68:161–72. doi: 10.1016/j.jacc.2016.03.596

3. Lane T, Fontana M, Martinez-Naharro A, Quarta C, Whelan C, Petrie A, et al. Natural history, quality of life, and outcome in cardiac transthyretin amyloidosis. *Circulation.* (2019) 140:16–26. doi: 10.1161/circulationaha.118.038169

4. Kelly J, Colon W, Lai Z, Lashuel H, McCulloch J, McCutchen S, et al. Transthyretin quaternary and tertiary structural changes facilitate misassembly into amyloid. *Adv Protein Chem.* (1997) 50:161–81. doi: 10.1016/s0065-3233(08)60321-6

5. Ferguson J, Sun X, Dyson H, Wright P. Thermodynamic stability and aggregation kinetics of EF helix and ef loop variants of transthyretin. *Biochemistry.* (2021) 60:756–64. doi: 10.1021/acs.biochem.1c00073

6. Conceição I, Coelho T, Rapezzi C, Parman Y, Obici L, Galán L, et al. Assessment of patients with hereditary transthyretin amyloidosis - understanding the impact of management and disease progression. *Amyloid.* (2019) 26:103–11. doi: 10.1080/13506129.2019.1627312

7. Sipe J, Benson M, Buxbaum J, Ikeda S, Merlini G, Saraiva M, et al. Amyloid fibril proteins and amyloidosis: chemical identification and clinical classification international society of amyloidosis 2016 nomenclature guidelines. *Amyloid.* (2016) 23:209–13. doi: 10.1080/13506129.2016.1257986

8. Zhang F, Hu C, Dong Y, Lin M, Liu J, Jiang X, et al. The impact of V30A mutation on transthyretin protein structural stability and cytotoxicity against neuroblastoma cells. *Arch Biochem Biophys.* (2013) 535:120–7. doi: 10.1016/j.abb.2013.03.005

9. Hammarström P, Jiang X, Hurshman A, Powers E, Kelly J. Sequence-dependent denaturation energetics: a major determinant in amyloid disease diversity. *Proc Natl Acad Sci USA.* (2002) 99(Suppl. 4):16427–32. doi: 10.1073/pnas.202495199

10. Groenning M, Campos R, Fagerberg C, Rasmussen A, Eriksen U, Powers E, et al. Thermodynamic stability and denaturation kinetics of a benign natural transthyretin mutant identified in a danish kindred. *Amyloid.* (2011) 18:35–46. doi: 10.3109/13506129.2011.560215

11. Rappley I, Monteiro C, Novais M, Baranczak A, Solis G, Wiseman R, et al. Quantification of transthyretin kinetic stability in human plasma using subunit exchange. *Biochemistry.* (2014) 53:1993–2006. doi: 10.1021/bi500171j

12. Fine N, Davis M, Anderson K, Delgado D, Giraldeau G, Kitchlu A, et al. Canadian cardiovascular society/Canadian heart failure society joint position statement on the evaluation and management of patients with cardiac amyloidosis. *Can J Cardiol.* (2020) 36:322–34. doi: 10.1016/j.cjca.2019.12.034

13. Witteles R, Bokhari S, Damy T, Elliott P, Falk R, Fine N, et al. Screening for transthyretin amyloid cardiomyopathy in everyday practice. *JACC Heart Fail.* (2019) 7:709–16. doi: 10.1016/j.jchf.2019.04.010

14. Hurshman Babbes A, Powers E, Kelly J. Quantification of the thermodynamically linked quaternary and tertiary structural stabilities of transthyretin and its disease-associated variants: the relationship between stability and amyloidosis. *Biochemistry.* (2008) 47:6969–84. doi: 10.1021/bi800636q

15. Sekijima Y, Wiseman R, Matteson J, Hammarström P, Miller S, Sawkar A, et al. The biological and chemical basis for tissue-selective amyloid disease. *Cell.* (2005) 121:73–85. doi: 10.1016/j.cell.2005.01.018

16. McCutchen S, Lai Z, Miroy G, Kelly J, Colón W. Comparison of lethal and nonlethal transthyretin variants and their relationship to amyloid disease. *Biochemistry.* (1995) 34:13527–36. doi: 10.1021/bi00041a032

17. Jiang X, Buxbaum J, Kelly J. The V122I cardiomyopathy variant of transthyretin increases the velocity of rate-limiting tetramer dissociation, resulting in accelerated amyloidosis. *Proc Natl Acad Sci USA.* (2001) 98:14943–8. doi: 10.1073/pnas.261419998

18. Mangione P, Porcari R, Gillmore J, Pucci P, Monti M, Porcari M, et al. Proteolytic cleavage of Ser52Pro variant transthyretin triggers its amyloid fibrillogenesis. *Proc Natl Acad Sci USA.* (2014) 111:1539–44. doi: 10.1073/pnas.1317488111

19. Ihse E, Rapezzi C, Merlini G, Benson M, Ando Y, Suhr O, et al. Amyloid fibrils containing fragmented ATTR may be the standard fibril composition in ATTR amyloidosis. *Amyloid.* (2013) 20:142–50. doi: 10.3109/13506129.2013.797890

20. Marcoux J, Mangione P, Porcari R, Degiacomi M, Verona G, Taylor G, et al. A novel mechano-enzymatic cleavage mechanism underlies transthyretin amyloidogenesis. *EMBO Mol Med.* (2015) 7:1337–49. doi: 10.15252/emmm.201505357

21. Purkey H, Dorrell M, Kelly J. Evaluating the binding selectivity of transthyretin amyloid fibril inhibitors in blood plasma. *Proc Natl Acad Sci USA.* (2001) 98:5566–71. doi: 10.1073/pnas.091431798

22. Beck F, Rosenthal T. Prealbumin: a marker for nutritional evaluation. *Am Fam Phys.* (2002) 65:1575–8.

23. Johnson S, Connelly S, Fearns C, Powers E, Kelly J. The transthyretin amyloidoses: from delineating the molecular mechanism of aggregation linked to pathology to a regulatory-agency-approved drug. *J Mol Biol.* (2012) 421:185–203. doi: 10.1016/j.jmb.2011.12.060

24. Buxbaum J, Anan I, Suhr O. Serum transthyretin levels in Swedish TTR V30M carriers. *Amyloid.* (2010) 17:83–5. doi: 10.3109/13506129.2010.483118

25. Buxbaum J, Koziol J, Connors L. Serum transthyretin levels in senile systemic amyloidosis: effects of age, gender and ethnicity. *Amyloid.* (2008) 15:255–61. doi: 10.1080/13506120802525285

26. Hanson J, Arvanitis M, Koch C, Berk J, Ruberg F, Prokaeva T, et al. Use of serum transthyretin as a prognostic indicator and predictor of outcome in cardiac amyloid disease associated with wild-type transthyretin. *Circ Heart Fail.* (2018) 11:e004000. doi: 10.1161/CIRCHEARTFAILURE.117.004000

27. Greve A, Christoffersen M, Frikke-Schmidt R, Nordestgaard B, Tybjaerg-Hansen A. Association of low plasma transthyretin concentration with risk of heart failure in the general population. *JAMA Cardiol.* (2021) 6:258–66. doi: 10.1001/jamacardio.2020.5969

28. Sekijima Y, Dendle M, Kelly J. Orally administered diflunisal stabilizes transthyretin against dissociation required for amyloidogenesis. *Amyloid.* (2006) 13:236–49. doi: 10.1080/13506120600960882

29. Judge D, Heitner S, Falk R, Maurer M, Shah S, Witteles R, et al. Transthyretin stabilization by AG10 in symptomatic transthyretin amyloid cardiomyopathy. *J Am Coll Cardiol.* (2019) 74:285–95. doi: 10.1016/j.jacc.2019.03.012

30. Monteiro C, Mesgazardeh J, Anselmo J, Fernandes J, Novais M, Rodrigues C, et al. Predictive model of response to tafamidis in hereditary ATTR polyneuropathy. *JCI Insight.* (2019) 4:e126526. doi: 10.1172/jci.insight.126526

31. Gertz M, Benson M, Dyck P, Grogan M, Coelho T, Cruz M, et al. Diagnosis, prognosis, and therapy of transthyretin amyloidosis. *J Am Coll Cardiol.* (2015) 66:2451–66. doi: 10.1016/j.jacc.2015.09.075

32. Ruberg F, Maurer M, Judge D, Zeldenrust S, Skinner M, Kim A, et al. Prospective evaluation of the morbidity and mortality of wild-type and V122I mutant transthyretin amyloid cardiomyopathy: the transthyretin amyloidosis cardiac study (TRACS). *Am Heart J.* (2012) 164:222–8.e1. doi: 10.1016/j.ahj.2012.04.015

33. Damrauer S, Chaudhary K, Cho J, Liang L, Argulian E, Chan L, et al. Association of the V122I hereditary transthyretin amyloidosis genetic variant with heart failure among individuals of African or hispanic/latino ancestry. *JAMA.* (2019) 322:2191–202. doi: 10.1001/jama.2019.17935

34. Chen Q, Yuan L, Deng X, Yang Z, Zhang S, Deng S, et al. A missense variant p.Ala117Ser in the transthyretin gene of a han Chinese family with familial amyloid polyneuropathy. *Mol Neurobiol.* (2018) 55:4911–7. doi: 10.1007/s12035-017-0694-0

35. Liu J, Guo Y, Zhou C, Ye Y, Feng J, Yin F, et al. Clinical and histopathological features of familial amyloidotic polyneuropathy with transthyretin Val30Ala in a Chinese family. *J Neurol Sci.* (2011) 304:83–6. doi: 10.1016/j.jns.2011.02.005

36. Liu T, Zhang B, Jin X, Wang W, Lee J, Li J, et al. Ophthalmic manifestations in a Chinese family with familial amyloid polyneuropathy due to a TTR Gly83Arg mutation. *Eye.* (2014) 28:26–33. doi: 10.1038/eye.2013.217

37. Liu Y, Lee Y, Yang C, Chen M, Lin K. Transthyretin Ala97Ser in Chinese-Taiwanese patients with familial amyloid polyneuropathy: genetic studies and phenotype expression. *J Neurol Sci.* (2008) 267:91–9. doi: 10.1016/j.jns.2007.10.011

38. Said G, Grippon S, Kirkpatrick P. Tafamidis. *Nat Rev Drug Discov.* (2012) 11:185–6. doi: 10.1038/nrd3675

39. Coelho T, Maia L, Martins da Silva A, Waddington Cruz M, Planté-Bordeneuve V, Lozeron P, et al. Tafamidis for transthyretin familial amyloid polyneuropathy: a randomized, controlled trial. *Neurology.* (2012) 79:785–92. doi: 10.1212/WNL.0b013e3182661eb1

40. Damy T, Garcia-Pavia P, Hanna M, Judge D, Merlini G, Gundapaneni B, et al. Efficacy and safety of tafamidis doses in the tafamidis in transthyretin cardiomyopathy clinical trial (ATTR-ACT) and long-term extension study. *Eur J Heart Fail.* (2021) 23:277–85. doi: 10.1002/ejhf.2027

frontiers | Frontiers in Cardiovascular Medicine

TYPE Case Report
PUBLISHED 19 June 2023
DOI 10.3389/fcvm.2023.1110392

OPEN ACCESS

EDITED BY
Neil Morgan,
University of Birmingham, United Kingdom

REVIEWED BY
Paola Mandich,
University of Genoa, Italy
Hiroki Yagi,
The University of Tokyo Hospital, Japan
Ashikh Seethy,
All India Institute of Medical Sciences, India
Hang Yang,
Chinese Academy of Medical Sciences and Peking Union Medical College, China

*CORRESPONDENCE
Jacopo Taurino
jacopo.taurino@grupposandonato.it

RECEIVED 28 November 2022
ACCEPTED 30 May 2023
PUBLISHED 19 June 2023

CITATION
Taurino J, Micaglio E, Russo Raucci A, Zanussi M, Chessa M, Udugampolage NS, Carrera P, Pappone C and Pini A (2023) Case report: Complex arterial findings in vascular ehlers-danlos syndrome with a novel *COL3A1* variant and death at young age.
Front. Cardiovasc. Med. 10:1110392.
doi: 10.3389/fcvm.2023.1110392

Case report: Complex arterial findings in vascular ehlers-danlos syndrome with a novel *COL3A1* variant and death at young age

Jacopo Taurino[1]*, Emanuele Micaglio[2], Annalisa Russo Raucci[3], Monica Zanussi[3], Massimo Chessa[4,5], Nathasha Samali Udugampolage[1], Paola Carrera[3,6], Carlo Pappone[2,5] and Alessandro Pini[1]

[1]Cardiovascular-Genetic Center, IRCCS Policlinico San Donato, Milan, Italy, [2]Arrhythmology & Electrophysiology, IRCCS Policlinico San Donato, Milan, Italy, [3]Laboratory of Clinical Genomics, IRCCS San Raffaele Scientific Institute, Milan, Italy, [4]ACHD Unit - Pediatric and Adult Congenital Heart Centre, IRCCS-Policlinico San Donato, Milan, Italy, [5]Vita & Salute San Raffaele University, Milan, Italy, [6]Genomics for the Diagnosis of Human Pathologies, IRCCS San Raffaele Scientific Institute, Milan, Italy

Vascular Ehlers-Danlos syndrome (vEDS) is a genetic disease caused by a pathogenic mutation in the *COL3A1* gene. Despite its severe course, the rarity and extreme clinical variability of the disease can pose significant obstacles to a timely diagnosis. Early and accurate diagnosis may lead to improved patient outcomes by providing access to targeted pharmacological treatments like celiprolol and enhancing the management of vEDS-related complications. Herein, we report a patient harboring a novel *de novo COL3A1* missense variant, in which the diagnosis was only possible belatedly due to delayed referral for genetic evaluation. The patient developed pulmonary complications, aneurysms, and vascular malformations, and died at the age of 26 years due to massive pulmonary bleeding.

KEYWORDS

COL3A1, vascular ehlers danlos syndrome, aneurysm - dissecting, pneumothorax, atypical onset

Introduction

Vascular Ehlers-Danlos syndrome (vEDS) is a rare connective tissue disorder characterized by a severe course involving fragility and easy rupture of arteries and bowel, transparent skin, easy bruising, and distinct facial features such as protruding eyes, thin nose and lips, sunken cheeks, and lobeless ears (1).

Respiratory manifestations of vEDS are uncommon but have been described, including spontaneous pneumothorax, intrapulmonary bleeding causing recurrent hemoptysis, and bulla or bleb formation (2).

vEDS can be life-threatening at a very young age, and its diagnosis is challenging, particularly in the absence of a family history, due to the rarity and extreme clinical variability associated with the disorder (3). However, primary diagnosis of vEDS can be suspected through careful genetic counseling based on clinical presentation and then confirmed by identifying the pathogenic variant in the *COL3A1* gene.

10.3389/fcvm.2023.1110392

Case report

The patient was born preterm at the 35th week of gestation due to premature rupture of membranes. At just four months of age, he experienced an apparent life-threatening event (ALTE) while crying, characterized by sudden loss of consciousness, generalized hypotonia, and cyanosis (no documentation was available). Two months later, a similar event occurred, and a head CT scan revealed bilateral subdural hematoma that was resolved via craniotomy. As a result, the patient suffered reduced visual acuity in the left eye, believed to be secondary to compression of the ipsilateral optic nerve, but he did not develop any other permanent neurological deficits over time.

Starting at the age of 14 years, the patient began experiencing recurrent episodes of hemoptysis, accompanied by right-sided paresthesias, headache, and photophobia. A brain MRI revealed cerebellar tonsil ectasia through the foramen magnum. That same year, the patient suffered a spontaneous right-sided pneumothorax, which was treated with mechanical pleurodesis and exeresis of a bullous lesion. Another pneumothorax occurred at the age of 17 years, this time managed with chemical pleurodesis. Between these two events, he underwent saphenectomy to address multiple vein ectasia in his left leg.

At 22 years old, after an episode of severe hemoptysis, an exploratory thoracotomy was performed, revealing a massive spontaneous right-sided hemothorax. Following suspicion of a coagulation disorder, a hematologic screening which included CBC, PT, aPTT, PFA-100, coagulation factor assay, and vWF dosage—was carried out; all results were normal. At the time of testing, vEDS was not suspected and genetic counseling was not advised. Lacking a definite diagnosis, the patient continued his active lifestyle without adopting any cautious behavior, including smoking.

At the age of 25 years, the patient presented to the emergency department of our institute with acute pain in the right thoraco-abdominal area. A thoracic-abdominal CT scan revealed a massive retroperitoneal hematoma in the right perirenal region, extending from the subdiaphragmatic region to the pelvic cavity (maximum diameter of 30 cm), adjacent to a large anastomotic circle between the aorta and the right pulmonary artery. Multiple dilations of the peripheral branches of the pulmonary artery were also observed.

The right diaphragmatic artery appeared hypertrophic, circumvoluted, with two aneurysmal formations one of which was also partially thrombosed. These findings were confirmed by the angiograms (**Figure 1A**) and treated via selective coil embolization (**Figure 1B**). The angiograms also revealed a small dissection flap in the right external iliac artery, and a hypertrophic and circumvoluted 12th intercostal artery. Later, selective catheterization of this artery demonstrated arterial-venous shunts between it and the pulmonary vein for the right lower pulmonary lobe (**Figure 2**). The shunts were then treated via selective embolization as well (**Figure 1B**).

One month later, the patient was readmitted to the emergency department due to another episode of hemoptysis. The chest CT scan revealed "ground glass" consolidation areas with a central consolidated component in the lung parenchyma, with the largest located at the left posterior costophrenic sinus, and several smaller ones in the left lower pulmonary lobe.

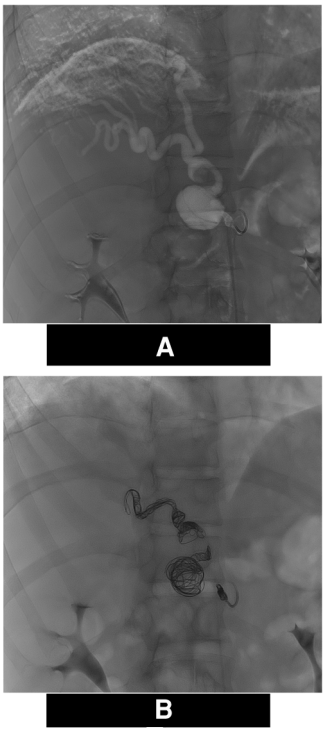

FIGURE 1
Angiograms of the right inferior diaphragmatic artery. (A) Digital Subtraction Angiography Hypertrophy of the right inferior diaphragmatic artery and evidence of 2 aneurisms (*). (B) Angiogram: Post Coil embolization using Interlock mechanically detachable coils (Boston Scientific, Natick, MA) and The Concerto^{TM} Helix and 3D detachable coil systems (Medtronic Inc Minneapolis MN, US).

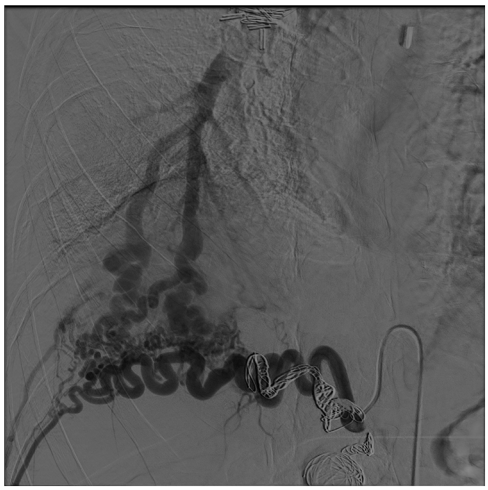

FIGURE 2
Digital subtraction angiography. Intercostal hypertrophic artery (*) and artero, venous fistula between this artery and the inferior right pulmonary vein (#).

These findings were consistent with alveolar hemorrhage, likely originating from the hypertrophic left bronchial artery, where a pseudoaneurysm was recognizable. A subsequent angiography showed markedly tortuous and ectasic proximal sections of the bronchial arteries and hyperemia of the distal bronchial circles.

Superselective catheterization attempts to reach the bleeding site of the left bronchial artery were unsuccessful. Consequently, as the hemoptysis resolved, the patient was not subjected to an embolization procedure; instead, he was started on tranexamic acid therapy without a clinical indication for whole blood transfusion.

During this hospitalization, the patient was referred to clinical genetics for further evaluation. Upon physical examination, the patient exhibited a muscular constitution; his height was 177 cm, and his weight was 75 kg. The skin assessment was challenging due to the presence of multiple tattoos covering the trunk and limbs. No facial anomalies or signs of joint hypermobility were evident; however, a high-arched palate, absence of the lingual frenulum, and flat feet with hammer toes were observed. A connective tissue disorder was finally suspected.

To verify this hypothesis, the patient underwent genetic testing from peripheral blood extracted DNA using a panel of 20 genes (*ACTA2, COL1A1, COL1A2, COL3A1, COL5A1, COL5A2, ELN, FBN1, FBN2, FLNA, MYH11, MYLK, NOTCH1, PLOD1, SMAD3, TGFB1, TGFB2, TGFBR1, TGFBR2, TNXB*) via next-generation sequencing. The analysis identified the novel heterozygous missense variant c.1889G > A causing the amino-acid substitution p.(Gly630Glu) in *COL3A1* (NM_000090.3) (**Figure 3**). Subsequent testing of parental samples demonstrated that the variant originated *de novo* (**Supplementary Figure S1**). A literature search (PubMed, Human Gene Mutation Database, LOVD, Ehlers-Danlos Syndrome variant Database, Internal data, ClinVar) confirmed that this variant has not been previously reported, indicating a novel mutation.

According to the ACMG standards for variant classification (4), the following criteria were applied to classify the variant as 'likely pathogenic': the variant was absent in both the unaffected parents (PS2), it is absent in the gnomAD database (PM2); it is located within the collagen triple helix repeat (PM1), and it is predicted in silico as deleterious by many different tools, including MetaRNN, M-CAP, MVP, Polyphen2 HDIV, Polyphen2 HVAR, SIFT, DEOGEN2, EIGEN, FATHMM, and MutPred (PP3).

The patient's clinical presentation, along with imaging and genetic test results, led to a diagnosis of vEDS, and pharmacological therapy with celiprolol 200 mg daily was started.

The patient was subsequently evaluated by a multidisciplinary team to determine the best approach for treating the frequent pulmonary hemorrhages.

The only resolutive treatment proposed was heart-lung transplantation. However, the surgical team deemed this option impossible due to the patient's previous chemical pleurodesis and tissue fragility. Later that year, the patient experienced a new spontaneous pneumothorax, followed by a massive pulmonary hemorrhage that proved fatal at the age of 26 years.

Discussion

Vascular Ehlers-Danlos syndrome (vEDS) is the most severe subtype among the Ehlers-Danlos syndromes (5); caused by pathogenic variants in the *COL3A1* gene, which encodes the α1 chain of type III procollagen [proα1(III)].

vEDS carries a high risk of sudden death due to the rupture of large arteries or hollow organs, such as the bowel and uterus. The median age for the first major vascular event is 24.6 years, and the median survival is only 48 years due to the high rate of complications (6).

Clinical diagnostic criteria for vEDS include: a positive family history of the disorder, early onset of arterial rupture or dissection before age of 40 years, unexplained rupture of the sigmoid colon, unexplained spontaneous pneumothorax or carotid-cavernous sinus fistula formation without trauma, and minor vEDS features (e.g., tendon and muscle rupture, easy bruising, thin translucent skin, hypermobility of small joints, aged appearance of extremities particularly the hands, gingival recession, keratoconus, early onset varicose veins) (5).

Imaging, including computed tomography angiography and magnetic resonance angiography, is an essential tool for diagnosing and monitoring vEDS. Aneurysms, dissections, arterial ectasia, and occlusions are the most common radiologic findings, with abdominal vessels being the most frequently affected (34%), followed by thoracic (33%), and head/cervical vessels (17%) (6).

Genetic testing is the definitive method for confirming the diagnosis of vEDS, through the identification and characterization of a *COL3A1* pathogenic variant, which may also offer a prognostic insight. According to Omar et al. (7), the majority of pathogenic variants in the *COL3A1* gene (approximately 65%) are missense variants, resulting in the substitution of a glycine residue within the triple helical domain. Aberrant splicing, occurring in about 25% of patients, is the second most common mutation mechanism. Additionally, 5% of patients have nonsense or frameshift variants, leading to unstable RNA that is degraded through nonsense-mediated decay without producing protein (null mutations or haploinsufficiency).

According to Pepin et al. (6), splicing variants are associated with the most severe disease course, followed by missense variants involving glycine residues, and finally haploinsufficient variants are associated with a milder course, including delayed symptom onset and increased life expectancy.

Diagnosing vEDS can be challenging, especially because 50% of *COL3A1* pathogenic variants occur *de novo*. As a result, vEDS is often only suspected after a significant or potentially fatal complication occurs (3).

For 70% of vEDS patients, the presenting sign is either a vascular rupture or an organ rupture (8). However, this means that a significant portion of patients have an atypical presentation of vEDS. Among these, 12% of patients have a spontaneous pneumothorax due to the rupture of a lung bleb as their first described manifestation (3). Additionally, pulmonary hemorrhages related to the rupture of small vascular nodules or arteriovenous fistulas have been reported as well (9, 2).

FIGURE 3
COL3A1 BAM from IGV. The c.1889G > A variant is detected in heterozygosity. Cov: coverage; AF: allelic fraction of alternative called base (A).

In 2015, Abrahamsen et al. (10) described a patient carrying a *COL3A1* pathogenic variant whose disease onset occurred at the age of 19 years, characterized by recurrent episodes of spontaneous pneumothorax. The patient also had other typical signs of the disease, such as a tall and slender build, mild scoliosis, asymmetry of the chest, long fingers with hypermobility of the thumb joints, thin and translucent skin, prominent eyes, and keratoconus, which further supported genetic testing for *COL3A1*. The authors suggested that the atypical presentation of vEDS with pneumothorax and pulmonary bleeding may be more common in young adults.

Treatment for vEDS primarily focuses on avoiding high-risk activities and procedures such as arterial punctures, elective surgeries, and gastrointestinal and uterine endoscopies. These procedures should be limited to cases with urgent complications, including arterial or organ rupture. Blood pressure control is crucial, and the use of antiplatelet and anticoagulation medications should be avoided unless strictly indicated. It is essential for patients to understand their risk factors and implement necessary lifestyle changes to reduce the risk of complications, such as avoiding strenuous physical activity and contact sports (8).

Atypical presentations of vEDS may delay diagnosis, resulting in suboptimal patient management and serious clinical consequences. In this regard, Diebels et al. (11) described a 58-year-old patient with Stanford type B aortic dissection who underwent thoracic endovascular repair (TEVAR) but experienced a retrograde dissection with rupture of the ascending aorta just two days later, which ultimately proved fatal. In this case, diagnosis was not possible through clinical criteria, but was only revealed post-mortem thanks to the identification of a pathogenic mutation in the *COL3A1* gene. The authors emphasized the importance of a conservative management approach for vascular events in patients even suspected of having vEDS, given the high fragility of their tissues and blood vessels, which can lead to very serious complications.

Currently, the only medical therapy that has been shown to improve outcomes for vEDS is the use of celiprolol, a β1-adrenoceptor antagonist and a β2-adrenoceptor agonist that reduces hemodynamic stress and the fragility of arterial walls (12).

The extent of evaluation at the time of initial diagnosis is currently a topic of ongoing debate. The most important step in managing vEDS is assembling an interdisciplinary care team, which should include a primary care physician, a geneticist, a vascular surgeon, and a general surgeon. This team will be responsible for coordinating both routine and emergency care (8).

In this work, we describe a patient with vEDS who died from the disease at a young age. Recurrent spontaneous pneumothorax and pulmonary hemorrhage in young individuals may indicate an atypical onset of vEDS and should warrant prompt genetic counseling, even in the absence of other common symptoms such as facial, skin, and joint anomalies.

Unfortunately, genetic counseling for our patient was recommended only after his condition worsened, and the delayed diagnosis precluded the proper clinical management that might have been potentially beneficial.

An earlier diagnosis might have allowed for timely treatment with celiprolol, which has been associated with better cardiovascular outcomes and longer life expectancy in vEDS patients. Furthermore, it might have led to alternative management strategies for the patient's recurrent pneumothoraces.

In this scenario, the typical tissue fragility of vEDS alone was not the reason to contraindicate heart and lung transplantation in our patient. However, this fragility, combined with the result of the previous chemical pleurodesis led the surgical team to deem any intervention unfeasible.

Conclusion

The usefulness of this case is to demonstrate the pivotal importance of referring to clinical genetics evaluation for all patients with a history of recurrent bleedings and spontaneous pneumothoraces. Early diagnosis of vEDS may enable better treatment choices, improved management, and ultimately, better outcomes.

Data availability statement

The original contributions presented in the study are included in the article/**Supplementary Material**, further inquiries can be directed to the corresponding author.

Ethics statement

Written informed consent was obtained from the individual(s) for the publication of any potentially identifiable images or data included in this article.

Author contributions

AR, JT, and AP evaluated the patient and collected his clinical history; JT and AP conceived the clinical study; MC conducted neuroimaging analyses at follow-up; AR, MZ, NU, PC, critically revised the clinical data and contributed to assembling the manuscript; MZ and PC performed NGS analysis and interpretation; JT and EM wrote the manuscript; PC, AP and CP critically revised the manuscript. All authors contributed to the article and approved the submitted version.

Funding

This study was partially supported by "Ricerca Corrente" funding from the Italian Ministry of Health to IRCCS Policlinico San Donato.

Conflict of interest

The authors declare that the research was conducted in the absence of any commercial or financial relationships that could be construed as a potential conflict of interest.

Publisher's note

Supplementary material

The Supplementary Material for this article can be found online at: https://www.frontiersin.org/articles/10.3389/fcvm.2023.1110392/full#supplementary-material

References

1. Malfait F. Vascular aspects of the ehlers-danlos syndromes. *Matrix Biol.* (2018) 71-72:380–95. doi: 10.1016/j.matbio.2018.04.013

2. Kawabata Y, Watanabe A, Yamaguchi S, Aoshima M, Shiraki A, Hatamochi A, et al. Pleuropulmonary pathology of vascular ehlers-danlos syndrome: spontaneous laceration, haematoma and fibrous nodules. *Histopathology*. (2010) 56(7):944–50. doi: 10.1111/j.1365-2559.2010.03574.x

3. Byers PH, Belmont J, Black J, De Backer J, Frank M, Jeunemaitre X, et al. Diagnosis, natural history, and management in vascular ehlers-danlos syndrome. *Am J Med Genet C Semin Med Genet*. (2017) 175(1):40–7. doi: 10.1002/ajmg.c.31553

4. Richards S, Aziz N, Bale S, Bick D, Das S, Gastier-Foster J, et al. Standards and guidelines for the interpretation of sequence variants: a joint consensus recommendation of the American college of medical genetics and genomics and the association for molecular pathology. *Genet Med.* (2015) 17:405–23. doi: 10.1038/gim.2015.30

5. Malfait F, Francomano C, Byers P, Belmont J, Berglund B, Black J, et al. The 2017 international classification of the ehlers-danlos syndromes. *Am J Med Genet C Semin Med Genet*. (2017) 175(1):8–26. doi: 10.1002/ajmg.c.31552

6. Pepin MG, Schwarze U, Rice KM, Liu M, Leistritz D, Byers PH. Survival is affected by mutation type and molecular mechanism in vascular ehlers-danlos syndrome (EDS type IV). *Genet Med.* (2014) 16(12):881–8. doi: 10.1038/gim.2014.72

7. Omar R, Malfait F, Van Agtmael T. Four decades in the making: collagen III and mechanisms of vascular ehlers danlos syndrome. *Matrix Biol Plus*. (2021) 12:100090. doi: 10.1016/j.mbplus.2021.100090

8. Byers PH. Vascular ehlers-danlos syndrome. In: Adam MP, Mirzaa GM, Pagon RA, et al., editors. *Genereviews®*. Seattle (WA): University of Washington (1993–2023). Available at: https://www.ncbi.nlm.nih.gov/books/NBK1494/

9. Ishiguro T, Takayanagi N, Kawabata Y, Matsushima H, Yoshii Y, Harasawa K, et al. Ehlers-Danlos syndrome with recurrent spontaneous pneumothoraces and cavitary lesion on chest x-ray as the initial complications. *Intern Med.* (2009) 48(9):717–22. doi: 10.2169/internalmedicine.48.1818

10. Abrahamsen BJ, Kulseth MA, Paus B. A 19-year-old man with relapsing bilateral pneumothorax, hemoptysis, and intrapulmonary cavitary lesions diagnosed with vascular ehlers-danlos syndrome and a novel missense mutation in *COL3A1*. *Chest*. (2015) 147(5):e166–70. doi: 10.1378/chest.13-3002

11. Diebels I, Hendriks JMH, Durnez J, Paelinck BP, El Addouli H, Laga S, et al. Retrograde type A aortic dissection 48 hours after TEVAR in a patient with a delayed diagnosis of vascular ehlers-danlos syndrome. *Aorta (Stamford)*. (2022) 10 (3):141–4. doi: 10.1055/s-0042-1749171

12. Ong KT, Perdu J, De Backer J, Bozec E, Collignon P, Emmerich J, et al. Effect of celiprolol on prevention of cardiovascular events in vascular ehlers-danlos syndrome: a prospective randomised, open, blinded-endpoints trial [published correction appears in lancet. 2016 aug 6;388(10044):564. Dosage error in published abstract; MEDLINE/PubMed abstract corrected; dosage error in article text]. *Lancet*. (2010) 376(9751):1476–84. doi: 10.1016/S0140-6736(10)60960-9

Frontiers in
Cardiovascular Medicine

Innovations and improvements in cardiovascular treatment and practice

Focuses on research that challenges the status quo of cardiovascular care, or facilitates the translation of advances into new therapies and diagnostic tools.

Discover the latest Research Topics

See more →

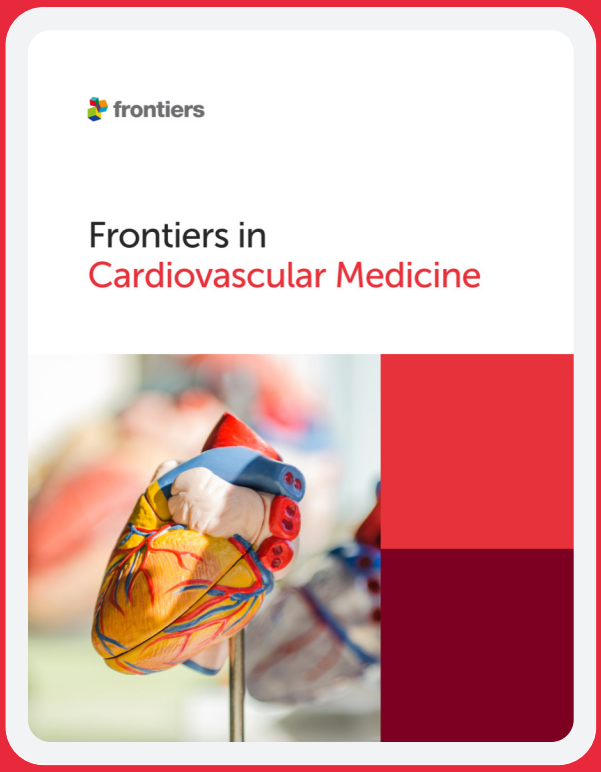

Frontiers

Avenue du Tribunal-Fédéral 34
1005 Lausanne, Switzerland
frontiersin.org

Contact us

+41 (0)21 510 17 00
frontiersin.org/about/contact